A026 223

TP-76-5

Wave Climate at Torrey Pines Beach, California

by

Steven S. Pawka, Douglas L. Inman,
Robert L. Lowe, and Linda Holmes

TECHNICAL PAPER NO. 76-5

MAY 1976

Approved for public release;
distribution unlimited.

Prepared for

U.S. ARMY, CORPS OF ENGINEERS

COASTAL ENGINEERING RESEARCH CENTER

Kingman Building
Fort Belvoir, Va. 22060

UNCLASSIFIED

SECURITY CLASSIFICATION OF THIS PAGE (When Data Entered)

REPORT DOCUMENTATION PAGE

READ INSTRUCTIONS BEFORE COMPLETING FORM

1. REPORT NUMBER TP 76-5	2. GOVT ACCESSION NO.	3. RECIPIENT'S CATALOG NUMBER
4. TITLE (and Subtitle) WAVE CLIMATE AT TORREY PINES BEACH, CALIFORNIA		5. TYPE OF REPORT & PERIOD COVERED Technical Paper
		6. PERFORMING ORG. REPORT NUMBER
7. AUTHOR(s) Steven S. Pawka, Douglas L. Inman, Robert L. Lowe, and Linda Holmes		8. CONTRACT OR GRANT NUMBER(s) DACW72-72-C-0021
9. PERFORMING ORGANIZATION NAME AND ADDRESS Scripps Institution of Oceanography La Jolla, California 92037		10. PROGRAM ELEMENT, PROJECT, TASK AREA & WORK UNIT NUMBERS A 31463
11. CONTROLLING OFFICE NAME AND ADDRESS Department of the Army Coastal Engineering Research Center (CERRE-OC) Kingman Building, Fort Belvoir, Virginia 22060		12. REPORT DATE May 1976
		13. NUMBER OF PAGES 372
14. MONITORING AGENCY NAME & ADDRESS(if different from Controlling Office)		15. SECURITY CLASS. (of this report) UNCLASSIFIED
		15a. DECLASSIFICATION/DOWNGRADING SCHEDULE

16. DISTRIBUTION STATEMENT (of this Report)

Approved for public release; distribution unlimited.

17. DISTRIBUTION STATEMENT (of the abstract entered in Block 20, if different from Report)

18. SUPPLEMENTARY NOTES

19. KEY WORDS (Continue on reverse side if necessary and identify by block number)

Array measurements
Directional spectra
Tilting spar
Wave climate
Torrey Pines Beach, California

20. ABSTRACT (Continue on reverse side if necessary and identify by block number)

The wave climate at a site off Torrey Pines Beach, California, was studied using a line array of four pressure sensors which roughly parallels the coastline at a depth of 10 meters. The pressure sensors were linked to a shelf station that contained accelerometers and, at times, electromagnetic current meters and a surface-piercing staff. The data were transmitted by radio link to a shore recording station.

(continued)

DD FORM 1 JAN 73 1473 EDITION OF 1 NOV 65 IS OBSOLETE

UNCLASSIFIED

SECURITY CLASSIFICATION OF THIS PAGE (When Data Entered)

20. Abstract.

Wave records were taken four times daily for a 16-month period from February 1973 to May 1974. The pressure-sensor array data were used to calculate estimates of the frequency-directional spectra of the wave field. The spectra were investigated in an effort to characterize the principal components of the wave field. The wave components were identified as peaks in the frequency spectra. The energy, peak frequency, bandwidth, and direction of these wave components were obtained in the data analysis. These parameters of the wave field are recorded in a tabular form. Seasonal groupings of the wave data reveal the variations of the typical wave conditions over the year.

Improvements to the anchoring of cables and connections of the shelf station eliminated most of its failure modes, and the SAS system remained on station and operative during some seven storms in the winter of 1974. The SAS shows promise of being a reliable long-term data collection system for nearshore waters.

PREFACE

This report is published to provide coastal engineers with climatic data to augment and help evaluate information and techniques obtained in the wave climate program of the U.S. Army Coastal Engineering Research Center (CERC).

This report is published, with only minor editing, as received from the contractor; results and conclusions are those of the authors and are not necessarily accepted by CERC or the Corps of Engineers.

This report was prepared by Steven S. Pawka, Research Assistant; Dr. Douglas L. Inman, Professor of Oceanography; Robert L. Lowe, Senior Development Engineer; and Linda Holmes, Research Assistant; Scripps Institution of Oceanography, La Jolla, California, under CERC Contract No. DACW72-72-C-0021. The authors acknowledge the assistance of Darold E. Palmer, John C. Boylls, Wayne Spencer, Michael Kirk, and Earl Murray in the collection of the data, and installation and maintenance of the equipment.

Dr. Dinorah Esteva was the CERC technical monitor for this contract under the supervision of Dr. D. Lee Harris, Chief, Coastal Oceanography Branch, Research Division.

Comments on this publication are invited.

Approved for publication in accordance with Public Law 166, 79th Congress, approved 31 July 1945, as supplemented by Public Law 172, 88th Congress, approved 7 November 1963.

JAMES L. TRAYERS
Colonel, Corps of Engineers
Commander and Director

CONTENTS

		Page
I	INTRODUCTION	9
	1. Background	9
	2. Scope of the Study	10
II	WAVE CLIMATE DATA SYSTEM	10
	1. Installation	10
	2. Data Acquisition	10
	3. Data Processing	12
	4. Sensors	16
	5. Underwater Cables and Connectors	19
	6. Field Operation of System	22
III	ARRAY THEORY	22
IV	CHARACTERISTIC PARAMETERS FOR WAVE SPECTRA	30
V	COMPARISONS OF VARIOUS METHODS AND TECHNIQUES	31
	1. Comparisons Among the Various Pressure Sensors	31
	2. Surface-Piercing Staff Versus Pressure Sensors	35
	3. Comparison with Visual Estimates of Wave Height and Direction	43
	4. Orbital Velocity as a Function of Wave Energy and Frequency	44
	5. Direction from Current Meters and a Single Pressure Sensor	51
	6. Direction from Accelerometers	60
	7. Directional Spectra of High Frequency Waves	63
VI	WAVE CLIMATE	70
VII	CONCLUSIONS	81
	LITERATURE CITED	86
APPENDIX		
A	THEORETICAL DEVELOPMENT OF DIRECTIONAL SPECTRA	89
B	DYNAMICS AND EXPECTED PERFORMANCE OF THE TILTING BAR	99
C	DESIGN AND OPERATION OF SURFACE-PIERCING WAVE STAFF	108
D	TABULAR REPRESENTATION OF CHARACTERISTIC PARAMETERS OF WAVE SPECTRA	116
E	FREQUENCY OF OCCURRENCE OF SPECTRAL PEAKS	174
F	COMPARISONS OF ENERGY LEVELS OF VARIOUS SENSORS	279

CONTENTS—Continued

Page

APPENDIX

G COMPARISONS OF DIRECTIONAL RESULTS OF VARIOUS GROUPINGS OF THE SENSORS 298

H COMPARISON OF SPECTRA OF WAVE STAFF AND PRESSURE SENSOR 320

I TABULAR COMPARISONS OF SENSORS 328

J SEASONAL ENERGY-DIRECTIONAL PLOTS FOR GIVEN FREQUENCY BANDS 344

TABLE

V-1 A comparison of directional results from the current meters with that of the pressure sensor array 46

FIGURES

II-1 Location map of pressure-sensor array and shelf station at Torrey Pines Beach 11

II-2 Schematic of pressure-sensor array 13

II-3 A sample analog record of pressure and accelerometer data . . 14

II-4 Photograph of pressure-sensor assembly 17

II-5 Underwater photograph of the current meter mounted on the shelf station 18

II-6 Photograph of the bottom section of the original shelf station 20

II-7 Photograph of the redesigned bottom section of the shelf station 21

III-1 Directional response of the 1-2-1 array to 14.2- and 4-second waves 27

III-2 Directional response of the 1-2-1 array to 4.7-second waves 29

IV-1 Comparison of a measured directional spectrum with a directional model for well directed southern swell 32

CONTENTS

FIGURES—Continued

		Page
IV-2	Comparison of a measured directional spectrum with a directional model for northern waves of period 6.9 seconds	33
V-1	Frequency spectra of records of two pressure sensors displaying a disparity at low frequencies	36
V-2	Frequency spectra of records of two pressure sensors displaying a disparity at high frequencies	37
V-3	Frequency spectra of two pressure sensors with depth correction factor applied from 0.0 to 0.5 hertz	39
V-4	Frequency and cross-spectra of a bottom-mounted pressure sensor and a surface-piercing resistive wire gage off Scripps Pier	40
V-5	Frequency and cross-spectra of accelerometers mounted on the tethered spar	42
V-6	Comparisons of measured with theoretical orbital velocity for SAS 1-13 Nov 73-01	47
V-7	Comparisons of measured with theoretical orbital velocity for SAS 1-12 Nov 73-04	48
V-8	Comparisons of measured with theoretical orbital velocity for SAS 1-09 Nov 73-01	49
V-9	Comparisons of measured with theoretical orbital velocity for SAS 1-11 Nov 73-03	50
V-10	Frequency and cross-spectra of longshore and onshore-offshore current measurements	52
V-11	Frequency and cross-spectra of onshore-offshore current measurements and bottom pressure	57
V-12	Current meter directional spectrum for a wave period of 8.8 seconds for SAS 1-14 Jun 73-02	58
V-13	Directional spectrum from pressure-sensor array for 8.8-second waves for SAS 1-14 Jun 73-02	59
V-14	Coordinate system defined by the axis of the accelerometers and that defined by the axis of the current meters	61

CONTENTS

FIGURES—Continued

		Page
V-15	Comparison of spectral results of orthogonal accelerometers mounted on the station	62
V-16	Directional response of the 1-2-1 array to 3.0-, 3.9-, and 4.5-second waves	64
V-17	A plot of coherence between pressure sensors versus separation distance for several wave frequencies	66
V-18	Frequency and cross-spectra of two pressure sensors for the data used in Figure 17	67
V-19	Directional spectra evaluated from the line array for wave periods 3.9 to 4.5 seconds	68
V-20	Frequency and cross-spectra of two pressure sensors for the data used in Figure 19	69
VI-1	Map displaying linear shadowing effects of offshore islands for the wave climate at Torrey Pines Beach	71
VI-2	Plot of peak energy versus peak period for spectral peaks recorded during the summer months of 1973	72
VI-3	Histogram displaying energy versus direction summed for 14.2-second waves for the summer months	73
VI-4	Frequency and cross-spectra of two pressure sensors displaying a typical bimodal summer form	74
VI-5	Plot of peak energy versus peak period for spectral peaks recorded during September, October, and November	76
VI-6	Plot of peak energy versus peak period for spectral peaks recorded during December, January, and February	77
VI-7	Histogram displaying energy versus direction summed for 14.2-second waves for the winter months	78
VI-8	Histogram displaying energy versus direction summed for 8.1-, 7.4-, and 6.9-second waves for the winter months	79

CONTENTS

FIGURES—Continued

Page

VI-9 Plot of peak energy versus peak period for spectral peaks recorded during the months of March, April, and May 80

VI-10 Comparison of sum energy recorded during a storm with the total energy budget of the project 82

VI-11 Plot of the probability distribution function for significant wave height for the four seasons 83

WAVE CLIMATE AT TORREY PINES BEACH, CALIFORNIA

by

Steven S. Pawka, Douglas L. Inman,

Robert L. Lowe, and *Linda Holmes*

I. INTRODUCTION

1. Background.

Wind-generated waves represent a significant energy input into the coastal region. Waves incident to the coast provide the principal driving force for several nearshore processes, including: longshore currents; rip currents; nearshore circulation cells; the seasonal changes in the equilibrium profile of the beach; and longshore transportation of sand. A full understanding of these processes in the natural environment requires knowledge of the incident wave characteristics, which collectively are referred to here as wave climate.

The primary objective of this study was an investigation into the nature of the frequency-directional spectra of waves in coastal waters, and, in particular, off Torrey Pines Beach, California. The site was selected for its straight coastline and offshore bathymetry in an effort to avoid complicated refraction effects. Torrey Pines Beach is exposed to several wave-generating regions in the North and South Pacific. However, offshore islands shelter the study site from waves propagating from certain sectors.

The frequency-directional spectrum may be obtained in a number of ways. Cote (1960) treated the use of stereo wave photographs as a means of deriving directional information. Longuet-Higgins, Cartwright, and Smith (1963) discussed the use of a tilt buoy for measurement of directional spectra. Barber (1963) discussed the directional resolving power of an array of wave detectors. Inman, Komar, and Bowen (1969) and Komar and Inman (1970) used wave arrays for determining the mean direction of near-breaking waves. Munk, et al. (1963) used a two-dimensional array of pressure sensors to resolve the directions of swell from distant sources. Simpson (1969) used a buoy system to make a limited number of observations of the directional spectra of waves in the coastal zone. Panicker and Borgman (1970) computed several directional spectra from the records of the nearshore five-gage CERC array at Pt. Mugu, California. The basic techniques employed in this study parallel the directional finding methods developed for electromagnetic wave antennas, and adapted for ocean waves by Barber (1963) and others.

2. Scope of the Study.

Both pressure-sensor arrays and buoy systems appear to be practical devices for daily measurement of frequency and directional properties of waves. However, a simple array can be constructed that gives much better directional resolution than a buoy recording system. The line array avoids problems of the shoaling transformation of the frequency-directional spectra as it is roughly parallel to the depth contours. Accordingly, a 1-2-1 spacing line array of pressure sensors was used in this study. This array is not an optimal design for directional resolution, but it does offer redundancy for a reliability analysis.

The spectra of the various sensors in the array were compared on a routine basis. The results of the directional analysis of the several groupings of pressure sensors were compared to determine the stability of the array's response to the waves. In addition, the results of a surface-piercing staff were compared to that of a pressure sensor. The frequency spectra of current meters at depth were also compared to those of the pressure sensors. Some parameters of the frequency spectra were compared to visual observations made from the beach and from a 300-foot cliff overlooking the site.

II. WAVE CLIMATE DATA SYSTEM

1. Installation.

The study site was on South Range off Torrey Pines Beach. This is a straight section of the coastline approximately 3 kilometers north of Scripps Pier. The location of the site is shown in Figure II-1.

A shelf station equipped with radio telemetry link to a shore station was located on South Range at a depth of 10 meters. The shelf station has a transmission capacity of 15 data channels. A line array of bottom-mounted pressure sensors was employed that had a measured alinement of 13° east (clockwise) to that of the coastline which in this area runs true north-south (Figure II-1). The sensors had relative spacings of 1-2-1 with 30.5 meters as the unit spacing. Sensor 3 was located on the base of the shelf station. The shelf station was also equipped with accelerometers and at times with current meters, and a surface-piercing staff.

2. Data Acquisition.

Data for the wave climate was collected using a shelf station with a PCM (Pulse Code Modulation) radio telemetry link to the shore station, referred to as a Shelf and Shore (SAS) system (Lowe, Inman, and Brush, 1972). The primary wave sensors were four absolute pressure sensors (Statham Model PA506-33) deployed in a linear array roughly parallel to the coastline. The mean water depth at all sensors was 10 meters.

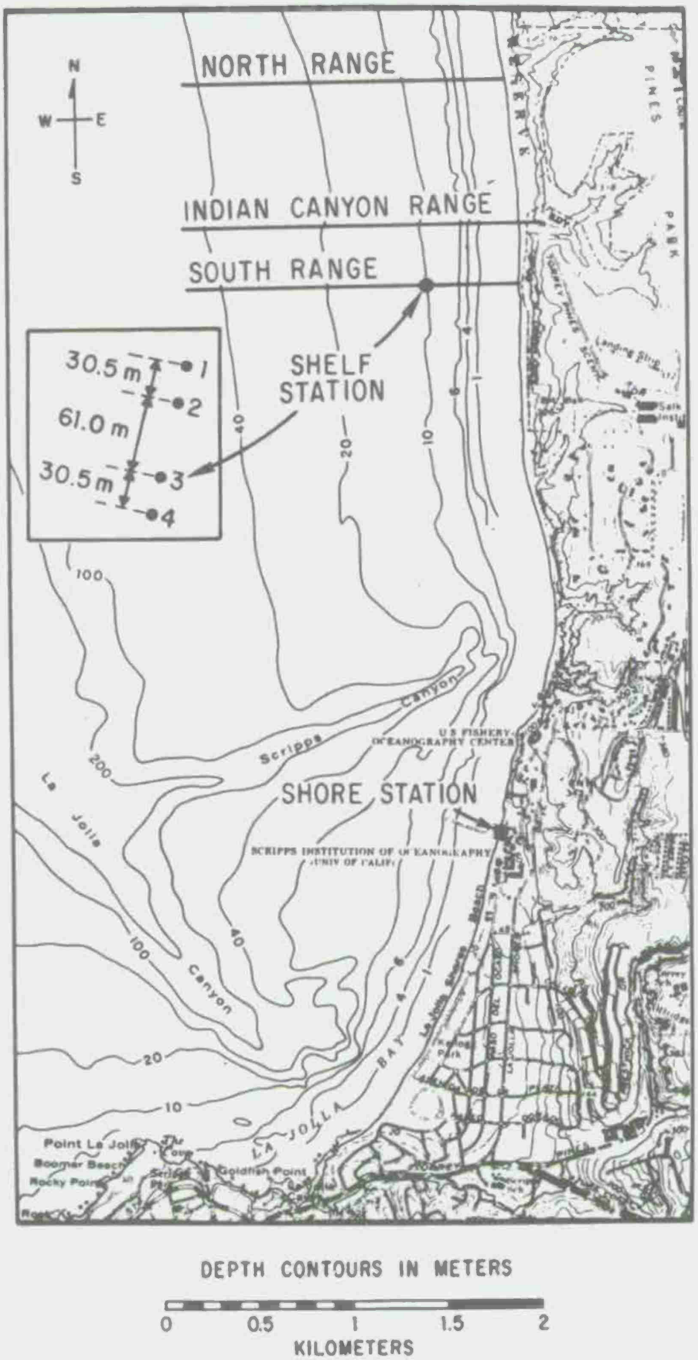

Figure II-1. The location of the shelf station and pressure-sensor array off Torrey Pines Beach, California.

The shelf station consists of an air-filled fiberglass spar having a 9 cm (3.5 inches) outside diameter. The spar section is coupled to an anchor assembly through a universal joint, so that the rigid spar is free to tilt in response to currents but not to rotate. A schematic diagram of the station complete with the pressure sensor array is shown in Figure II-2.

Signals from the pressure sensors pass through underwater cables, enter the glass spar through underwater bulkhead connectors, and finally pass up the center of the spar to the telemetry package in the top section of the spar. The signal conditioning and analog to digital conversion for each pressure sensor are performed in the telemetry package.

A timing circuit in the telemetry package controls the period during which data are gathered. This circuit is set to sample waves four times per day (0400, 1000, 1600 and 2200 hours PST). Each sampling period lasts for 1 hour. The data from each sensor are sampled 125 times per sec, each sample is converted to a 10-bit binary number and transmitted back to the shore station over a PCM telemetry radio link. The high sampling rate before transmission of the data is required to provide virtually simultaneous sampling of the data. At the shore station the data are received and processed by PCM synchronizing equipment. The data are filtered by a specially designed digital filter to eliminate digital noise due to transmission of the data. The cutoff frequency of this filter is approximately 10 Hz which will not affect the wave data being collected. The digital filter is part of the data communication system and contains, in addition to the digital filter, a small buffer memory. The memory is loaded with the data at the high rate of the communication system and unloaded at the slower rate of the digital magnetic tape, which for this study was four samples per second. The data in between the slower samples were not used in this study.

Each data channel is converted back to analog voltages and displayed on an oscillographic recorder, and recorded on IBM compatible magnetic tape. The analog record (Figure II-3) acts as a data quality monitor. Only 4,096 data points are recorded on the magnetic tape at four samples per second, producing one raw data file. The digital record represents only the first 17 minutes of the 1-hour sampling period. In retrospect, all of the data should have been recorded on digital tape. If the entire 1-hour sample were available, more sophisticated data analysis procedures could have been used to avoid some of the noise problems discussed later in this report.

3. <u>Data Processing</u>.

After the data has been recorded on magnetic tape, it is ready for processing on an 1130 IBM computer. A special data reduction system was devised which produces processed tapes, a printed output of the

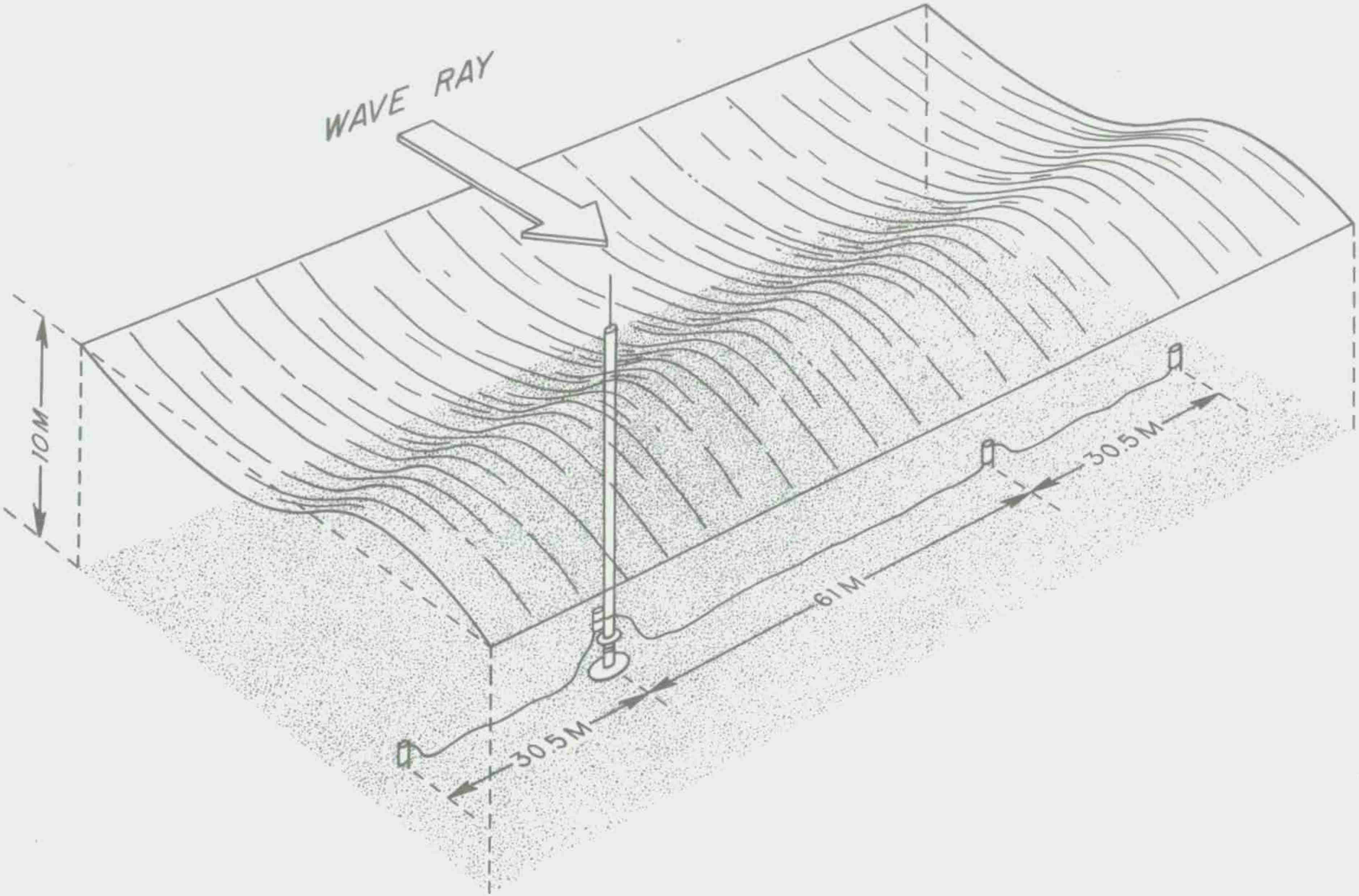

Figure II-2. Schematic of the shelf station and pressure sensor array.

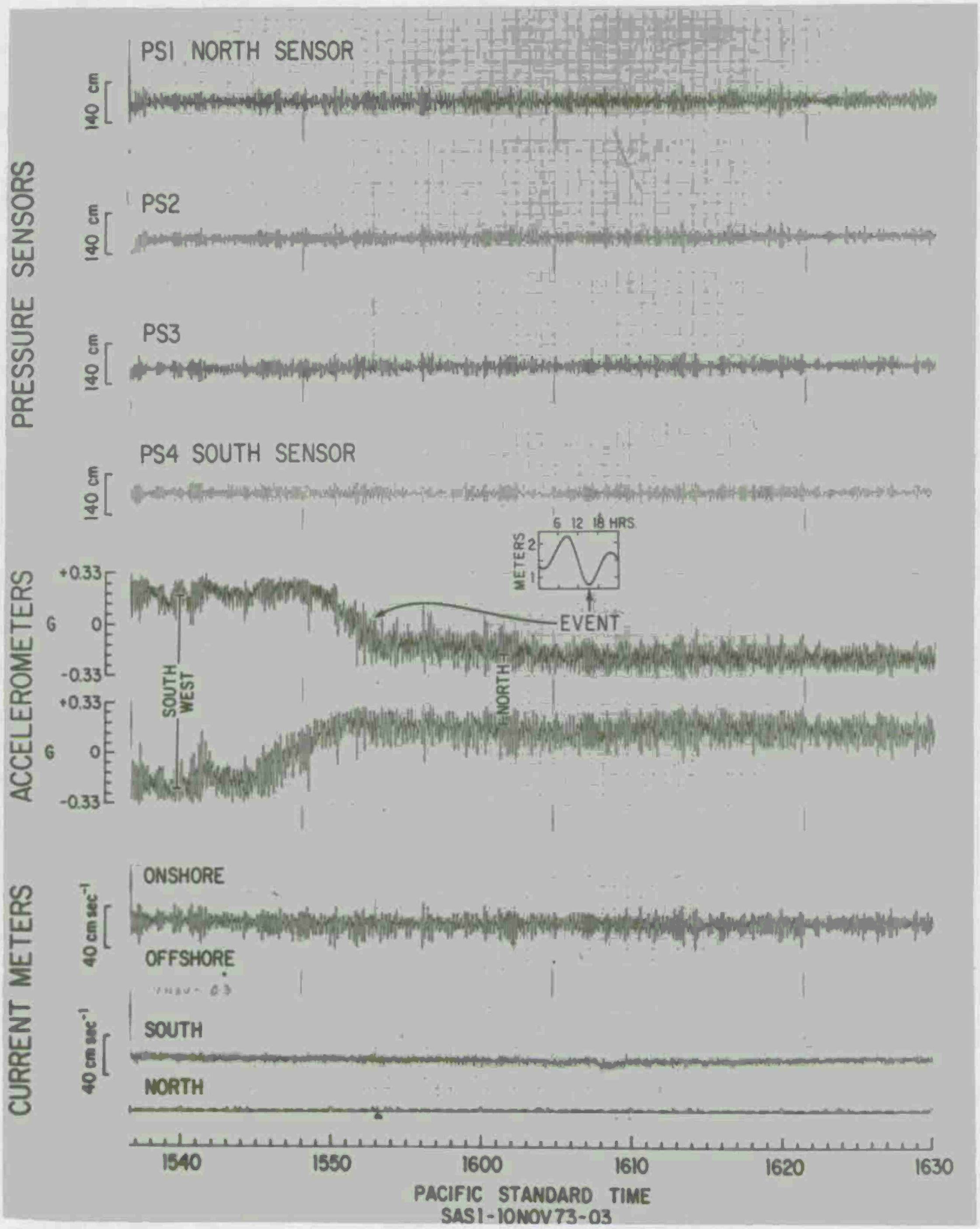

Figure II-3. Analog record from Torrey Pines Station. The top four traces are from the pressure-sensor array; the tilt of the station is indicated by accelerometer traces 5 and 6, and current near the base of the station is shown on traces 7 and 8. The occurrence of the change in tilt of the shelf station is referenced to local tide in the insert above traces 5 and 6.

statistics for each pressure sensor (including the mean, maximum, minimum, and standard deviation values) and a summary of the energy values of each pressure sensor.

The data reduction system reads and processes each specified magnetic tape data file from the raw data tape produced by the telemetry system. If magnetic tape or sequencing errors exist, the data run is aborted and the system resumes processing at the next specified file. The raw data of each channel of a run are then reformatted and calibrated. Next, a Fast Fourier Transform (Cooley and Tukey, 1965) is performed and cross-spectra of all combinations of the four pressure sensor channel pairs are calculated. The Fourier coefficients are multiplied by a depth correction coefficient up to a cutoff frequency of 0.25 Hz. The cross-spectral values allow phase and coherence to be calculated for each of the six possible channel pairs. These, together with the energy values, are used to calculate the directional spectra; first using all four sensors (1, 2, 3, 4), then for the two redundant three-sensor arrays (1, 2, 3 and 2, 3, 4). This procedure gives a degree of redundancy in the calculations which was desired by CERC. The Fourier coefficients are then squared and grouped by 11 to form the frequency spectra values. Grouping by 11 was desired for compatibility with CERC data. However, in light of the poor resolution in the lower frequency bands, grouping by a smaller number of bands would be desirable (e.g., band 6 includes wave periods ranging from 18.4 to 15.4 seconds). Considering the trade-off between frequency resolution and statistical reliability, we feel that grouping of eight is optimum for investigation of surface waves with this sample rate and record length. Finally, a program which selects spectral peaks in the frequency spectrum, gives their energy and bandwidth, and also sums the energy of the spectrum (up to 0.25 Hz), outputs this information for each pressure-sensor channel on the line printer. This printout is used in tabulating the tables for Appendixes A and B. The processed data tapes contained the following seven files for each SAS run (when all four sensors were functioning):

File 1. Identification information and contents list.

2. Reformatted and calibrated raw data time series for each channel (4,096 data points each).

3. Fifty spectral values (energy density) for each channel.

4. Fourier coefficients, consisting of 1,024 floating point numbers per channel (i.e., 512 real, 512 imaginary which give phase).

5. Directional spectra values for four-sensor array (181 real words giving values from 0° to ±90°).

6. Directional spectra values for three sensors (i.e., 1, 2, 3).

7. Directional spectra values for three sensors (i.e., 2, 3, 4).

For other purposes, such as analyzing current meter or accelerometer data, or any other time series recorded on one of the available channels, the individual programs used in the data reduction system were available to supplement any further programing. Plotter programs exist which plot frequency spectra for any pair of channels along with the phase and coherence between that pair. Directional spectra plots for either the pressure-sensor array method, or the current meter method can be obtained when desired.

4. Sensors.

The four-pressure-sensor array is the primary wave measuring instrument. These sensors are Statham Model PA506-33 absolute pressure transducers with accuracy of ±0.2%. These sensors are housed in a PVC container to protect them from the seawater. Pressure is coupled to the transducer through a flexible rubber diaphragm and a silicone oil bath. A photograph of this assembly is shown in Figure II-4.

Accelerometers are used to measure the tilt of the station as it responds to waves and currents. Appendix B describes dynamic response of the spar and provides the analysis procedure used to obtain tilt angle from the raw accelerometer data. A high quality servo-type accelerometer is used. These accelerometers are Donner Model 4311AS-2A. Accelerometer data were found to be a valuable indication of the wave direction as well as current speed and direction (Section V-6).

An electromagnetic current meter was used on occasion to measure currents near the base of the station. The current meter resolves the current vector into two orthogonal components. In all cases, the probe was positioned to measure horizontal velocity. The meter was manufactured by Marsh-McBirney (Model 711) and has a velocity threshold of 1 cm/sec, and 0.2 second time constant. A picture of the meter installed on the shelf station is shown in Figure II-5. Wave directional spectra obtained from current meter data are discussed in Section V-5.

Wave height measurements of the sea surface were to be made using a recently developed digital wave staff. The digital staff was 5 meters long with contact spacing of 0.5 cm. Although the digital wave staff functioned properly, it did not prove to be adaptable to the shelf station. The positive buoyancy of the station was not sufficient to hold the staff vertical during low tide. A detailed description of this wave staff is provided in Appendix C.

Figure II-4. A view of the disassembled pressure sensor showing the sensor and its PVC housing.

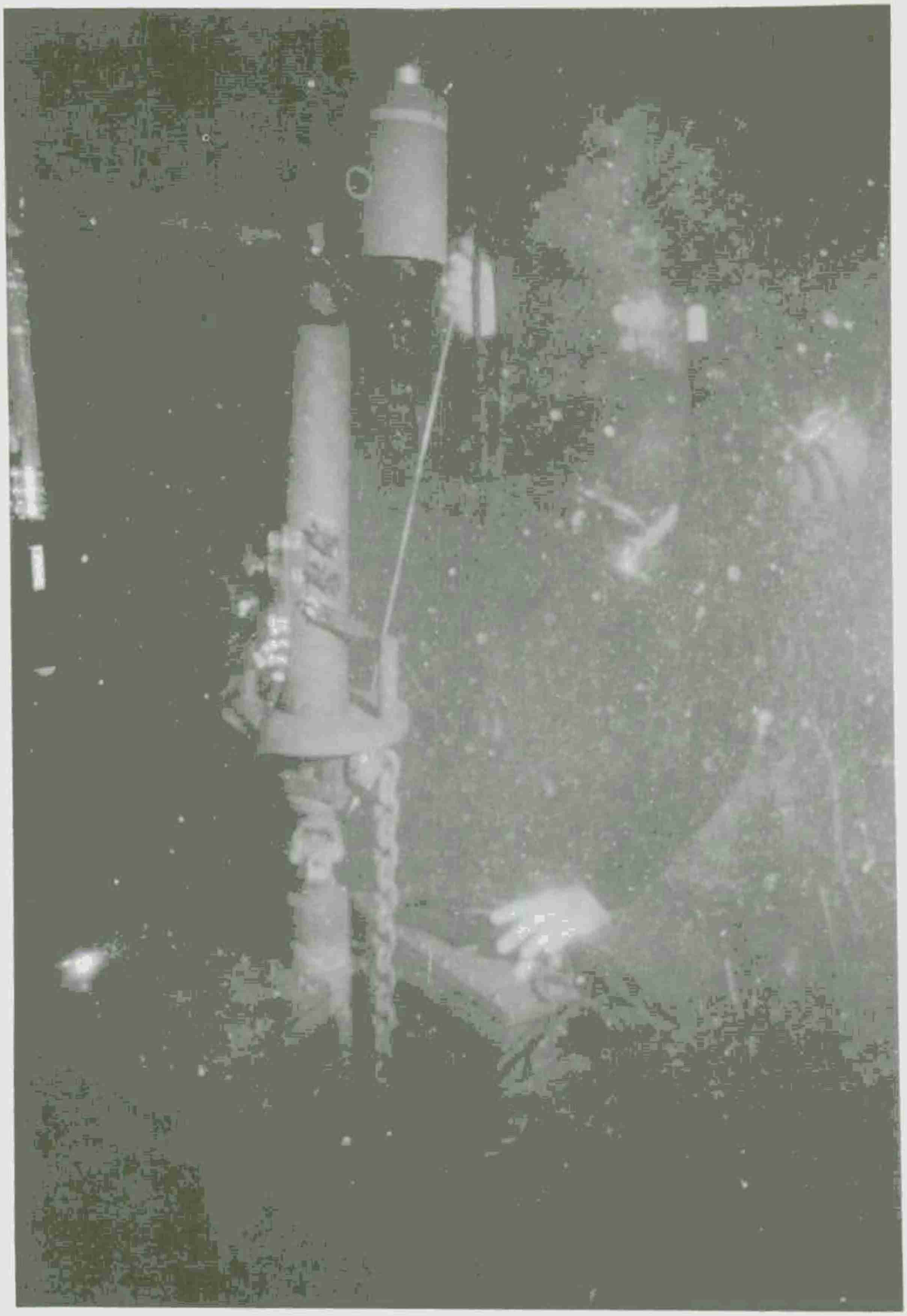

Figure II-5. Underwater photograph of the lower section of shelf station anchor assembly, universal joint, and electromagnetic current meter.

A resistive wire gage was constructed for use on Torrey Pines shelf station. This gage is similar to others developed at Scripps Institution of Oceanography and used for wave studies off the research vessel *FLIP*. This gage is also described in detail in Appendix C. Data obtained from the resistive wire gage were compared with the pressure gage mounted directly below the staff. Two sets of data were taken, one set with the station free to tilt, and one set with the station tethered. Comparisons of these data are reported in Section V-2.

5. Underwater Cables and Connectors.

The electrical cables used to connect the pressure sensor to the shelf station proved to be a major source of problems in the early phase of the study. The pressure sensors were tied to 1.5-inch steel pipes that were driven approximately 4 feet into the sand bottom. Neoprene-jacketed cables with four 16-gage conductors were used to carry power to the sensor and the return signal from the sensor. These cables were weighted by 16-pound shackles placed about 20 feet apart. The idea was that the cables would quickly bury in the sand, thus protecting them from the wave forces. However, it was found that high waves uncovered the cable and caused it to loosen from the weights. Once freed from the weights, the cables were carried back and forth in the wave surge. This constant motion would "workharden" the electrical conductors causing them to break. Several different cable-weighting techniques were tried, with little success. The final solution to the cable problem was to use four conductor armor cable. This cable consists of four wires individually insulated with polypropylene inside a two-layer, counterlaid, steel wire outer jacket. A steel pipe, 2 inches in diameter, was jetted approximately 6 feet into the sandy bottom near the base of the shelf and at the pressure sensor locations. The armor cable was strung between these pipes by scuba divers. Care was taken to ensure that the cable had no sharp bends.

Of course, armor cables are more expensive and more difficult to install than are neoprene-jacketed cables, but this factor is more than offset by the reliability of the armor cables.

Problems were experienced with underwater connectors in the early phase of this study. Originally, a flush-mounted, right-angle connector (510F) manufactured by Electro Oceanics was used at the base of the shelf station (Figure II-6). These connectors were found to be unsatisfactory because they are structurally weak and were easily loosened. Both of these connector problems caused seawater to enter the shelf station, thus shorting out unprotected wires. A redesign of the base of the station (Figure II-7) allowed stronger connectors (Electro Oceanics 53E) with an improved "O" ring seal to be used. This new design completely eliminated the connector problems.

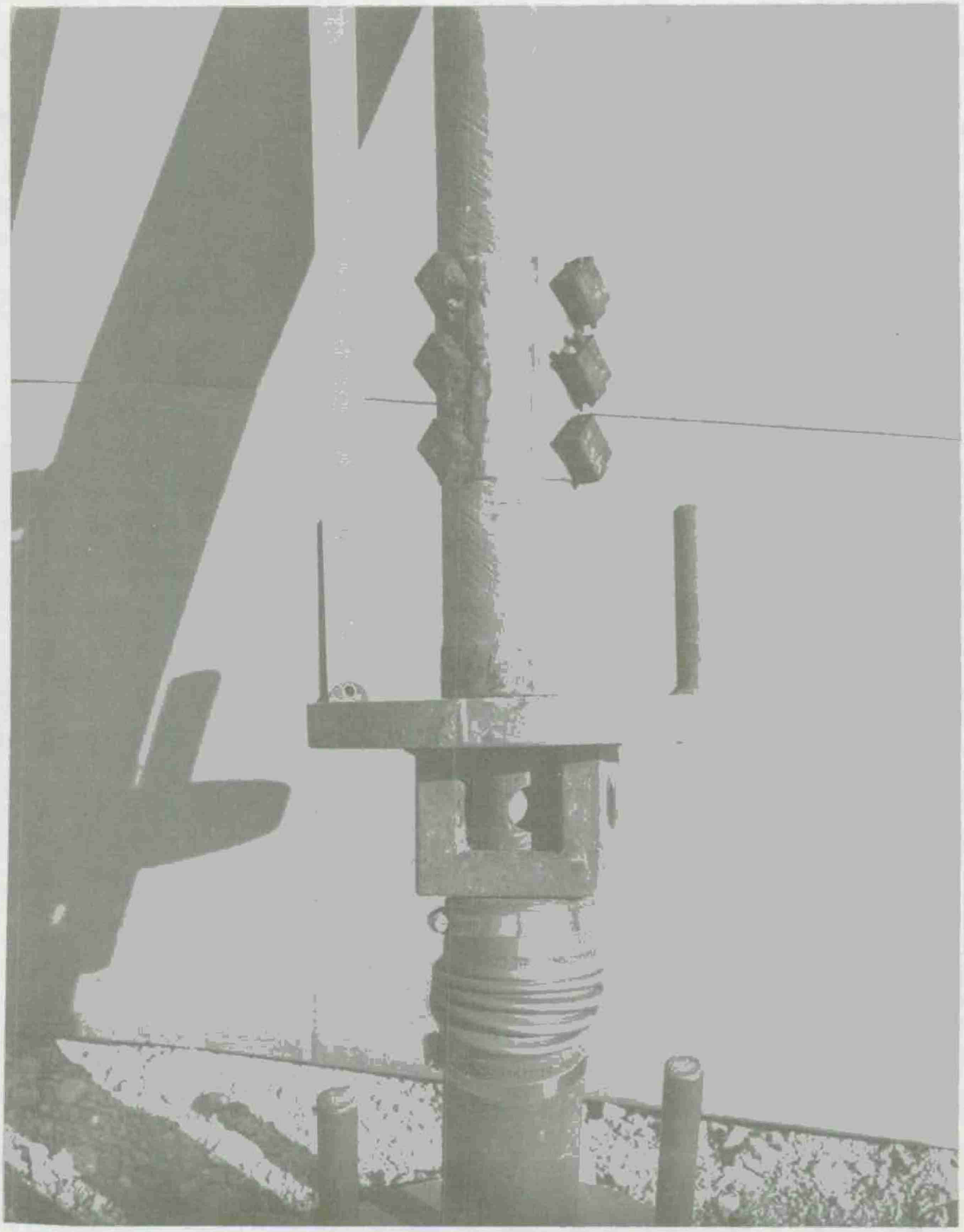

Figure II-6. Detail of the bottom section of the original shelf station showing the right-angle underwater connectors. The scale is in centimeters.

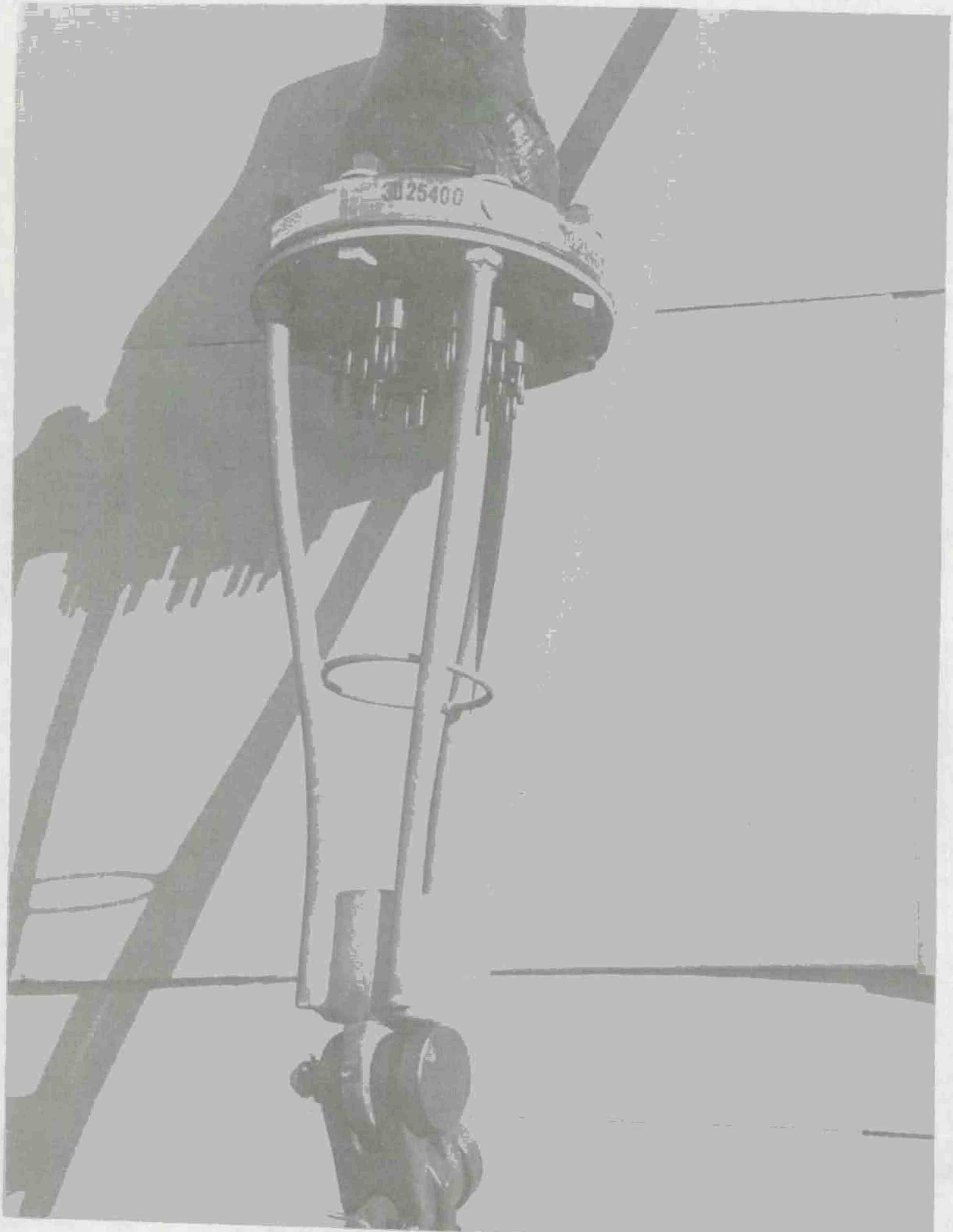

Figure II-7. Detail of the redesigned bottom section showing the improved connectors. The scale is in centimeters.

6. Field Operation of System.

The performance of the system used to obtain wave climate has been evaluated for the 16-month period from 5 February 73 to 31 May 74. A total of 1,130 data runs was collected during this period, or approximately 59 percent of the scheduled runs (i.e., four per day). Of the 1,130 runs, 71 percent was with all four pressure sensors working, 25 percent with three sensors working, and 5 percent with two sensors functioning. The efficiency of the data collection system increased after several hardware improvements were made. During the period of February to May 1974, which followed the system improvements, 76 percent of the data runs was recorded, of which 80 percent had all 4 pressure sensors properly functioning. Forty-three percent of the data loss was due to structural failure of the fiberglass spars. There were two such occurrences which account for over one-third of the lost data. Both these events were structural failure of the fiberglass spars which required replacement of the entire shelf station. Close inspection revealed that the resin had fatigued causing the spar to develop pinhole leaks at the point of maximum bending stress. The first failure occurred on 18 April 73, and the second occurred on 14 November 73. After the first failure, the system was down for 1 month; the second time for 2½ weeks.

Other major causes of loss of data were problems with the telemetry package which accounted for 14 percent of the data loss, 13 percent of data loss was due to faulty cables and connectors, and 13 percent as a result of problems with the recording system. The remaining data loss was due to a number of minor causes, such occurrences as low batteries combined with long periods of bad weather preventing their replacement; storm waves breaking over the station interrupting data transmission; and component failures in the receiving system.

With the exception of failures due to fatigue, the SAS system has proved to be a very reliable system. With the experience and improvement of the system components, we are convinced that the system's major failure modes have been overcome. This has been proven to some extent by the successful operation of the system during the winter months of 1974 when 74 percent of the anticipated runs were recorded. It is important to note that the shelf station as a system remained intact and on station even during several storms when waves were breaking over the station in 10 meters of water.

III. ARRAY THEORY

An ocean wave field is composed of waves of various frequency, amplitude and direction of propagation. The total energy per unit surface area of the wave field, E, is related to the sea surface displacement η, by the relation:

$$E = \rho g \langle \eta^2 \rangle \qquad \text{(III-1)}$$

where ρ is the water density, g is the acceleration of gravity, and $\langle\eta^2\rangle$ is the variance of the time series of η, which gives the mean-square elevation of the water surface due to waves. Spectral analysis is a determination of how $\langle\eta^2\rangle$ is distributed with respect to wave frequency and direction. The frequency spectrum, S(f), is energy density as a function of wave frequency, in units of cm^2 per Δf, where Δf is the frequency bandwidth. The area under the frequency spectrum equals the variance of the sea surface displacement,

$$\langle\eta^2\rangle = \int_0^\infty S(f)\, df \,, \tag{III-2}$$

where S(f) is the Fourier transform of the autocovariance function

$$R_{11}(\tau) = \langle\eta_1(t) \cdot \eta_1(t + \tau)\rangle \,, \tag{III-3}$$

so that

$$S(f) = 2\int_{-\infty}^{\infty} R_{11}(\tau)\, e^{-2\pi i f \tau}\, d\tau \,, \tag{III-4}$$

where τ is a timelag, $i = \sqrt{-1}$, and $\eta_j(t)$ is a time series of sea surface displacements as measured by the sensor labeled j. The subscripts j, k of the function $R_{jk}(\tau)$ reference the sensors that were sampled for the data used in the computation of $\langle\eta_j(t)\, \eta_k(t + \tau)\rangle$. In general, R_{jk} is termed the covariance function and is referred to as the autocovariance function when $j = k$. The autocovariance function has the units of cm^2, which is proportional to energy, and it preserves the frequency structure inherent in the original time series.

The analysis of wave direction requires more than one blind sensor. Assuming that the waves are known to approach within a 180° arc, the direction of a single wave train can be determined from the relative arrival time of a wave crest at two blind sensors. The phase difference between the signals of two sensors expressed in radians is related to the direction of the wave train by the equation:

$$\phi = 2\pi \frac{\ell}{L} \sin\alpha \,, \tag{III-5}$$

where $\ell < L/2$ is the distance between the sensors, α is the angle of the wave's approach relative to the normal to a line separating the sensors, and L is the wavelength. The phase difference of the wave signals of two sensors as a function of frequency is obtained from the frequency cross-spectrum. The frequency cross-spectrum, $C_{12}(f) - iQ_{12}(f)$, between two sensors is defined as the Fourier transform of their covariance function,

$$C_{12}(f) - iQ_{12}(f) = \int_{-\infty}^{\infty} R_{12}(\tau)\, e^{-2\pi i f\tau}\, d\tau, \qquad \text{(III-6)}$$

where

$$R_{12}(\tau) = \langle \eta_1(t) \cdot \eta_2(t + \tau) \rangle \qquad \text{(III-7)}$$

and the subscripts reference the sensors.

If the wave field is made up of a single wave train, then

$\eta_1 = \sqrt{2A_o} \cos 2\pi ft$ and $\eta_2 = \sqrt{2A_o} \cos(2\pi ft + \phi)$, where $A_o = \langle \eta^2 \rangle$.

The cross-spectrum is then

$$C_{12} = A_o \cos\phi, \qquad \text{(III-8)}$$

and

$$Q_{12} = A_o \sin\phi, \qquad \text{(III-9)}$$

where

$$\phi = 2\pi \frac{\ell}{L} \sin\alpha = \tan^{-1}(Q_{12}/C_{12}).$$

Thus, the phase is related to the relative sizes of the real and imaginary parts of the cross-spectrum.

Equations (III-8) and (III-9) show that the cross-spectrum varies sinusoidally with the separation distance of the sensors. The frequency of this variation is $k \sin\alpha$, where $k = 1/L$ is the magnitude of the wave number and is fixed by the frequency of the waves by the dispersion relation,

$$(2\pi f)^2 = gk \tanh(2\pi kh) ,$$

where h is the depth. If the cross-spectrum is known for all separation distances in the two orthogonal horizontal directions x and y, then the complex function $C(X, Y, f) - iQ(X, Y, f)$ may be defined as a continuous function analogous to the frequency cross-spectrum given in equation (III-6). $C(X, Y, f) - iQ(X, Y, f)$ is the directional cross-spectrum and is defined by its relation to $\eta(x, y, t)$:

$$C(X, Y, f) - iQ(X, Y, f) = \int_{-\infty}^{\infty} R(X, Y, \tau)\, e^{-2\pi i f\tau} d\tau , \qquad \text{(III-10)}$$

where

$$R(X, Y, \tau) = \langle\eta(x, y, t)\ \eta(x + X, y + Y, t + \tau)\rangle ,$$

and X and Y are horizontal component lags. The Fourier transform of $C(X, Y, f) - iQ(X, Y, f)$ over X and Y space yields $S(f, \alpha)$, the frequency-directional spectrum:

$$S(f, \alpha) = \int_{-\infty}^{\infty}\int_{-\infty}^{\infty} \left[C(X,Y,f) - iQ(X,Y,f)\right] e^{-2\pi i(kX \sin\alpha + kY \cos\alpha)} dXdY. \qquad \text{(III-11)}$$

The frequency-directional spectrum is the energy density as a function of wave frequency and direction, and has units of $cm^2/\Delta f\Delta\alpha$, where $\Delta\alpha$ is the directional bandwidth.

In reality the cross-spectrum is known only for the separations of the finite number of sensors in the array. For the linear 1-2-1 array with a unit spacing of ℓ_0 equal to 30.5 meters the separations $X = 0$, ±1, ±2, ±3 and ±4 are known, and there are no Y separations. The equation for $S(f,\alpha)$ reduces to the summation:

$$S(f, \alpha) = C(X = 0, f) + 2 \sum_{n=1}^{4} \Big[C(X = \ell_o n, f) \cos(2\pi nk \sin\alpha)$$

$$+ Q(X = \ell_o n, f) \sin(2\pi nk \sin\alpha) \Big], \qquad \text{(III-12)}$$

where $n = 1, 2, \ldots$ are the number of unit spacings, ℓ_o in the array.

Equation (III-12) was used for the calculation of the frequency-directional spectra. The cross-spectra were calculated using the Fast Fourier Transform (FFT) method (Bendat and Piersol, 1971). The outline of how equation (III-11) reduces to equation (III-12) and a more detailed development of spectral theory in general are included in Appendix A.

The approximation of $S(f,\alpha)$ through the use of the summation in equation (III-12) rather than the integral in its definition, equation (III-11), leads to problems of "aliasing" and poor resolution. The spectral analysis problems in the frequency domain are analogous but less severe. Therefore, only inadequacies of the spatial transformation are discussed.

The finite total length of the array introduces a smearing of the directional spectra estimates leading to a lack of resolution in direction. This poor resolution is analogous to the spreading of light through a diffracting slit. The wave analogy to this application of the uncertainty principal (Dicke and Wittke, 1960) states that a wave packet with a finite width will have an uncertainty in wave number. Our finite array forces us to assume a finite width of the wave packet which leads to uncertainty in wave number, and thus in the direction as well.

This effect can be seen by using a cross-spectrum calculated for a single wave train in the summation of equation (III-12) for the estimation of $S(f,\alpha)$. The estimated $\hat{S}(f,\alpha)$ will have a spread in direction and is termed the array's response to a single wave train. The 1-2-1 array's response to 14 second waves propagating at normal incidence to the array is shown in Figure III-1.

The knowledge of the covariance function at discrete points in space, rather than in a continuous line, leads to the problem of aliasing or the confusion of wave directions. An inappropriately designed array will respond to waves from a particular direction with several peaks in its directional spectrum. All but the true peak are referred to as aliased spectral peaks. This problem can be easily seen for the case of only two sensors. Equation (III-5) does not have

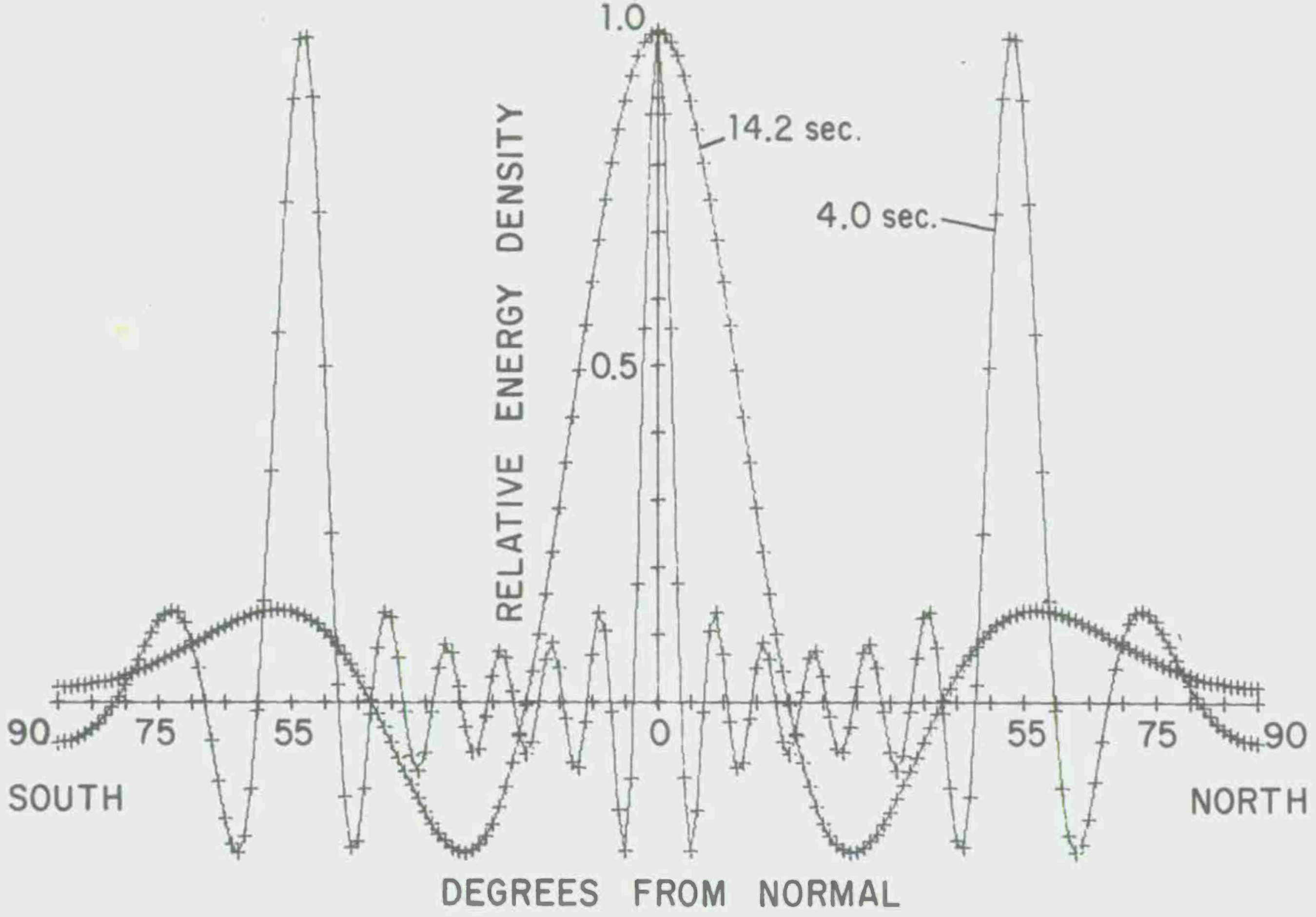

Figure III-1. The directional response of the 1-2-1 linear array for waves with periods of 4.0 and 14.2 seconds approaching from 0°. The wide peak for the 14.2-second wave results from smearing due to the finite length of the array. The two "aliased" peaks at ± 54° for the 4-second wave are caused by the discrete spacing for which $L < 2\ell_o$. This response function is referred to as a Barber Window and is obtained through equal weighting of the cross-spectral information.

an unique solution for α given ϕ, ℓ, and L if the wavelength L is not greater than 2ℓ. As an example, if $\ell = 3/2L$ and the phase equals 0, then equation (III-5) gives:

$$\phi = 0 = 3\pi \sin\alpha = n2\pi , \qquad \text{(III-13)}$$

where n is an integer. This equation can be satisfied with $\alpha = 0$ and $\pm 41.8°$.

This problem becomes quite severe for higher frequency waves whose wavelength is short relative to the smallest sensor spacing of the array. A more mathematical treatment of the techniques of array analysis, and these analysis problems, is included as Appendix A.

It is apparent that while a long total length of array is desired, a small spacing between any two adjacent sensors is also necessary. With a maximum spacing specified for any two adjacent sensors, and a finite number of sensors, a line array will obviously give the maximum possible length of sensor arrangement, and hence the maximum resolution in direction. However, a line array has a 180° ambiguity in direction. The coast is effective in eliminating possible sources from two quadrants, providing wave reflection can be neglected.

With a set number of wave sensors, the size of the spacings desired is dependent upon the length of the waves of interest. For example, an array with large spacings that gives good resolution for long waves will seriously alias the spectra of the higher frequency waves. A good display of an array's performance with respect to waves of a particular frequency is the directional response function. This is the response of the array, in energy density versus direction, to waves of a single direction. Figure III-1 displays the response of the 1-2-1 line array, with 30.5-meter unit spacing, to 14.2 and 4-second waves approaching the array from 0° from the normal to the array. While there is better central peak resolution of the 4-second waves, two alias peaks are also present. The array is best designed for waves of a period around 5.5 sec. That is, this is the period of waves for which the array has the best resolution while still having no serious aliasing problems. The response of the array to 4.7-second waves is plotted in Figure III-2. Aliasing is a serious problem for wave periods less than 4.5 sec (Section V-7). Although a longer array would have been desirable for the investigation of waves with periods of 10 to 18 sec, the total length used, 122 meters, appeared to be a practical limit considering problems of cable maintenance, continuity in bathymetry, and coherence of the wave field.

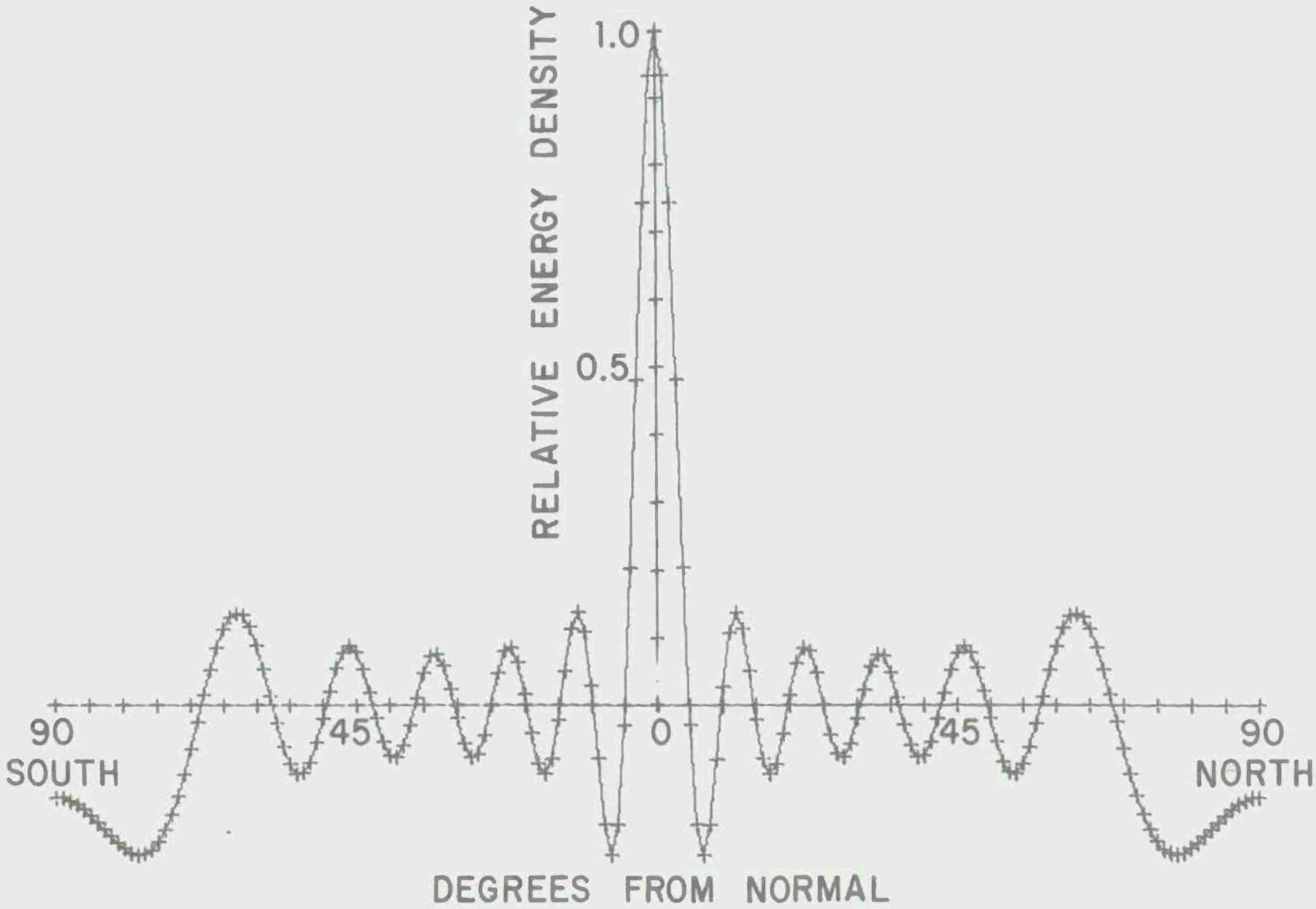

Figure III-2. The directional response of the 1-2-1 array to normally incident waves of period 4.7 seconds. This response function was obtained using a Barber Window, i.e., equal weighting of the cross-spectral information.

IV. CHARACTERISTIC PARAMETERS FOR WAVE SPECTRA

The wave field at any particular time may be complex and include components that differ in their place and circumstances of origin. These wave components can usually be identified as relative peaks in the frequency spectrum. In an effort to specify the principal wave components, the dominant peaks of the measured frequency spectra were routinely identified. The spectral peaks are characterized by three parameters: (1) peak frequency f_o; (2) bandwidth Δf; and (3) energy E_p. The center frequency of the frequency band with the greatest energy density is designated the peak frequency. The cutoff frequency band for a peak is defined as the frequency band of minimum energy density between two adjacent peaks or the frequency band in which the energy density equals approximately 10^{-2} of the energy at the peak frequency if there is no adjacent peak. The energy density in the cutoff frequency band between adjacent peaks is used in the determination of the energy of the peak with the lower frequency. The details of the peak selection procedure are included in Appendix A. A tabular display of the characteristic parameters evaluated for the data runs of this project is included as Appendix D.

Three directional parameters were developed to characterize the directional spectra. The directional parameters resulted from a comparison of the measured directional spectra with model directional spectra computed with the assumption of a single direction of wave propagation. This technique was used by Munk, et al. (1963) in observations of long-period swell. The model spectra were least-squares fit to the measured spectra, the variables of the fit being the energy and direction of the single wave train. The parameter α_o is the direction of propagation of the single wave train model which best fits the measured directional spectrum. With well directed swell this angle will approximately equal the direction of maximum spectral density. The parameter $P(\alpha_o)$ is an indication of goodness of fit and is essential for the interpretation of α_o . $P(\alpha_o)$ is related to the residual of the least-squares fit:

$$P(\alpha_o) = \frac{\sum_{\alpha=-90}^{90} \left[S(f_o,\alpha) - \hat{S}_{\alpha_o}(f_o,\alpha)\right]^2}{\sum_{\alpha=-90}^{90} \left[S(f_o,\alpha)\right]^2}, \qquad \text{(IV-1)}$$

where $S(f_o,\alpha)$ is the measured directional spectrum for the frequency band centered on f_o, and $\hat{S}_{\alpha_o}(f_o,\alpha)$ is the model directional spectrum. The summation was routinely computed for steps of 5° from $\alpha = 90°$ north to $\alpha = 90°$ south. For a mean value of $S(f_o,\alpha) - \hat{S}_{\alpha_o}(f_o,\alpha)$ around $10^{-2}S(f_o,\alpha)$, $P(\alpha_o)$ would equal 4×10^{-3}. Values as low as 1×10^{-3} have been recorded which imply a very narrow directional spectrum. Values of $P(\alpha_o)$ below about 10^{-1} are considered to be good fits and indicate the directional spectrum is unimodal and narrow. Figure IV-1 is a plot of the measured directional spectrum for 16.8-second waves versus the residual directional spectrum, $S(f_o,\alpha) - \hat{S}_{\alpha_o}(f_o,\alpha)$, for the run SAS-1-21 July 73-04. $P(\alpha_o)$ was 2×10^{-3} for this fit, indicating a good fit. Figure IV-2 is a plot of the measured and residual directional spectra for the 6.9-sec waves of SAS-1-21 July 73-04. The residual spectrum shows definite peaks indicating the multidirectional character of the incoming waves. $P(\alpha_o)$ for this fit was 0.5, which is considered to be a poor fit.

There is an uncertainty in direction of best fit, α_o, when $P(\alpha_o)$ is a slowly varying function of the trial values of α_o. The spread in trial values of α_o for which $P(\alpha_o)$ is approximately the same is defined as the parameter $\Delta\alpha_o$. $\Delta\alpha_o$ has typical values ranging from ±1° to ±4°.

The spectral parameters are useful in the identification and characterization of waves from the various source regions. They may also be used as direct input into computational models. The practical validity of representing the spectra by the peak frequency, the total energy in the peak, and the mean direction in calculation of longshore wave power available for transport of sand was shown by Inman, Komar, and Bowen (1969) and Komar and Inman (1970).

V. COMPARISONS OF VARIOUS METHODS AND TECHNIQUES

1. Comparisons Among the Various Pressure Sensors.

The records of the various pressure sensors in the linear array were systematically compared to evaluate the stability of the measurement process. Wave by wave comparisons were deemed to be unrealistic because of the short crestedness of waves; further, the comparisons of the frequency spectra computed for the several pressure sensors yield easily interpretable results.

The total energy for each of the four sensors, their average, and the range about this average have been computed for the SAS runs analyzed, and included in Appendix E. The "total" energy included data ranging from 0.0 to 0.25 Hz. From a sample of 587 runs it was determined that 68 percent of the time the total range of the energy values was less than 20 percent of the mean. The total range was less than 30 percent of the mean for 90 percent of the runs. For 2 percent of the runs, the range of the energy values was greater than 50 percent of mean.

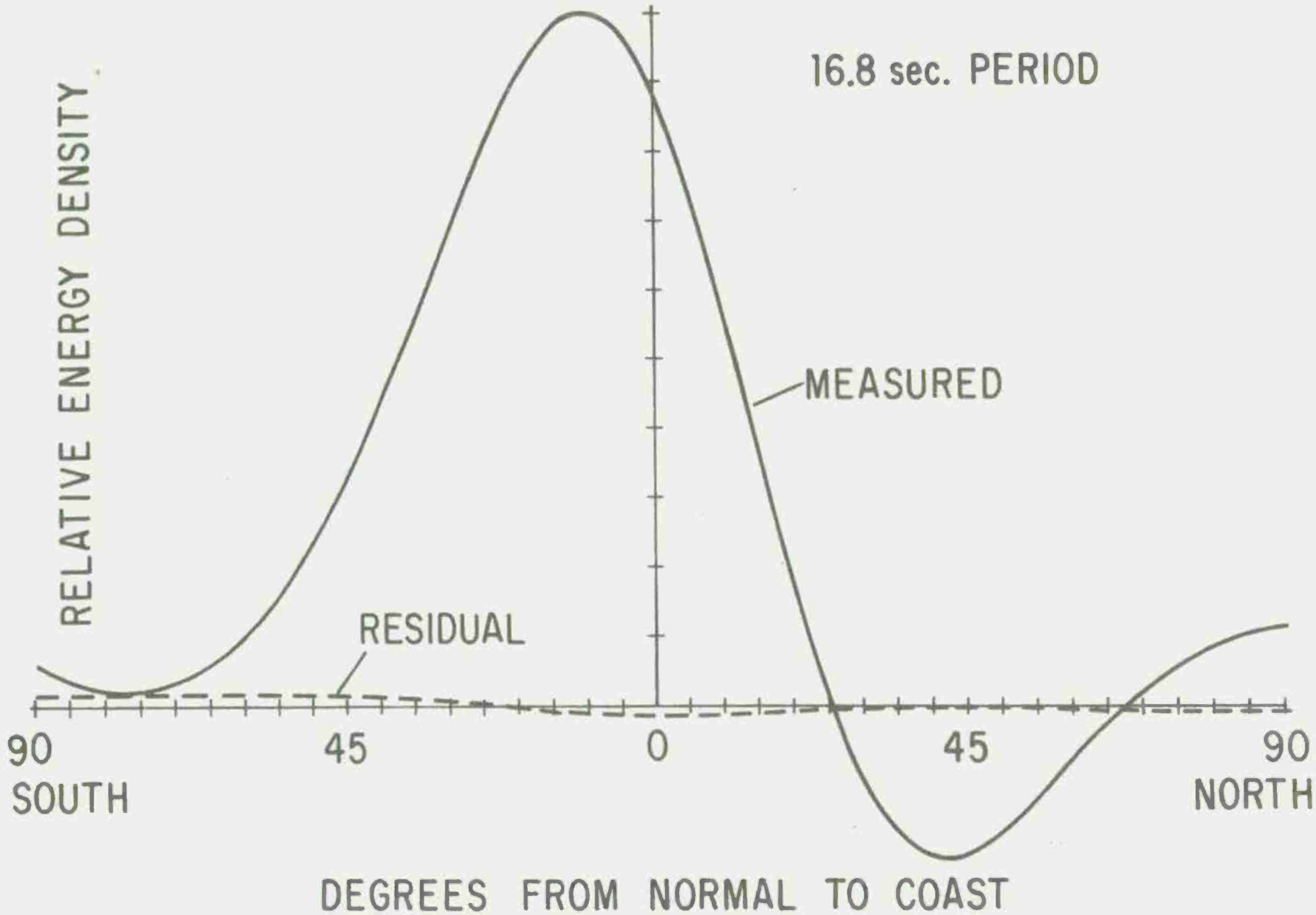

Figure IV-1. The measured directional spectrum and residual spectrum for southern swell of SAS 1-21, Jul 73-04. The residual spectrum is the difference between the measured and single direction model spectra. The fact that the residual spectrum is very small relative to the measured spectrum indicates the waves are approximately unidirectional.

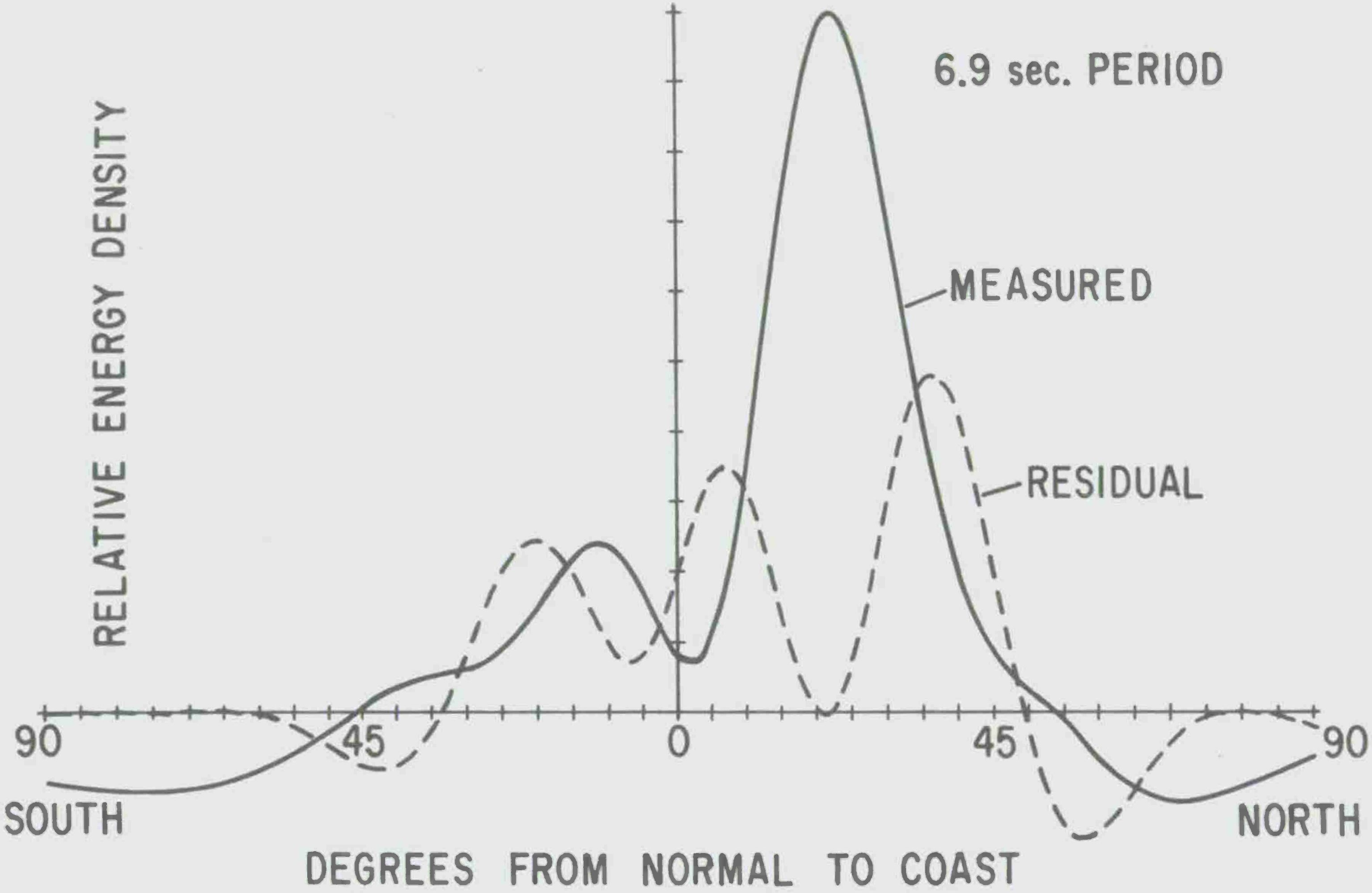

Figure IV-2. The measured and residual spectra for northern waves of SAS 1-21, Jul 73-04. The bimodality and broadness of the measured spectrum are reflected in the peaks of the residual spectrum.

The sum energies recorded by each of the four sensors over two periods of extended four sensor operation were computed. The results are listed below:

	Sum Energy cm^2			
60 Runs	Sensor 1	Sensor 2	Sensor 3	Sensor 4
29 Jan 74-31 Mar 74	49,649	50,061	47,853	46,456
24 Runs				
16 May 73-22 July 73	8,447	8,980	8,588	7,999

The range in the sum energies for the 60 runs in 1974 was 7.4 percent. Although this indicates some systematic difference in the energy levels of the various sensors, this range is small relative to the average range of energy levels over these runs, which was 15 percent. The range in the sum energies for the 24 runs in 1973 was 20.7 percent. The systematic difference in the energy levels of the sensors may be explained in part by the slight angle that the array makes with the bottom contours. This orientation has sensor 1 in the shallowest water; therefore, this sensor should see a slightly more shoaled version of the spectrum. The mean pressure difference between sensors 1 and 4 is equivalent to 0.6 meter of water.

A band by band comparison was made for the spectra of the four sensors for 27 SAS runs. The mean range of energy density values was calculated for the first 24 frequency bands, 0.0 Hz - 0.25 Hz. The range in the total energy of the first 24 bands, and the energy of the dominant spectral peak were also calculated for each of the SAS runs. There was some inconsistency in the selection of bandwidths of peaks in the records of the various sensors by the computer procedure. Therefore, the peak energy values were recalculated by visual inspection of the spectra. The results of these sensor comparisons are summarized in Appendix F, Table F-1. The mean range of energy density values of the four sensors over all the runs, 63.8 percent, was significantly higher than the mean of the ranges of total energy, 20.4 percent. This suggests that the sensors are measuring somewhat independent samples of a stochastic process. Since this is not a wholly deterministic process, the variance is to be expected. The estimate of the total energy has more degrees of freedom than the individual band estimate. However, the estimates of the energy contained in the dominant spectral peak appear to agree better than those for the total energy. The mean range of the peak energies for the 27 runs was 12.1 percent. This implies the waves of the dominant peak are more deterministic in their nature.

The runs which display a very large range in the total energy (>35%) as measured by the four sensors are affected by noise problems. Figure V-1 displays the more infrequent disparity in energy of the lower frequency bands. This may be caused by the "turn-on" transients of the pressure sensors and will only significantly affect the comparability of the total energy among the sensors when the wave energy is very low. The more common problem of variability of the high frequency region of the spectra is pictured in Figure V-2. This problem is due to noise in the system which in the more severe cases manifests itself in the form of data "dropouts." These dropouts are of sufficient length that no simple quality control measures could accurately recover the unaltered spectra. In 90 percent of the runs where the total range of the energy levels vary by more than 50 percent of the mean, most of the variation is in one sensor. The cause of these very high variations is an erratic sensor whose record is marred with dropouts.

Various groupings of 3 of the 4 sensors of the array have been used to calculate directional spectra. For example, the sensor groupings 1, 2, 3 and 2, 3, 4 represent redundant 1-2 spacing arrays. The direction of best fit to a single direction of propagation, α_0, defined in Section III, was calculated for the directional spectra of each 3 sensor grouping. The results are included as Appendix G. The directions obtained for the lower frequency peaks agree well in general. A sample of 103 runs was selected which included runs from each of the seasons. For 90.7 percent of these runs, the range in α_0 for the dominant spectral peak was 3° or less. The maximum range in the values of α_0 was 7°. The range in α_0 was not well correlated with the range of total energy of the various sensors. Therefore, even though the range in total energy of the sensors indicates a possibility of nonstationarity in the wave field, it is not reflected in the directional estimates.

2. Surface-Piercing Staff Versus Pressure Sensors.

Measurement of the wave field by use of pressure sensors at depth requires that a rigorous relationship between the surface height and vertical pressure field be known. Linear wave theory has been assumed to relate the pressure signal at depth to the surface elevation. To validate the use of bottom-mounted pressure sensors for the measurement of sea surface elevations, a comparison was made of simultaneous records of a surface-piercing staff and a pressure sensor at depth. A continuous wire staff was designed which resembled other staffs developed at Scripps Institution of Oceanography. The staff is described in detail in Section II and Appendix C of this report.

Linear wave theory yields a solution which has a wave-induced pressure which decreases with depth as a function of its frequency. The pressure at distance z' from the bed of waves of frequency f is given as:

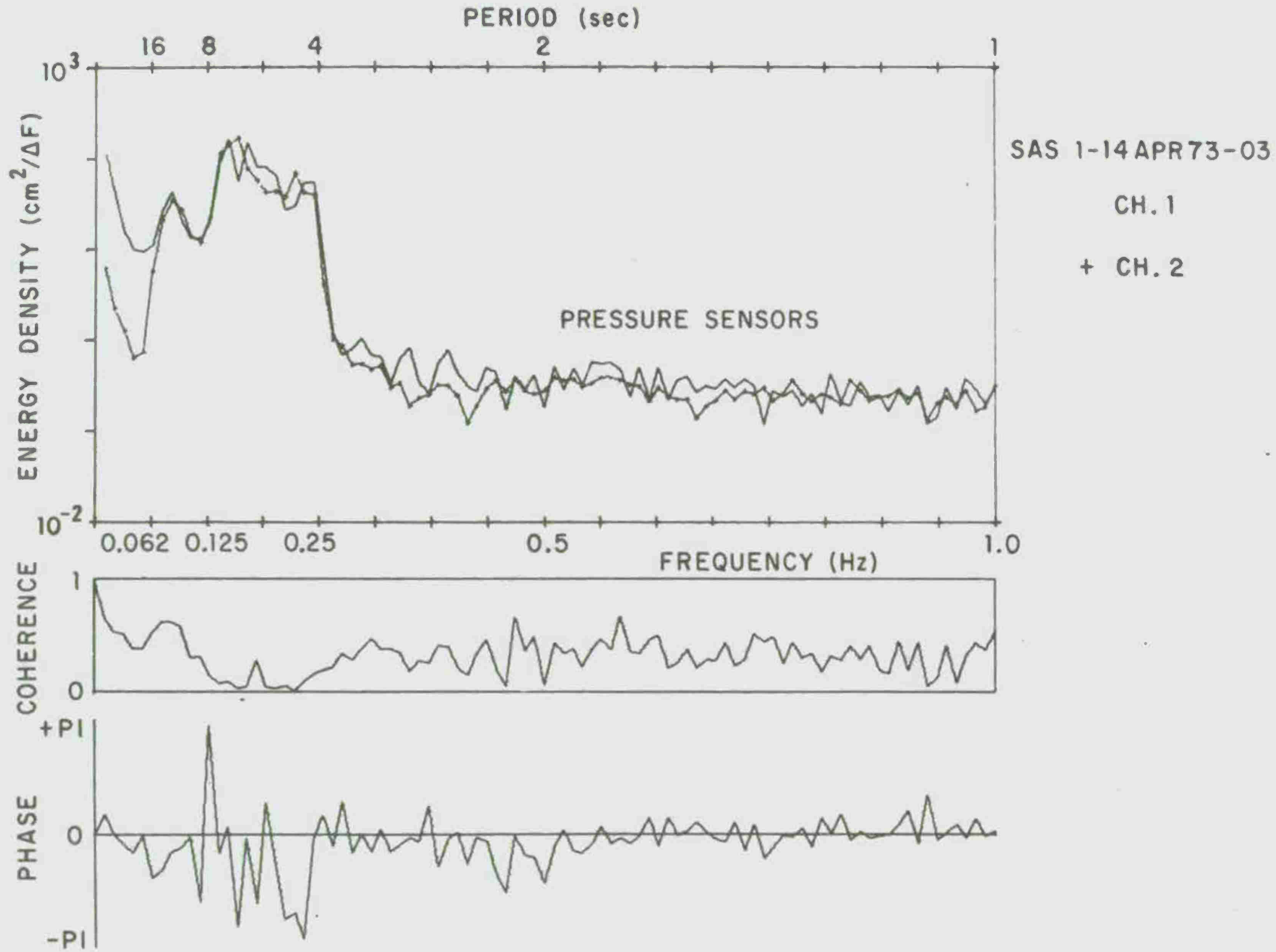

Figure V-1. Frequency spectra and the cross-spectral results for sensors 1 and 2 showing a large discrepancy in the energy density levels of the low frequency bands.

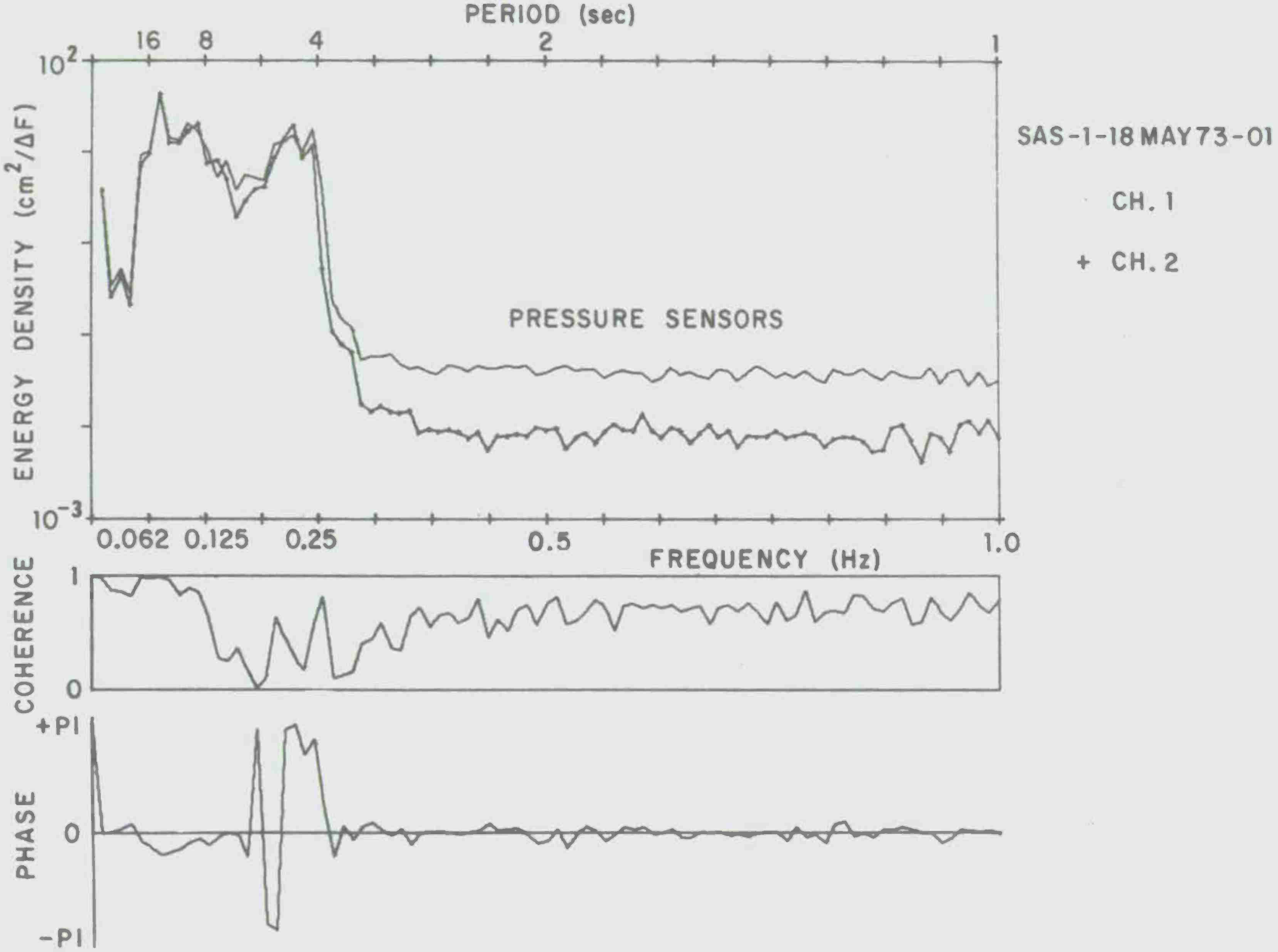

Figure V-2. Frequency spectra and the cross-spectral results for sensors 1 and 2 displaying a large discrepancy in the energy density levels of the high frequency part of the spectrum.

$$p(h,k) = p_o \frac{\cosh(kz')}{\cosh(kh)} \qquad \text{(V-1)}$$

where $p_o = gH/2$ is the pressure fluctuation due to sinusoidal waves of height H at $z = 0$, k is the absolute value of the wave number, and h is the depth of the water column. The frequency spectra of the pressure records may be corrected to account for this filtering by the water column. The correction factor becomes exponentially larger for increasing frequency. Therefore, it is necessary to cutoff the correction beyond a frequency to avoid bringing the noise region of the spectrum up to the signal level. To determine where to fix the cutoff point, several spectra were corrected for depth out to 0.5 Hz. A high frequency trough (Figure V-3), at approximately 0.25 Hz to 0.3 Hz, appeared beyond which the increasing correction factor dominated the measured spectral trends. Therefore, the frequency 0.25 Hz was selected as the correction cutoff for these pressure sensors located at a mean depth of 10 meters. The frequency spectra were uncorrected for frequencies higher than 0.25 Hz.

A prototype of the continuous wire staff was tested off the end of Scripps Pier. The staff was maintained in a vertical position by nylon lines. Simultaneous records were taken with this staff and a bottom-mounted pressure sensor at a depth of approximately 5.5 meters. A representative plot of the frequency spectra obtained is shown in Figure V-4. The spectral values for the staff and the pressure sensor agree well across the spectral peaks. The spectral amplitude of the pressure sensor falls below that of the wave staff beyond the cutoff of the spectral correction for depth. Both spectra show a small peak around 0.3 Hz and there is a relative peak in the coherence at this frequency. As expected, the wave staff shows a higher level of energy in the high-frequency region of the spectrum. The staff in the pier configuration had a lower signal to noise ratio than that of the pressure sensor.

Following the experiment off the pier, a staff was attached to the SAS station at Torrey Pines Beach. The station was tethered temporarily by steel cables to restrict its motion. The results of the four runs of this experimental setup are included in Appendix H. A quantitative comparison was made of the spectral values across the coherent band, that is for wave periods of 4 to 18 seconds. The energy density of the grouped frequency bands was compared for the spectra from the two different sensors. A mean percent difference of the spectral values in the bands was calculated as follows:

$$D_B(\%) = \sum_{n=5}^{24} \frac{|S_{ws}(f= n\Delta f) - S_{ps}(f=n\Delta f)| \times 10}{\left((S_{ws}(f=n\Delta f) + S_{ps}(f=n\Delta f)\right)}, \qquad \text{(V-2)}$$

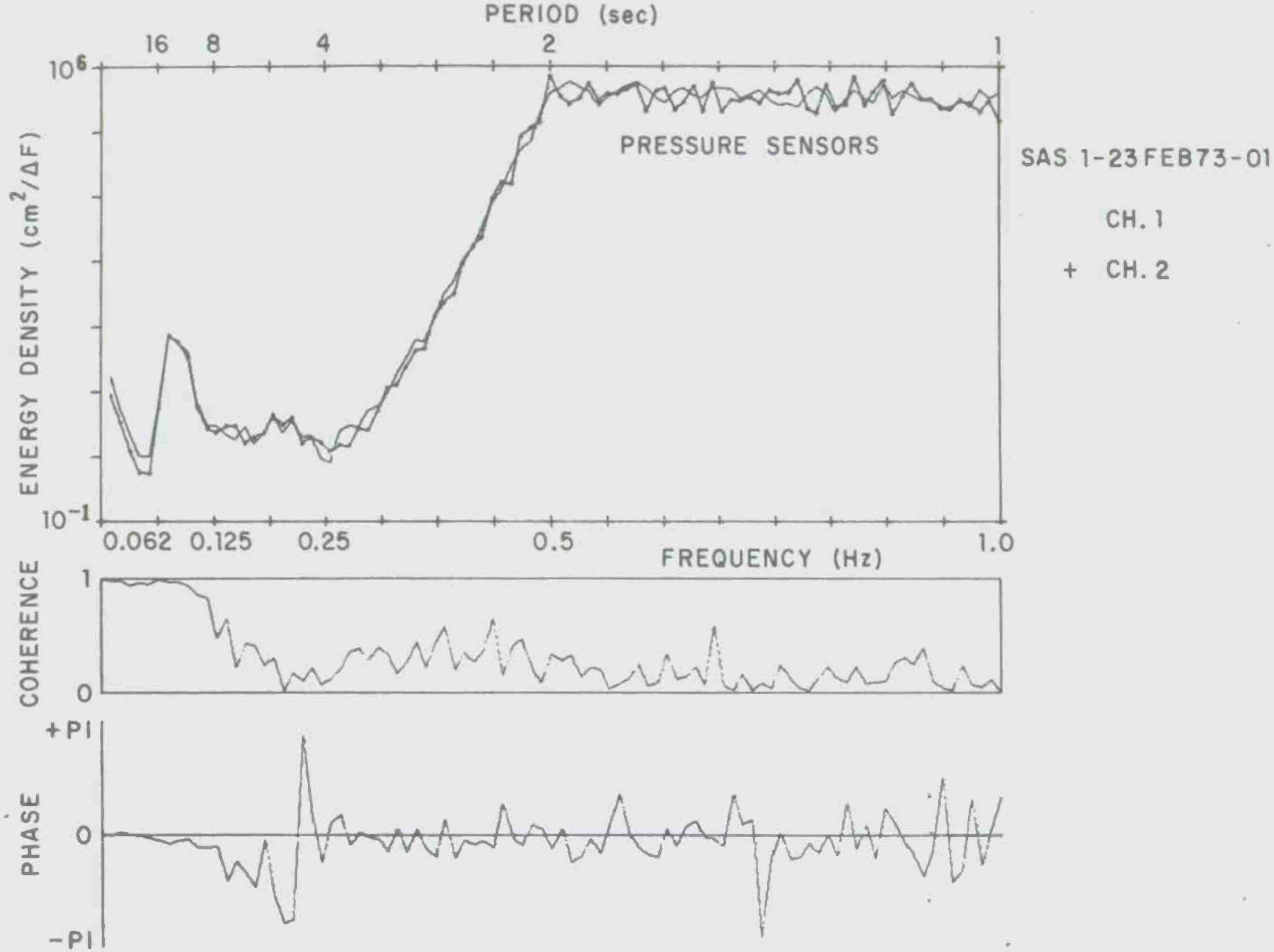

Figure V-3. Frequency and cross-spectra computed for pressure sensors 1 and 2 of the sensor array. The depth correction factor was carried out from 0.0 to 0.5 Hz. The rise in energy in the high-frequency region, above 0.25 Hz, is due to the unbounded nature of the correction factor.

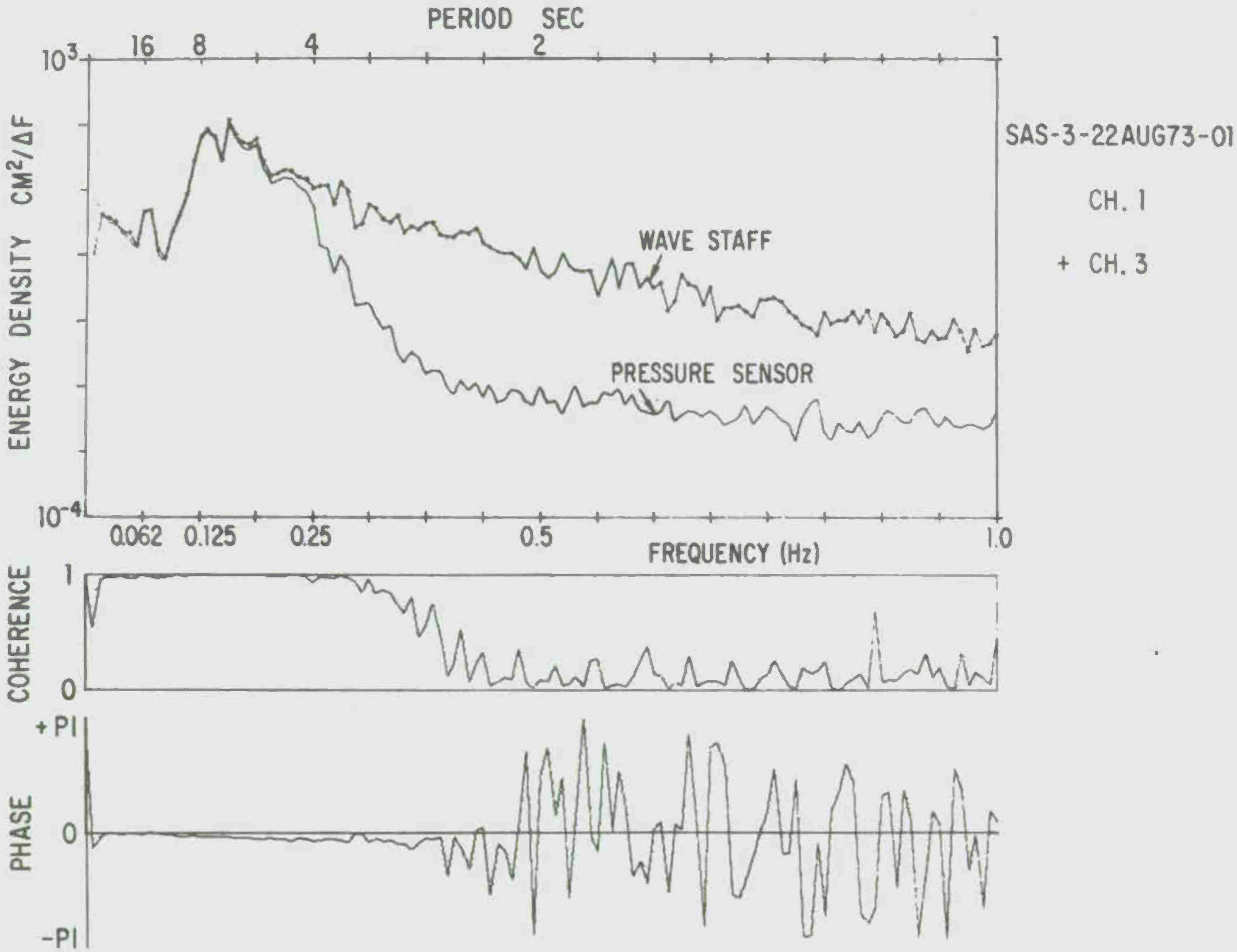

Figure V-4. Frequency and cross-spectra of a bottom-mounted pressure sensor and the surface-piercing resistive wire gage for simultaneous runs off Scripps Pier. The pressure-sensor spectrum is depth corrected for a 5.3-meter depth from 0.0 to 0.25 Hz. The sensors show good spectral agreement below 0.3 Hz.

where D_B is the defined percent difference of the band energy, S_{ws} and S_{ps} are the frequency spectrum values for the wave staff and pressure sensor respectively, n is the frequency band number, and Δf is the bandwidth, 0.0107 Hz. Also considered was the percent difference of the total energy as calculated from the spectra of the two different sensors. The total energy was calculated as the area under the coherent region of the spectrum. The results of the comparisons are listed below:

Run	D_B	% Difference of Total Energy	Sensor with Largest Total Energy
SAS 1-15 Feb 74-03	14.0	13.2	P.S.
SAS 1-15 Feb 74-04	27.0	25.3	W.S.
SAS 1-16 Feb 74-03	11.9	20.9	W.S.
SAS 1-16 Feb 74-04	12.7	8.4	P.S.
Average	16.4	17.0	

In three of the four runs the spectral values of one of the sensors were consistently higher than those of the other. However, for the run SAS 1-16 Feb 74-03 the lower frequency bands of the wave staff had larger energy density while for the higher frequency bands, from 6.0 to 4.0 seconds, the pressure-sensor values were higher.

Although the shelf station was tethered, there was some motion which was recorded by the accelerometers. The spectra of the accelerometers for SAS 1-15 Feb 74-03 are shown in Figure V-5. Although the standard deviation of the angle of tilt of the spar was only 2°, the spectra of the accelerometers closely resembled the spectrum of surface elevation.

The coherence of the records of the wave staff and pressure sensor drops off around 0.25 Hz and at the very low frequency bands. The run SAS 1-15 Feb 74-03 displays two fairly coherent higher frequency peaks located at 0.27 Hz and 0.34 Hz. This suggests that the wave staff used with a pressure sensor is useful in the identification of higher frequency peaks. The peak in coherence helps identify a spectral peak while the energy of the peak will be indicated by the spectrum of the wave staff. Generally, there is very low coherence at these frequencies between pressure sensors which are separated by large distances, the smallest spacing in our array is 30.5 meters. Therefore, positive identification of these low-energy peaks is difficult with the pressure sensors alone.

Figures H-6 and H-7 (App. H) are representative plots of results of cross-spectral analysis between a pressure sensor and the wave staff when the station was untethered. The spectral peak shapes appear quite similar, but the staff recorded more energy, particularly in the lower frequency bands. Also, the high-frequency region levels off at a much higher

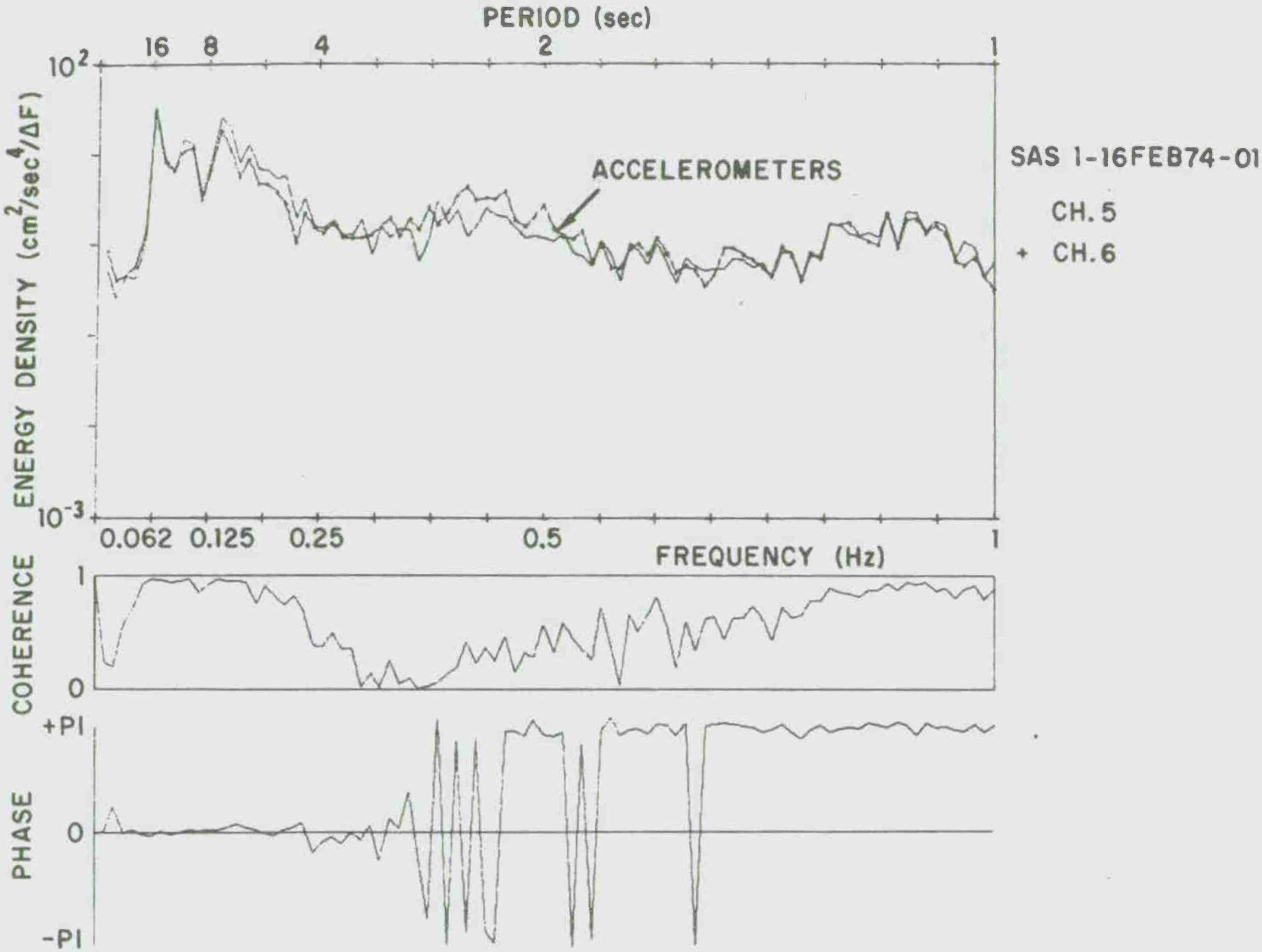

Figure V-5. Frequency and cross-spectra of accelerometers mounted on the tethered spar. Although the standard deviation of the angle of tilt is only 2°, the motions have a close resemblance to the wave spectra (sec Fig. H-4 in App. H).

energy than the case when the station was tethered. It is apparent that the tilt of the untethered station biases the data from the wave staff.

3. Comparison with Visual Estimates of Wave Height and Direction.

An effort was made to compare the measured wave spectra with visually observed wave conditions. Several of the characteristic parameters of the wave spectra (Section IV) are compared with observed wave parameters. The observations were made on a daily basis from the top of a 300-foot cliff overlooking the site of the Torrey Pines Station. The observer makes an estimation of an average breaker angle, and period of the dominant train of waves. An estimation of average wave height is made from the beach. The comparison of these observations with the spectral information should be most meaningful when the energy spectrum is largely composed of one narrow peak. With these conditions the observed wave period should be close to the peak period of the spectrum.

The root-mean-square wave height H_{rms} measured at the station in 10 meters of water (h = 10 m) is related to the energy in a spectral peak by:

$$H^2_{rms} = 8 \langle\eta^2\rangle , \qquad \text{(V-3)}$$

where $\langle\eta^2\rangle$ is the mean-square elevation of the water surface as measured at the station. From this and a knowledge of h/L_∞ where L_∞ is the deepwater wavelength, H_∞ can be obtained. Taking $\langle\eta^2\rangle$ as the energy under a spectral peak and assigning it to the peak frequency allows the relationship for breaking solitary waves (Munk, 1949) to be used:

$$H_b = H_\infty /3.3 \left(H_\infty/L_\infty\right)^{+ 1/3} \qquad \text{(V-4)}$$

which uses the assumption $H_b/h_b = 0.78$, where h_b is the breaking depth, H_b is the height of the wave at breaking, H_∞ is the deepwater wave height, and L_∞ is the deepwater wavelength. Snell's law was then used to compute the breaker angle at the depth at breaking.

Table F-2 (App. F) is a summary of the comparisons between the observed and measured parameters. The peak with period nearest the observed period generally agrees best in height and angle of approach with the visual observations. Since it is hard to judge angles accurately to the nearest degree, visual angles are usually recorded as 0° or 5° north or south and are useful mainly in checking the north-south tendency of direction.

The observed wave heights agree well with the H_{rms} of the major spectral peak when the peak is relatively narrow (bandwidth <0.15 Hz) and contains most (>80%) of the energy in the spectrum. In general, H_{rms} of the major spectral peak, the sum of the rms wave heights of the peaks, and $H_{1/3}(=4(\langle\eta^2\rangle^{1/2})$ do not correlate well with observed wave height. The observed wave height is generally smaller than $H_{1/3}$ and the sum of the rms wave heights.

4. Orbital Velocity as a Function of Wave Energy and Frequency.

A Marsh-McBirney Electromagnetic Current Meter, Model 711, was installed 1 meter above the bottom and 5 meters south of pressure sensor 3, which was mounted on the shelf station. The meter is a solid state water velocity sensor operating on the principle of electromagnetic induction and consisting of an electronics case, powered by ±6 volts, and a transducer probe 2.5 cm (1 inch) in diameter and 20 cm long with a permanently attached cable. The meter, which measures two orthogonal components of water flow perpendicular to the longitudinal axis of the probe, was calibrated in a wave channel by measuring voltage outputs for various known input velocities. The relation between velocity and voltage was linear. The meter has a resolution of 1.0 cm/sec with a response time of 0.2 sec, and a velocity range of 0.01 to 2.5 m/sec, as determined by tests conducted at SIO Hydraulics Laboratory and at the Naval Undersea Research and Development Center, San Diego, California.

Current meter data collected during special runs on 14 June 73, 16 June 73, and during routine runs in November allowed a comparison to be made between the field measurements of orbital velocities and the value predicted by linear wave theory. If u and v are the orbital velocity components of wave motion in the onshore-offshore and longshore directions respectively, then the magnitude of the orbital velocity as measured by the current meter is given by:

$$U_{cm} = \sqrt{u^2 + v^2} \ , \qquad \text{(V-5)}$$

where the subscript cm denotes the measurement by current meters. The values of u,v are obtained from the velocity variance-frequency spectrum where the u, v signals are treated as is η in equations (III-3) and (III-4). From linear theory, the orbital velocity measured at a height z' above the seabed is:

$$U = \frac{\pi H}{T} \frac{\cosh kz'}{\sinh kh} \cos(\sigma t) \ ; \qquad \text{(V-6)}$$

here H is the wave height, T the wave period, k the wave number, and h the mean water depth. Or, since $\sigma = \frac{2\pi}{T}$ is the angular frequency of the wave,

$$U = \frac{H\sigma}{2} \frac{\cosh kz'}{\sinh kh} \cos(\sigma t). \qquad \text{(V-7)}$$

The wave amplitude is obtained from the pressure signal recorded by pressure sensor 3 which has been depth corrected (equation V-1).

Equations (V-5) and (V-7) were then used to compare the horizontal orbital velocities obtained from the electromagnetic current meter with the values predicted from linear wave theory.

Values were obtained for the 20 usable runs of November 1973 during which the current meter was installed. For these runs the value calculated from linear theory (equation V-7) was higher than the measured value (equation V-5) with an average ratio of 1.2 when the values for each run were averaged over the first 24 elementary frequency bands, that is, to 0.25 Hz.

However, most of the variation between the measured current velocity values and the theoretical ones is found at the high energy, low frequency peaks. The largest waves of these 20 runs were recorded on 13 November 73 (Table V-1) where the ratio of the theoretical current value to the measured value of the high energy-peak (872 cm^2) located at 10.9 sec was 1.7 (Figure V-6). Comparatively high waves were also present on 12 November 73. The 10.9 sec peak, 579 cm^2 of energy, (Figure V-7) has a peak ratio of 1.4.

For lower energy waves the ratio at the low-frequency peak is typically 1.2, such as those on 9 November 73 (Figure V-8), where the peak at 14.2 sec contains 85.5 cm^2 of energy; and on 11 November 73 (Figure V-9) where the 14.2 sec peak contains only 26.3 cm^2 of energy.

The discrepancy may be a calibration problem. However, the results indicate that another theory should be used in place of the linear one, especially for waves with periods larger than 10 sec, where the linear theory no longer gives the best approximation of wave characteristics. Similarly, there is a need for a better understanding of the relation between properties measured at or near the bottom and the actual surface behavior.

Table V-1. Directional information for SAS 1-14 June 73-01 and SAS 1-14 June 73-02 showing the results of the preliminary current meter runs. The periods, E_p and BW were obtained from the pressure sensor data; α_o and $P(\alpha_o)$ were computed from the directional array; α and $\bar{\alpha}$ are angles obtained from the current meter data.

Run	Period(sec)	$E_p(cm^2)$	BW(Hz)	Array α_o	Array $P(\alpha_o)$%	Current Meter α	Current Meter $\bar{\alpha}$
SAS 1-14 June 73-01	14.2	481	.075	5°S	1.7	5°S	7°N
	8.8	547	.107	1°N	0.2	4°N	7°N
SAS 1-14 June 73-02	12.3	463	.070	2°S	0.2	4°N	9°N
	8.8	692	.097	1°N	0.3	4°N	7°N

Definition of Terms:

Period : The period of the spectral peak at which the directional information was obtained.

E_p : The energy contained in the spectral peak, average of the data of all four sensors.

BW : The bandwidth, an average of the data of all four sensors.

α : The angle where the directional spectrum obtained from orbital velocity records reaches a maximum, measured from the normal to the beach, but corrected to the alinement of the array.

$\bar{\alpha}$: The mean angle obtained from the current meter data as defined in the text.

α_o : The direction of the best fit to a single wave train obtained from the four-pressure-sensor array, measured from the vertical to the array. The fitting technique is based on the minimum value of $P(\alpha_o)$.

$P(\alpha_o)$: A measurement of the effectiveness of the fit for the four-sensor array.

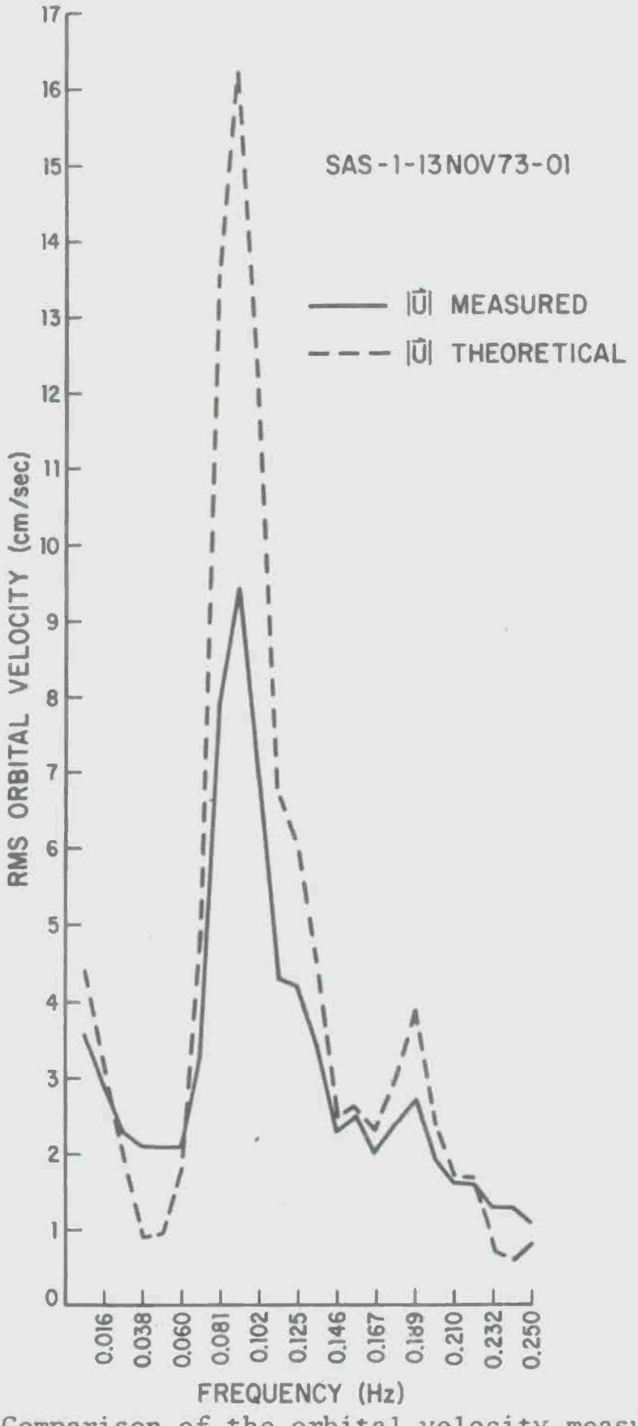

Figure V-6. Comparison of the orbital velocity measured by the current meter with that predicted by linear theory using the energy density values measured at pressure sensor 3. This run had the largest current velocities for which a comparison was made between the theoretical and measured velocity. This run also showed the largest discrepancy between the theoretical and measured rms velocity at the low-frequency peak.

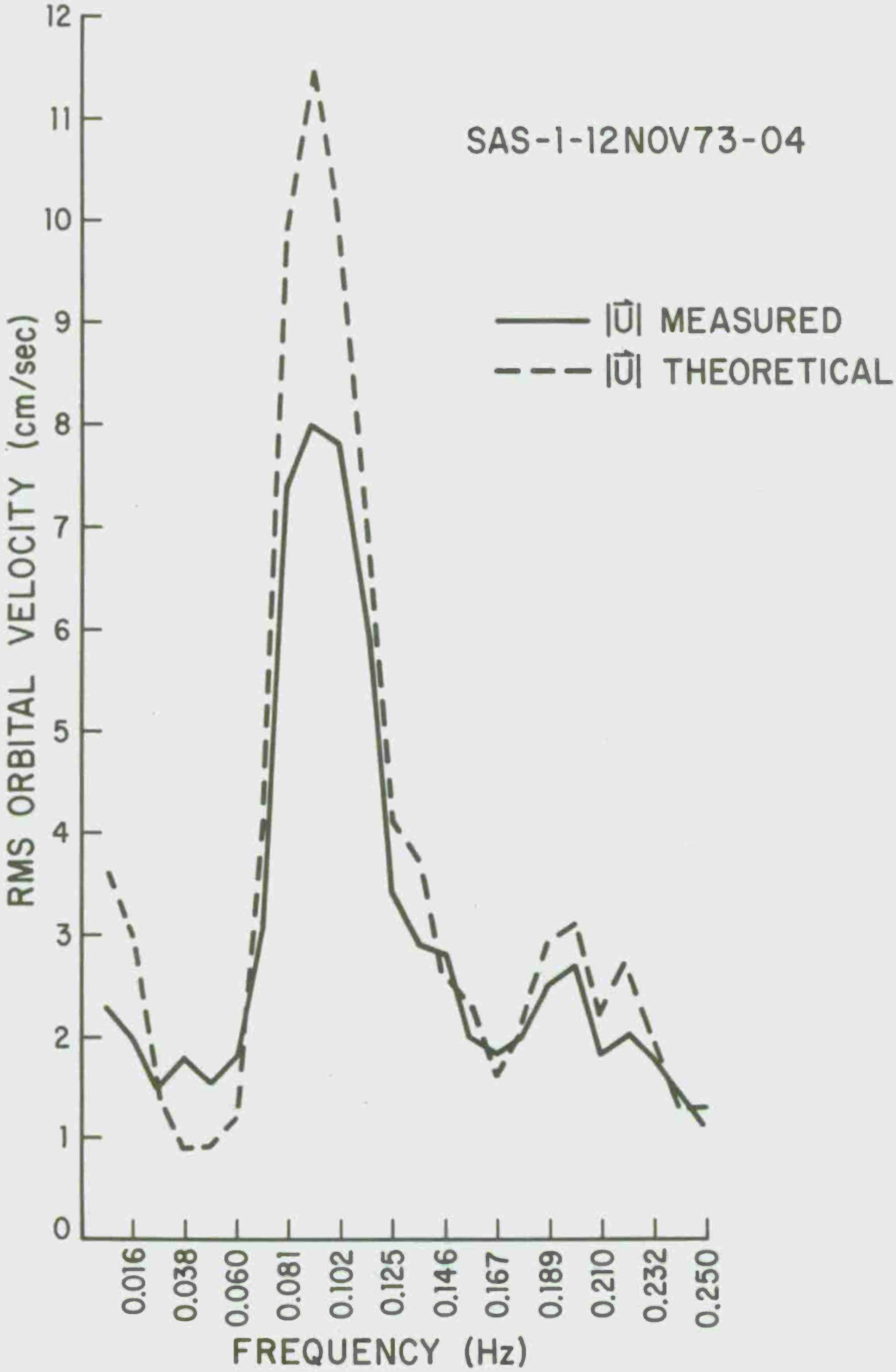

Figure V-7. Comparison of the orbital velocity measured by the current meter with that predicted by linear theory using the energy density values measured at pressure sensor 3.

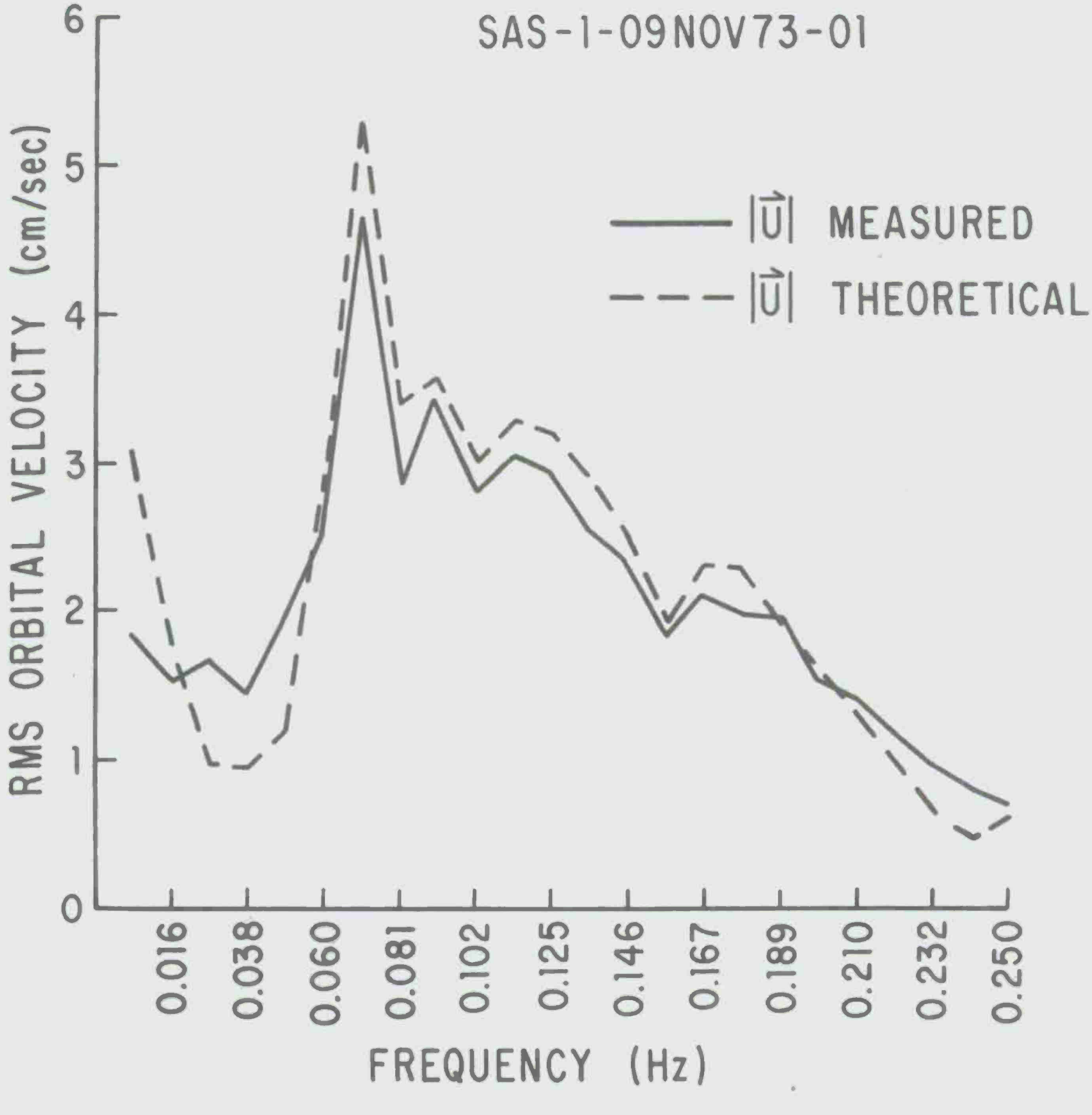

Figure V-8. Comparison of the orbital velocity measured by the current meter with that predicted by linear theory using the energy density values measured at pressure sensor 3.

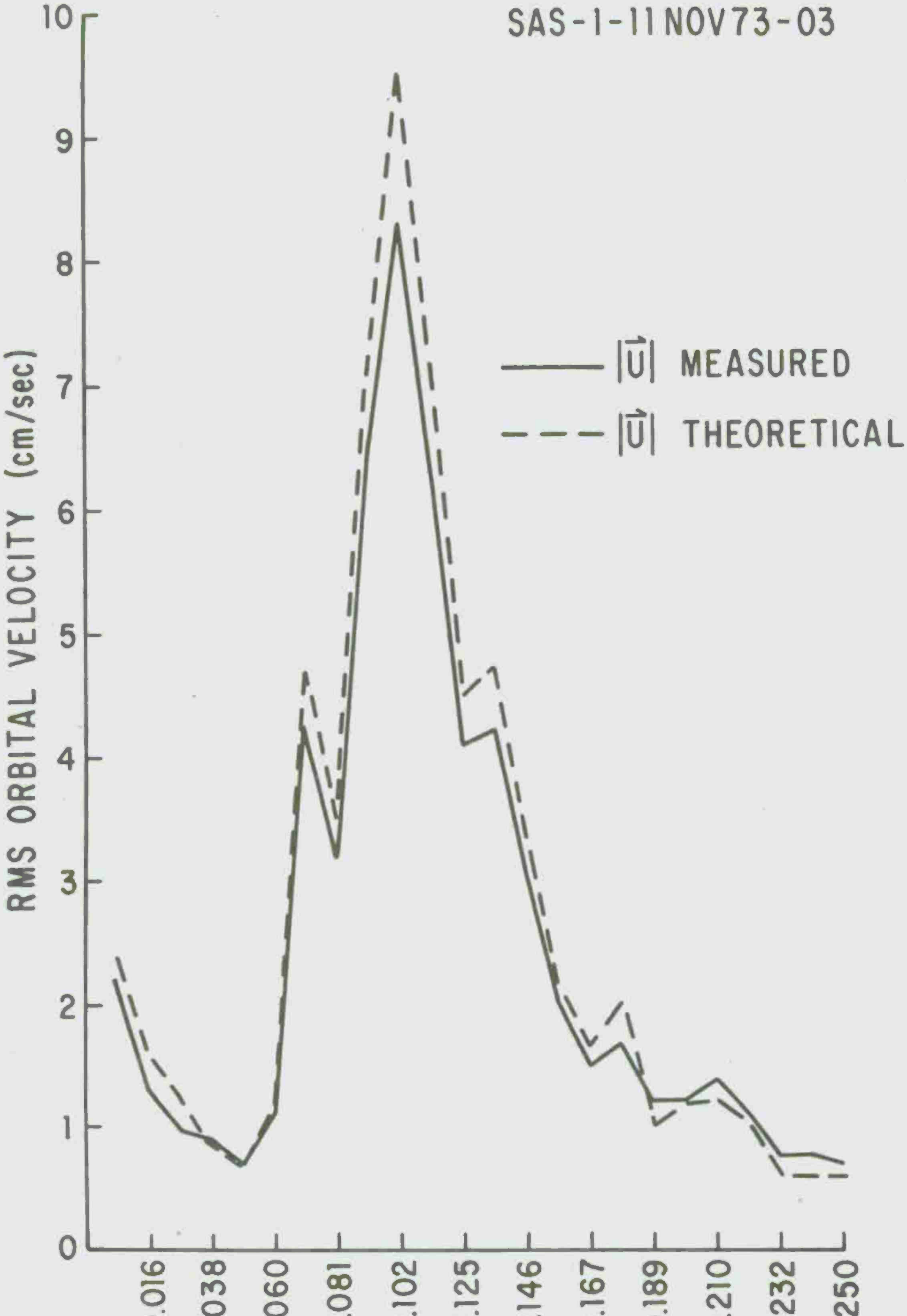

Figure V-9. Comparison of the orbital velocity measured by the current meter with that predicted by linear theory using the energy density values measured at pressure sensor 3.

There is generally low coherence between the onshore-offshore and longshore velocities with significant coherence only at the low-frequency peak. Figure V-10 shows a plot of spectrum of onshore-offshore and longshore current velocities for SAS 1-09 Nov 73-01.

5. Direction from Current Meters and a Single Pressure Sensor.

Following Bowden and White (1966), the frequency-directional spectrum is defined by:

$$S(f, \alpha) = \frac{1}{df d\alpha} \sum_{df} \sum_{d\alpha} \frac{1}{2} \bar{a}_n^2 , \qquad \text{(V-8)}$$

where $\bar{a}_n$ denotes the mean value of the amplitudes a_n which represent the amplitudes of the n wave components. The summations are of the mean-square value of all wave component amplitudes contained in the infinitesimal ranges of frequency and direction $(f, f + df)$ and $(\alpha, \alpha + d\alpha)$. Thus, $S(f,\alpha) df d\alpha$ is the contribution to the mean-square value of η due to the wave components in the ranges $(f, f + df)$ and $(\alpha, \alpha + d\alpha)$.

The frequency-directional spectrum $S(f,\alpha)$ can be written as a Fourier Series:

$$S(f,\alpha) = \frac{1}{2} a_o + a_1 \cos\alpha + b_1 \sin\alpha + a_2 \cos 2\alpha + b_2 \sin 2\alpha \qquad \text{(V-9)}$$

$$+ \ldots + a_n \cos n\alpha + b_n \sin n\alpha + \ldots .$$

This sum is similar in form to the one of equation (III-12) where the coefficients are the directional cross-spectra. $C(X, f) - iQ(X, f)$ in equation (III-12) is a function of the horizontal component lags X and is well defined in array theory due to the separation distances of the sensors in the array. The time series of pressure and two horizontal velocity do not involve separation distances. Other methods are used to obtain the coefficients a_n and b_n.

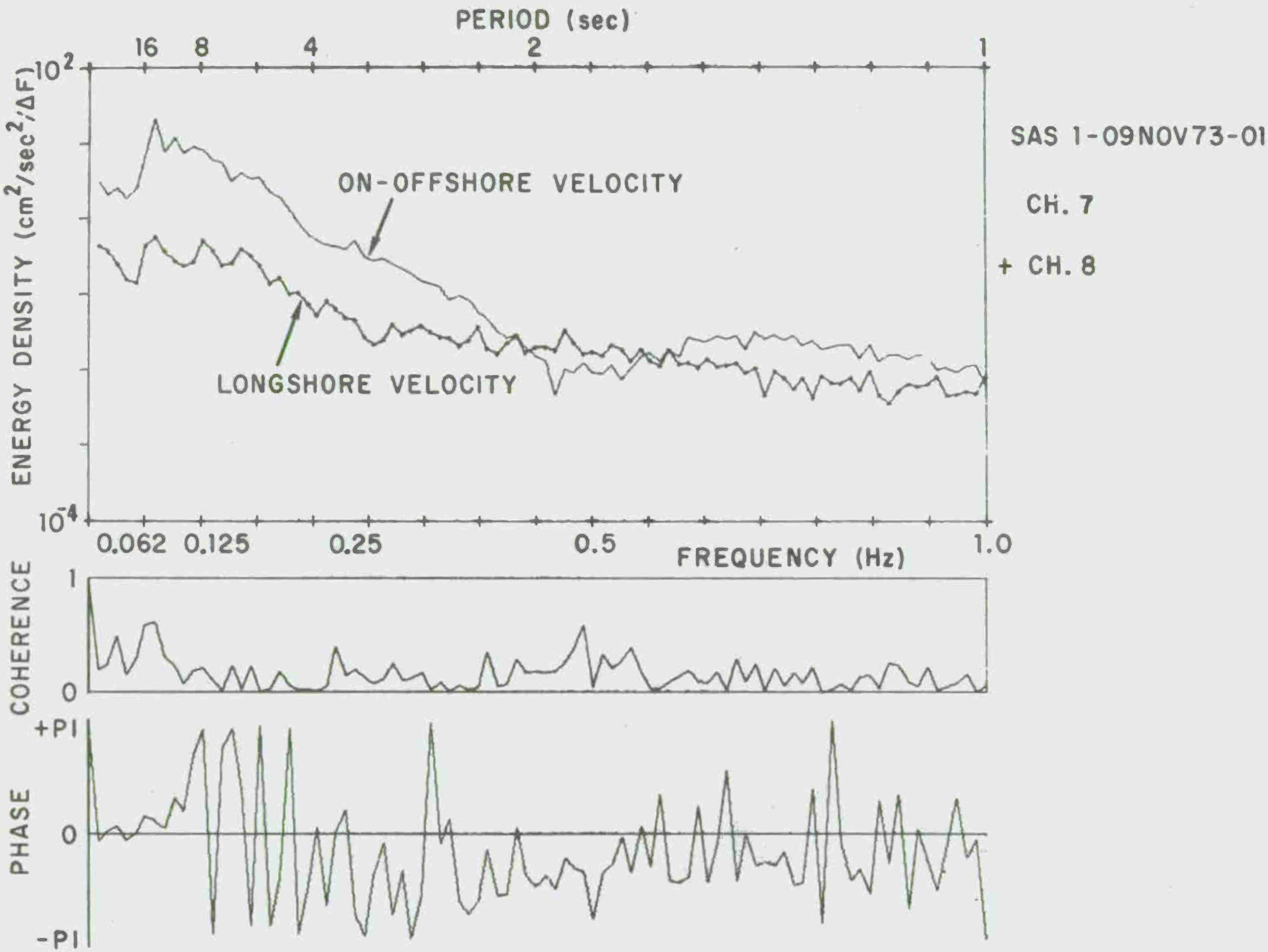

Figure V-10. Frequency and cross-spectra for channels 7 and 8 (*in situ* onshore-offshore and longshore velocities) used in calculating wave direction from the current meters.

If p represents the pressure fluctuations near the seabed and u, v the orbital velocity components of wave motion in the onshore-offshore and longshore directions respectively, then the frequency cospectra C_{ij} (as in equation III-6) can be formed of any pair of quantities, p, u, v:

$$C_{pp}(f) = \frac{1}{\cosh^2 kh} \int_0^{2\pi} S(f, \alpha)\, d\alpha$$

$$C_{uu}(f) = \left(\frac{gk}{2\pi f}\right)^2 \frac{\cosh^2 kz'}{\cosh^2 kh} \int_0^{2\pi} \cos^2\alpha \; S(f,\alpha)\, d\alpha$$

$$C_{vv}(f) = \left(\frac{gk}{2\pi f}\right)^2 \frac{\cosh^2 kz'}{\cosh^2 kh} \int_0^{2\pi} \sin^2\alpha \; S(f,\alpha)\, d\alpha$$

$$C_{pu}(f) = \left(\frac{gk}{2\pi f}\right) \frac{\cosh kz'}{\cosh^2 kh} \int_0^{2\pi} \cos\alpha \; S(f, \alpha)\, d\alpha \qquad \text{(V-10)}$$

$$C_{uv}(f) = \left(\frac{gk}{2\pi f}\right)^2 \frac{\cosh^2 kz'}{\cosh^2 kh} \int_0^{2\pi} \sin\alpha \; \cos\alpha \; S(f,\alpha)\, d\alpha$$

$$C_{pv}(f) = \left(\frac{gk}{2\pi f}\right) \frac{\cosh kz'}{\cosh^2 kh} \int_0^{2\pi} \sin\alpha \; S(f,\alpha)\, d\alpha.$$

The above are related to the Fourier coefficients

$$a_n + ib_n = \frac{1}{\pi} \int_0^{2\pi} e^{ni\alpha} \; S(f,\alpha)\, d\alpha \qquad \text{(V-11)}$$

of the spectrum $S(f, \alpha)$ so that:

$$a_o(f) = \frac{1}{\pi} \cosh^2 kh \, C_{pp}(f)$$

$$a_1(f) = \frac{1}{\pi} \left(\frac{2\pi f}{gk}\right) \frac{\cosh^2 kh}{\cosh kz'} C_{pu}(f)$$

$$a_2(f) = \frac{1}{\pi} \left(\frac{2\pi f}{gk}\right)^2 \frac{\cosh^2 kh}{\cosh^2 kz'} \left(C_{uu}(f) - C_{vv}(f)\right) \quad . \quad . \quad . \qquad \text{(V-12)}$$

$$b_1(f) = \frac{1}{\pi} \left(\frac{2\pi f}{gk}\right) \frac{\cosh^2 kh}{\cosh kz'} C_{pv}(f)$$

$$b_2(f) = \frac{2}{\pi} \left(\frac{2\pi f}{gk}\right)^2 \frac{\cosh^2 kh}{\cosh^2 kz'} C_{uv}(f),$$

where z' is the distance of the instrument from the seabed, h is the mean water depth, g is the acceleration due to gravity, f is the frequency of the waves, and α is the direction of wave approach.

From the pressure and orbital velocity data, the first five Fourier coefficients of the frequency-directional spectrum can be obtained. So, the first five terms of the series in equation (V-9) are known giving the partial Fourier sum, or an estimate of the frequency-directional spectrum,

$$\hat{S}(f,\alpha) = \frac{1}{2} a_o + a_1 \cos\alpha + b_1 \sin\alpha + a_2 \cos 2\alpha + b_2 \sin 2\alpha. \qquad \text{(V-13)}$$

If the terms of higher order are small, equation (V-13) may be a good approximation to the true frequency-directional spectrum given by the infinite series in equation (V-9).

This method does not involve spatial aliasing as described in array theory (Section III). The spectrum obtained in this manner is broader than for the array method since only five terms are obtained as compared to nine for the four-sensor array (Equation III-12). If the directional spectrum for a fixed frequency is plotted, it will attain a maximum for some directional value which will be referred to as the peak direction, α_m. A look at equations (V-10 and V-12) indicate that a mean direction $\bar{\alpha}$ can be found:

$$\tan\bar{\alpha} = \frac{b_1}{a_1} . \qquad \text{(V-14)}$$

This mean direction $\bar{\alpha}$ has meaning only for unimodal narrow angular distributions. The better the agreement between the peak direction α_m and the mean direction $\bar{\alpha}$, the more the spectra can be considered as due to a single wave train approaching from the direction α.

The above method was used on data collected at the SAS station off Torrey Pines Beach. A Marsh-McBirney Electromagnetic Current Meter, Model 711 (described in Section V-4) installed 1 meter above the bottom and 5 meters south of pressure sensor 3 collected preliminary data during special long-term runs on 14 June 73 (0945 to 1120 hours PST), and 16 June 73 (1029 to 1200 hours PST) at a rate of 2 samples per second. Data on 16 June 73 were eliminated because of erratic pressure sensors and magnetic tape errors. Two segments of data from 14 June 73 were analyzed. The first 34-minute segment of 4,096 points was labeled as SAS 1-14 Jun 73-01, and the segment from 1019 to 1053 hours PST as SAS 1-14 Jun 73-02.

A computer program was written which used equation (V-12) to compute the coefficients a_0, a_1, a_2, b_1, and b_2. A grouping of 22 adjacent bands was used in the calculation of the spectra. With the sampling rate of 2/sec and a total of 4,096 data points, this grouping yielded a frequency resolution of $\Delta f = 0.0107$ Hz. The coefficients were then used to calculate an estimate of the directional spectrum. Equation (V-14) was used to obtain $\bar{\alpha}$. Directional information was also determined from the four pressure-sensor array using the procedure described in Appendix A. The uncertainty in direction of positioning the orthogonal current meters is estimated to be of the order of ±5° to 10°. This results from the difficulty in adjusting a 2.5-centimeter-diameter cylinder to a compass direction underwater. On the other hand, the position of the pressure sensor array has been determined to within 1° by horizontal sextant angles from known shore station. The array was measured to be alined 1.5° west of magnetic north. This indicates that the normal to the array is rotated 13° clockwise of true east-west, which is the normal to the beach shoreward of the array. Current meter directional values have been corrected to account for the alinement of the array.

For SAS 1-14 June 73-01 peak spectral energies were located at periods of 14.2 sec and 8.8 sec. The peaks have a similar amount of energy. However, the peak for the 8.8-sec waves is broader than that for the 14.2-sec waves (Table V-1). $S(f,\alpha)$, when calculated using pressure and two horizontal velocity components reaches a peak direction at 5°S for the 14.2-sec waves, the mean direction, $\bar{\alpha}$, is 7°N. The directional spectrum obtained from a four-pressure sensor array peaks at 5°S with $P(\alpha_0) = 1.7$ (where $P(\alpha_0)$ is defined by equation (IV-1)). For the 8.8-sec peak, the method using orbital velocities peaks at 4°N as the direction of the energy with $\bar{\alpha} = 7°N$. The array method gives peaks at 1°N with $P(\alpha_0) = 0.2$. In both procedures, the 8.8-sec peak fits better to a single wave model.

The energy spectrum from SAS 1-14 June 73-02 has peaks at periods of 12.3 sec and 8.8 sec. The peak direction from the current meter for the 12.3-sec wave is 4°N and from the array, 2°S. Here $P(\alpha_0) = 0.2$ while $\bar{\alpha} = 9°N$. The 8.8-sec wave has a directional array spectral peak at 1°N with $P(\alpha_0) = 0.3$ and a current meter spectral peak at 4°N with $\bar{\alpha} = 7°N$. In this run both peaks fit to a single wave since $P(\alpha_0)$ is small and α and $\bar{\alpha}$ are close in value. The frequency spectral plots for the *in situ* onshore-offshore orbital velocity and pressure data is shown in Figure V-11. Normalized directional spectra plots for the 8.8-second peak of SAS 1-14 June 73-02 are shown in Figures V-12 and V-13. Figure V-12 shows the directional spectrum as calculated from the time series of pressure and orbital velocities. Figure V-13 is the spectrum calculated from the array. Both figures also show the response of each method to a delta function. The current meter method has a much broader response than the array method. The current meter method response is broad since only five terms in the Fourier expansion of $S(f,\alpha)$ can be calculated from a knowledge of pressure and velocities. The advantage is, however, that the direction spectral windows are independent of frequency. This makes comparisons between different frequencies easier than for the array method whose windows are frequency dependent. Another advantage to the current meter method besides the frequency independent windows is that less instrumentation is required.

Visual observations made on 14 June 73 indicate waves with a period of approximately 10 sec were breaking at an angle of 5° from the north. The significant height was given as 2 meters. When shoaling and refraction are considered, these values correspond reasonably well with a breaker angle of 6°N calculated for the 8.8-sec spectral peak.

The fairly good agreement between the directions obtained using these two methods for the runs on 14 June 73 suggested that further comparisons would be useful. The current meter was reinstalled on 2 November 73 and operated through 13 November 73 during routine runs at the SAS station so that more comparisons with the directional array method could be made.

Twenty of these November 73 runs were usable, yielding a total of 38 peaks which were analyzed. Results are shown in Table F-3 (App. F).

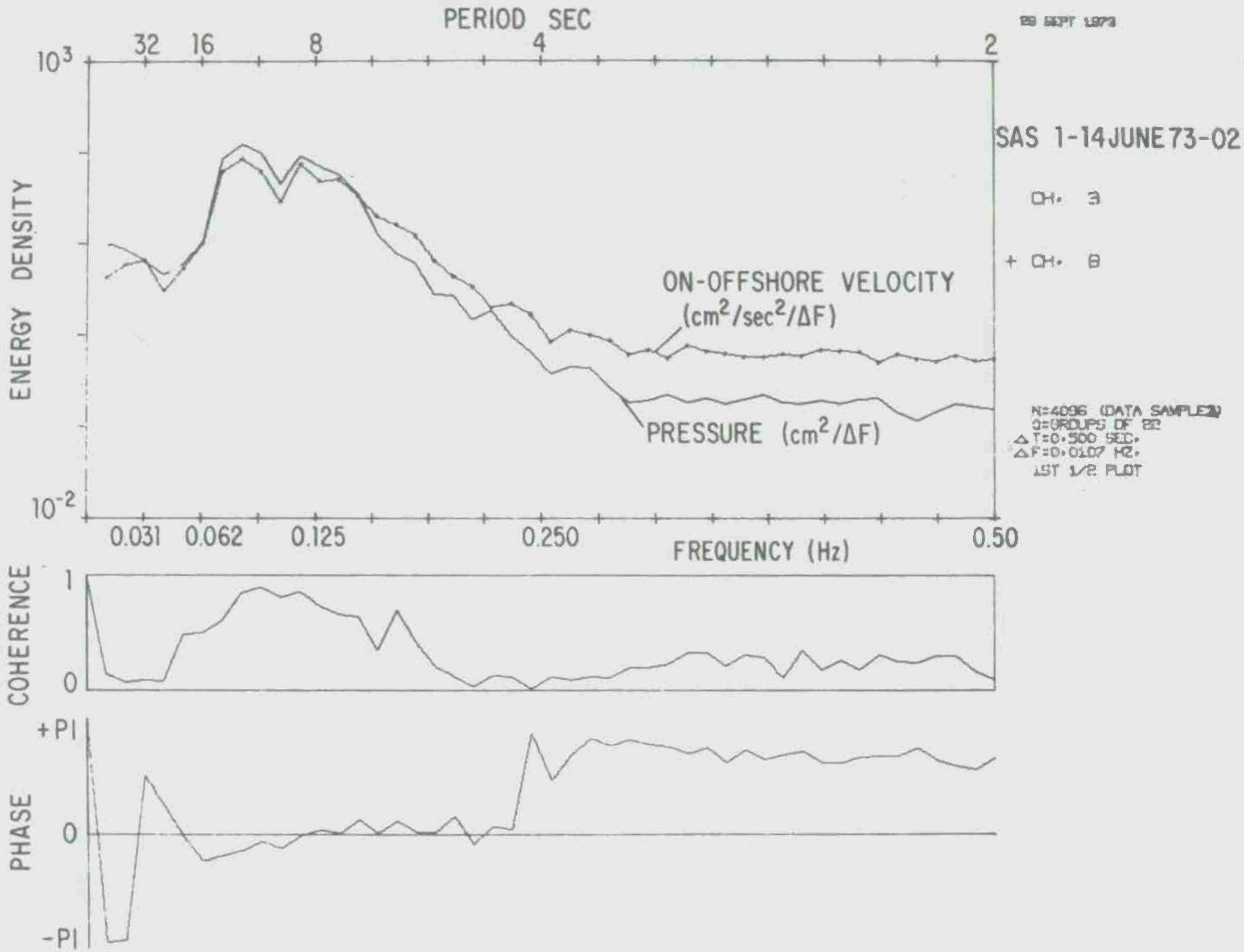

Figure V-11. Frequency and cross-spectra of the *in situ* pressure (channel 3) and onshore-offshore orbital velocity (channel 8) used in calculating wave direction from the current meters.

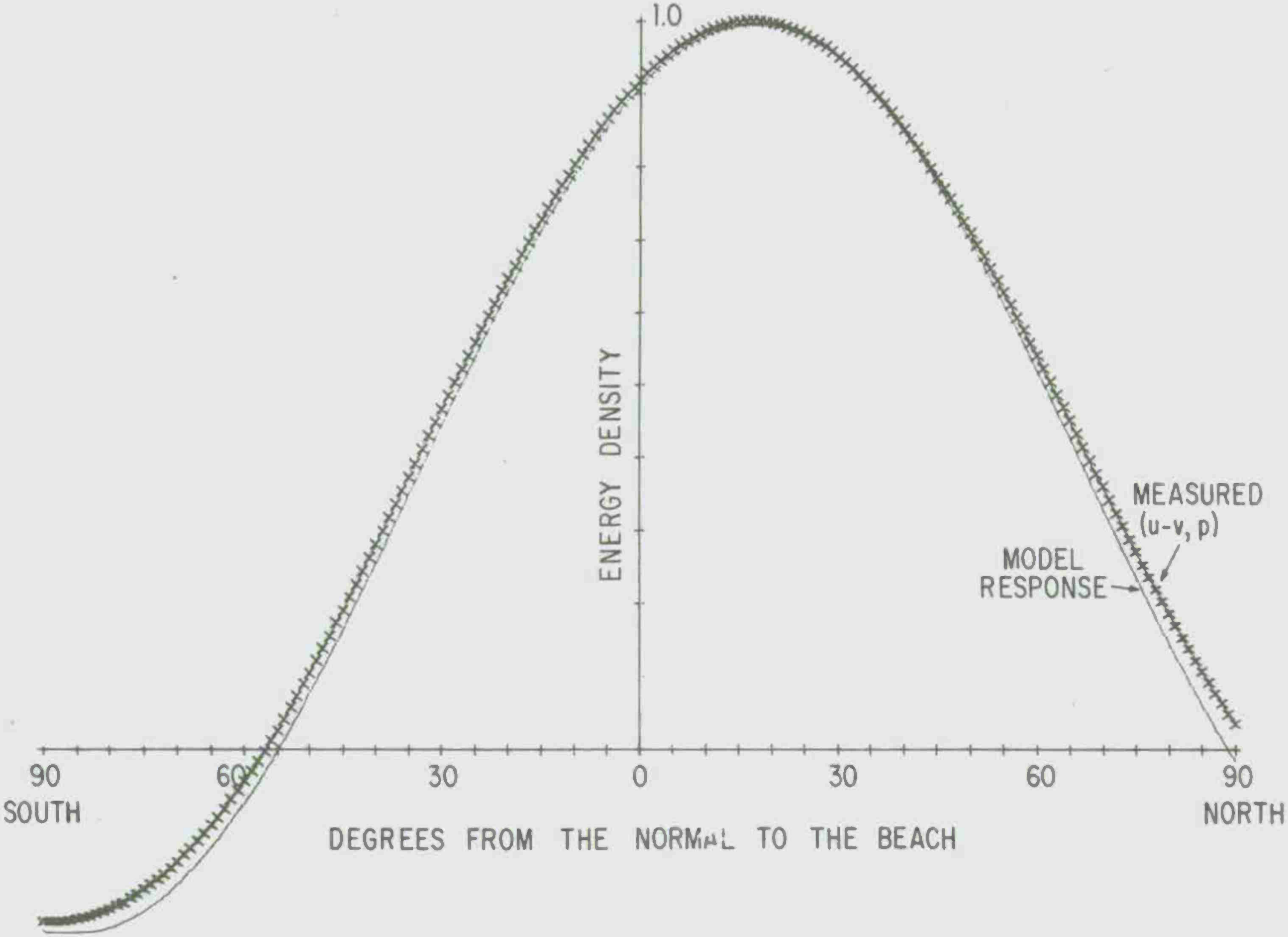

Figure V-12. Calculated current meter directional spectrum (hatched line) and the spectrum of a single wave train of the same period having the direction of the spectral peak (smooth line). The broad spectrum is the result of having only five terms in the expansion of S(f, α) on a delta function. The spectrum is for 8.8-second waves from run SAS 1-14 Jun 73-02. The energy density values are normalized by the maximum value at 17° north, which was the angle obtained before the 13° correction was made to account for the alinement of the pressure-sensor array.

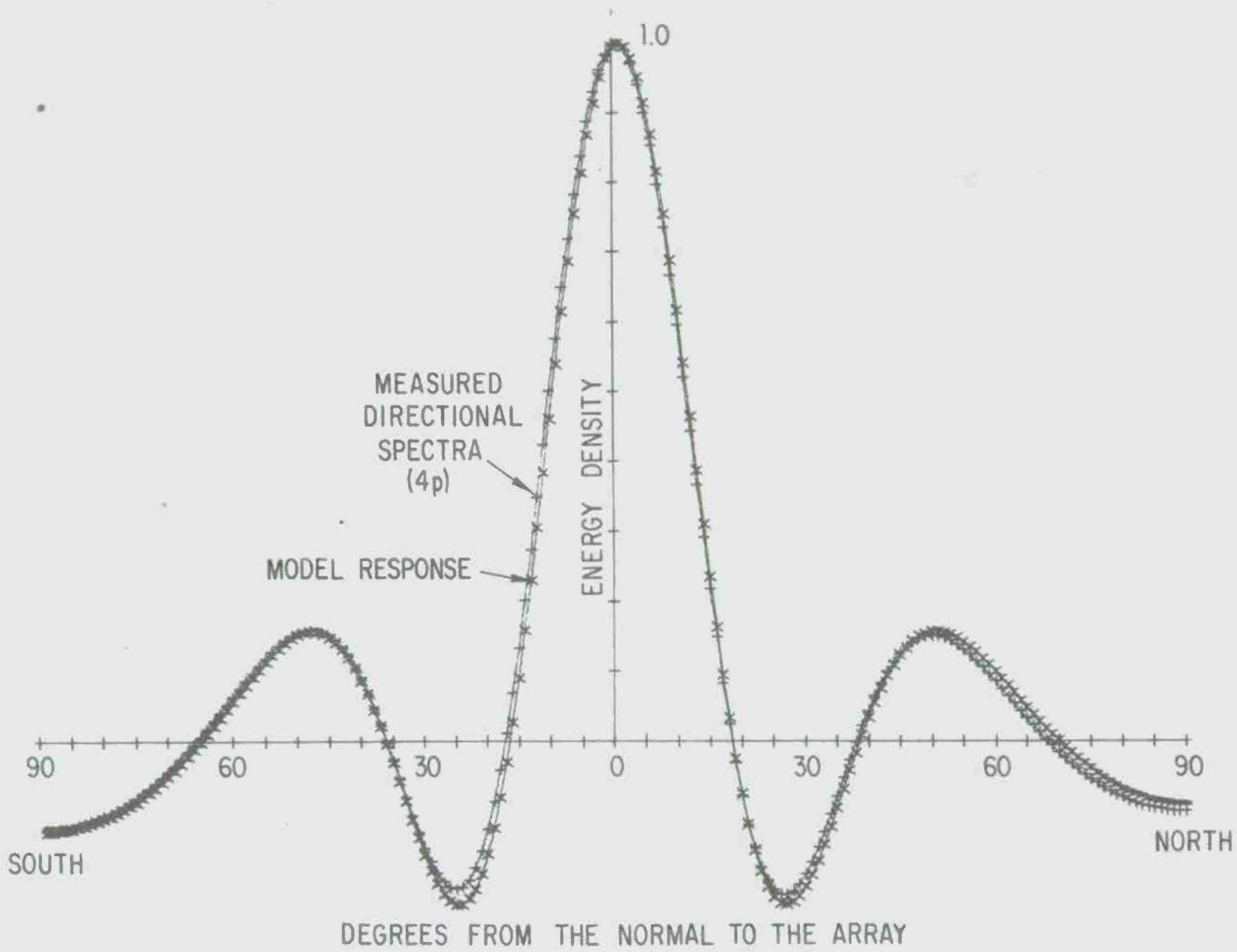

Figure V-13. Plot of measured directional spectrum for 8.8-second waves of run SAS 1-14 Jun 73-02. Also plotted is the response of the array to an input model of a single direction wave train. The good agreement between the measured directional spectrum and the model response indicates that the 8.8-second waves are unidirectional.

Assuming the normal to the array is rotated 13° clockwise of true east-west directional agreement is within ±5° for 21 of the peaks (55.3%). Agreement in direction is within ±10° for 92.1 percent of the peaks. In some of the runs with large disagreement, noise is noticeably present in the data. This is true, for example, of SAS 1-07 Nov 73-02 for pressure sensors 1 and 2 and in all pressure sensors for SAS 1-04 Nov 73-04. A faulty plug which was replaced 5 Nov 73 may have presented some of the difficulty. In other cases $P(\alpha_0)$ is large, indicating a poor single wave fit. For instance, $P(\alpha_0)$ = 59.7 percent for the first peak on 11 Nov 73-04, $P(\alpha_0)$ = 61.7 percent for the second peak on 12 Nov 73-03, and $P(\alpha_0)$ = 50.2 percent for the second peak on 12 Nov 73-04 (refer to Table F-3, App. F). In other cases the higher frequency peaks are not necessarily well defined consistently throughout the pressure sensor and current meter data. This is true for the 8 Nov 73 runs. Comparisons with visual observations and with direction obtained from accelerometer data (Section V-6) are also included in Table F-3 (App. F).

6. Direction from Accelerometers.

Due to the difficulty in maintaining an array of pressure sensors, it would be desirable to obtain wave climate information using only the motion of the spar and one pressure sensor. To determine the feasibility of this, the accelerometer records were also used to obtain a direction for the 20 available runs during November 73 to augment the directional comparison between the current meter and array values. The accelerometers measure horizontal acceleration in orthogonal directions. Each is oriented 45 degrees from the normal to the beach. Since waves do not usually arrive from directions greater than ± 45 degrees from the normal to the beach, there is no ambiguity as to which quadrant the waves are coming from (Figure V-14). Thus, the spectral values (Figure V-15) of the accelerometers at the peak frequency are sufficient to obtain an angle. For each peak of interest, the square root of the spectral value of accelerometer 2 was divided by the square root of the spectral value of accelerometer 1 (Figure V-14). The arctangent of the result gives an angle which must then be corrected by 45 degrees to allow for the orientation of the accelerometers. It should be noted that a method similar to this was not used in the current meter analysis since the orientation of the current meters was such that waves could be arriving from either of the offshore quadrants (Figure V-14, quadrant II or III). The magnitudes of the onshore-offshore and longshore velocities alone is not sufficient to obtain a unique angle. At the shelf station, the ambiguity in the onshore-offshore axis is eliminated due to the presence of the beach (no waves would be arriving from quadrant I or IV (Figure V-14). The pressure record can be used to remove the ambiguity in the longshore axis by distinguishing between crests and troughs of the waves as was done in the current meter analysis discussed previously (Section V-5).

Results for the accelerometer analysis are also in Table F-3 (App. F) along with comparisons with visual observations when available, since they were not taken on weekends. Of the 38 peaks analyzed, 12 (26.3 percent) disagreed more than ±5° in direction between the accelerometer method

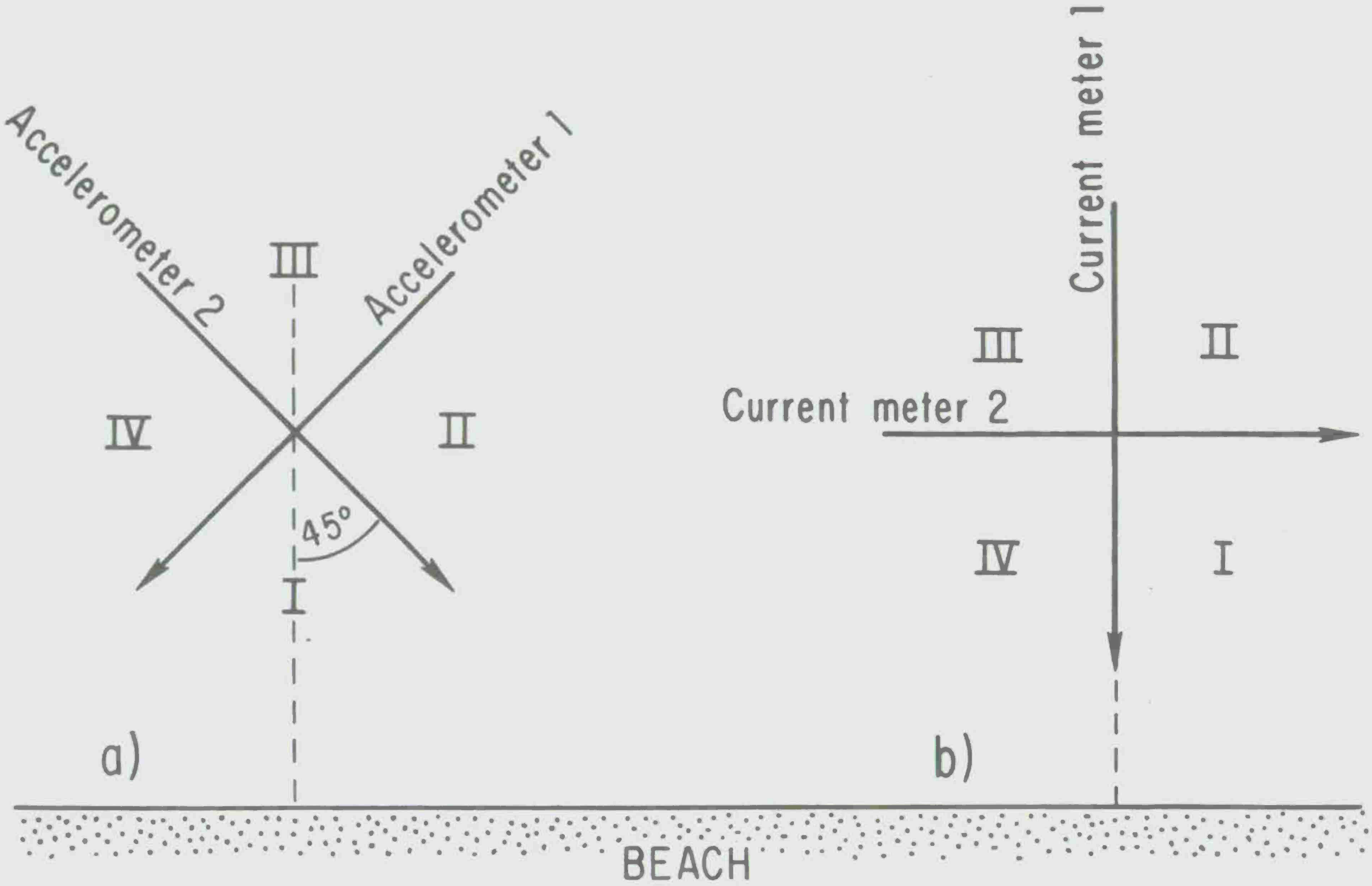

Figure V-14. The orientation of: (a) accelerometers; and (b) the current meters illustrating the coordinate system (and corresponding quadrants) defined by the axis of each instrument.

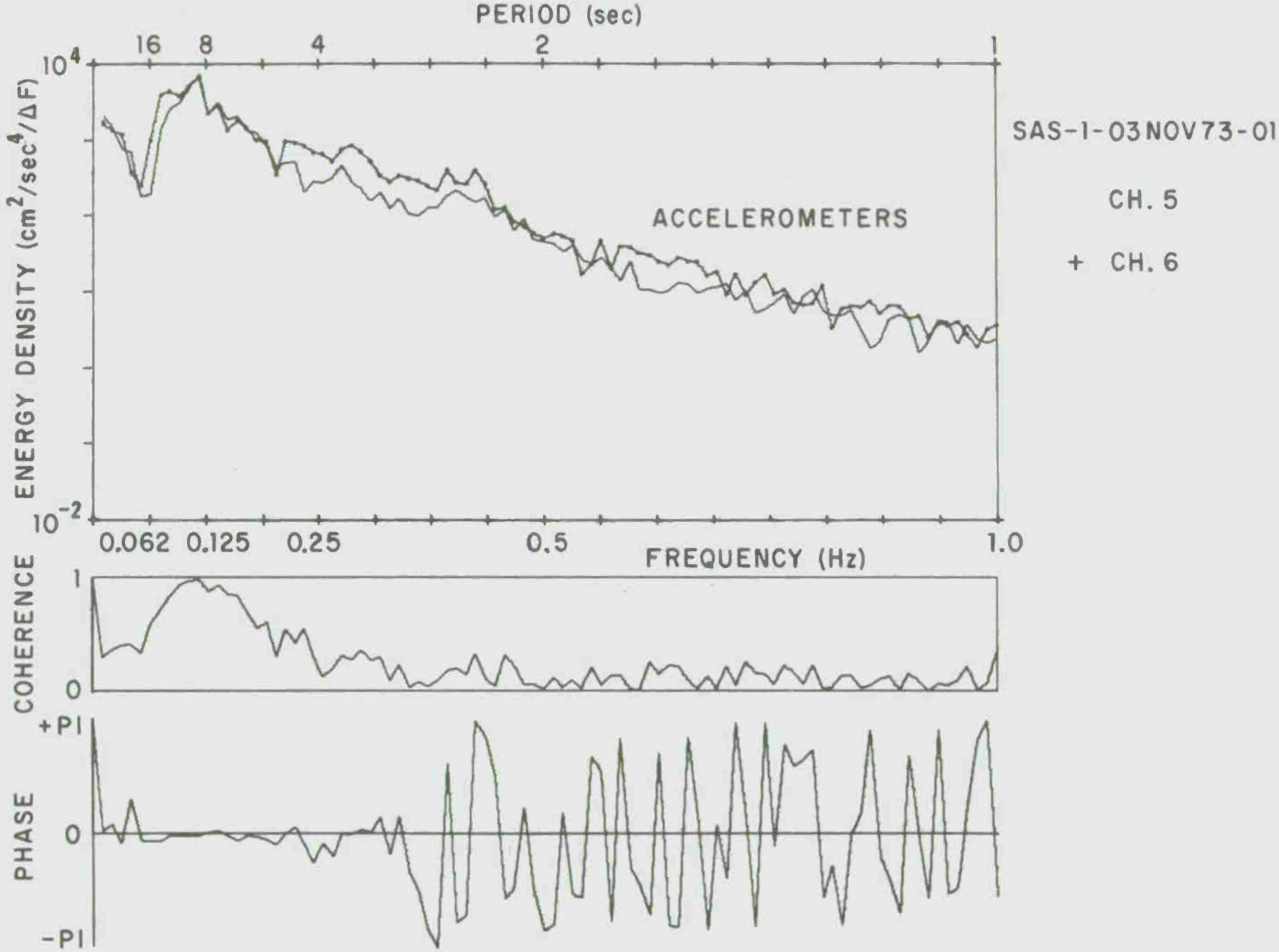

Figure V-15. Frequency and cross-spectra for accelerometer channels 5 and 6 (accelerometers 1 and 2 respectively in Fig. V-14) used in calculating wave direction from the accelerometers.

employed and the array method. Thus 73.7 percent of the peaks agreed within ±5°. All but four (10.5 percent) of these runs were within ±10°. However, direction from the current meter (Section V-5) and accelerometer agree to within ±5° for 65.8 percent of the runs. All but three of these runs (7.9 percent) were within ±10°. Again, noise in the data records is evident in some runs such as SAS 1-07 Nov 73-02 due to a faulty plug. Most of the poor agreement occurs at the low-energy peaks. For the runs SAS 1-03 Nov 73-02, SAS 1-10 Nov 73-01, SAS 1-11 Nov 73-03, SAS 1-12 Nov 73-03, SAS 1-12 Nov 73-04, and SAS 1-13 Nov 73-01, directions for the high-energy peaks agree better than for the low-energy peaks of the same run (refer to Table F-3, App. F). However, this is not always the case as in SAS 1-08 Nov 73-03 where directions agree well for the low-energy peak also. There may be other causes for the disagreement, as in run SAS 1-11 Nov 73-03 where a jump occurs in the record due to a change in current. Once these effects are understood, the accelerometer records may prove valid for obtaining wave directional properties. General conclusions are not possible since the usable runs where array, current meter, and accelerometer data were all available, represent a small sample obtained under similar wave climate conditions.

7. Directional Spectra of High Frequency Waves.

The directional spectra were routinely evaluated up to a frequency of 0.25 Hz. This cutoff was based on the limited interpretative value of the directional spectra in the band from 0.25 Hz to 0.5 Hz. Also, the directional data stored and reported were unnecessarily bulky due to the inclusion of the generally meaningless directional spectra of the higher frequencies. The difficulty of interpreting the high-frequency directional spectra is discussed below.

The problems of sampling a directional spectrum with a finite number of sensors include aliasing and resolution. The problem of aliasing as discussed in Section III results in an ambiguity of the direction of approach of the waves. Figure V-16 displays the spectral response of the linear array to 3.9-second waves approaching the array at 0°. The measured directional spectrum has a peak at 0° but also at ±54°. The distance between these alias peaks and the true peak is a function of the wavelength compared to the smallest spacing array. For set spacings in the array, the distance between these peaks decreases as the frequency increases. Figure V-16 shows the response of the array to 4.5-second waves, the longest period waves for which the alias peaks appear with an input of energy at 0°. As the distance between the peaks decreases at higher frequencies, more peaks will appear and the problem becomes more complex. The response of the array to 3-second waves propagating normal to the array is also plotted in Figure V-16. For this input there are four aliased peaks in the computed directional spectrum.

These serious problems of aliasing are compounded by the nature of the higher frequency waves. Significant peaks are rare in the higher

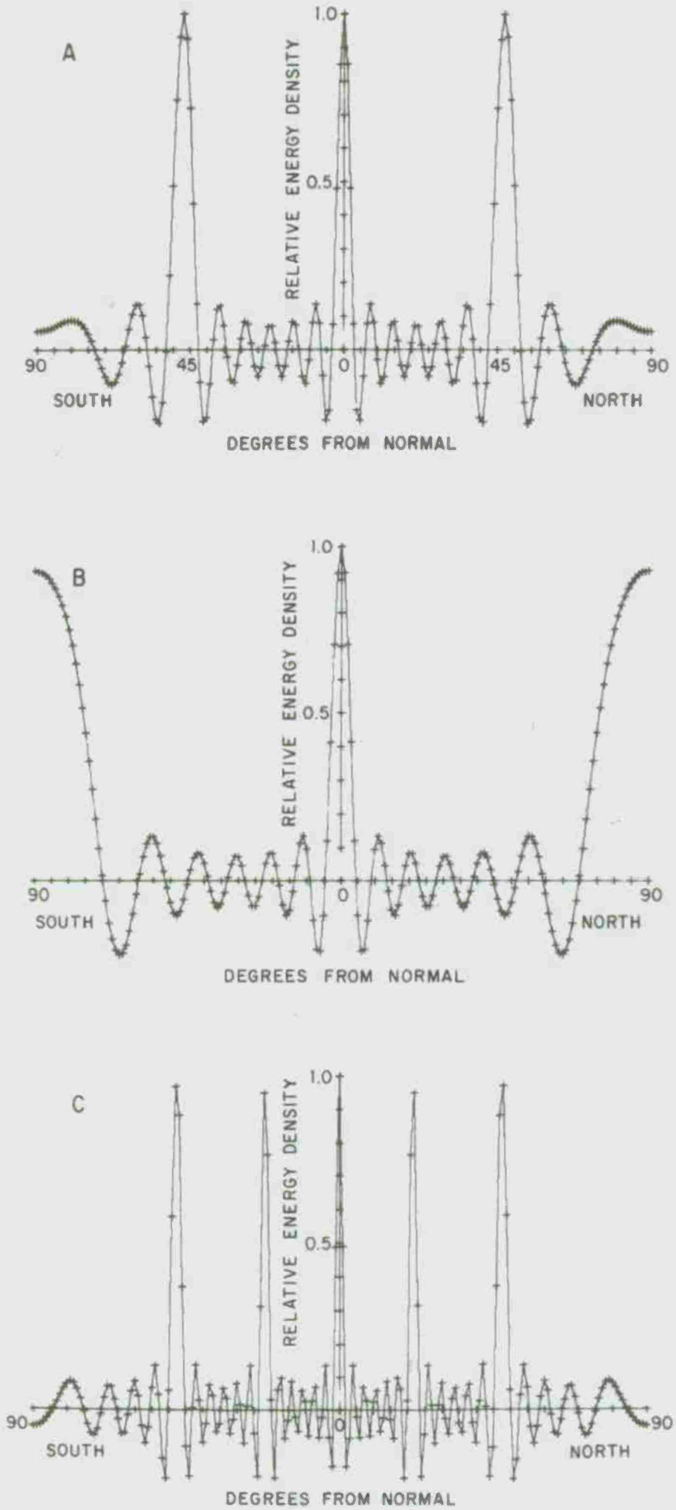

Figure V-16. The directional response of the 1-2-1 array to waves approaching from 0° with periods 3.9 seconds (A), 4.5 seconds (B), and 3 seconds (C). All peaks but those at 0° are "alias" peaks.

frequency, >0.25 Hz, area of the energy spectrum and the coherence is quite low. This implies a very wide band of directions bordering on directionless noise. The normal situation is for the energy spectrum to slope sharply from the region of 0.25 Hz, and for coherence above 0.25 Hz to be very low. Figure V-17 shows the coherence values of a frequency band on the slope of the spectrum as it compares with the coherence of the spectral peaks. The associated frequency spectra are plotted in Figure V-18. However, on occasion there have been fairly significant peaks recorded for wave periods from about 4.1 to 4.7 sec. The run SAS 1-17 May 73-02 is an example of this type of wave record. The coherence at the spectral peak, which is at 4.5 sec, is not very high (approximately 0.6) when compared to the values for the major peak. The interpretation of the directional spectra is still quite difficult. The directional spectra for wave periods, 4.5, 4.3, 4.1, 4.0, and 3.9 sec are included in Figure V-19. The associated frequency spectra of the run are plotted in Figure V-20. With no additional knowledge one should not be able to discount any of the major peaks present in the directional spectra. However, it is apparent that as one of the peaks shifts with increasing frequency, the peak around 10°N remains stationary. This implies that the peak around 10°N is a true peak and the other is an alias which shifts its position for the various frequencies.

The directional spectrum at 4.5 sec is quite clean and it probably can be concluded that a significant portion of the energy is well directed. The spectrum fits well into a single direction model, $P(\alpha_o)$ is approximately 20 percent for α_o equal to 8°N. However, at the higher frequencies, the directional spectra are quite complex and possess many significant side lobes. There is no way of distinguishing which lobes are real or if they result from aliasing . The resulting ambiguity becomes quite severe, particularly in the case of 4.1 sec waves. Obviously, one could not expect to approximate the true spectrum in practical problems with these results.

The case illustrated above was for relatively coherent high frequency waves. The only information obtained from the spectra was that the energy is propagating from approximately 8°N. This result can also be derived from the phases between sensors. An average angle computed from the phases for 4.5-sec waves is 8.9°N. As with the directional spectrum, there is an ambiguity in this calculation as an angle of 60°S will also satisfy the phase relationships. However, as with the directional spectra this ambiguity may be eliminated by inspection of the results for a neighboring band if the energy in the adjacent bands is from approximately the same direction. The phases for 4.7-sec waves, for example, give estimates of 7.9°N and 73°S. Once again the stable peak around 8°N is indicated as the true peak.

It is therefore apparent that the interpretable information contained in directional spectra of coherent high-frequency waves is recoverable through simple phase calculations. The additional information the spectrum does contain is masked hopelessly by the aliasing problems.

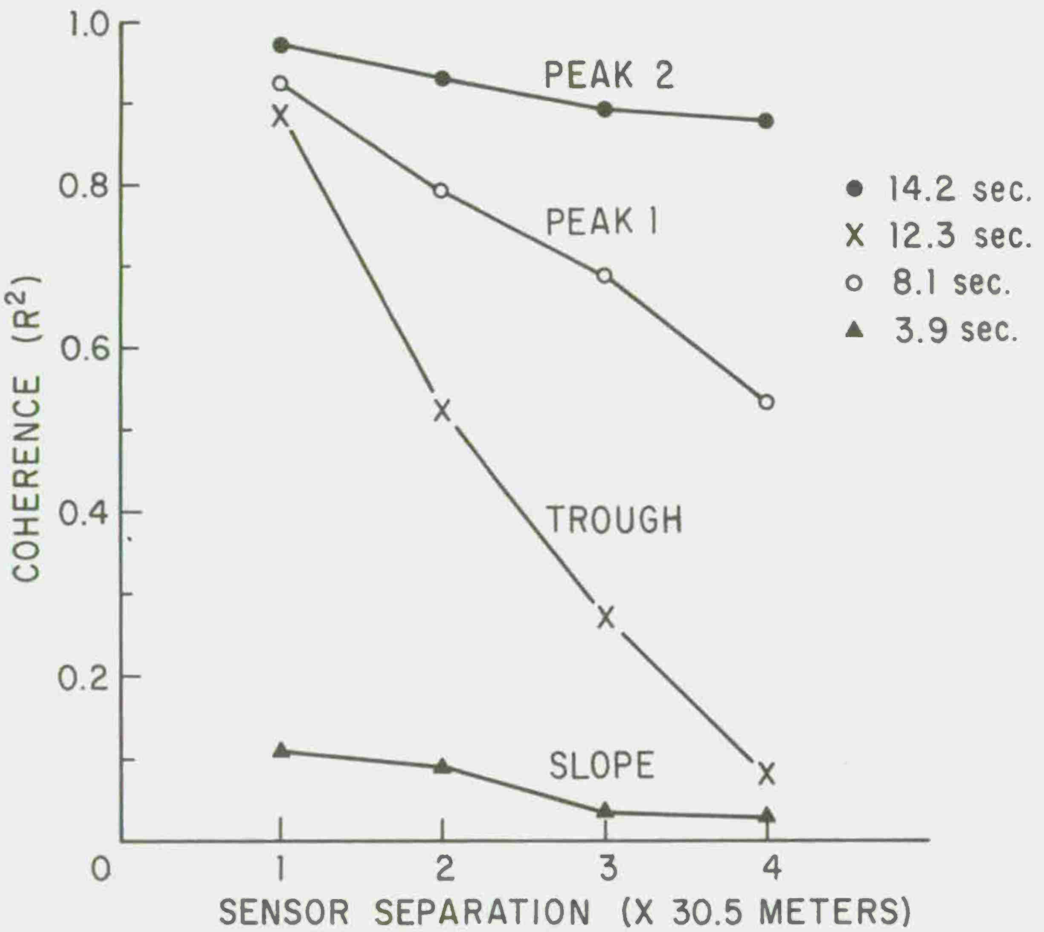

Figure V-17. The coherence between the various sensors as a function of their separation. The data were taken from SAS 1-27 May 73-03. The associated frequency spectra are plotted in Figure V-18. The low-frequency waves, peak 2, are very coherent at separation distances comparable to their wavelength. The wavelength of 14.2-second waves in 10-meter depths is 137 meters. The coherence between sensors 1 and 2 in terms of the cross-spectrum (defined in equation III-6) is: $R^2 = (C_{12}^2 + Q_{12}^2/C_{11}C_{22})$.

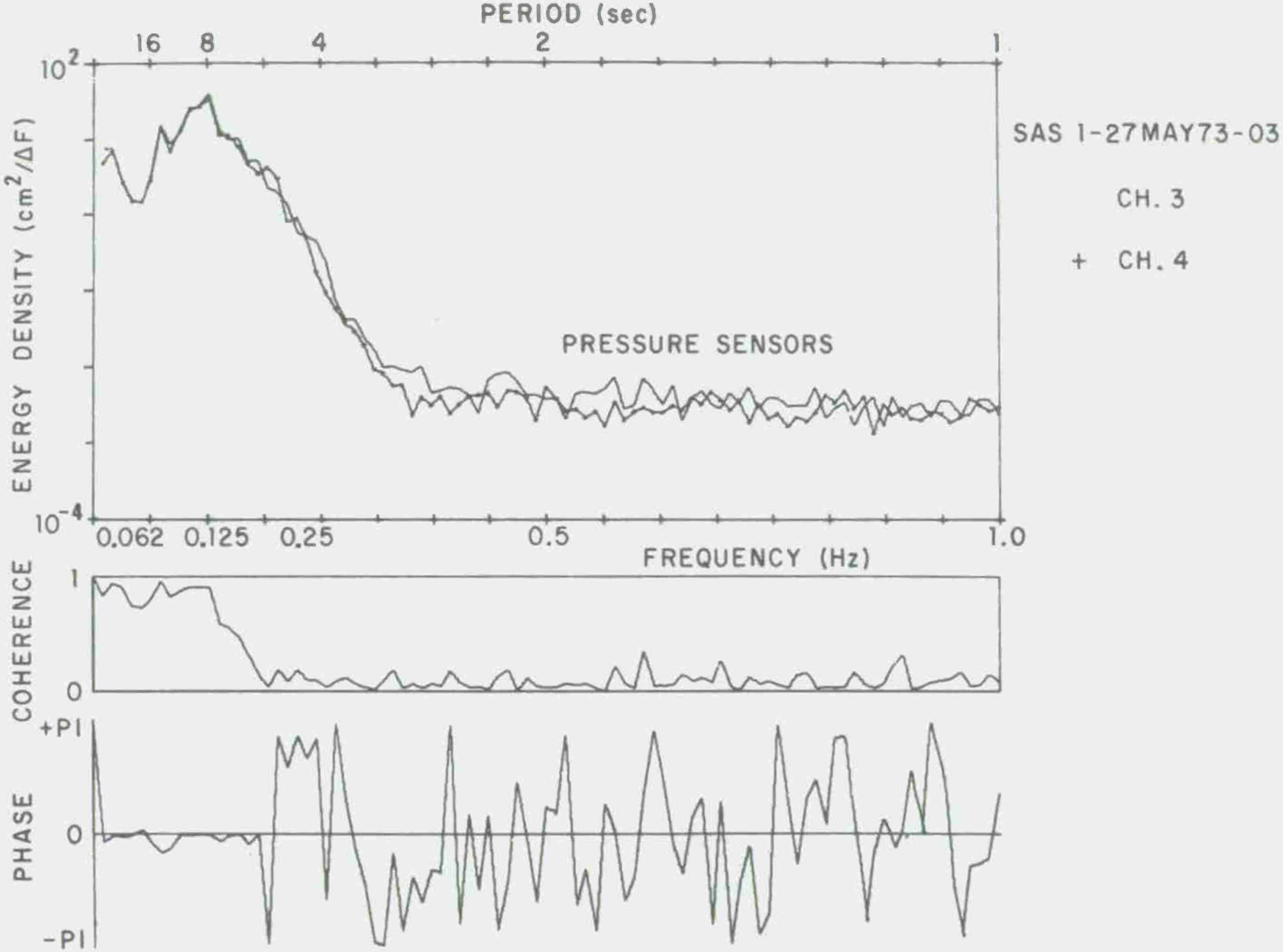

Figure V-18. Frequency and cross-spectra of sensors 3 and 4 of the 1-2-1 array. These are the associated spectra for the coherence plot of Figure V-17. Most of the energy of the wave field is contained in the higher frequency peak.

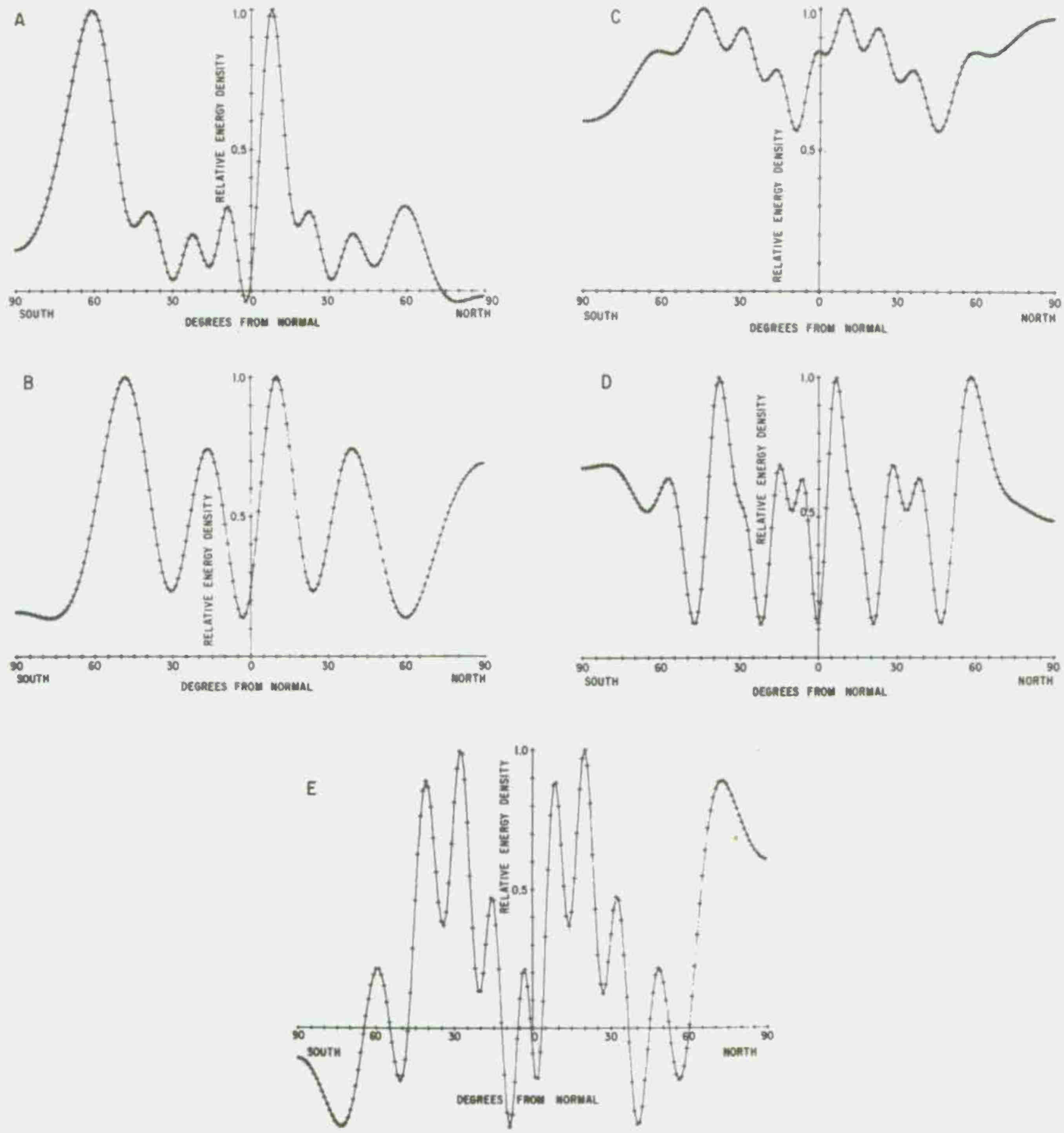

Figure V-19. The directional spectra for 4.5- (A), 4.3- (B), 4.1- (C), 4.0- (D), and 3.9-second waves (E) for SAS 1-17 May 73-02. The peak at 8° north appears for each of the higher frequency bands while the southern peak shifts its position. This suggests the peak at 8° north is the true peak while the peak at 60° south is an "alias" peak.

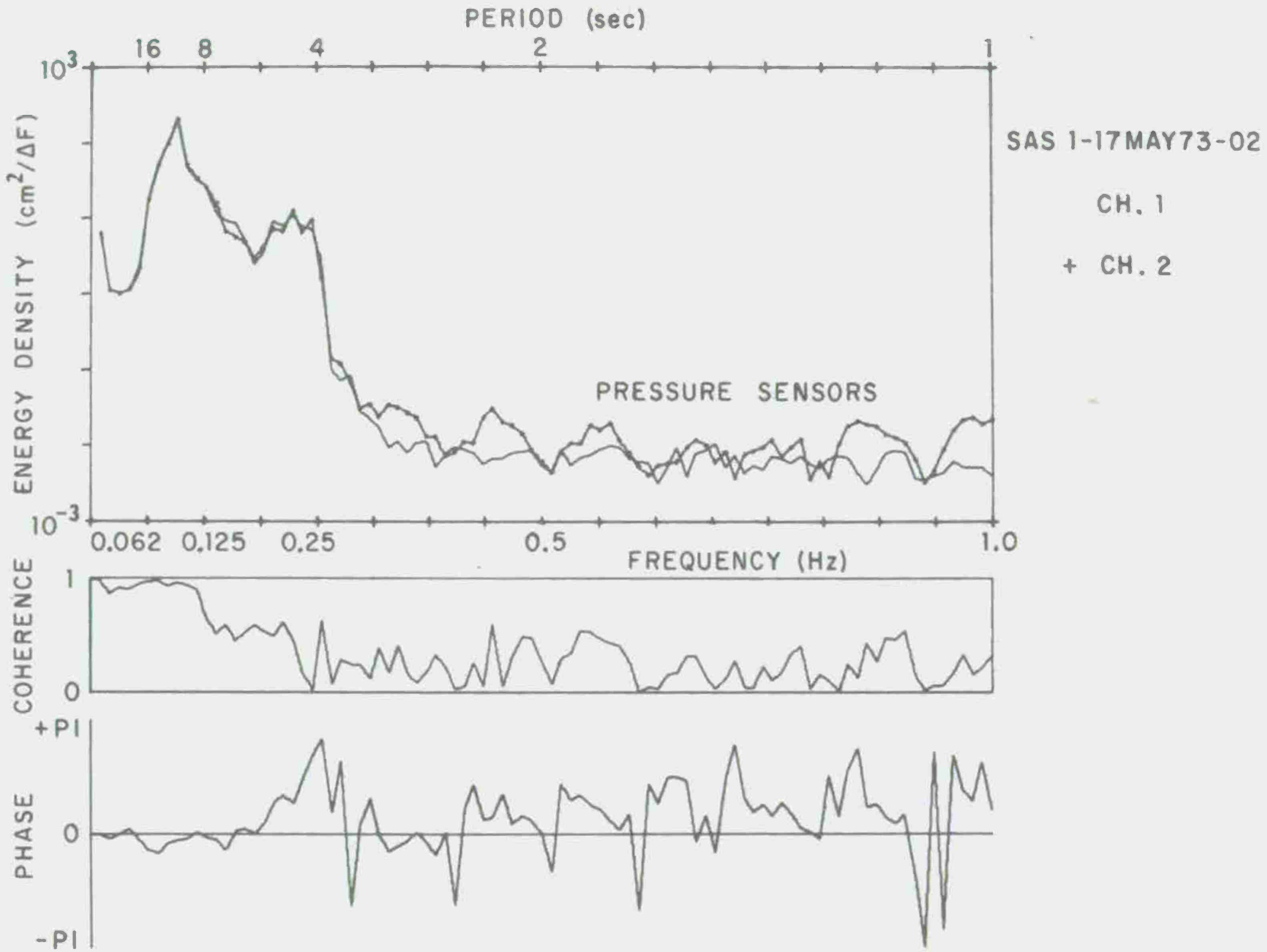

Figure V-20. Frequency and cross-spectra computed for sensors 1 and 2 of the pressure-sensor array. These are the associated frequency spectra for the directional spectra plotted in Figure V-19. The coherence of the higher frequency peak is relatively high.

The high-frequency directional spectra would probably be useful if either one of two situations existed: 1) there be a limited band of directions that one would expect energy, thus enabling one to ignore other regions of the spectrum; 2) the sampling be of the nature as to give a high resolution, unaliased picture of the directional spectrum. Condition 1) can never be satisfied because of the wide directional band nature of the high-frequency waves. The higher frequency waves not only are refracted less than the longer period waves but many times come from local winds at large angles to the shore. Condition 2) could be met with a suitably designed array. However, it is evident that our array was not designed well for the investigation of higher frequency waves with periods less than about 4.8 sec. There is a trade-off, of course, between a good design for looking at high-or low-frequency waves with a limited array. It is felt that our array was designed more properly for the investigation of the lower frequency waves, wave periods of 5.5 sec and longer, which contain most of the energy along this coast.

VI. WAVE CLIMATE

The wave climate at Torrey Pines Beach is controlled by many factors. The location and intensity of wave-generating storms are important in determining the nature of the swell which approaches the area. The blocking effect of the continental land mass and offshore islands causes the study region to be shadowed from waves from certain directions. Figure VI-1 displays the directions shadowed at the Torrey Pines site. No diffraction or refraction effects were taken into account when calculating the extent of the island's shadows. Therefore, Figure VI-1 should be treated as only a rough approximation of the shadowing effects. The refraction of waves, both by offshore and nearshore topography, also affects the nature of the waves measured.

Investigations were made into both the specific and average characteristics of the wave data. To display the average tendency of the wave climate, the data were grouped in terms of the four seasons. Figure VI-2 and Table I-1 (App. I) are two displays of the general wave climate for the summer runs of 1973. Figure VI-2 is a plot of energy versus period of the waves. A point has been plotted for each spectral peak for the summer records. Figures V-11, 12, and 13 are equivalent plots for the other three seasons. It should be noted that at each frequency there is a wide spread of recorded energies. This may differ greatly from the results of a visual study. For example, the long-period southern swell is only visually detectable at medium to high amplitudes. This is particularly true when there is another significant wave component present. Table I-1 (App. I) includes much the same information, but has the directional data included.

Figure VI-3 is a histogram which displays for the summer months the sum of the energy measured at a given frequency for each direction of propagation. Only the data when the frequency is a peak frequency are included in this presentation. This type of data grouping is of particular help in determining the importance of the several wave-generating

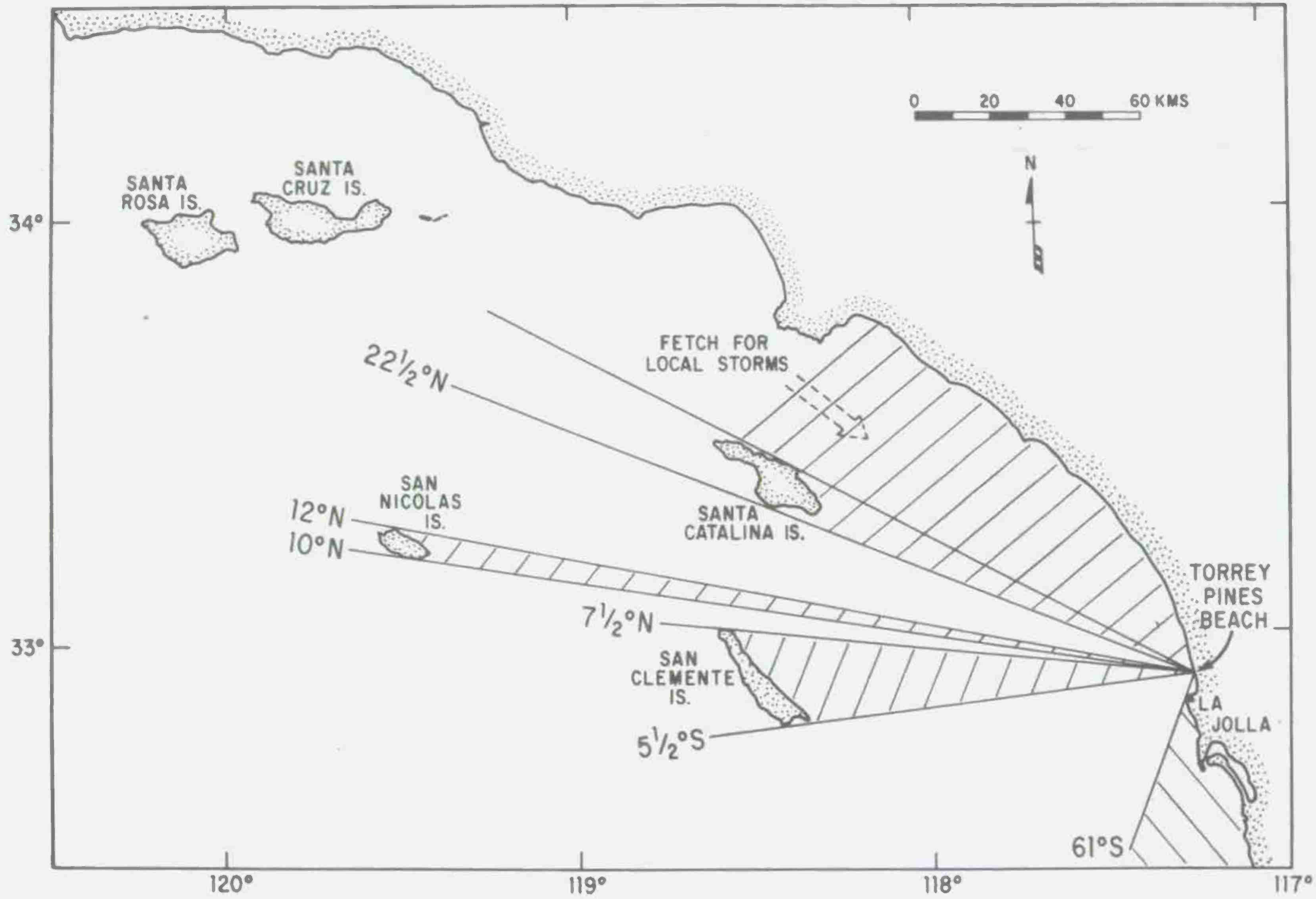

Figure VI-1. A rough chart of the continental borderland off southern California which displays wave shadowing effect of the islands. The unshaded regions show unaffected angles of deepwater approach of waves from distant storms incident to Torrey Pines Beach. The angles are given in degrees from normal to the beach, which is oriented true north and south at the site of measurement.

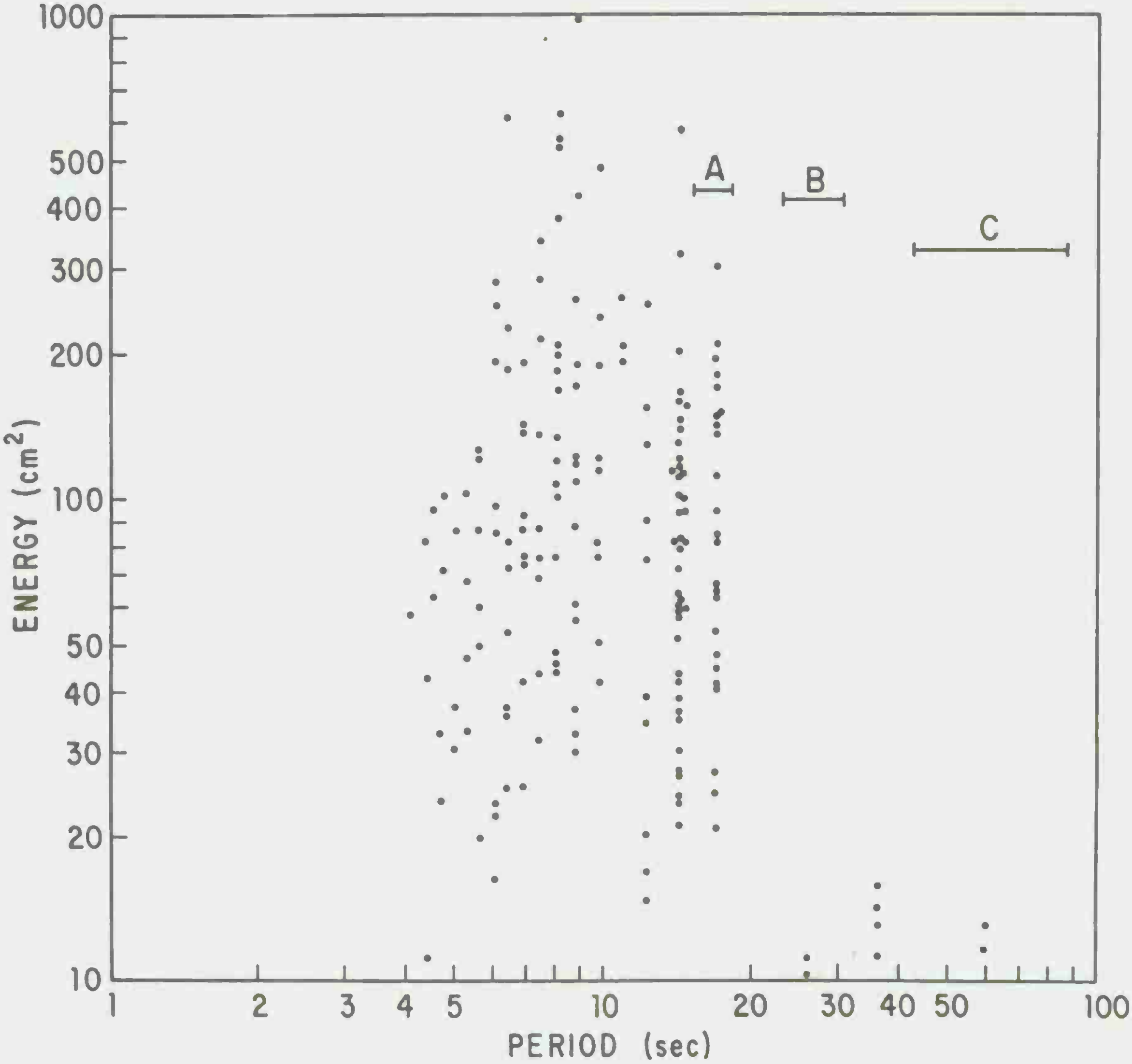

Figure VI-2. A representation of the wave climate for the months June, July, and August 1973. Each point represents the energy and central period for a spectral peak in a wave record. The bands A, B, and C represent the bandwidth of the frequency groups with central periods 16.8 sec, 26.2 sec, and 59.2 sec respectively. One hundred and nine runs were analyzed for the summer months. There are relatively few spectral peaks in the period range of 9 to 12 seconds. This fact reflects the persistence of the spectral trough shown in Figure VI-4 over the summer runs.

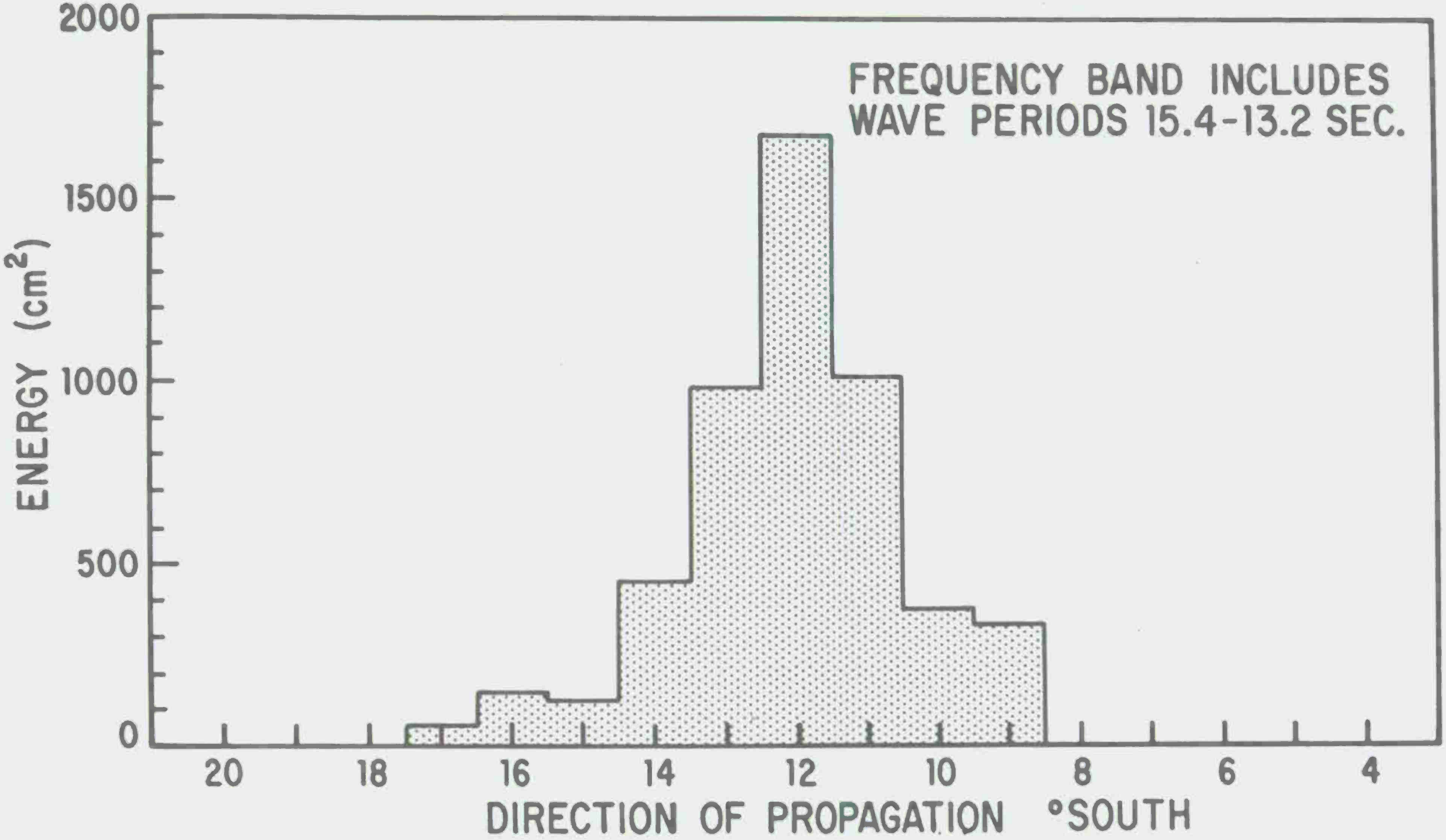

Figure VI-3. A plot of the total energy versus direction of propagation summed over 109 runs during June, July, and August 1973 for spectral peaks with a peak period of 14.2 seconds. The directions are in degrees from normal to the coast at Torrey Pines Station.

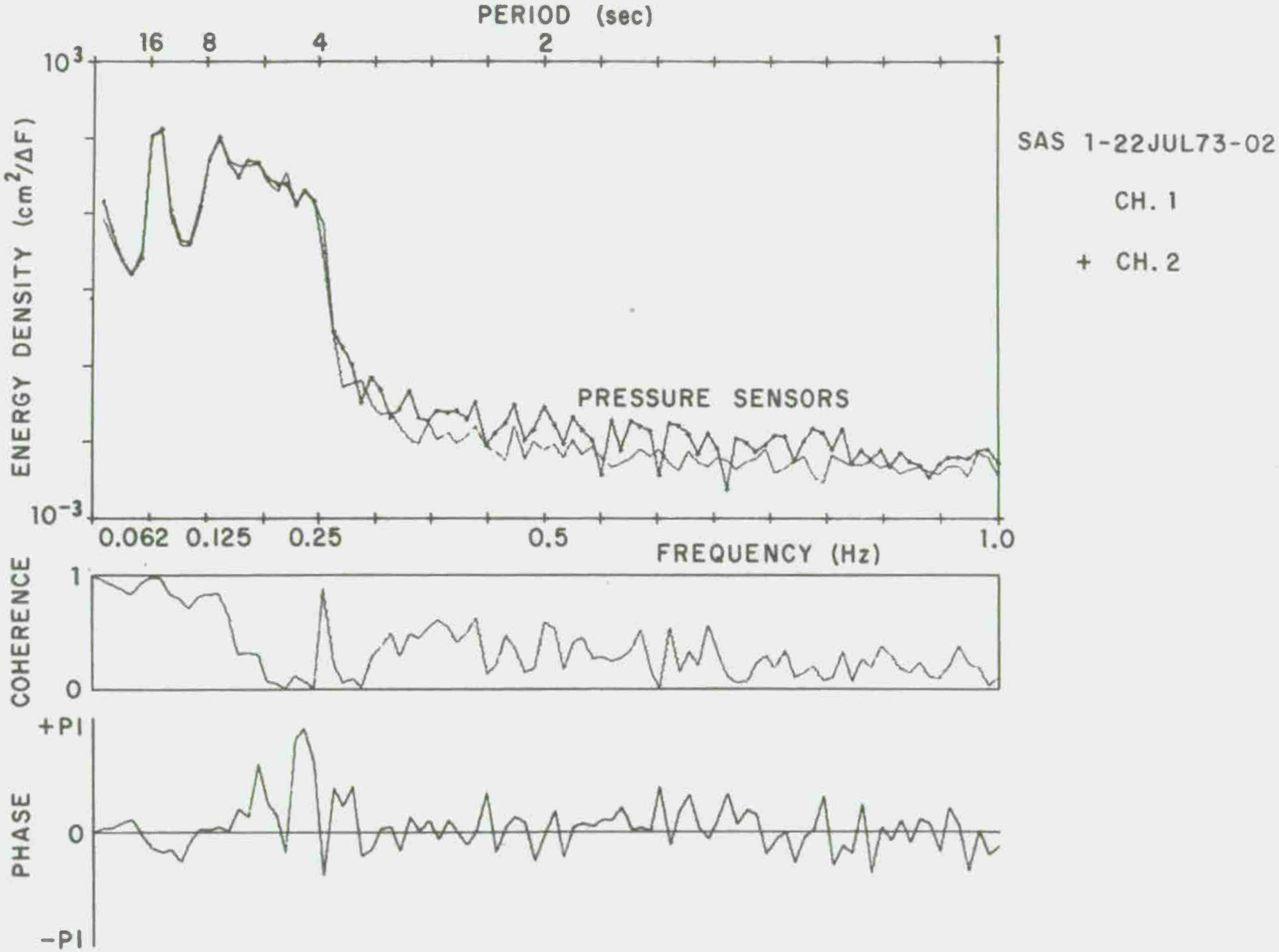

Figure VI-4. Frequency and cross-spectral results of two pressure sensors of the 1-2-1 array displaying the typical bimodal spectral form of summer wave field. The narrow low-frequency peak is south swell while the higher frequency waves are from a relatively local storm in the North Pacific.

regions during the various seasons. Appendix J includes the directional plots for the various wave periods and seasons.

The characteristics of the wave spectra generated from the several source regions determine the specific nature of the local wave field. A common summer form of the frequency directional spectra was observed. The characteristic bimodal form of the frequency spectra measured in the summer months is shown in Figure VI-4. The lower frequency peak is relatively narrow, about 0.04-Hz bandwidth, and the peak period is usually between 12-17 sec. The higher frequency peak is much broader, about 0.1 Hz in width, and its peak period is usually between 6-10 sec. The energy of the lower frequency peak is usually between 20-200 cm^2 with a mean energy of 100 cm^2. The higher frequency peak varies from 30-500 cm^2 with a mean of approximately 170 cm^2.

The directional data reveals that the lower frequency waves are very well directed and have angles to the beach at the 10-meter depth of 5° to 15° from the south. The higher frequency waves are in general less well directed and the peak is usually from 5° to 18° from the north. The bimodality of the spectra of the summer waves in this region has been noted in previous work (Inman, 1953).

The scatter diagram for fall (Figure VI-5) showing peak energy versus period is very similar to the plot for summer months. The directional plots reveal, however, that some of the long-period swell is coming from a northerly direction. In particular, the 12- to 14-second waves show a source around 6° to 9° north. The shorter period waves, below 12 seconds, are primarily coming from 8° to 20° north, while the waves around 16 seconds are still from the south.

The wave climate of the winter months differs greatly from that of summer and fall. Figure VI-6 shows the generally high-energy level of the spectral peaks in the winter. There is also an increase in the occurrence of medium to low energy 4-5 sec chop waves. The directional information indicates there are many components to the winter wave climate. The longer period waves are generally coming from 2° to 8° north, indicating North Pacific swell, but Figure VI-7 shows a definite southern component for the 14-sec waves. This south swell was also observed visually. The shorter period waves display a wider spread in directions, with primary sources from 2° to 15° north. However, Figure VI-8 shows a strong southern component to the 6.6- to 6.3-second waves. These relatively short southern waves are due to severe local storms which approach the area from approximately due west. The winds in the southeast quadrant of the approaching storm are southerly to southwesterly and are quite intense.

Figure VI-9 reveals a severe wave climate for the spring months. This is due primarily to storms which occur in the early part of the season. Figure VI-9 also shows that there is a larger occurrence of 9-12 sec waves in this season. The trough in this region of the spectrum for the summer months is definitely not evident here. The primary

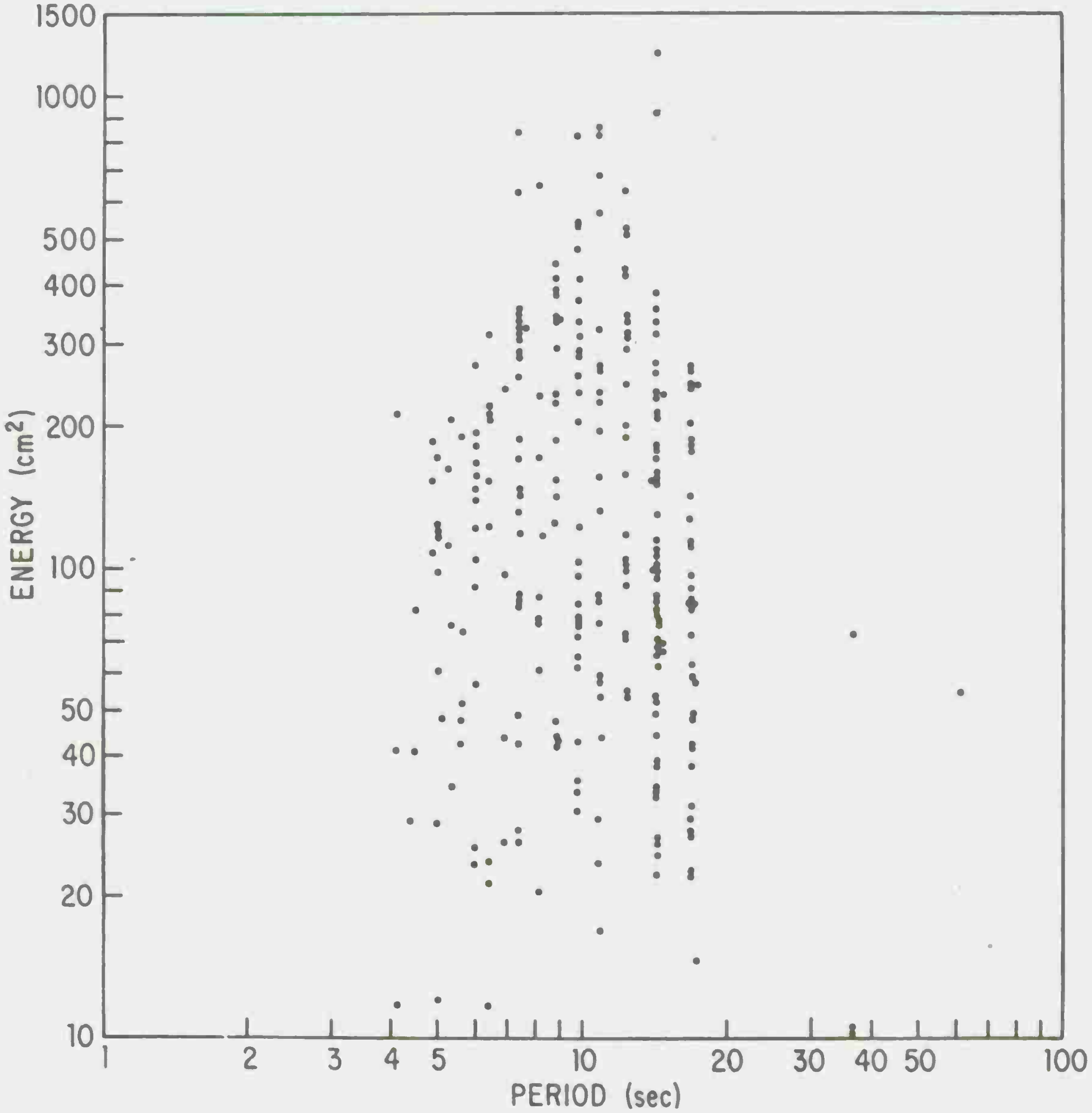

Figure VI-5. A representation of the wave climate for September, October, and November 1973. Each point represents the energy and central period for a spectral peak in a wave record. One hundred and twenty runs were analyzed for the fall months.

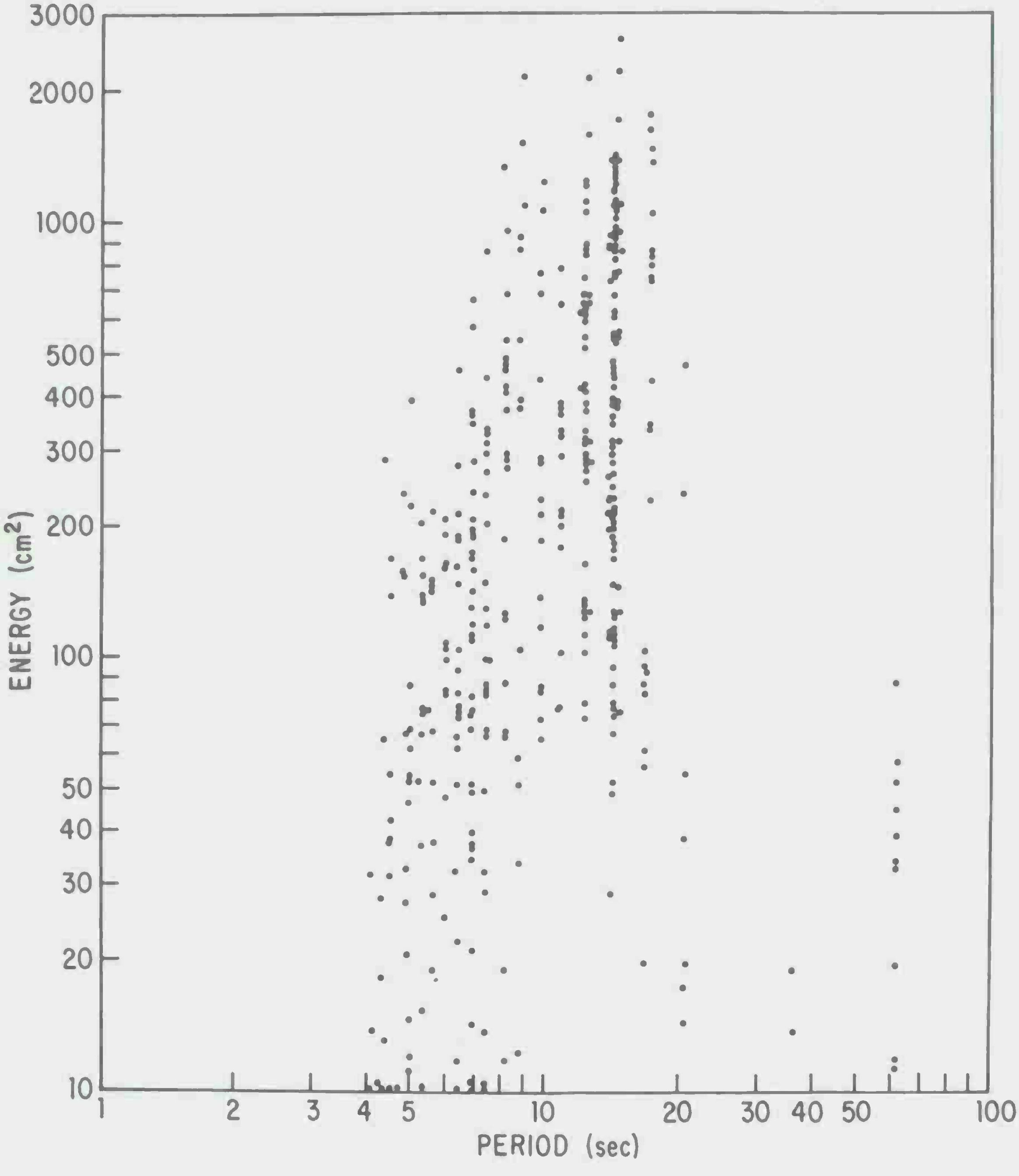

Figure VI-6. A representation of the wave climate for December, January, and February. A total of 181 runs was analyzed. The energy levels of the low-frequency peaks are significantly higher than for the summer and fall quarters. There is also more occurrence of the very long-period (∿ 60 seconds) peaks.

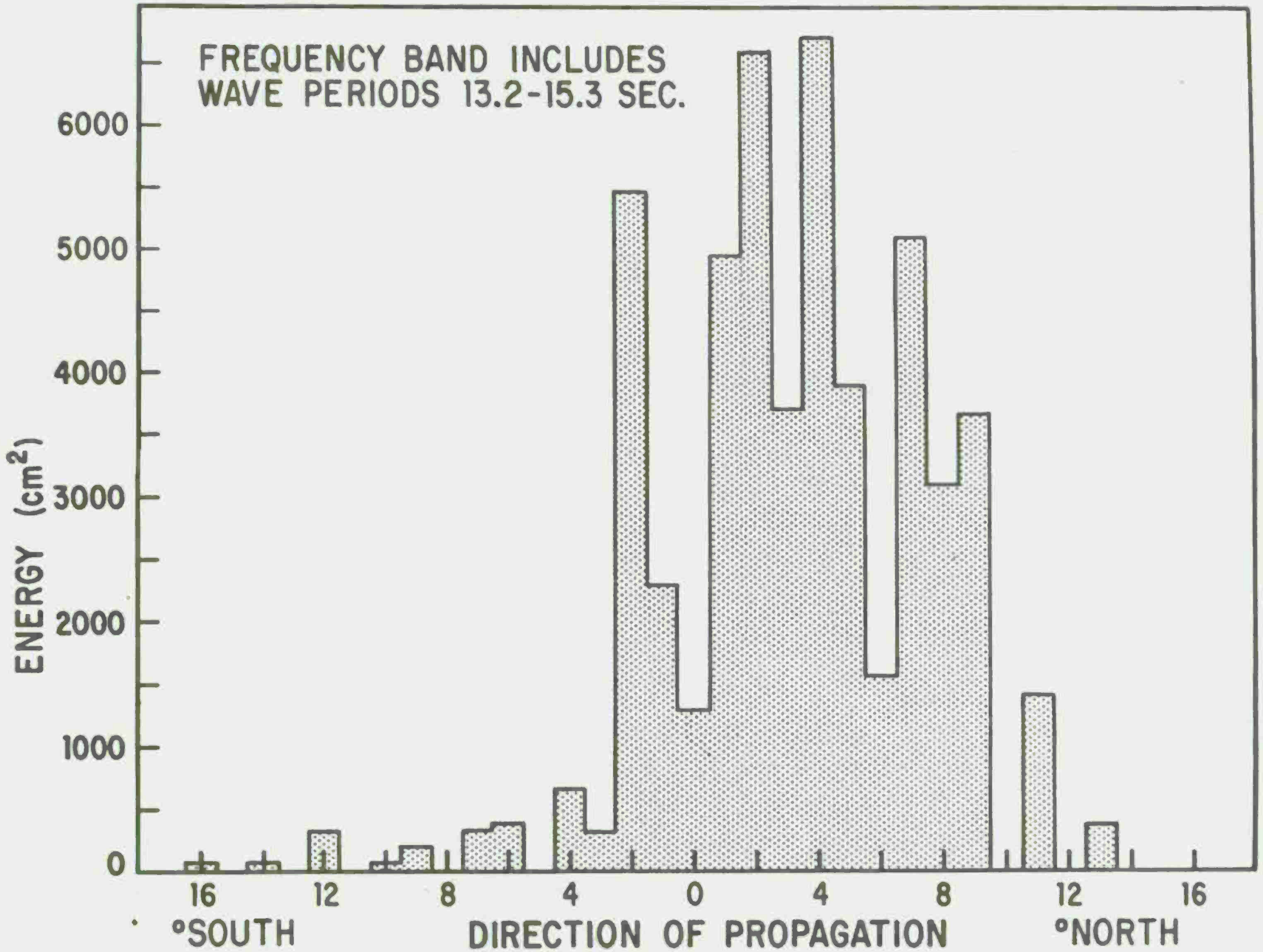

Figure VI-7. A plot of the total energy versus direction of propagation summed over 181 runs during December, January, and February for spectral peaks with a peak period of 14.2 seconds. The directions are in degrees from normal to the coast at the Torrey Pines Station. The plot indicates a southern source of wave energy as well as at least two significant sources in the northern quadrant.

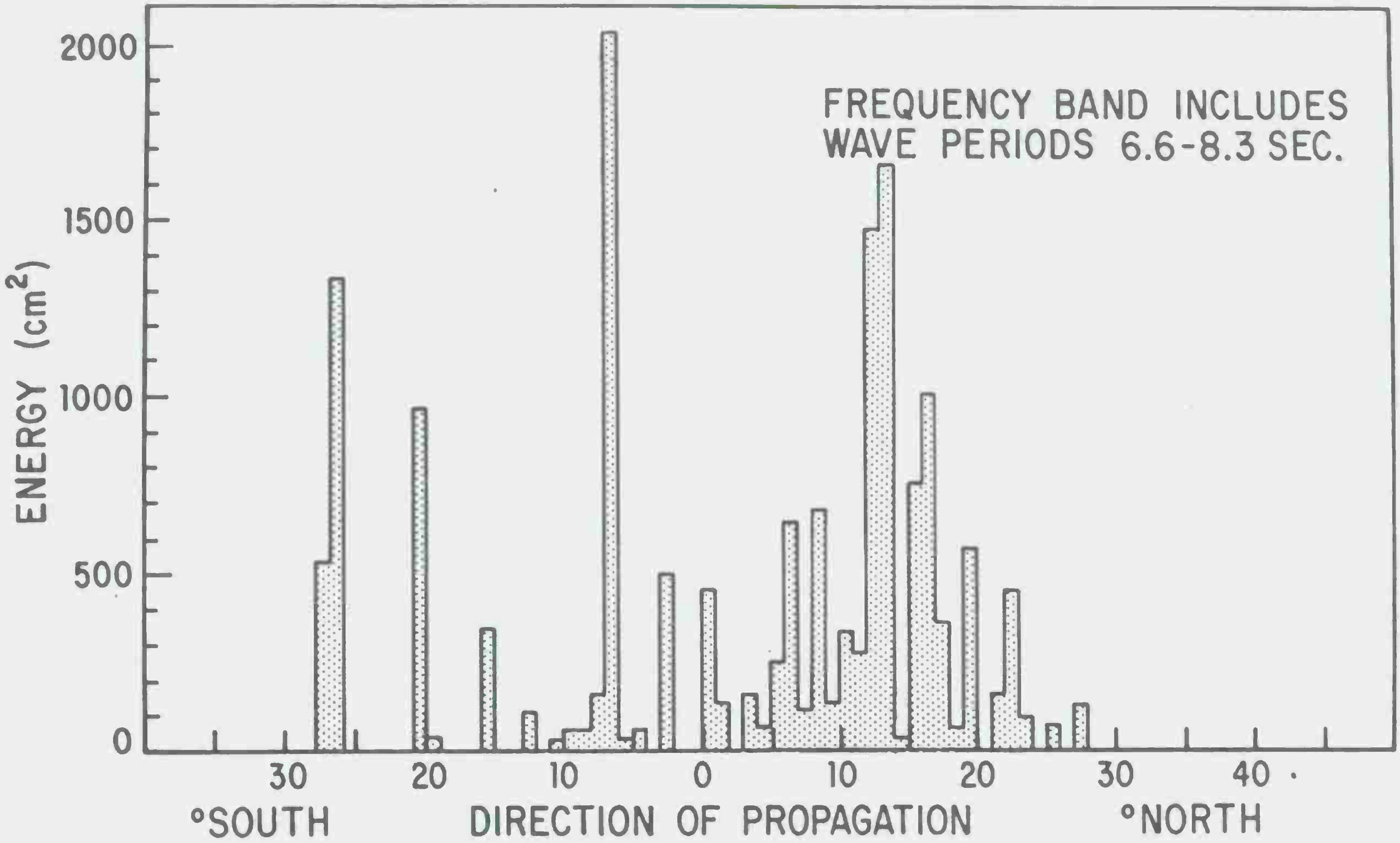

Figure VI-8. A plot of the total energy versus direction of propagation summed over 181 runs during December, January, and February for spectral peaks with peak period of 8.1, 7.4, and 6.9 seconds. The directions are in degrees from normal to the coast at the Torrey Pines Station. This plot displays a very wide directional band for higher frequency waves.

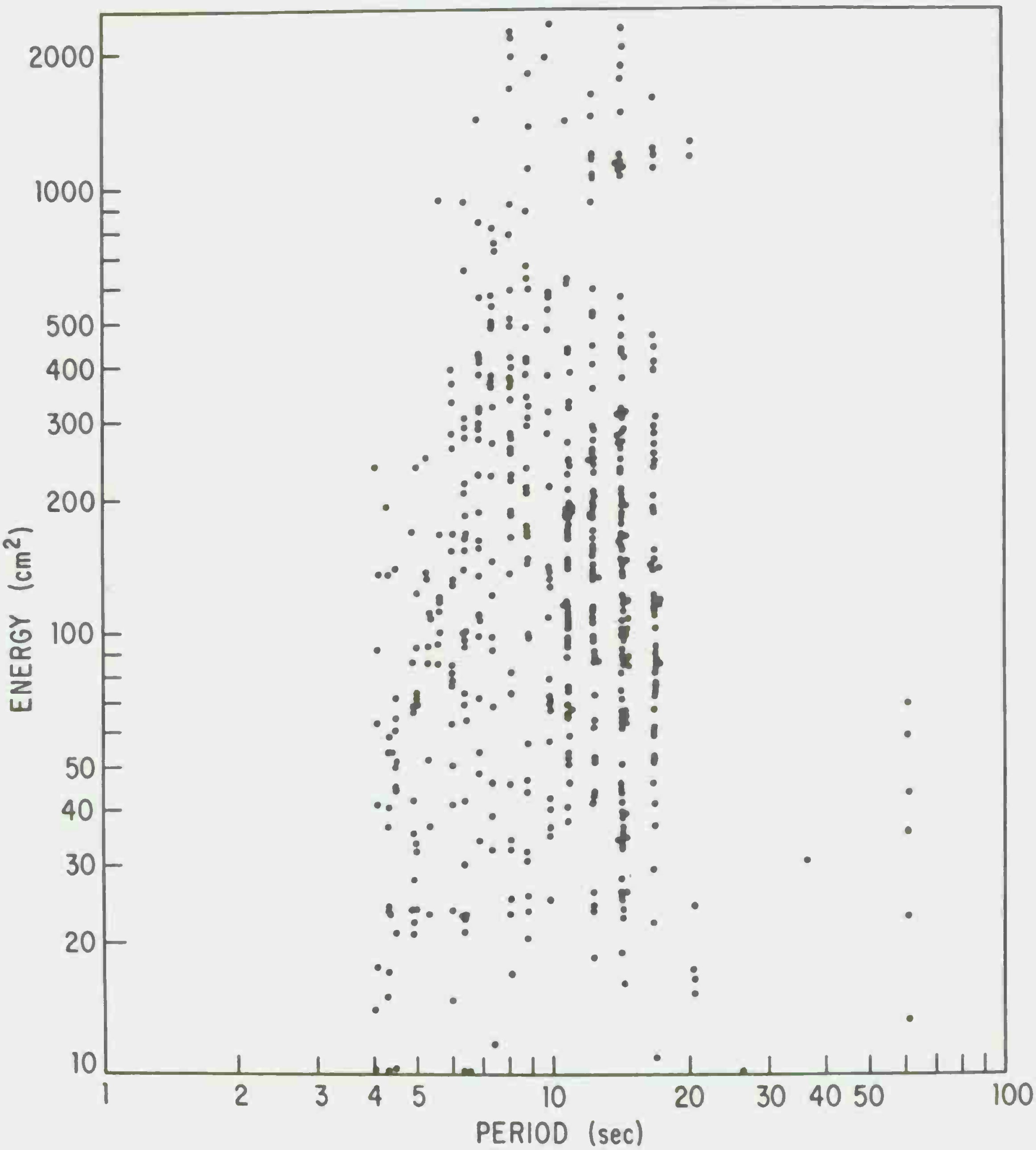

Figure VI-9. A representation of the wave climate for March, April, and May. The data were analyzed from 247 SAS runs. This quarter is a period of transition of wave climate and the result represents a mix of the summer and winter distributions. Therefore, the spectral peaks are relatively evenly distributed over the various energy levels and wave periods.

source of waves in this season are the North Pacific storms which generate waves with periods from 10 to 15 seconds coming from 2° to 8° north. The waves with periods around 16 seconds have both a northerly and southerly component but have generally much less energy than the shorter period waves.

Figure VI-10 displays the total energy of the 13.2- to 15.4-second waves recorded for all the runs analyzed. The figure reveals at least three principal sources of energy: 10° to 12° south, 1° to 3° south, and 2° to 8° north. The shaded portion of the plot reveals the energy recorded during nine runs of the storm which occurred from 27 to 30 March 74. This indicates the importance that local storms play in the total energy budget for the year in this region.

The significant height, $H_{1/3}$, or the mean height of the highest 1/3 waves, is related to the variance $\langle\eta^2\rangle$ by Longuet-Higgins (1952) for a narrow band Gaussian wave field,

$$H_{1/3} \sim 4 \langle\eta^2\rangle^{1/2}. \qquad \text{(VI-1)}$$

This has been empirically justified by many researchers, including Longuet-Higgins (1952), Goda (1974), and Larsen (1974), for open ocean waves. The significant height was calculated from each run and the probability distribution function for the significant height is plotted in Figure VI-11. The plot reveals that the waves of winter and spring have a higher mean $H_{1/3}$ than summer or fall, but a larger expected variance of $H_{1/3}$ values also.

VII. CONCLUSIONS

The wave climate study off Torrey Pines Beach has provided considerable insight into the problems associated with obtaining wave energy and directional spectra in shallow nearshore waters. A summary of the findings from this study are presented below:

1. A trial performance of the system off Scripps Pier which was directed toward determining the likely long-term performance of the system was only moderately successful. This was because long-term structural fatigue of the fiberglass shelf station, which later led to flooding and station malfunctioning, could not be evaluated in a short period trial.

2. The SAS system has proven to be a viable method for obtaining data from the nearshore waters. It remained on station and intact during severe storm conditions. Identification of major failure modes and the elimination of these failures have resulted in increasing the recovered data to better than 75 percent of the scheduled observations.

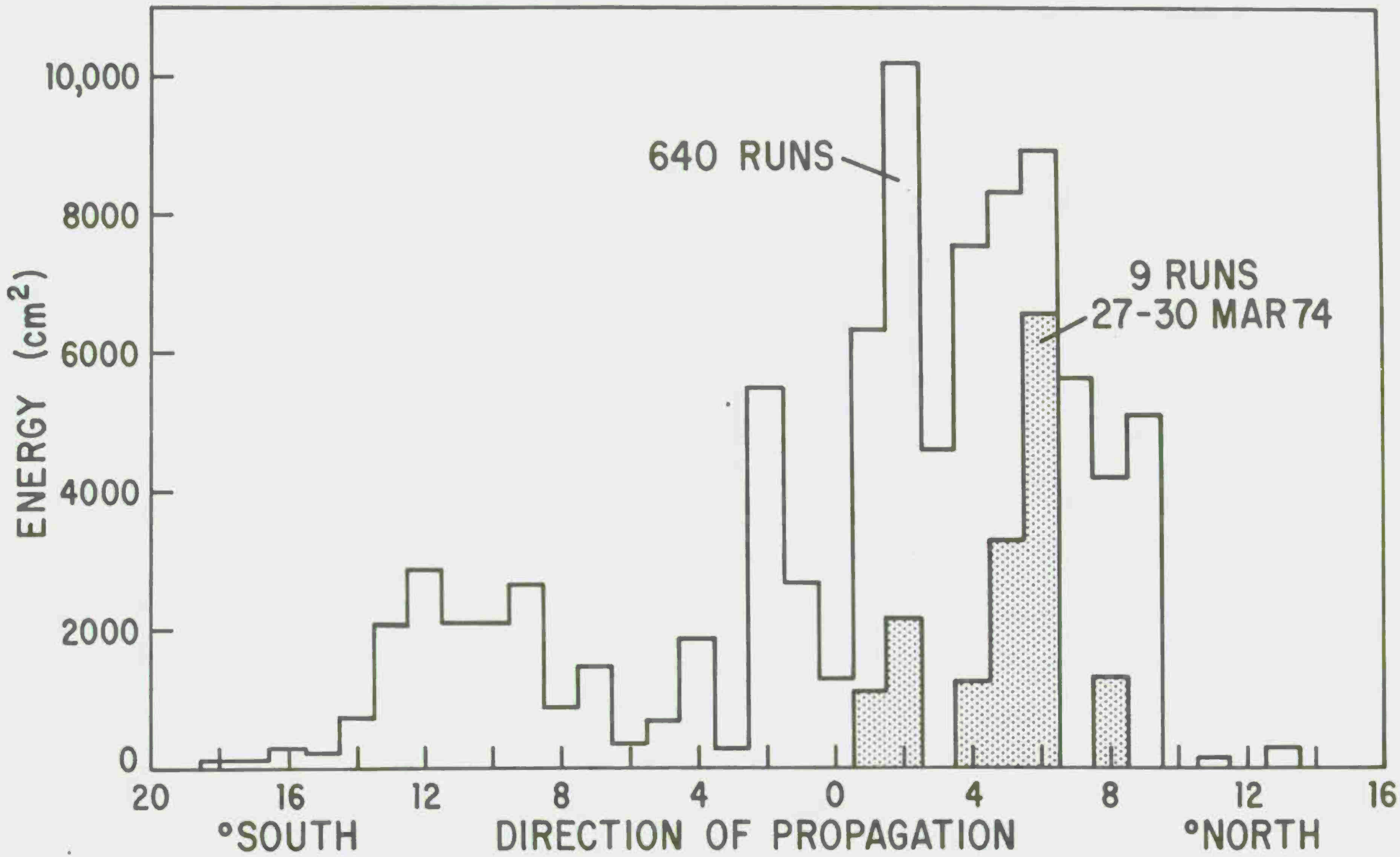

Figure VI-10. A display of the total energy measured for the spectral peaks with a wave period of 14.2 seconds evaluated from all the measured runs. The 27 to 30 March 1974 data (shaded) shows the importance of storm waves in the total energy budget.

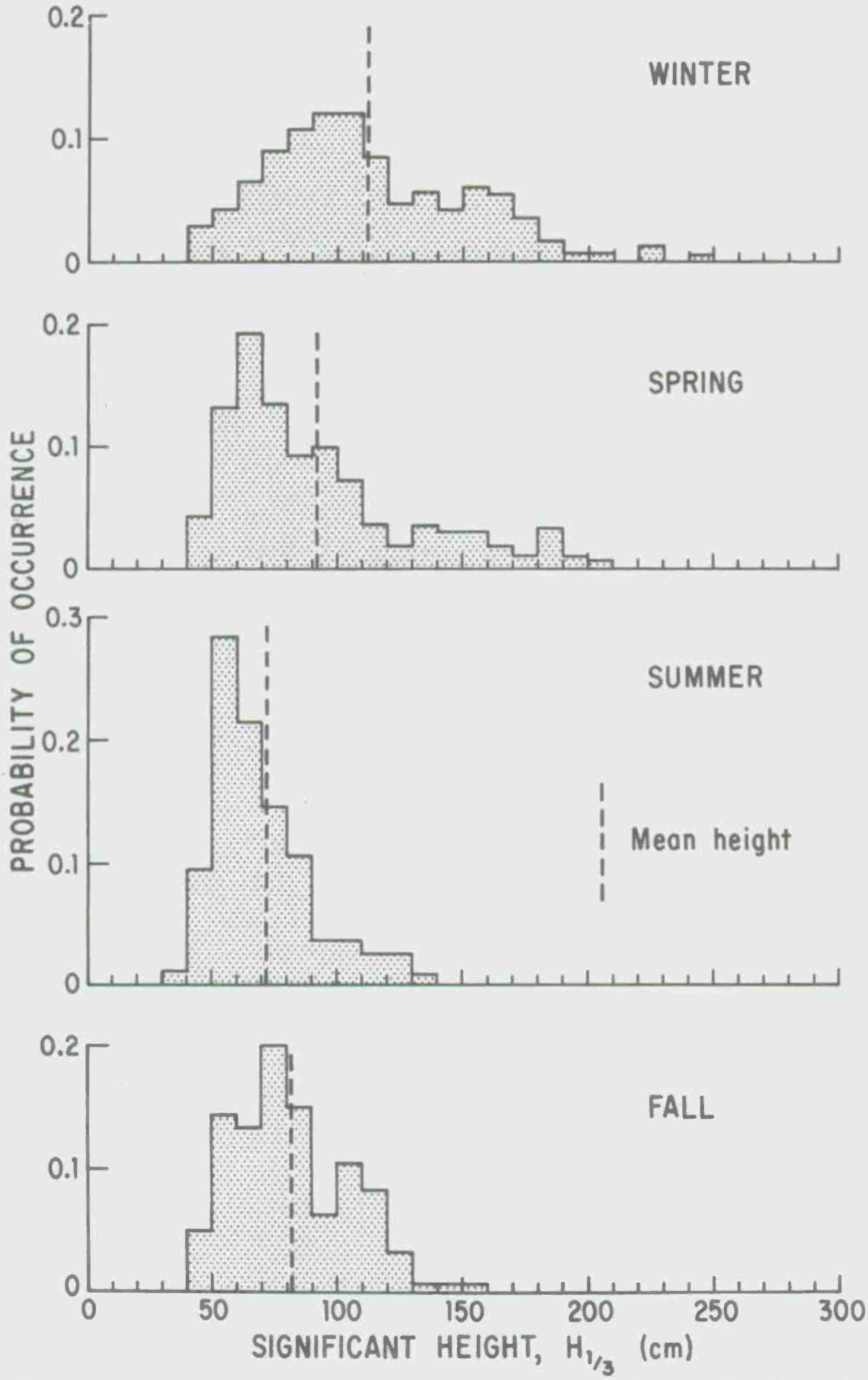

Figure VI-11. A plot of the distribution functions of significant wave height for the various seasons. The height of the plot gives the probability of occurrence of the associated 10-cm wave height class. The wave heights were calculated from the pressure-sensor data in 10-meter depths. The mean significant height is also indicated for each season.

3. The frequency and directional information derived from the line array of pressure sensors were sufficient for the specification of wave climate. That is, the energy and primary direction of dominant spectral peaks (waves from 5 to 20 seconds) were obtained with some degree of confidence.

4. The array was best suited for measuring the directional spectra of waves with periods around 5.5 seconds. Directional measurements of lower frequency waves lacked resolution, while "aliasing" problems made the interpretation of higher frequency directional spectra difficult.

5. The measurement of directional spectra through the use of current meters suffers a lack of resolution relative to the array measurements. The determination of the primary direction of wave propagation from the two different methods agreed within ±4°.

6. The total wave energy estimated by the various pressure sensors of the array had an average range in values of approximately 20 percent of its mean. The results of a sample of 27 runs indicated the range in energy of the dominant spectral peak as estimated from the four sensors varied by only 12 percent of the mean value.

7. The total wave energy obtained from the surface-piercing wave staff differed from the pressure sensor value by an average of 17 percent of the mean. The average difference of band energy density between the frequency spectra of the wave staff and pressure sensor was also approximately 17 percent of the mean. This suggests a systematic nature to the differences between the spectra of the wave staff and the pressure sensor. However, the sensor which recorded the highest energy level of the two varied over the runs.

8. The visual measurements of wave period and direction agreed with the array measurements when the wave spectra were narrow band in frequency and direction. The visual estimates of wave height did not agree consistently with the results from the pressure sensors.

9. The frequency band comparisons of spectral density of velocity fluctuations measured by a current meter with those estimated by a pressure signal yielded an average difference between the two of 20 percent of this mean. Significant differences up to 50 percent occurred at the frequency bands of maximum spectral density.

10. Accelerometer data used to obtain wave direction gave values which agree with direction from the array to within ±5° for 75 percent of the peaks compared. The motion of the spar was recorded by the accelerometers can provide a convenient method of obtaining wave direction.

11. Waves of dominant spectral peaks are well correlated (coherence 0.75) over distances greater than their wavelength. The coherence

between sensors for relative minimums in the energy spectra drops sharply with sensor separation. The coherence for frequencies on the higher frequency slope of the energy spectra was consistently low for all sensor separations.

12. The frequency spectra of summer waves have a characteristic bimodal form. The relatively narrow lower frequency peak (10 to 16 seconds) is southerly and well directed. The broader high-frequency peak (peak period around 6 to 10 seconds) is generally less well directed and usually from 5° to 10° north.

13. The wave climate of the fall months closely resembles the summer results with the addition of a small northern component to the longer period waves.

14. The wave climate of the winter and spring months is much more severe than the summer and fall; the average total energy recorded for the spring and winter months was over two times as great as the average for the summer. The cumulative results for winter and spring showed a large amount of energy for waves of periods 12 to 15 seconds approaching the beach at angles of 5° to 15° north in 10-meter depth.

15. A small southern component to the longer period waves 13 to 18 seconds appeared in the wave climate of the winter months. Some higher frequency southerly waves, periods of 5 to 18 seconds, were correlated with local frontal passages.

16. The energy supplied by brief but severe storms of winter and spring contributes significantly to the total energy budget for a year.

LITERATURE CITED

BARBER, N.F., "The Directional Resolving Power of an Array of Wave Detectors," *Ocean Wave Spectra*, Prentice-Hall, Englewood Cliffs, N.J., 1963, pp. 137-150.

BENDAT, J.S., and PIERSOL, A.G., *Random Data: Analysis and Measurement Procedures*, Wiley-Interscience, New York, 1971.

BOWDEN, K.F., and WHITE, R.A., "Measurements of the Orbital Velocities of Sea Waves and their Use in Determining the Directional Spectrum," *Geophysical Journal, Royal Astronomical Society*, Vol. 12, 1966, pp. 33-54.

COOLEY, J.W., and TUKEY, J.W., "An Algorithm for the Machine Calculation of Complex Fourier Series," *Mathematics of Computations*, Vol. 19, No. 90, 1965, pp. 297-301.

COTE, L.J., et al., "The Directional Spectrum of a Wind Generated Sea as Determined from Data Obtained by the Stereo Wave Observation Project," *Meteorological Papers*, Vol. 2, No. 6, New York University, N.Y., 1960.

DICKE, R.H., and WITTKE, J.P., *Introduction to Quantum Mechanics*, Addison-Wesley, Reading, Mass., 1960.

GODA, Y., "Estimation of Wave Statistics from Spectral Information," *Proceedings of the International Symposium on Ocean Wave Measurement and Analysis*, New Orleans, La., Sept. 1974.

INMAN, D.L., "Areal and Seasonal Variations in Beach and Nearshore Sediments at La Jolla, California," TM-39, U.S. Army, Corps of Engineers, Beach Erosion Board, Washington, D.C., Mar. 1953.

INMAN, D.L., KOMAR, P.D., and BOWEN, A.J., "Longshore Transport of Sand," *Proceedings of the 11th Conference on Coastal Engineering*, American Society of Civil Engineers, London, Vol. 1, 1969, pp. 298-306.

KOMAR, P.D., and INMAN, D.L., "Longshore Sand Transport on Beaches," *Journal of Geophysical Research*, Vol. 75, No. 30, 1970, pp. 5914-5927.

LARSEN, L.H., and FENTON, D.R., "Observations of Waves in the North Pacific," *Proceedings of the International Symposium on Ocean Wave Measurement and Analysis*, New Orleans, La., Sept. 1974.

LONGUET-HIGGINS, M.S., "On the Statistical Distribution of the Heights of Sea Waves," *Journal of Marine Research*, Vol. XI, No. 3, Yale University, New Haven, Conn., 1952, pp. 245-266.

LONGUET-HIGGINS, M.S., CARTWRIGHT, D.E., and SMITH, N.D., "Observations of the Directional Spectrum of Sea Waves Using the Motions of a Floating Buoy," *Ocean Wave Spectra*, Prentice-Hall, Englewood Cliffs, N.J., 1963, pp. 111-136.

LOWE, R.L., INMAN, D.L., and BRUSH, B.M., "Simultaneous Data System for Instrumenting the Shelf," *13th International Conference on Coastal Engineering*, American Society of Civil Engineers, 1972, pp. 95-112.

MUNK, W.H., "The Solitary Wave and its Application to Surf Problems," *Annals of the New York Academy of Science*, Vol. 51, 1949, pp. 376-424.

MUNK, W.H., et al., "The Directional Recording of Swell from Distant Storms," *Philosophical Transactions of the Royal Society of London*, Vol. 255, No. 1062, Series A, 1963, pp. 505-584.

PANICKER, N.N., and BORGMAN, L.E., "Directional Spectra from Wave Gage Arrays," *12th International Conference on Coastal Engineering*, American Society of Civil Engineers, 1970, pp. 117-135.

SIMPSON, J.H., "Observations of the Directional Characteristics of Sea Waves," *Geophysical Journal of the Royal Astronomical Society*, Vol. 17, 1969, pp. 93-120.

APPENDIX A

THEORETICAL DEVELOPMENT OF DIRECTIONAL SPECTRA

The intent of this appendix is to give a more detailed description of the procedure for obtaining directional spectra. The problems introduced due to finite sampling are detailed. In addition, the procedures used in the interpretation of the analysis are developed and the terms used in the results of the analysis are defined.

Time series consisting of surface wave heights measured simultaneously at several points in space can be used to estimate a frequency-directional spectrum for surface waves. The assumption of stationarity in space, that is, a frequency spectrum and cross-spectrum independent of position in the wave field has been used in the calculation of the energy-directional spectrum. The assumption of stationarity in time is required only for the interpretation of the results.

Before discussing the frequency-directional spectrum a few definitions will be introduced. Define the Fourier transform pair:

$$\begin{aligned} f(x) &= \int_{-\infty}^{\infty} F(k_x)\, e^{2\pi i k_x x}\, dk_x \\ F(k_x) &= \int_{-\infty}^{\infty} f(x)\, e^{-2\pi i k_x x}\, dx\ , \end{aligned} \qquad \text{(A-1)}$$

where $F(k_x)$ is the one-dimensional Fourier transform of $f(x)$; x is a coordinate in the onshore-offshore direction; and $k_x = 1/L_x$ is the wave number in the x-direction. Allow the above operations to be represented by the following notation:

$$\begin{aligned} F(k_x) &\supset f(x) \\ f(x) &\supset F(k_x)\ , \end{aligned} \qquad \text{(A-2)}$$

where the transform notation $F(k_x) \supset f(x)$ indicates that $f(x)$ is

the Fourier transform of $F(k_x)$. Now, define the convolution of two arbitrary functions of x, $f(x)$ and $g(x)$, to be $H(X)$ where X is a distance in the x-direction:

$$H(X) = \int_{-\infty}^{+\infty} f(x)\, g(X - x)\, dx , \qquad \text{(A-3)}$$

and let this operation be represented by the notation:

$$H(X) = g(x) * f(x).$$

The convolution theorem states:

$$\begin{aligned} f(x) \cdot g(x) &\supset F(k_x) * G(k_x) \\ f(x) * g(x) &\supset F(k_x) \cdot G(k_x) , \end{aligned} \qquad \text{(A-4)}$$

where

$$f(x) \supset F(k_x) \quad \text{and} \quad g(x) \supset G(k_x). \qquad \text{(A-5)}$$

Barber (1963) has a good treatment of the convolution theorem.

The treatment of frequency-directional spectra below follows the development of Barber (1963). Consider the surface elevation, $\eta(x,y,t)$ as a function of the onshore-offshore coordinate x; the longshore coordinate y; and, time t. If $\eta(x,y,t)$ is known over a region extending in the x-direction from 0 to A, in the y-direction from 0 to B, and over the times $t = 0$ to $t=C$, the surface elevations may be represented by the following Fourier series:

$$\eta(x,y,t) = \sum_{\ell=-\infty}^{\infty} \sum_{m=-\infty}^{\infty} \sum_{n=-\infty}^{\infty} A_{\ell,\,m,\,n} e^{2\pi i\left(\frac{\ell x}{A} + \frac{my}{B} + \frac{nt}{C}\right)}, \tag{A-6}$$

where ℓ , m, and n are integers; and, $A_{\ell\ n,m}$ is an infinite three-dimensional matrix. The convolution of $\eta(x,y,t)$ with itself gives the function called the lag correlogram, $R(X,Y,\tau)$ where X is a spatial lag in the x-direction; Y is a spatial lag in the y-direction; and, τ is the lag in time

$$R(X,Y,\tau) = \frac{1}{ABC} \int_{x=0}^{A} \int_{y=0}^{B} \int_{t=0}^{C} (x,y,t)\cdot(x+X,y+Y,t+\tau)dx\ dy\ dt. \tag{A-7}$$

From the convolution theorem, the lag correlogram can be represented by the following series:

$$R(X,Y,\tau) = \sum_{\ell=-\infty}^{\infty} \sum_{m=-\infty}^{\infty} \sum_{n=-\infty}^{\infty} |A|^2_{\ell,m,n}\ e^{2\pi i\left(\frac{\ell X}{A} + \frac{mY}{B} + \frac{n\tau}{C}\right)}, \tag{A-8}$$

where $|A|^2_{\ell,m,n}$ is the squared modulus of $A_{\ell,m,n}$ Allow equation (8) to be expressed in the following integral form:

$$R(X,Y,\tau) = \int_{-\infty}^{\infty} \int_{-\infty}^{\infty} \int_{-\infty}^{\infty} S(k_x,k_y,f)\ e^{2\pi i(k_x X,k_y Y,f\ )} dk_x\ dk_y\ df, \tag{A-9}$$

where k_x and k_y are the x and y components of the wave number; f is the frequency, and $S(k_x,k_y,f)$ is a set of Dirac delta functions occurring at integer values of k_x,k_y, and f with integrated values equal to the appropriate $|A|^2_{\ell,m,n}$. The function $S(k_x,k_y,f)$ represents the frequency-directional spectrum and has the units $cm^2/(\Delta f\ \ \Delta k_x\ \Delta k_y)$. $S(k_x,k_y,f)$ can be found exactly if

the lag correlogram is known for all separations X, Y, and τ. Assume $R(X, Y, \tau)$ is given for all values of X, Y, τ. Then,

$$R(X, Y, \tau) \supset S(k_x, k_y, f), \tag{A-10}$$

where $S(k_x, k_y, f)$ is the true spectrum.

The results of finite sampling can be seen in the following way: Let $\hat{R}(X,Y,\tau)$ be a finite sampled version of $R(X,Y,\tau)$; in other words $\hat{R}(X,Y,\tau)$ is the function that we would actually measure:

$$\hat{R}(X, Y, \tau) = R(X, Y, \tau) \cdot g(X, Y, \tau), \tag{A-11}$$

where $g(X, Y, \tau)$ is a set of unit delta functions which weights the known values of the lag correlogram. That is $g(X, Y, \tau)$ is 0 except for values of X and Y that correspond to separation of sensors. At these space intervals $g(X, Y, \tau)$ is equal to 1 (Barber, 1963). The spectrum that we calculate, $\hat{S}(k_x, k_y, f)$, is then tne transform of $\hat{R}(k_x, k_y, f)$.

In the analysis of the frequency-directional spectra it will be assumed that the time domain is sufficiently well known so that the sampling problems in the space domain can be treated separately. In this case $g(X,Y,\tau)$ is not a function of τ and the spectrum becomes:

$$\hat{S}(k_x,k_y,f) \supset \left[\hat{R}(X,Y,\tau) = R(X,Y,\tau) \cdot g(X,Y)\right]. \tag{A-12}$$

From the convolution theorem:

$$\hat{S}(k_x, k_t, f) = S(k_x, k_y, f) * G(k_x, k_y) \tag{A-13}$$

$$\hat{S}(k_x,k_y,f) = \int_{-\infty}^{\infty} \int_{-\infty}^{\infty} S(k_{xo},k_{yo},f)\, G(k_{xo}- k_x,k_{yo}-k_y)\, dk_{xo}\, dk_{yo} ,$$

where k_{xo}, k_{yo} are dummy variables and

$$g(X,Y) \supset G(k_x, k_y). \tag{A-14}$$

$G(k_x, k_y)$ is called the spectral window. For the linear array with four sensors, $g(X,Y)$ is a set of 13 delta functions: one at $X=0$, $Y=0$, and the others at the ± 6 lags available in the array. Each delta function in theory has an arbitrary integrated value; i.e., the known values of the lag correlogram may be weighted to optimize our estimate of the spectrum. The 1-2-1 configuration reduces the set of lags to 9 as the 1 and 3 lags are redundant.

A window suggested by Barber (1963) for its narrow central peak has equal integral values of all the delta functions, that is all equal to unity. This rectangular lag window introduced by Barber has the form:

$$G(k_x, k_y, f) = 1 + 2 \sum_{n=1}^{4} \cos 2(k_x x_n + k_y y_n). \tag{A-15}$$

It should be noted that if $G(k_x, k_y, f)$ were a delta function, the calculated spectrum would equal the true spectrum (neglecting noise). Therefore, one attempts to construct a window which is close in shape to a delta function. The finite width of the central peak of this function introduces smearing of the spectral estimates and thus introduces a reduction in resolution. The major lobes of the function cause an ambiguity in direction or aliasing. A sample of a Barber window is plotted in Figure A-1.

The first step toward obtaining the frequency-directional spectrum is to transform the lag correlogram in time:

$$\int_{-\infty}^{\infty} R(X,Y,\tau)\, e^{-2\pi i f \tau} d\tau = C(X,Y,f) - iQ(X,Y,f). \tag{A-16}$$

The functions $C(X,Y,f)$ and $Q(X,Y,f)$ are obtained from the band averaged Fourier coefficients from the FFT results. This, of course, only approximates the infinite integral of equation (A-16). The problems

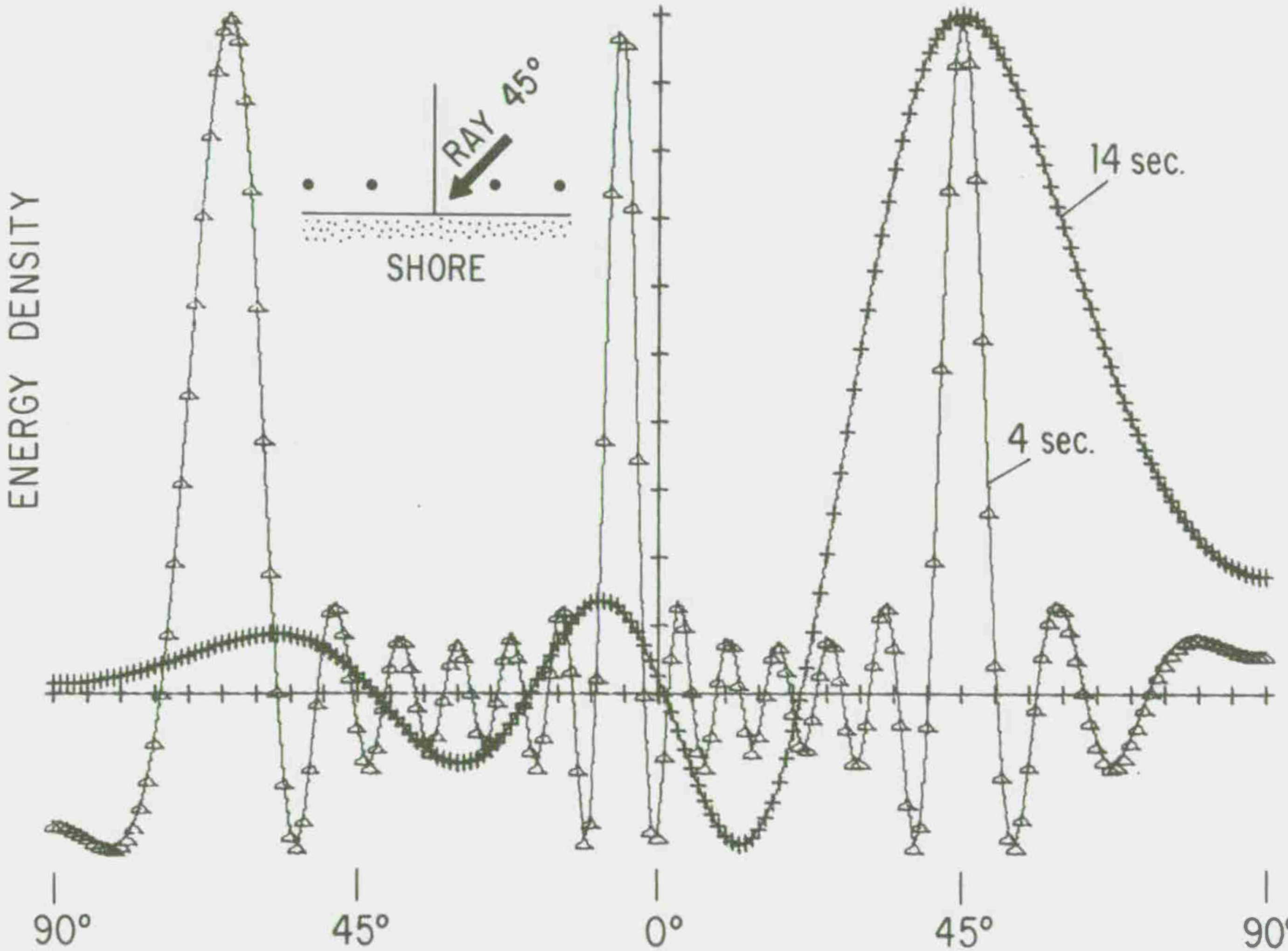

Figure A-1. A plot of the Barber Window for waves of period 14 and 4 seconds. The Window gives the response of the array to waves of a single direction propagating at an angle of 45° north relative to the normal to the array. The energy density values are in relative units.

resulting from this approximation are analogous to those of the approximation of the space transformation, but are much less severe due to the large amount of time lags. The sampling rate of four samples per second is high enough to avoid aliasing problems in the frequency spectrum.

The analysis is now carried out at a frequency, f_o. The frequency-directional spectrum is obtained from the transformation:

$$S(k_x,k_y,f_o) = \int_{-\infty}^{\infty} \int_{-\infty}^{\infty} \left[C(X,Y,f_o)-iQ(X,Y,f_o)\right] e^{-2\pi i(k_xX+k_yY)} dX\,dY. \tag{A-17}$$

If it is assumed that C and Q are zero except at the spacial lags given by the array, the above integral becomes the summation:

$$S(k_x,k_y,f_o) = \sum_{n=-N}^{N} \left[C(X_n,Y_n,f_o)-iQ(X_n,Y_n,f_o)\right] e^{-2\pi i(k_xX_n + k_yY_n)} \tag{A-18}$$

for the 1-2-1 array where $N = 4$.

Let α be an angle measured from the normal to the array. Then $k_x = k \cos\alpha$ and $k_y = k \sin\alpha$ where k is the magnitude of the wave number. The only spatial lags are in the y-direction. Since

$$P(X_n,Y_n,f_o) = P(-X_n, -Y_n,f_o) \quad \text{and} \quad Q(X_n,Y_n,f_o) = -Q(-X_n, -Y_n,f_o),$$

equation (A-18) becomes:

$$S(f_o, \alpha) = C(0,f_o) + 2 \sum_{n=1}^{4} \left[C(Y_n,f_o)\cos(2\pi kY_n\sin\alpha)+Q(Y_n,f_o)\sin(2\pi kY_n\sin\alpha)\right], \tag{A-19}$$

where k is fixed by f_o, and the depth by the linear wave theory dispersion relation (note that k was defined as $1/L$ instead of the usual $2\pi/L$):

$$2\pi f_o^2 = g\ k \tanh(2\pi kh). \tag{A-20}$$

Equation (A-19) is used for the practical calculation of the directional spectrum, i.e., the energy density as a function of the directions of propagation of waves of frequency f_o.

The limited number of sensors and the finite length of the array produce a window, $G(k_x,k_y,f_o)$ which smears sharp spectral peaks into broader ones. In an attempt to better resolve the directional structure of the incoming waves, a fitting technique was implemented. It is assumed in this procedure that the wave trains present are well directed and few in number. The procedure begins with a fit of the measured spectra with a hypothesized result due to a wave train of single frequency f_o coming from a single direction. This procedure will be referred to as a fit to a single wave train. A model spectrum is generated by convolution of an ideal single wave train spectra with the spectral window. The model directional spectrum is least-squared fit to the measured space spectrum, the variables being the direction of propagation and energy of the hypothesized incoming waves. If $S(f_o,\alpha)$ = measured spectrum value, $\hat{S}_{\alpha_o}(f_o,\alpha)$ = computed value of the model spectrum as a function of the hypothesized direction of propagation, α_o, then the relation,

$$P(\alpha_o) = \frac{\sum_{\alpha=-90}^{90} \left[S(f_o,\alpha) - \hat{S}_{\alpha_o}(f_o,\alpha)\right]^2}{\sum_{\alpha=-90}^{90} \left[S(f_o,\alpha)\right]^2} \tag{A-21}$$

becomes a measure of best fit.

The function is given in percent and it is a measure of effectiveness of the fit as it is the ratio of the sum of squared residuals to the sum of data values squared. A plot of $P(\alpha_o)$ versus α_o reveals a minimum and it is the α_o which produces the minimum $P(\alpha_o)$ that is assumed to be the best direction of fit to a single wave train. The broadness of the minimum region suggests an uncertainty to the direction obtained. The spread in values of α_o for which $P(\alpha_o)$ is approximately the same, within roughly 10 percent of the lowest value, is termed the uncertainty, $\Delta\alpha_o$. The size of $P(\alpha_o)$ suggests the effectiveness of the one wave fit. The summation (A-21) was routinely evaluated for

steps in α of 5°. Values of $P(\alpha_o)$ (in percent) below 10.0 were considered indications of a good fit. This implies the true directional spectrum is unimodal and narrow. Values of $P(\alpha_o)$ between 10.0 and roughly 50.0 indicate some departure from the single direction model but α_o should be the dominant direction of energy propagation. If $P(\alpha_o)$ is above 50.0, the fit is considered to be poor.

CHARACTERIZATION OF SPECTRAL PEAKS

The characterization of the frequency spectrum attempts to describe the total spectrum as a finite sum of significant peaks.

Energy peaks are selected for each channel of a run by a computer program which seeks the maximum energy value of the spectrum and then proceeds on a change of slope technique to choose the right and left limits defining the bandwidth of the peak. The values in the peak are then set equal to zero and the process continues for a maximum of four peaks. In order to avoid calling a single jump a peak, a condition is imposed that the energy value in question should be either at least twice as high as the previous value or higher than two previous ones.

Using this method, it is possible to compare the spectra obtained from the time series record of each of the four pressure sensors for any run. It is seen that the bandwidth of a given peak agrees among these four spectra to within $2\Delta f$ (where $\Delta f = 0.0107$). There were some instances where the bandwidths were more than $2\Delta f$ apart, but in these cases channels 1 and 2 agreed to within $2\Delta f$, while channels 3 and 4 agreed. This pairing of channels (1 with 2 and 3 with 4) is also evident in both the total energy of the spectrum and the energies of the individual peaks. Whether this is due to instrumentation, wave direction, or some other factor is not yet known.

The peak energy, peak period, and bandwidth of each spectral peak for the spectra of all four sensors were evaluated. The peak energy and bandwidth listed for each spectral peak in the tables of Appendix D are mean values of the results for the four sensors. The peak period given is the mode period of the results of the various sensors.

Figure A-2 displays a sample spectra which is used in the following example of how the peak investigation is carried out.

Single jumps, as at A_3 and A_6 are counted as separate peaks if their value is either: 1) higher than twice the previous one; or 2) higher than two previous values. For instance, A_3 is not counted as a peak since neither condition holds ($A_3=24<2A_2=32$; $A_3=24<A_1=56$). On the other hand, A_6 is counted as a peak since condition 2) holds ($A_6=8>A_4=6$) even though condition 1) does not hold ($A_6=8<2A_5=10$). In this case three peaks would be chosen. Each peak is given the period of its highest energy value. Peak 3 is assigned the period of the point A_6.

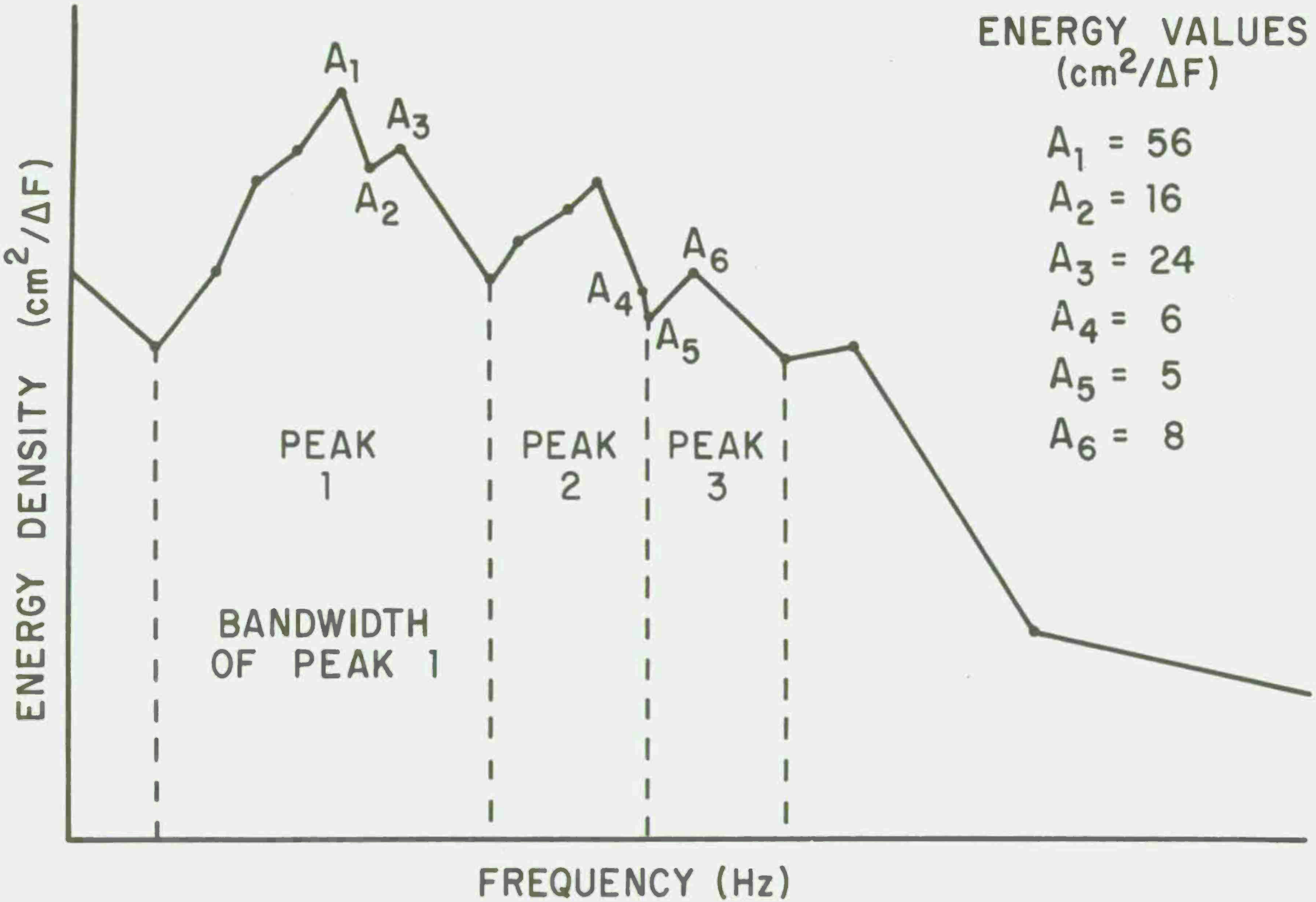

Figure A-2. Sample spectra illustrating the results of the peak selection procedure. The method employed has defined three peaks.

APPENDIX B

DYNAMICS AND EXPECTED PERFORMANCE OF THE TILTING SPAR

The dynamic response of the spar to oscillatory flow has been examined by laboratory modeling as well as by computer analysis of the nonlinear differential equations. The method of measuring the tilt angle using orthogonally mounted accelerometers is presented.

LABORATORY STUDY

The shelf station is a forced, damped oscillator and as such will have a resonant frequency. A model study was conducted to determine if this resonant frequency could be observed.

A one-seventh scale model of the station was constructed and tested in the wind-wave channel at Scripps Institution of Oceanography. Displacements of the station were measured photographically and wave height and period were measured using digital wave staff. The model was driven by waves of periods from 2.0 to 9.0 seconds.

Obtaining a meaningful resonance curve as a function of variable wave frequency requires that the maximum forcing torque, the restoring moment, the drag coefficient, and the coefficient of inertia remain the same for each driving frequency. This is accomplished by adjusting wave height with frequency to maintain a constant Strouhal number (the Strouhal number is defined as $u_m T/D$ where u_m is the maximum orbital velocity, T is the wave period, and D is the spar diameter), and by normalizing the displacements to equivalent maximum acceleration and displaced volume.

Figure B-1 gives the resonance curve for angular displacement normalized to the resonant frequency (f_1 = 0.16 Hz) for equivalent maximum acceleration and displaced volume. The curve is of the proper shape and should reflect with some accuracy the resonant frequency of the full-size spar. However, the model does not accurately reflect the magnitude of the resonance. While constant Strouhal conditions preserve the drag coefficient, the smaller orbital velocities under scaled conditions generate drag torques that are only 2 percent of what is necessary to compare in scale to those of the full scale spar.

ANALYSIS OF EQUATION OF MOTION

The tilting spar's motion can be described by considering the various forces acting on it. Because the spar is firmly anchored, only forces that produce torques about the universal joints are considered. Four moment-producing forces act on the spar. A buoyant force acts with a moment arm equal to the distance from the U-joint to the center of buoyancy times the sine of the tilt angle (θ). This moment is represented by the first term on the left-hand side of equation (B-1).

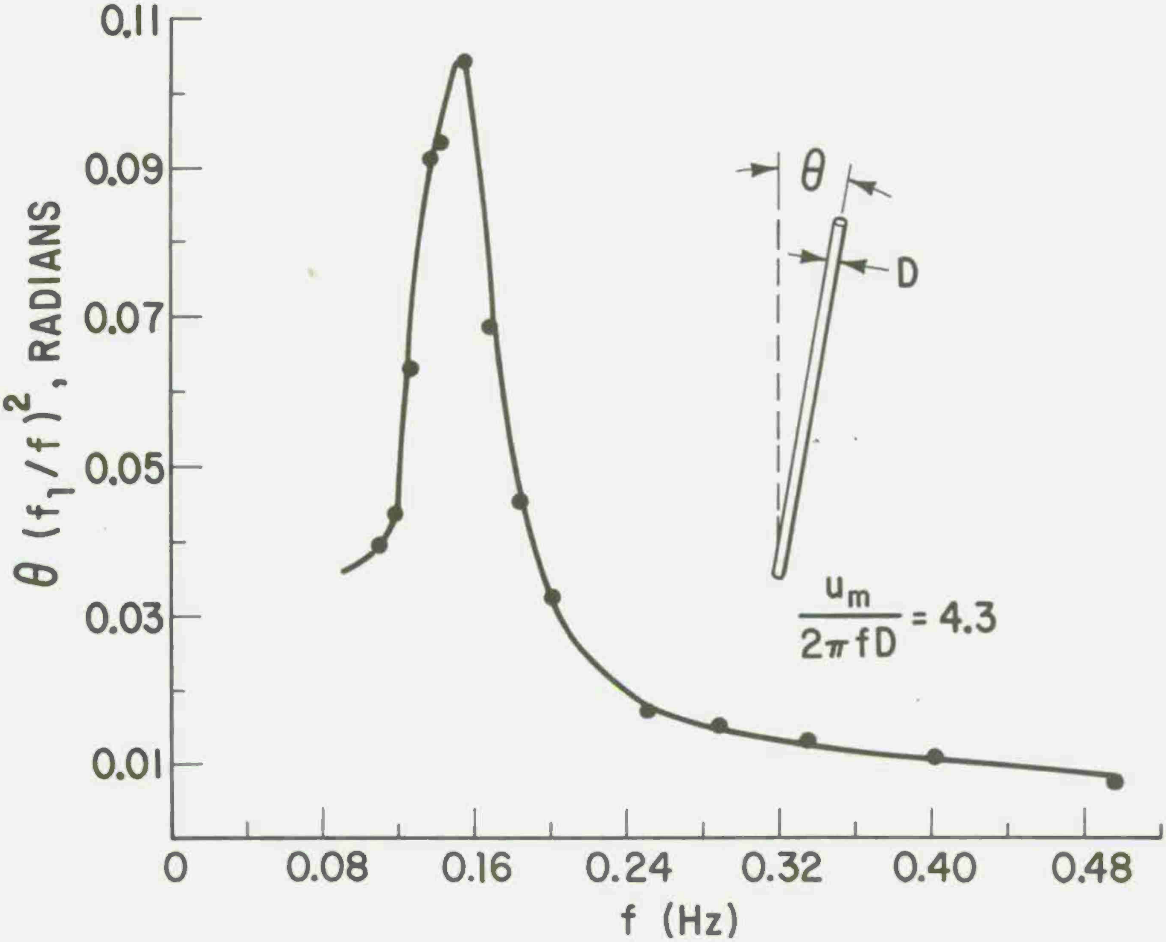

Figure B-1. Response curve obtained from 1/7th scale model of spar. Resonance is observed at 0.16 Hz. The magnitude of the resonant peak does not reflect the full-scale spar.

Two forces caused by the waves are represented by the second and third terms of equation (B-1). The first of these forces is the force that would exist on the water particles within the enclosed volume of the submerged spar in the absence of the spar. This force is distributed along the vertical axis of the spar. The second of the wave-generated forces is the virtual mass force, caused by a moving body in an accelerating fluid.

A drag force must also be included which is chosen to be proportional to the square of the relative velocity of the water and the spar. This force is also distributed along the vertical axis of the spar and is represented by the fourth term on the left of equation (B-1).

These moment-producing forces must be balanced by inertial forces which accelerate the spar. The term of the right-hand side of equation (B-1) is the moment of the spar itself:

$$\sin(\theta) g\, Z_B M_B - \rho a \int_{-h}^{0} \pi r^2 \, z \, dz - \rho c_a \int_{-h}^{0} (a - \ddot{\theta} z) \, \pi r^2 \, z \, dz$$

$$- \frac{1}{2} c_f \rho \int_{-h}^{0} |u - \dot{\theta} z| \, (u - \dot{\theta} z) \, 2rz \, dz = \ddot{\theta} I_s \, , \qquad \text{(B-1)}$$

where θ is the angle of tilt of the spar measured from the vertical, $\dot{\theta}$ is the angular velocity of the spar, g is the acceleration of gravity, Z_B is the distance from the U-joint to the center of buoyancy, M_B is the net buoyancy, ρ is the density of seawater, u is the horizontal water particle velocity, a is the horizontal water particle acceleration, r is the radius of the spar, z is the water depth, c_f is the drag coefficient and for a cylinder is approximately equal to 1.0, $\ddot{\theta}$ is the angular acceleration of the spar, I_s is the moment of inertia of the spar, and, $c_a = c_m - 1$ where c_m is the virtual mass coefficient and is approximately 2.0 for a cylinder.

The equation of motion (B-1) is a nonlinear ordinary differential equation which has been numerically integrated. It was assumed that the spar did not flex and that the velocity profile under the wave was independent of depth (i.e., shallow water wave theory applies). These assumptions were necessary in order to simplify the analysis. θ was small such that $\sin\theta \approx \theta$ for all cases anlayzed. Response of tilt angle versus wave frequency for various maximum orbital velocities were computed. Figure B-2 is a plot of these response curves. It is clear from these curves that at high velocities (large waves) resonance is not apparent. At low orbital velocities, however, there is a marked resonance occurring at about 0.1 Hz.

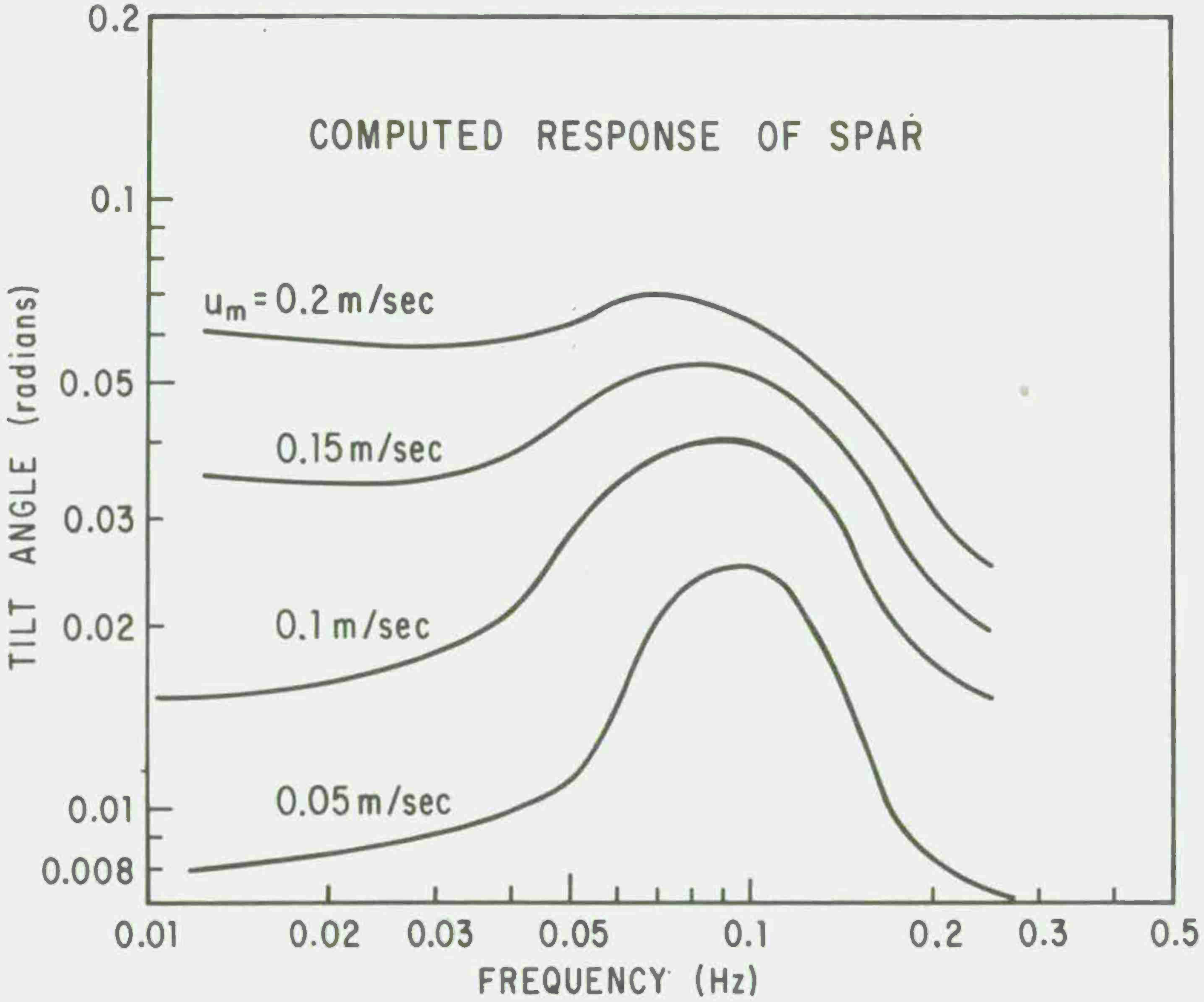

Figure B-2. Computed response of the spar for various maximum orbital velocities (u_m). These curves were obtained by integrating equation B-1.

MEASUREMENT OF TILT ANGLE

Two accelerometers orthogonally mounted in the top of the spar detect the motion caused by the water movement. These accelerometers sense acceleration normal to the major axis of the spar. For waves with periods ranging from 5 sec to 16 sec, both the acceleration due to gravity and the motion must be taken into account. Equation (B-2) describes the acceleration sensed by one of the accelerometers:

$$\tilde{a}(t) = -g \sin\theta(t) + L\,\frac{d^2\theta(t)}{dt^2}, \qquad \text{(B-2)}$$

where $\tilde{a}$ is the measured acceleration, g is the acceleration of gravity, L is the length of the spar, θ is the angle of tilt from the vertical in the x,z plane or the y,z plane. $\tilde{a}(t)$ can be expressed in terms of its Fourier components:

$$\tilde{a}(t) = \sum_{n=0}^{k} A_n e^{in\Delta\sigma t}, \qquad \text{(B-3)}$$

where the A_n are Fourier components, i is $\sqrt{-1}$, k is the number of incremental frequencies, $\Delta\sigma$ is the angular frequency resolution.

Solving equation (B-2) for each of the coefficients defined in equation (B-3) gives:

$$A_n e^{in\Delta\sigma t} = -g \sin\theta_n(t) + L\,\frac{d^2\theta_n(t)}{dt^2}. \qquad \text{(B-4)}$$

Let $X_n = \theta_n(t)$, $\sin\theta_n(t) \sim \theta_n(t)$ for small angles,

$$\frac{d^2X_n}{dt^2} - \frac{g}{L}X_n = \frac{A_n}{L} e^{in\Delta\sigma t} \qquad \text{(B-5)}$$

The general solution of this differential equation is:

$$X_n = B_n e^{i(n\Delta\sigma t + \phi)} , \tag{B-6}$$

where ϕ is an arbitrary phase angle, thus,

$$\frac{d^2X_n}{dt^2} = -B_n(n\Delta\sigma)^2 \; e^{i(n\Delta\sigma t + \phi)}. \tag{B-7}$$

Substituting for X_n and $\frac{d^2X_n}{dt^2}$ in equation (B-5) gives:

$$-B_n(n\Delta\sigma)^2 e^{i(n\Delta\sigma t + \phi)} - \frac{g}{L} B_n e^{i(n\Delta\sigma t + \phi)} = \frac{A_n}{L} e^{in\Delta\sigma t} \tag{B-8}$$

Dividing them by $e^{in\Delta\sigma t}$ and replacing $e^{-i\phi}$ with $(\cos\phi - i \sin\phi)$ gives:

$$-B_n(n\Delta\sigma)^2 - \frac{g}{L} B_n = \frac{A_n}{L} \left(\cos\phi - i \sin\phi\right). \tag{B-9}$$

ϕ can be eliminated by noting $i \sin\phi = 0$; therefore $\phi = 0$. Solving for B_n gives:

$$B_n = - \frac{A_n}{g + L(n\Delta\sigma)^2}. \tag{B-10}$$

We can now write $\sin\theta_n(t)$ in terms of the Fourier coefficient of $\tilde{a}(t)$:

$$\theta(t) = \sum_{n=0}^{k} - \frac{A_n}{g + L(n\Delta\sigma)2} e^{in\Delta\sigma t} \tag{B-11}$$

With the above procedure the spectrum and the time series of the angle of tilt can be obtained from the accelerometer data.

Figure B-3 is a plot of the position (in the x-y plane) of the shelf station as a function of time. The predominant motion is on-offshore which is caused by the swell and wind-driven wave. However, a longshore motion is also present and has a period on the order of 60 seconds as illustrated in Figure B-4.

3073-3584

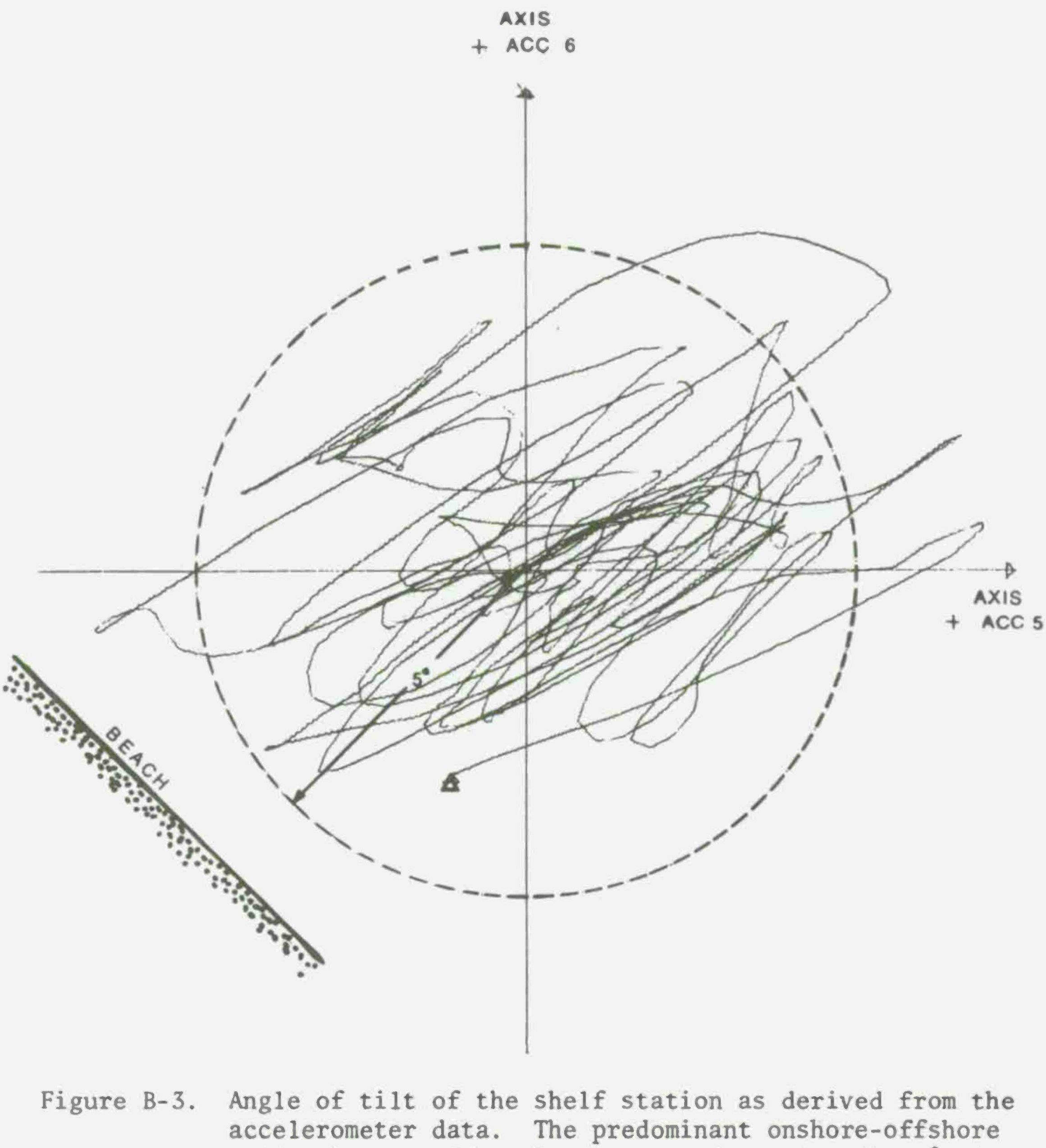

Figure B-3. Angle of tilt of the shelf station as derived from the accelerometer data. The predominant onshore-offshore motion is caused by wind waves and swell. The 5° tilt grid represents a displacement of 0.9 meter from the vertical. Unfiltered loci of motion for 256 seconds of data is represented in this plot. Shelf station was in 10 meters of water on B Range of SIO.

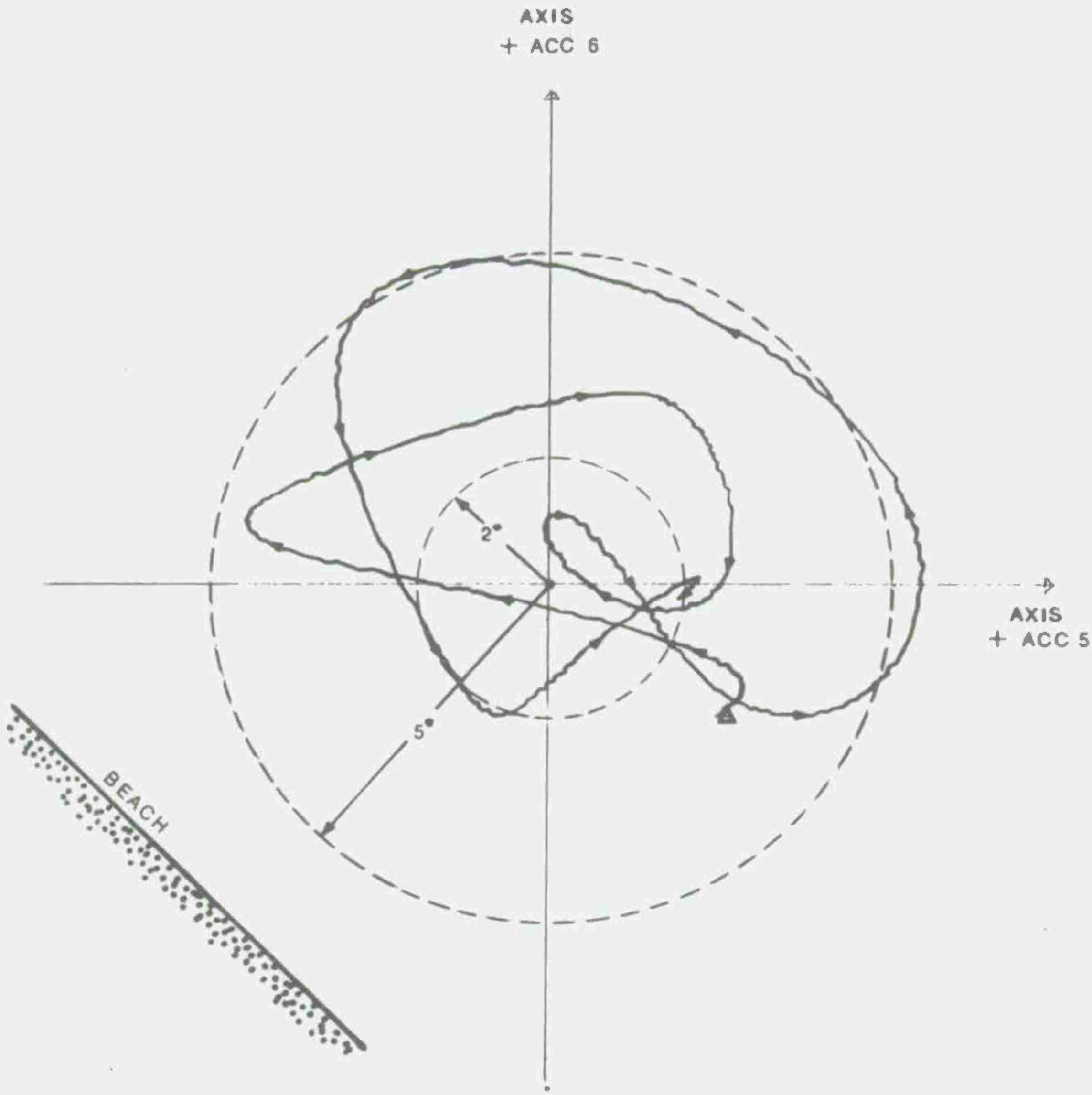

Figure B-4. Angle of tilt of the shelf station with the wind waves and swell removed using inverse FFT filter. Only oscillations with periods greater than 40 seconds are shown. This motion is in general agreement with edge wave theory.

APPENDIX C

DESIGN AND OPERATION OF SURFACE-PIERCING WAVE STAFFS

It was our intention to use a digital wave staff on the shelf station installed off Torrey Pines Beach. However, these plans proved to be impractical to implement on a shelf station placed in 10 meters of water with a 2-meter tidal range because of undesirable drag and buoyancy characteristics induced by the wave staff. A new surface-piercing wave staff (resistive wire gage) was developed with characteristics more compatible with the shallow water installation. Digital wave staffs appear to be promising for rigid mountings and for shelf stations in water 20 meters and deeper.

DIGITAL WAVE STAFF

Under the sponsorship of Sea Grant, a 1000 contact, surface-piercing wave staff was designed to be used with the shelf station. The design approach was to construct the wave staff on printed circuit (PC) glass epoxy boards. The 1000 contact staff is constructed from 10 duplicate PC boards, each having 100 contacts spaced one-half cm apart (Figure C-1). The individual PC boards bolt together with no overlap of the contacts.

The wide copper conductor at one edge of the board provides +5 volts through the seawater for the contacts on the opposite edge. The wave staff electronic system operates on +5 volts current. Each contact is held to system ground by a 1 megohm resistor when not exposed to seawater. When a contact is shorted by seawater, the voltage is pulled to +5 volts, thus providing a logic level change to the electronic circuit.

A block diagram of the wave staff electronic system is shown in Figure C-2. The basic sensing portion consists of a 1,024 bit shift register. This register is parallel loaded with the information generated by the contacts. If the contact is out of the water, a binary "0" is loaded, but if the contact is underwater a binary "1" is loaded into the register. Once the contact information is loaded, the bit information in the register is shifted out serially as data. The data signal is used to control a 10-bit binary counter which is reset to an all zero state with the parallel load command. The binary counter is only advanced if the data line is a "1". Therefore, only contacts that are underwater are counted. After 1,024 clock cycles the binary counter contains, in binary format, the number of contacts underwater. The content of the binary counter is transferred to a holding register when the next load command is received. The holding register drives a digital to analog converter whose output is a voltage proportional to the number of contacts underwater. With a clock rate of 50,000 Hz the contacts of the staff are examined approximately 500 times per second.

The electronics necessary to form the shift register are located on the PC board. These electronic components are protected from seawater by a heavy coat of polyurethane. Interconnection between boards

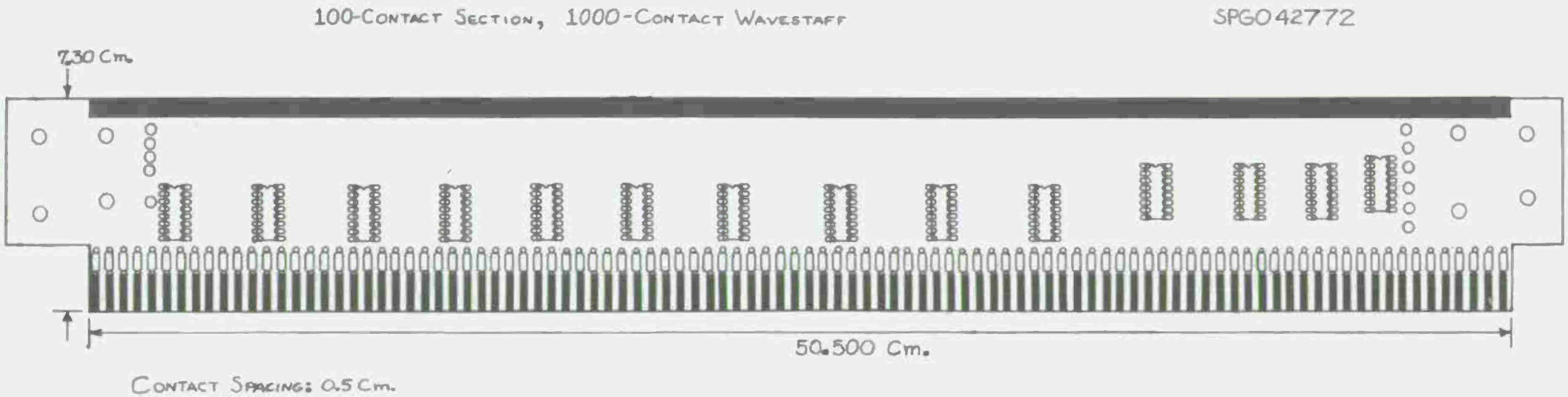

Figure C-1. Detail of 100 contact printed circuit board. Ten PC boards are used for the digital wave staff.

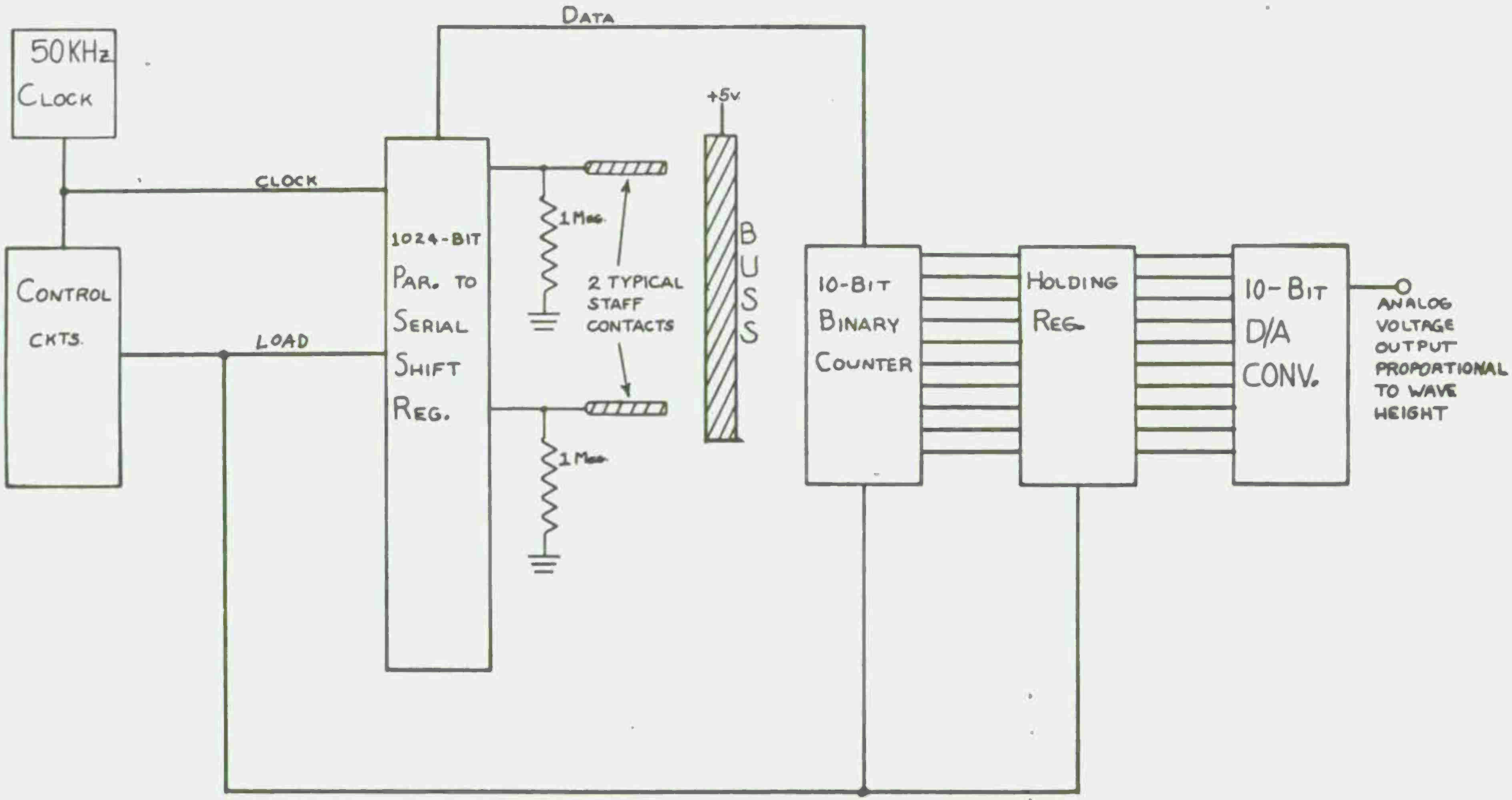

Figure C-2. Block diagram of the electronics for the digital wave staff.

is made with jumper wires (only five are needed). The wave staff is attached to the shelf station spar by aluminum brackets.

The wave staff was tested off Scripps Pier in 10 meters of water with unsatisfactory results. It was found that the buoyancy characteristics of the shelf station were greatly altered by the wave staff. At low tide the station listed almost 30°, which is more than twice the tilt experience without the wave staff. This large tilt angle is experienced because shallow depth results in a small buoyancy of the spar which cannot support the additional weight of the wave staff. This unwanted characteristic of the digital wave staff made it incompatible with the shelf station when placed in shallow water. It would appear (although not proven by test) that the digital wave staff-shelf station combination would work successfully if placed in deeper water where the total buoyancy force is greater, or in a less dynamic environment such as tideless seas and large lakes.

RESISTIVE WIRE GAGE

Because of the unsatisfactory results experienced with the digital wavestaff when mounted on the station in shallow water, a second attempt was made to develop a surface-piercing staff that would function with the shelf station. A resistive wire gage was constructed. Two taut 30-gage nichrome high-resistive wires were flush mounted in teflon onto the face of a 3.5-cm aluminum U-channel (Figure C-3). The wires form a resistance loop when shorted by the sea surface. The total resistance of the loop changes proportionally to the path length of the wires which depends on the relative water level along the major axis of the gage.

An AC bridge circuit is used to measure the change in resistance of the wire loop. The block diagram of this circuit is shown in Figure C-4. A 5-KHz oscillator with a 20-volt peak-to-peak output is used to excite the bridge. The voltage unbalance caused by the resistance change is transformer coupled to a high-gain amplifier. The resulting signal is detected by a synchronous demodulator whose output is a DC voltage proportional to the resistance in the wire loop. A calibration of the gage was performed. This test showed the linearity to be within ±1 percent of full scale and that the linear range was 4.5 meters.

The resistive wire gage was attached to the Torrey Pines Shelf Station and the station was held vertical by the tethering system shown in Figure C-5. Several data runs were made with the station tethered. Comparisons between the resistive wire gage and the pressure sensor were made for all these runs. A detailed discussion of this comparison is given in Section V-2; but in general, good agreement was found. Based on these comparisons, it is felt that under normal conditions the pressure sensors are adequate for general wave climate.

It should be noted that the shelf station is not designed to be tethered. A storm front moved through the area while the station was

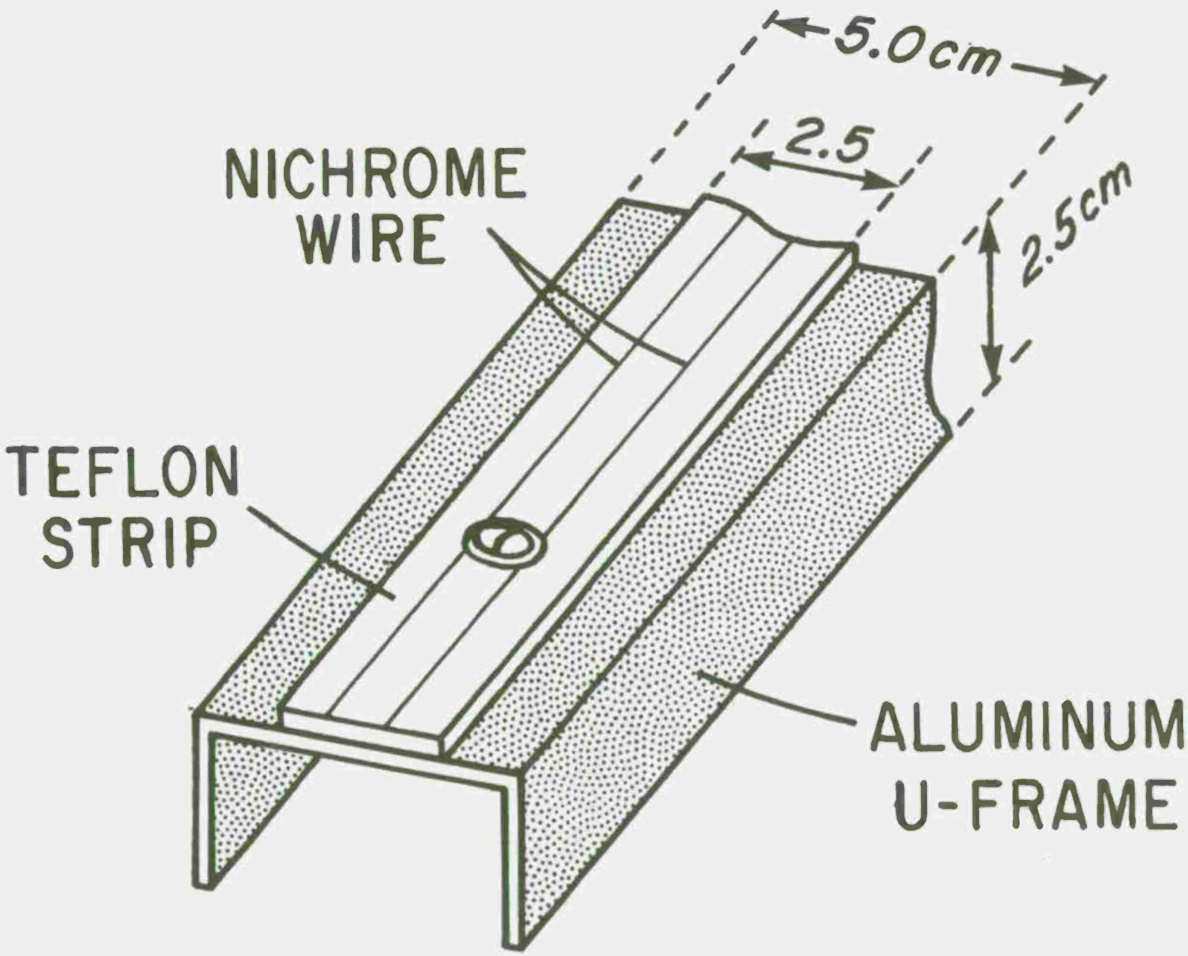

Figure C-3. Detail of the mounting for the resistive wire gage.

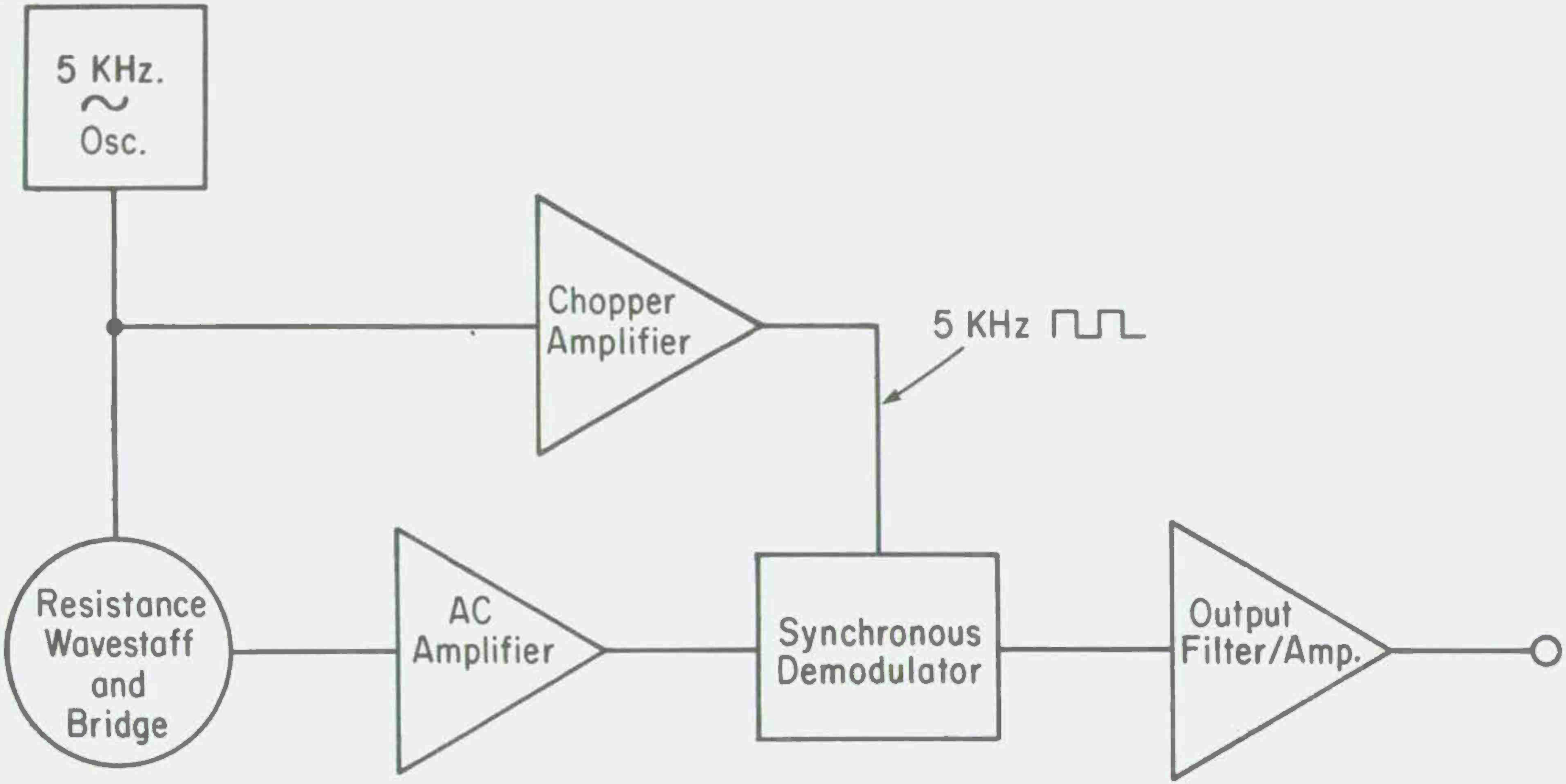

Figure C-4. Function block diagram of the electronic circuits of the resistive wire gage.

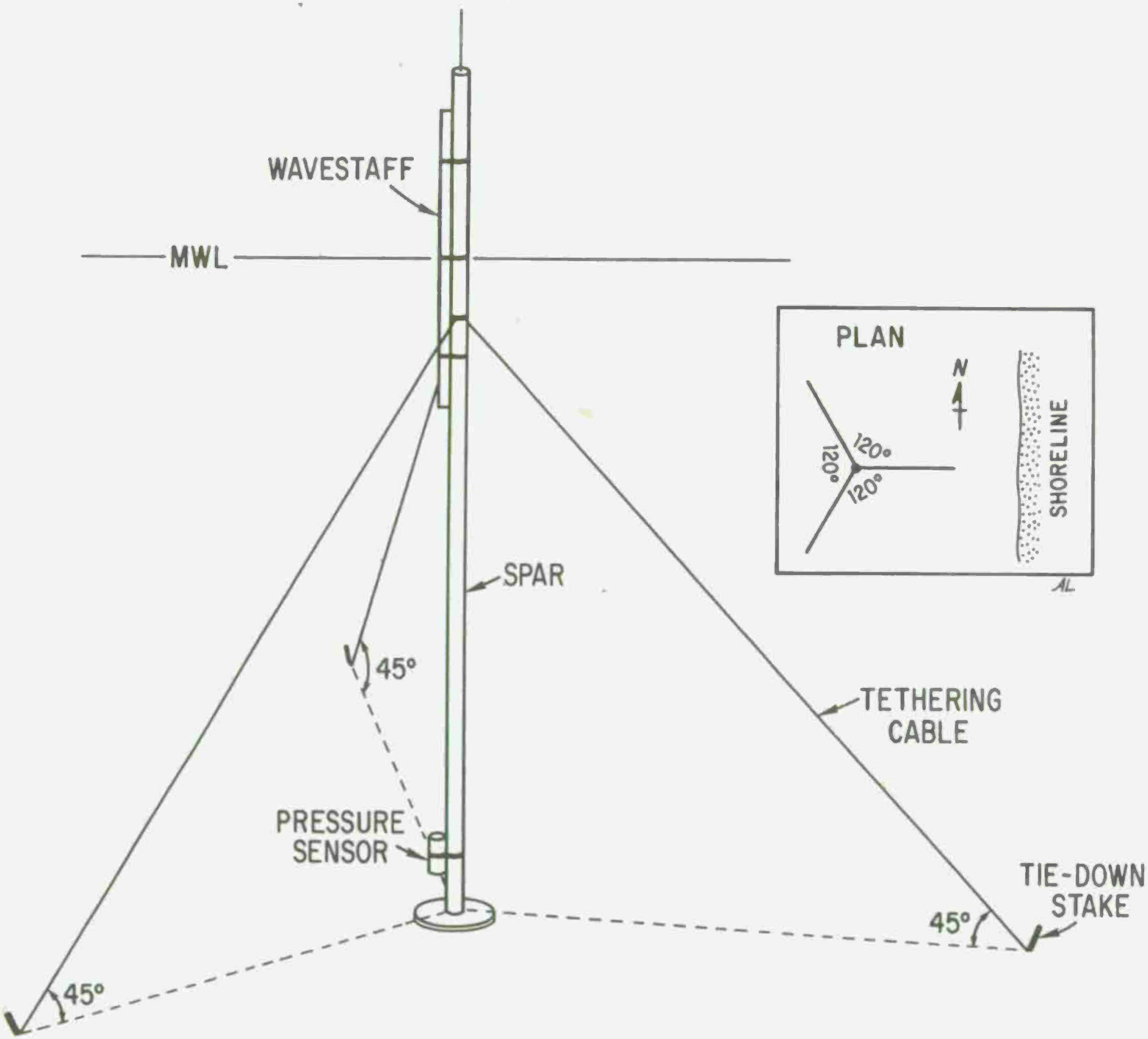

Figure C-5. Shelf station as tethered off Torrey Pines Beach.

tethered, causing the tethering system to be torn loose, and resulted in structural damage to the shelf station. For this reason more comparisons were not made.

Several data runs were made with the station untethered. It was found that the energy-density spectra for the resistive wire gage were too high. This overestimate of wave height is caused by the tilting of the station due to currents and waves. By using the data from the accelerometer, it is conceptually possible to correct the gage but there were not sufficient funds in the contract to accomplish this work.

Appendix D. A tabular presentation of the parameters characterizing wave energy and directional spectra for a four element line array in water 10 meters deep off Torrey Pines Beach, California. The terms are defined at the end of the table and are derived in Appendix A.

Run	Peak	Period (sec)	BW(Hz)	E_T(cm^2)	E_p(cm^2)	α_o	P(α_o)%	$\Delta\alpha_o$
SAS 1-6 Feb 73-01	1	14.2	.056	866	364	0°	11	±3°
	2	8.1	.065		296	1°S	45	±3°
	3	6.9	.064		166			
SAS 1-12 Feb 73-01	1	14.2	.150	3840	3380	15°S	.80	±2°
SAS 1-12 Feb 73-04	1	12.3	.078	1490	1100	17°S	1.2	±2°
	2	7.4	.111		334	29°S	56	
SAS 1-13 Feb 73-01	1	12.3	.104	1650	1200	15°S	8.2	±3°
	2	5.0	.100		395	39°S	51	±5°
SAS 1-13 Feb 73-02	1	12.3	.107	1720	1220	12°S	10	±3°
	2	6.4	.110		452			
SAS 1-13 Feb 73-04	1	9.8	.165	1060	965	20°S	33	±5°
SAS 1-14 Feb 73-01	1	14.2	.193	2050	2000	11°S	.44	±1°
SAS 1-14 Feb 73-02	1	14.2	.143	1860	1640	9°S	8.5	±2°
	2	6.4			103	10°S	50	±2°
SAS 1-14 Feb 73-03	1	14.2	.080	1400	1060	9°S	.80	±2°
	2	6.9	.027		130	7°S	51	±3°
	3	5.6	.085		148			
SAS 1-14 Feb 73-04	2	60.2	.043	789	11.5			
	1	14.2	.197		770	12°S	.72	±2°
SAS 1-15 Feb 73-03	2	10.9	.064		374	13°S	2.3	±2°
	1	6.9	.118	1120	670	1°S	18	±2°
SAS 1-16 Feb 73-02	2	60.2	.064	1110	50	7°S	.01	
	1	14.2	.133		986	14°S	.21	±1°

Appendix D. (Cont'd)

Run	Peak	Period (sec)	BW(Hz)	$E_T(cm^2)$	$E_p(cm^2)$	α_o	$P(\alpha_o)\%$	$\Delta\alpha_o$
SAS 1-17 Feb 73-01	2	20.4	.027	746	4.2			
	1	12.3	.171		623	12°S	4.2	± 3°
SAS 1-17 Feb 73-04	1	12.3	.094	849	631	12°S	1.0	± 2°
	2	6.9	.059		142	4°S	44	± 3°
	3	5.9	.048		97			
SAS 1-18 Feb 73-01	1	14.2	.061	1420	1080	8°S	.40	± 2°
	2	8.1	.082		268	5°S	24	± 2°
	3	5.3	.068		52			
SAS 1-18 Feb 73-02	1	14.2	.075	1690	1420	10°S	.60	± 1°
	2	7.4	.054		118	9°S	50	± 4°
SAS 1-18 Feb 73-03	1	14.2	.079	1580	1250	10°S	.51	± 1°
	2	7.4	.075		240	8°S	11	± 2°
	3	5.0	.054		51.2			
SAS 1-18 Feb 73-04	1	14.2	.107	1590	1420	4°S	.43	± 1°
	2	6.9	.059		109	10°S	13	± 2°
	3	4.8	.059		27			
SAS 1-19 Feb 73-02	3	60.2	.043	1090	58			
	1	14.2	.075		876	15°S	2.4	± 2°
	2	8.1	.095		120	6°S	28	± 3°
	4	4.3	.054		4.2			
SAS 1-20 Feb 73-01	3	60.2	.032	837	34			
	1	20.5	.043		473	14°S	.19	± 2°
	2	12.3	.064		283	12°S	12	± 3°
	4	6.4	.093		33			
SAS 1-20 Feb 73-03	1	16.8	.089	1330	1130	13°S	.26	± 1°
	2	8.8	.043		135	14°S	2.5	± 2°
	3	5.9	.043		38			
	4	5.0	.021		9.3			

Appendix D. (Cont'd)

Run	Peak	Period (sec)	BW(Hz)	$E_T(cm^2)$	$E_p(cm^2)$	α_o	$P(\alpha_o)$%	$\Delta\alpha_o$
SAS 1-21 Feb 73-02	1	16.8	.111	790	722	13°S	.65	±1°
	3	6.9	.021		12	10°S	56	±3°
	2	5.6	.038		15			
SAS 1-21 Feb 73-05	1	14.2	.125	670	627	11°S	1.1	±2°
	2	6.4	.091		20	2°S	52	±4°
SAS 1-22 Feb 73-01	1	14.2	.032	687	430	15°S	5.0	±2°
	2	10.9	.097		226	13°S	32	±5°
	3	5.3	.029		4.4			
	4	4.1	.047		4.2			
SAS 1-22 Feb 73-02	1	14.2	.136	584	523	17°S	1.7	±2°
	2	5.0	.068		7.5	6°S	110	
SAS 1-23 Feb 73-01	1	14.2	.091	217	182	7°S	2.0	±2°
	2	5.3	.070		15.2	33°S	44	±2°
SAS 1-23 Feb 73-02	1	12.3	.097	163	134	3°S	6.9	±2°
	2	6.9	.043		6.8	33°S	48	±3°
	3	4.5	.048		4.7			
SAS 1-24 Feb 73-01	1	12.3	.091	147	129	3°S	4.8	±2°
	2	6.4	.054		6.9	38°S	44	±3°
SAS 1-24 Feb 73-02	1	12.3	.095	150	127	4°S	10	±3°
	2	7.4	.064		7.6	22°S	11	±3°
SAS 1-24 Feb 73-03	1	9.8	.129	745	692	3°S	21	±2°
	2	4.5	.054		37	37°S	70	
SAS 1-24 Feb 73-04	1	9.8	.142	1390	1250	10°S	41	±3°
	2	5.3	.070		76	33°S	37	±2°
SAS 1-25 Feb 73-01	1	12.3	.148	2200	1870	2°S	.40	±1°
	2	4.3	.051		126			

Appendix D. (Cont'd)

Run	Peak	Period (sec)	BW(Hz)	$E_T(cm^2)$	$E_p(cm^2)$	α_o	$P(\alpha_o)$%	$\Delta\alpha_o$
SAS 1-25 Feb 73-02	1	10.9	.086	3060	2420			
	2	7.4	.021		154			
	3	6.4	.021		119			
SAS 1-25 Feb 73-03	1	14.2	.091	2710	2320			
	2	6.4	.027		153			
SAS 1-25 Feb 73-04	3	36.6	.043	2340	33			
	2	14.2	.032		925			
	1	10.9	.097		1000			
SAS 1-26 Feb 73-01	1	12.3	.145	1660	1580			
SAS 1-27 Feb 73-01	1	14.2	.091	1720	1490			
	2	8.1	.086					
SAS 1-22 Mar 73-01	3	60.2	.043	1230	13.3			
	2	14.2	.043		156	6°S	1.5	±3°
	1	6.9	.107		834	2°S	49	±5°
SAS 1-06 Apr 73-01	1	5.0	.093	207	93.0			
	2	14.2	.040		34.9	7°N	92	±3°
SAS 1-07 Apr 73-03	1	6.9	.075	451	186	87°N	60	
	2	10.9	.032		40.3			
SAS 1-10 Apr 73-02	1	14.2	.102	149	108			
	2	9.8	.054		25			
	3	4.1	.048		7			
SAS 1-10 Apr 73-03	1	12.3	.062	160	107			
	2	9.8	.056		35			
	3	6.4	.048		5			
	4	4.3	.035		3			
SAS 1-11 Apr 73-01	1	12.3	.078	147	90			
	2	9.8	.097		40			
	3	4.1	.049		14			

Appendix D. (Cont'd)

Run	Peak	Period (sec)	BW(Hz)	$E_T(cm^2)$	$E_p(cm^2)$	α_o	$P(\alpha_o)\%$	$\Delta\alpha_o$
SAS 1-11 Apr 73-03	3	16.8	.032	172	11			
	1	12.3	.110		88			
	2	4.5	.333		45			
SAS 1-12 Apr 73-01	1	10.9	.078	198	117			
	3	8.1	.050		25			
	2	4.8	.064		28			
SAS 1-12 Apr 73-03	1	14.2	.064	740	302			
	2	6.4	.070		194			
SAS 1-13 Apr 73-03	2	14.2	.067	1081	283			
	1	5.9	.075		368			
	3	4.1	.030		135			
SAS 1-14 Apr 73-01	2	12.3	.056	760	135			
	1	6.4	.070		284			
	3	4.1	.027		63			
SAS 1-14 Apr 73-03	3	12.3	.050	1072	106			
	1	6.4	.091		659			
	2	4.5	.040		140			
SAS 1-15 Apr 73-02	2	12.3	.046	719	86			
	1	6.9	.099		431			
SAS 1-16 Apr 73-03	2	16.8	.048	564	101			
	1	6.9	.086		293			
SAS 1-17 Apr 73-01	1	14.2	.086	463	145			
	2	5.6	.069		117			
	3	4.1	.046		92			
SAS 1-17 Apr 73-03	1	12.3	.056	679	208			
	4	9.8	.026		69			
	2	6.4	.047		154			
	3	5.3	.054		133			

Appendix D. (Cont'd)

Run	Peak	Period (sec)	BW(Hz)	$E_T(cm^2)$	$E_p(cm^2)$	α_o	$P(\alpha_o)$%	$\Delta\alpha_o$
SAS 1-18 Apr 73-01	1	8.1	.134	2250	1630			
SAS 1-16 May 73-02	2	14.2	.029	172	19	22°S	4.8	±3°
	1	9.8	.110		131	0°	4.4	±2°
	3	4.3	.059		15	28°S	76	±5°
SAS 1-17 May 73-01	1	10.9	.121	241	187	6°S	11.5	±2°
	2	4.3	.060		37	30°N	66.4	±5°
SAS 1-17 May 73-02	1	10.9	.140	301	270	2°S	2.0	±2°
	2	4.5	.059		21	8°N	25.4	±3°
SAS 1-18 May 73-01	1	14.2	.048	220	78	25°S	0.1	±1°
	2	9.8	.054		57	2°S	17.4	±3°
	3	4.5	.067		50	22°S	74.1	±3°
SAS 1-18 May 73-03	1	12.3	.089	292	186	10°S	5.2	±2°
	2	4.5	.059		60	2°S	54.2	±5°
SAS 1-18 May 73-04	1	12.3	.110	218	158	13°S	4.6	±2°
	2	4.8	.064		22	43°S	63.2	±4°
SAS 1-19 May 73-01	1	12.3	.118	270	230	11°S	5.7	±2°
	2	4.8	.083		21	40°S	70.3	±3°
SAS 1-19 May 73-02	2	14.2	.040	261	46	28°S	0.6	±1°
	1	10.9	.083		117	4°S	3.7	±2°
	3	4.8	.083		42	28°S	73.3	±4°
SAS 1-19 May 74-04	1	16.8	.137	204	154	21°S	1.8	±2°
	2	5.0	.089		32	40°N	63.2	±5°
SAS 1-20 May 73-01	1	16.8	.088	234	143	26°S	.4	±1°
	2	4.8	.113		54.3	48°S	87.2	±4°
SAS 1-20 May 73-02	1	16.8	.043	241	115	24°S	.5	±1°
	2	10.9	.080		69.7	5°S	15.0	±2°
	3	4.5	.032		10.2			

Appendix D. (Cont'd)

Run	Peak	Period (sec)	BW(Hz)	$E_T(cm^2)$	$E_p(cm^2)$	α_o	$P(\alpha_o)\%$	$\Delta\alpha_o$
SAS 1-20 May 73-03	2	16.8	.038	244	86.7	25°S	1.5	±1°
	1	10.9	.083		111	2°S	10.1	±2°
	3	5.9	.035		14.8			
SAS 1-20 May 73-04	2	14.2	.048	162	43.3	21°S	10.8	±2°
	1	10.9	.069		51.5	2°S	28.2	±2°
	3	6.4	.046		22.6			
SAS 1-21 May 73-01	2	14.2	.038	232	70.5	28°S	24.9	±3°
	1	9.8	.064		78.5	1°N	11.8	±2°
	3	4.8	.051		35.2			
SAS 1-21 May 73-03	2	14.2	.064	314	89.3	20°S	50.0	±5°
	1	5.6	.078		120			
SAS 1-21 May 73-04	1	14.2	.056	267	88.7	20°S	27.4	±5°
	2	4.8	.043		69.3			
SAS 1-22 May 73-03	1	10.9	.093	262	175	0°	7.9	±2°
	2	6.0	.061		62.7			
SAS 1-23 May 73-02	2	12.3	.054	195	42.9	18°S	12.6	±3°
	1	9.8	.064		72.0	3°S	18.6	±3°
SAS 1-23 May 73-03	1	10.9	.125	175	101	4°S	19.8	±3°
	2	6.0	.050		50.6	30°N	85	±5°
SAS 1-24 May 73-01	2	9.8	.059	271	36.8	6°S	6.2	±2°
	1	6.9	.061		110	3°S	9.6	±2°
SAS 1-24 May 73-02	2	12.3	.054	284	23.3	8°S	43.0	±5°
	1	6.9	.158		229	4°N	47.8	±3°
SAS 1-24 May 73-03	2	14.2	.054	159	25.0	36°S	56.2	±5°
	1	6.9	.122		107	4°N	33.7	±3°
SAS 1-24 May 73-04	2	14.2	.100	212	85.8	21°S	4.7	±2°
	1	6.4	.086		93.8			

Appendix D. (Cont'd)

Run	Peak	Period (sec)	BW(Hz)	$E_T(cm^2)$	$E_p(cm^2)$	α_o	$P(\alpha_o)$%	$\Delta\alpha_o$
SAS 1-25 May 73-01	3	12.3	.082	853	151	2°S	5.5	± 2°
	1	6.9	.072		323			
	2	4.1	.050		240	17°N	92.2	± 4°
SAS 1-25 May 73-03	1	12.3	.082	373	168	5°S	4.5	± 2°
	2	6.4	.047		79	6°S	82.2	± 5°
SAS 1-25 May 73-04	2	12.3	.081	358	112	7°S	85.3	± 3°
	1	5.6	.064		113	25°S	66.5	± 4°
SAS 1-26 May 73-01	1	12.3	.105	600	248	5°S	1.1	± 2°
	2	6.4	.051		207	2°N	42.1	± 2°
SAS 1-26 May 73-02	2	12.3	.051	733	131	8°S	4.7	± 2°
	1	7.4	.105		502	0°	30.6	± 3°
SAS 1-26 May 73-03	2	10.9	.067	548	197	3°S	2.8	± 2°
	1	7.4	.081		270	1°S	31.3	± 3°
SAS 1-26 May 73-04	2	10.9	.075	670	185	4°S	2.7	± 2°
	1	7.4	.078		328	1°N	55.2	± 4°
SAS 1-27 May 73-01	2	14.2	.032	656	39.0	27°S	1.4	± 3°
	1	8.1	.113		516	2°N	10.6	± 3°
SAS 1-27 May 73-02	2	14.2	.032	610	34	31°S	4.1	± 2°
	1	8.1	.193		373	2°N	22.1	± 2°
SAS 1-27 May 73-03	3	14.2	.032	431	24.1	29°S	.3	± 1°
	1	8.1	.193		223	1°S	53.2	± 5°
	2	6.9	.036		97.3			
SAS 1-27 May 73-04	2	14.2	.043	244	25.2	30°S	1.2	± 1°
	1	7.4	.083		121	2°N	26.1	± 2°
SAS 1-28 May 73-01	3	12.3	.048	176	26	30°S	3.6	± 2°
	1	8.8	.054		56.3	3°N	20.0	± 2°
	2	6.0	.043		41.2			

Appendix D. (Cont'd)

Run	Peak	Period (sec)	BW(Hz)	$E_T(cm^2)$	$E_p(cm^2)$	α_o	$P(\alpha_o)\%$	$\Delta\alpha_o$
SAS 1-28 May 73-02	2	12.3	.048	235	24.2	32°S	3.6	± 2°
	1	7.4	.091		145	0°	38.2	± 2°
SAS 1-28 May 73-04	3	12.3	.054	124	18.4	30°S	7.1	± 2°
	1	8.8	.072		44.1	3°S	10.1	± 2°
	2	6.4	.035		23.2			
SAS 1-29 May 73-02	2	14.2	.048	176	34.2	23°S	2.0	± 2°
	1	8.8	.080		99.0	1°N	13.1	± 2°
SAS 1-29 May 73-03	1	14.2	.059	106	33.1	23°S	.5	± 1°
	2	8.8	.067		32.3	0°	49.6	± 3°
SAS 1-30 May 73-01	1	16.8	.057	176	51.2	20°S	.8	± 1°
	2	8.1	.059		45.1	1°S	39.1	± 3°
	3	5.3	.046		23.0			
SAS 1-29 May 73-04	2	14.2	.043	121	28.1	26°S	1.0	± 2°
	1	8.8	.070		46.2	4°S	39.3	± 3°
SAS 1-30 May 73-02	1	14.2	.060	133	38.3	23°S	.7	± 1°
	2	8.1	.062		32.1	3°N	50.8	± 3°
SAS 1-30 May 73-03	2	14.2	.075	106	38.4	21°S	8.8	± 2°
	1	7.4	.088		46.0			
SAS 1-30 May 73-04	1	14.2	.064	142	35.0	22°S	2.0	± 1°
	2	8.1	.037		23.2	0°	53.3	± 2°
SAS 1-31 May 73-01	4	14.2	.038	1080	60.1	22°S	21.8	± 4°
	3	8.1	.035		73.2	1°S	77.8	± 3°
	2	5.6	.054		167			
	1	4.1	.056		525			
SAS 1-31 May 73-02	2	14.2	.046	209	60.1	23°S	1.0	± 1°
	1	10.9	.051		88.5	1°N	8.6	± 2°
	3	6.4	.051		22.6			

Appendix D. (Cont'd)

Run	Peak	Period (sec)	BW(Hz)	$E_T(cm^2)$	$E_p(cm^2)$	α_o	$P(\alpha_o)$%	$\Delta\alpha_o$
SAS 1-31 May 73-03	1	16.8	.040	254	116	24°S	.3	± 1°
	2	10.9	.043		58.5	2.S	6.7	± 2°
	3	7.4	.051		38.3			
SAS 1-31 May 73-04	2	14.2	.054	333	74.2	22°S	2.0	± 2°
	3	10.9	.035		51.6	2°S	9.1	± 2°
	1	4.3	.080		135			
SAS 1-01 Jun 73-02	1	16.8	.036	243	96.2	23°S	.1	± 1°
	2	12.3	.056		90.3	1°S	7.3	± 2°
	3	6.4	.083		25.3			
SAS 1-01 Jun 73-04	1	14.2	.113	260	205	25°S	2.8	± 2°
	2	6.4	.093		37	4°N	76.8	± 4°
SAS 1-02 Jun 73-03	1	10.9	.091	446	266	0°	.6	± 1°
	3	7.4	.064		75.6	2°N	11.4	± 2°
	2	4.3	.064		83.7			
SAS 1-02 Jun 73-04	1	12.3	.056	462	256	12°S	18.4	± 3°
	2	8.8	.032		110	4°N	16.2	± 2°
	3	6.9	.046		42.1			
SAS 1-03 Jun 73-01	2	14.2	.046	234	49.6	26°S	.4	± 1°
	1	10.9	.062		116	1°S	8.1	± 2°
	3	6.4	.054		30.3			
SAS 1-03 Jun 73-02	1	10.9	.183	234	210	0°	17.1	± 3°
SAS 1-03 Jun 73-03	1	12.3	.114	198	157	12°S	41.9	± 4°
	2	6.0	.047		16.4	10°N	80.9	± 5°
SAS 1-03 Jun 73-04	2	14.2	.032	357	51.4	25°S	3.8	± 2°
	1	8.8	.153		246	2°N	5.4	± 2°
SAS 1-04 Jun 73-01	1	14.2	.094	274	115	25°S	2.9	± 2°
	2	5.0	.067		86.9			

Appendix D. (Cont'd)

Run	Peak	Period (sec)	BW(Hz)	$E_T(cm^2)$	$E_p(cm^2)$	α_o	$P(\alpha_o)$%	$\Delta\alpha_o$
SAS 1-04 Jun 73-02	1	14.2	.065	193	90.1	23°S	2.9	± 2°
	2	8.8	.079		66.9	5°N	9.2	± 2°
	3	4.3	.061		23.9			
SAS 1-04 Jun 73-03	2	12.3	.027	182	130	15°S	15.3	± 3°
	1	8.8	.126		32.8	5°N	7.2	± 2°
	3	4.3	.043		11.9			
SAS 1-04 Jun 73-04	1	12.3	.149	170	139	15°S	48.4	± 5°
	2	4.5	.046		15.7	52°S	77.3	± 5°
SAS 1-04 Jun 73-05	1	12.3	.054	114	36.1	5°S	16.1	± 3°
	2	9.8	.039		26.2	3°N	8.2	± 1°
	3	6.9	.050		15.7			
SAS 1-05 Jun 73-01	3	12.3	.038	194	39.8	10°S	23.8	± 4°
	1	9.8	.029		52.3	8°N	16.3	± 3°
	2	8.1	.065		48.4			
SAS 1-05 Jun 73-02	3	16.8	.027	134	7.9	28°S	9.8	± 1°
	2	12.3	.035		23.2	29°S	34.4	± 3°
	1	8.8	.070		40.2			
SAS 1-05 Jun 73-03	2	12.3	.051	198	34.7	6°S	36.6	± 3°
	1	8.8	.081		89.5	1°S	8.7	± 2°
SAS 1-05 Jun 73-04	1	8.8	.107	498	126	0°	2.4	± 2°
	2	5.6	.099		41.5	0°	63.8	± 3°
SAS 1-06 Jun 73-01	2	14.2	.089	204	39.6	23°S	2.3	± 2°
	1	4.5	.107		140	53°S	83.6	± 4°
	3	6.9	.016		4.7			
SAS 1-06 Jul 73-05	2	14.2	.040	625	60.9	30°S	.5	± 1°
	1	9.8	.105		488	0°	6.3	± 2°
	3	5.3	.054		47.5			

Appendix D. (Cont'd)

Run	Peak	Period (sec)	BW(Hz)	$E_T(cm^2)$	$E_p(cm^2)$	α_o	$P(\alpha_o)$%	$\Delta\alpha_o$
SAS 1-06 Jul 73-06	1	9.8	.142	811	632	1°S	7.2	±2°
	2	5.0	.062		64.8	20°S	83.7	±5°
SAS 1-06 Jul 73-07	2	14.2	.029	692	584	26°S	.8	±1°
	1	8.8	.102		37.1	1°N	14.6	±2°
SAS 1-07 Jul 73-01	3	12.3	.040	346	43.1	26°S	.8	±1°
	1	9.8	.070		196	1°N	10.8	±2°
	2	6.4	.051		76.0			
SAS 1-07 Jul 73-02	1	8.8	.134	305	211	2°N	3.2	±1°
	2	6.0	.065		55.6	9°N	51.5	±3°
SAS 1-07 Jul 73-03	1	8.8	.096	372	191	5°N	51.2	±3°
	2	6.9	.043		75.7	5°S	62.5	±4°
SAS 1-07 Jul 73-04	1	8.8	.121	351	256	4°S	4.3	±2°
	2	5.6	.115		81.0			
SAS 1-07 Jul 73-05	1	8.8	.102	366	254	1°N	10.9	±2°
	2	6.4	.099		108	12°N	58.6	±4°
SAS 1-07 Jul 73-07	2	10.9	.107	268	197	27°S	29.9	±3°
	1	7.4	.054		39.4	3°N	27.3	±3°
SAS 1-08 Jul 73-01	3	12.3	.051	136	14.8	30°S	7.4	±2°
	1	7.4	.115		88.0	2°S	28.5	±2°
	2	4.8	.038		24.1			
SAS 1-08 Jul 73-03	3	12.3	.051	209	23.4	30°S	2.9	±2°
	1	7.4	.079		120	1°S	36.2	±2°
	2	5.6	.075		41.6			
SAS 1-08 Jul 73-05	2	14.2	.051	206	26.8	24°S	.5	±1°
	1	7.4	.075		138	6°N	20.7	±4°
	3	6.0	.056		23.9			

Appendix D. (Cont'd)

Run	Peak	Period (sec)	BW(Hz)	$E_T(cm^2)$	$E_p(cm^2)$	α_o	$P(\alpha_o)$%	$\Delta\alpha_o$
SAS 1-08 Jul 73-07	3	14.2	.057	188	18.6	26°S	.2	±1°
	1	8.1	.079		109	1°N	34.2	±3°
	2	6.0	.057		42.4			
SAS 1-09 Jul 73-01	3	12.3	.035	152	20.1	26°S	2.1	±2°
	1	8.1	.080		76.3	5°N	12.8	±2°
	2	5.0	.059		37.2			
SAS 1-09 Jul 73-03	2	16.8	.043	187	25.0	25°S	.8	±1°
	1	8.1	.115		137	3°N	16.4	±3°
SAS 1-10 Jul 73-01	2	14.2	.043	226	52.2	25°S	3.7	±2°
	1	8.8	.062		123	2°N	26.2	±3°
	3	6.9	.056		25.3			
SAS 1-10 Jul 73-02	3	14.2	.039	268	24.9	24°S	.7	±1°
	1	8.8	.093		174	3°N	36.4	±3°
	2	4.8	.036		33.4			
SAS 1-11 Jul 73-01	3	14.2	.032	327	30.2	25°S	2.1	±1°
	1	9.8	.083		194	1°N	44.1	±3°
	2	6.9	.071		77.0			
SAS 1-11 Jul 73-02	3	14.2	.043	202	23.6	26°S	1.4	±1°
	1	9.8	.094		120	0°	39.5	±3°
	2	5.3	.064		33.5			
SAS 1-16 Jul 73-03	3	14.2	.035	269	26.7	22°S	1.4	±1°
	1	9.8	.070		120	1°N	36.9	±4°
	2	5.9	.083		86.0			
SAS 1-16 Jul 73-04	2	14.2	.056	174	35.8	24°S	.3	±1°
	1	9.8	.166		120			
SAS 1-17 Jul 73-01	2	14.2	.091	260	72.9	22°S	.5	±1°
	1	5.0	.115		171			

Appendix D. (Cont'd)

Run	Peak	Period (sec)	BW(Hz)	$E_T(cm^2)$	$E_p(cm^2)$	α_o	$P(\alpha_o)\%$	$\Delta\alpha_o$
SAS 1-18 Jul 73-04	1	16.8	.070	208	60.8	25°S	.4	±1°
	3	5.6	.057		50			
	2	4.1	.064		59.1			
SAS 1-19 Jul 73-01	1	16.8	.064	304	124	24°S	.9	±1°
	3	5.6	.061		60.3	2°N	81.4	±5°
	2	4.7	.078		102			
SAS 1-19 Jul 73-03	1	16.8	.070	259	140	22°S	3.3	±3°
	2	5.9	.126		98	7°N	76.8	±4°
SAS 1-19 Jul 73-04	1	16.8	.070	420	229	24°S	.5	±1°
	2	5.9	.142		177	6°N	74.9	±3°
SAS 1-20 Jul 73-01	2	14.2	.059	368	147			
	1	6.0	.140		193			
SAS-1-20 Jul 73-03	2	16.8	.061	390	151	25°S	0.4	±1°
	1	6.9	.139		195	5°S	40.0	±2°
SAS-1-20 Jul 73-04	2	14.2	.061	461	101	23°S	0.6	±1°
	1	6.4	.150		345	27°S	75.7	
SAS 1-21 Jul 73-01	2	14.2	.059	425	95	25°S	0.7	±1°
	1	6.4	.139		290	2°N	46.1	±5°
SAS 1-21 Jul 73-02	2	14.2	.069	740	238	22°S	1.2	±2°
	1	6.9	.140		456	6°N	26.4	±3°
SAS 1-21 Jul 73-03	2	14.2	.078	395	143	24°S	1.0	±2°
	1	7.4	.161		218	1°N	33.1	±3°
SAS 1-21 Jul 73-04	2	16.8	.059	612	261	25°S	0.2	±1°
	1	7.4	.140		306	8°N	54.3	±3°
SAS 1-22 Jul 73-01	2	16.8	.054	699	199	27°S	0.4	±1°
	1	8.1	.140		464	4°N	8.9	±2°

Appendix D. (Cont'd)

Run	Peak	Period (sec)	BW(Hz)	$E_T(cm^2)$	$E_p(cm^2)$	α_o	$P(\alpha_o)$%	$\Delta\alpha_o$
SAS 1-22 Jul 73-02	2	14.2	.064	733	258	25°S	0.4	±1°
	1	7.4	.118		436	3°N	17.0	±2°
SAS 1-22 Jul 73-03	1	16.8	.064	515	211	25°S	.2	±1°
	2	8.1	.097		205	9°N	20.9	±3°
SAS 1-22 Jul 73-04	2	14.2	.054	442	166	27°S	.8	±1°
	1	8.1	.075		186	3°N	57.9	±3°
SAS 1-23 Jul 73-01	2	14.2	.043	495	64.7	25°S	1.2	±2°
	1	8.8	.078		260	67°N	51.6	
SAS 1-23 Jul 73-03	3	14.2	.048	466	58.7	23°S	.6	±1°
	1	9.8	.075		241	3°N	58.3	±3°
	2	5.6	.075		123			
SAS 1-24 Jul 73-02	2	16.8	.037	680	64.3	29°S	.1	±1°
	1	8.1	.097		625	3°N	67.3	±4°
SAS 1-27 Jul 73-04	1	14.2	.050	220	118	28°S	1.0	±2°
	2	8.8	.129		60.4	42°S	39.8	±4°
SAS 1-28 Jul 73-02	1	14.2	.082	141	64.2	24°S	7.5	±2°
	2	8.8	.154		57.4	3°N	57.6	±4°
SAS 1-29 Jul 73-02	2	16.8	.062	191	48.1	26°S	.5	±1°
	1	5.6	.100		87.4	8°S	83.4	±5°
SAS 1-29 Jul 73-04	1	16.8	.086	243	146	26°S	3.2	±3°
	2	4.5	.136		63.1			
SAS 1-30 Jul 73-01	1	14.2	.094	251	146	29°S	.2	±1°
	2	4.7			72.3			
SAS 1-30 Jul 73-02	1	14.2	.061	268	162	26°S	.8	±1°
	3	8.8	.047		30.0	2°N	44.3	±3°
	2	5.3	.093		64.1			

Appendix D. (Cont'd)

Run	Peak	Period (sec)	BW(Hz)	$E_T(cm^2)$	$E_p(cm^2)$	α_o	$P(\alpha_o)\%$	$\Delta\alpha_o$
SAS 1-31 Jul 73-01	1	14.2	.057	218	158	27°S	.4	±1°
	2	8.1	.161		46.4	2°N	20.1	±3°
SAS 1-01 Aug 73-02	2	14.2	.079	204	60.0	25°S	.1	±1°
	1	5.3	.096		103	1°S	87.3	±4°
SAS 1-01 Aug 73-03	2	14.2	.071	149	42.7	24°S	1.0	±2°
	1	6.9	.143		93.9	9°N	20.9	±4°
SAS 1-02 Aug 73-01	2	14.2	.082	245	103	24°S	.5	±1°
	1	8.1	.118		109	5°N	10.8	±3°
SAS 1-02 Aug 73-03	2	14.2	.046	233	44.9	25°S	.1	±1°
	1	8.1	.161		170	6°N	11.4	±3°
SAS 1-02 Aug 73-04	3	14.2	.043	220	40.0	27°S	.4	±1°
	2	8.8	.043		66.0	5°N	17.6	±3°
	1	6.9	.100		127			
SAS 1-03 Aug 73-01	1	14.2	.068	181	83.6	26°S	1.8	±2°
	2	7.4	.132		69.9	5°N	24.4	±3°
SAS 1-10 Aug 73-01	4	14.2	.067	917	115	24°S	2.4	±2°
	3	8.1	.054		209	5°N	7.2	±2°
	2	6.0	.056		251			
	1	4.3	.056		328			
SAS 1-10 Aug 73-03	2	14.2	.064	207	88.4	25°S	.3	±1°
	1	8.1	.153		100	7°N	11.3	±4°
SAS 1-11 Aug 73-01	2	14.2	.072	178	81.4	27°S	2.9	±2°
	1	6.9	.134		87.9	5°N	11.9	±2°
SAS 1-11 Aug 73-02	2	14.2	.080	175	53.6	25°S	1.3	±2°
	1	5.6	.129		82.4			
SAS 1-11 Aug 73-03	2	14.2	.072	322	95.1	23°S	.3	±1°
	1	6.4	.140		184	12°S	86.8	±6°

Appendix D. (Cont'd)

Run	Peak	Period (sec)	BW(Hz)	$E_T(cm^2)$	$E_p(cm^2)$	α_o	$P(\alpha_o)$%	$\Delta\alpha_o$
SAS 1-11 Aug 73-04	2	14.2	.056	314	63.1	26°S	1.3	± 2°
	1	4.1	.118		103			
SAS 1-12 Aug 73-01	2	14.2	.054	391	134	25°S	.6	± 1°
	1	8.1	.140		187	22°S	52.2	± 3°
SAS 1-12 Aug 73-02	2	14.2	.056	281	82.6	25°S	.2	± 1°
	1	8.8	.145		121	6°N	62.1	± 4°
SAS 1-14 Aug 73-04	1	16.8	.102	89.8	42.6	27°S	.3	± 1°
	2	6.0	.115		22.2	15°N	73.4	± 4°
SAS 1-15 Aug 73-01	1	16.8	.080	132	82.4	26°S	.1	± 1°
	2	6.4	.123		36.9	1°N	55.8	± 4°
SAS 1-15 Aug 73-02	1	16.8	.099	197	151	23°S	.1	± 1°
	2	5.6	.113		20.0	4°N	80.1	± 4°
SAS 1-16 Aug 73-03	1	16.8	.048	360	302	23°S	1.4	± 3°
	2	8.1	.140		45.4	7°N	57.7	± 4°
SAS 1-16 Aug 73-04	1	14.2	.080	387	314	24°S	.3	± 1°
	2	7.4	.121		32.2	4°N	32.4	± 3°
SAS 1-20 Aug 7303	2	12.3	.069	246	74.7	24°S	4.5	± 3°
	1	5.6	.083		125	6°N	73.9	± 4°
SAS 1-20 Aug 73-04	1	16.8	.059	169	54.6	24°S	.1	± 1°
	2	6.4	.067		53.8	11°N	38.3	± 3°
SAS 1-21 Aug 73-01	1	16.8	.075	291	84.2	27°S	.3	± 1°
	2	6.4	.072		71.9	8°N	40.8	± 3°
SAS 1-21 Aug 73-02	1	16.8	.067	264	107	25°S	1.5	± 1°
	2	7.4	.064		75.0			
	3	5.9	.074		70.3			
SAS 1-21 Aug 73-03	1	16.8	.056	369	183	26°S	1.7	± 1°
	2	8.1	.068		122			

Appendix D. (Cont'd)

Run	Peak	Period (sec)	BW(Hz)	$E_T(cm^2)$	$E_p(cm^2)$	α_o	$P(\alpha_o)\%$	$\Delta\alpha_o$
SAS-1-22 Aug 73-02	2	16.8	.040	572	213	26°S	14.8	±2°
	1	8.1	.161		349	1°S	40.0	±3°
SAS 1-22 Aug 73-03	3	16.8	.056	764	167	27°S	3.0	±2°
	1	7.4	.070		342			
	2	6.0	.099		284			
SAS 1-22 Aug 73-04	2	16.8	.064	897	198	27°S	.8	±1°
	1	6.4	.137		621			
SAS 1-23 Aug 73-01	2	14.2	.038	1220	122	25°S	.5	±1°
	1	8.8	.153		1010			
SAS 1-23 Aug 73-02	2	14.2	.032	1026	107	24°S	0.6	±1°
	1	8.1	.161		851	1°S	10.6	±2°
SAS 1-23 Aug 73-03	3	14.2	.043	937	114	25°S	0.1	±1°
	1	8.1	.081		556	2°S	20.5	±2°
	2	6.4	.075		228	7°S	41.3	±3°
SAS 1-24 Aug 73-02	2	14.2	.046	674	101	25°S	1.5	±2°
	1	8.1	.171		552	6°S	37.2	±2°
SAS-1-24 Aug 73-03	2	16.8	.046	603	45.4	24°S	1.7	±2°
	1	8.1	.148		386	4°S	2.3	±2°
SAS 1-24 Aug 73-04	2	16.8	.035	480	59.0	30°S	0.4	±1°
	1	8.1	.161		361	2°S	23.9	±3°
SAS 1-25 Aug 73-01	2	14.2	.032	489	35.2	27°S	10.1	±3°
	1	8.8	.129		423	1°S	0.6	±1°
SAS 1-25 Aug 73-02	3	14.2	.038	400	32.6	24°S	1.8	±2°
	1	8.1	.080		265	2°S	2.5	±1°
	2	5.6	.056		64.2	6°N	39.4	±2°

Appendix D. (Cont'd)

Run	Peak	Period (sec)	BW(Hz)	$E_T(cm^2)$	$E_p(cm^2)$	α_o	$P(\alpha_o)\%$	$\Delta\alpha_o$
SAS 1-25 Aug 73-03	3	14.2	.048	208	21.2	25°S	0.9	±1°
	1	8.1	.062		102	0°S	4.7	±2°
	2	5.6	.083		55.7			
SAS 1-25 Aug 73-04	3	12.3	.052	232	17.9	36°S	30.0	±3°
	1	8.1	.070		105	3°N	10.3	±3°
	2	6.4	.092		83.2			
SAS-1-26 Aug 73-01	2	12.3	.036	247	17.0	33°S	10.3	±3°
	1	6.9	.110		142	5°N	34.0	±2°
SAS 1-26 Aug 73-02	2	16.8	.039	129	18.3	24°S	0.1	±1°
	3	12.3	.032		13.1	33°S	15.2	±2°
	1	6.9	.122		72.0	9°S	60.9	±4°
SAS 1-26 Aug 73-03	2	16.8	.046	121	27.8	23°S	0.1	±1°
	1	6.9	.156		73.9	1°N	25.2	±3°
SAS 1-26 Aug 73-04	2	16.8	.064	127	31.3	26°S	0.2	±1°
	1	8.8	.089		46.3	0°	4.1	±2°
	3	5.0	.046		16.3			
SAS 1-27 Aug 73-01	2	16.8	.035	219	43.5	27°S	0.1	±1°
	3	9.8	.056		42.2	1°N	12.1	±2°
	1	4.5	.075		95.6			
SAS 1-27 Aug 73-02	2	16.8	.040	208	67.7	27°S	0.1	±1°
	1	9.8	.078		77.7	1°S	5.2	±2°
	3	5.0	.078		30.7			
SAS 1-31 Aug 73-01	3	16.8	.027	204	21.9	27°S	11.3	±4°
	1	9.8	.102		82.1	3°N	27.9	±2°
	2	4.3	.059		43.1			
SAS 1-06 Sept 73-01	2	16.8	.043	350	97.6			
	3	8.1	.054		79.2			
	1	4.8	.107		138			

Appendix D. (Cont'd)

Run	Peak	Period (sec)	BW(Hz)	$E_T(cm^2)$	$E_p(cm^2)$	α_o	$P(\alpha_o)$%	$\Delta\alpha_o$
SAS 1-06 Sept 73-02	2	16.8	.043	522	179	22°S	51.7	± 4°
	1	7.4	.128		302	0	58.0	± 4°
SAS 1-06 Sept 73-03	2	16.8	.043	533	203	26°S	24.6	± 5°
	1	8.8	.132		298	1°S	60.0	± 5°
SAS 1-07 Sept 73-01	2	14.2	.039	934	238	24°S	25.9	± 4°
	1	8.1	.143		646	2°S	79.7	± 4°
SAS 1-07 Sept 73-02	2	14.2	.043	678	260	25°S	52.4	± 3°
	1	8.8	.143		317	0°	80.9	± 5°
SAS 1-07 Sept 73-03	2	14.2	.059	776	309	26°S	41.9	± 4°
	1	8.8	.097		446	1°S	85.4	± 5°
SAS 1-08 Sept 73-01	2	14.2	.048	749	273	25°S	34.9	± 4°
	1	8.8	.097		414	0°	69.6	± 5°
SAS 1-08 Sept 73-02	2	12.3	.043	668	73.8	7°S	13.3	± 3°
	1	9.8	.140		534	4°S	37.0	± 5°
SAS 1-08 Sept 73-04	2	36.6	.042	792	10.8			
	1	10.9	.097		685			
SAS 1-09 Sept 73-01	1	12.3	.140	590	507			
SAS 1-14 Sept 73-01	1	14.2	.054	192	106	23°S	41.3	± 4°
	2	10.9	.096		59.7	5°S	23.7	± 3°
SAS 1-14 Sept 73-02	1	14.2	.054	199	82.3	24°S	50.8	± 4°
	2	10.9	.064		77.2	4°S	15.9	± 3°
SAS 1-14 Sept 73-03	2	14.2	.054	197	80.3	22°S	41.7	± 5°
	1	10.9	.086		88.8	2°S	17.4	± 3°
SAS 1-15 Sept 73-01	2	14.2	.054	184	70.5			
	1	10.9	.089		87.8	1°S	68.3	± 4°
SAS 1-17 Sept 73-02	1	16.8	.036	323	111			

(cont'd)

Appendix D. (Cont'd)

Run	Peak	Period (sec)	BW(Hz)	$E_T(cm^2)$	$E_p(cm^2)$	α_o	$P(\alpha_o)$%	$\Delta\alpha_o$
SAS 1-17 Sept 73-02	2	12.3	.047		105			
(cont'd)	3	6.0	.129		91.7			
SAS 1-17 Sept 73-03	1	16.8	.032	263	112	22°S	57.5	± 5°
	2	12.3	.057		70.3	2°N	15.5	± 4°
	3	5.0	.097		60.6			
SAS 1-17 Sept 73-04	1	16.8	.039	203	87.3	22°S	32.8	± 3°
	2	12.3	.043		55.3	7°S	24.4	± 4°
	3	5.6	.122		47.5			
SAS 1-18 Sept 73-01	1	16.8	.032	373	249	19°S	23.2	± 4°
	2	10.9	.057		53.7	1°N	10.0	± 3°
	3	5.6	.107		42.5			
SAS 1-18 Sept 73-03	2	14.2	.036	343	88.5	20°S	28.4	± 4°
	3	9.8	.043		75.7	1°S	19.5	± 4°
	1	6.4	.129		153			
SAS 1-18 Sept 73-04	1	14.2	.032	338	185	22°S	25.1	± 4°
	2	9.8	.054		62.4	3°S	26.4	± 4°
	3	6.0	.068		57.1			
SAS 1-19 Sept 73-02	2	14.2	.050	353	115	25°S	27.0	± 3°
	1	6.0	.129		195	11°S	67.5	± 4°
SAS 1-19 Sept 73-03	2	14.2	.075	298	67.8	21°S	28.0	± 4°
	1	6.0	.160		140	4°S	67.4	± 3°
SAS 1-19 Sept 73-04	2	14.2	.043	254	94.6	20°S	20.7	± 3°
	1	6.0	.143		122	1°S	78.5	± 4°
SAS 1-20 Sept 73-01	1	14.2	.047	243	79.8	17°S	26.3	± 4°
	3	9.8	.025		34.2	0°	11.2	± 3°
	2	5.6	.079		71.6			

Appendix D. (Cont'd)

Run	Peak	Period (sec)	BW(Hz)	$E_T(cm^2)$	$E_p(cm^2)$	α_o	$P(\alpha_o)$%	$\Delta\alpha_o$
SAS 1-20 Sept 73-03	2	14.2	.064	346	152	22°S	20.2	±4°
	3	9.8	.021		35.4	1°N	11.8	±3°
	1	6.4	.125		213			
SAS 1-20 Sept 73-04	3	12.3	.043	461	92.1	4°S	20.9	±3°
	2	9.8	.043		123	5°S	18.8	±4°
	1	6.4	.122		220			
SAS 1-21 Sept 73-01	2	10.9	.079	431	156	3°S	32.0	±3°
	3	8.8	.021		44.1	3°S	26.0	±2°
	1	6.4	.122		211			
SAS 1-21 Sept 73-02	2	10.9	.072	876	225	5°S	21.2	±3°
	1	7.4	.143		625	6°S	42.2	±2°
SAS 1-21 Sept 73-03	1	12.3	.072	663	317	5°S	36.5	±3°
	2	7.4	.140		315	3°S	46.9	±3°
SAS 1-22 Sept 73-01	1	12.3	.075	509	338	2°S	27.2	±3°
	2	7.4	.107		149	2°N	62.3	±4°
SAS 1-22 Sept 73-02	1	12.3	.072	629	318	9°S	10.9	±4°
	2	7.4	.125		279	1°S	61.7	±3°
SAS 1-22 Sept 73-03	1	9.8	.096	418	256	1°N	13.7	±3°
	2	6.4	.107		124	8°N	55.0	±4°
SAS 1-23 Sept 73-03	2	12.3	.072	387	98.9	1°S	41.2	±4°
	1	6.0	.139		272	11°N	63.6	±4°
SAS 1-23 Sept 73-04	2	12.3	.061	452	104	2°S	29.7	±3°
	1	6.4	.147		309	9°N	43.4	±4°
SAS 1-24 Sept 73-03	2	10.9	.067	640	197	0°	29.3	±3°
	1	7.4	.072		339	9°N	67.7	±3°
SAS 1-24 Sept 73-04	1	10.9	.067	693	261	3°S	3.7	±2°
	2	8.1	.110		254	1°N	6.4	±2°

Appendix D. (Cont"d)

Run	Peak	Period (sec)	BW(Hz)	$E_T(cm^2)$	$E_p(cm^2)$	α_o	$P(\alpha_o)$%	$\Delta\alpha_o$
SAS 1-25 Sept 73-01	2	9.8	.032	632	65.4	1°N	3.4	±2°
	1	7.4	.075		336	9°N	65.1	±3°
SAS 1-27 Sept 73-01	3	16.8	.032	475	83.0	21°S	2.1	±2°
	1	12.3	.054		246	5°S	46.6	±4°
	2	8.8	.093		125			
SAS 1-02 Oct 73-01	2	14.2	.043	104	34.0	18°S	27.6	±4°
	1	10.9	.023		58.6	1°S	1.6	±2°
SAS 1-02 Oct 73-02	2	16.8	.032	131	14.8	15°S	0.8	±2°
	1	12.3	.086		54.8	24°S	5.0	±3°
SAS 1-02 Oct 73-03	3	16.8	.040	119	23.2	18°S	5.0	±3°
	1	10.9	.067		44.3	17°S	56.5	±4°
	2	6.4	.043		23.8			
SAS 1-03 Oct 73-02	2	16.8	.054	294	49.8	19°S	2.2	±3°
	1	8.1	.072		119	3°N	52.4	±3°
SAS 1-03 Oct 73-03	2	16.8	.038	325	82.9	23°S	0.7	±2°
	1	6.0	.141		181	10°N	56.5	±3°
SAS 1-03 Oct 73-04	2	16.8	.046	198	59.9	23°S	0.2	±1°
	1	9.8	.091		85.1	1°N	38.8	±3°
SAS 1-04 Oct 73-01	2	16.8	.048	222	58.8	25°S	0.3	±1°
	1	9.8	.078		96.6	4°N	9.3	±2°
SAS 1-06 Oct 73-03	1	14.2	.051	205	101	25°S	2.0	±3°
	2	9.8	.044		30.9	4°N	6.1	±2°
	3	6.0	.096		25.4			
SAS 1-08 Oct 73-01	2	14.2	.054	111	32.6	23°S	0.6	±2°
	1	8.8	.070		47.2	0°	5.3	±1°

Appendix D. (Cont'd)

Run	Peak	Period (sec)	BW(Hz)	$E_T(cm^2)$	$E_p(cm^2)$	α_o	$P(\alpha_o)\%$	$\Delta\alpha_o$
SAS 1-08 Oct 73-02	3	14.2	.043	310	26.8	23°S	3.1	± 3°
	1	7.4	.081		131	2°N	40.0	± 4°
	2	5.0	.086		123			
SAS-1-09 Oct 73-02	2	16.8	.043	917	47.9	26°S	0.1	± 2°
	1	7.4	.161		841	5°N	35.7	± 3°
SAS 1-10 Oct 73-01	2	16.8	.081	284	82.0	24°S	0.1	± 1°
	1	6.0	.121		166	5°N	57.0	± 3°
SAS 1-10 Oct 73-03	2	14.2	.043	329	69.8	26°S	0.2	± 2°
	1	6.9	.172		241	0°	39.7	± 3°
SAS 1-10 Oct 73-04	2	16.8	.043	321	72.5	25°S	0.2	± 1°
	1	7.4	.118		189	2°N	23.8	± 4°
SAS 1-11 Oct 73-01	2	14.2	.048	182	54.1	24°S	0.6	± 2°
	1	8.1	.107		88.0	6°S	36.9	± 3°
SAS 1-11 Oct 73-02	2	14.2	.043	213	49.2	22°S	1.2	± 3°
	1	7.4	.143		118	45°S	37.2	± 4°
SAS 1-11 Oct 73-03	1	14.2	.036	213	44.8	25°S	1.3	± 4°
	2	9.8	.043		43.0	1°S	13.1	± 4°
SAS 1-12 Oct 73-04	2	14.2	.043	146	34.8	25°S	1.0	± 3°
	1	8.8	.064		44.8	8°S	45.9	± 4°
	4	6.4	.032		11.6			
	3	5.0	.068		29.3			
SAS 1-13 Oct 73-02	1	14.2	.072	187	66.4	24°S	1.0	± 3°
	2	8.8	.039		41.9	7°S	32.8	± 3°
	3	7.4	.032		25.6	4°N	24.3	± 3°
	4	6.0	.047		23.6			
SAS 1-13 Oct 73-03	2	14.2	.064	151	39.9	23°S	2.0	± 2°
	1	7.4	.129		83.2	8°N	24.4	± 4°

Appendix D. (Cont'd)

Run	Peak	Period (sec)	BW(Hz)	$E_T(cm^2)$	$E_p(cm^2)$	α_o	$P(\alpha_o)\%$	α_o
SAS 1-14 Oct 73-01	1	16.8	.072	190	91.2	22°S	0.5	± 1°
	3	7.4	.047		27.5	6°N	29.5	± 3°
	4	6.4	.039		21.1	1°N	48.2	± 4°
	2	4.1	.064		41.0			
SAS 1-14 Oct 73-02	1	14.2	.054	230	130	21°S	1.7	± 3°
	4	10.9	.029		23.7	5°S	8.5	± 2°
	3	6.9	.057		26.4			
	2	4.3	.075		29.4			
SAS 1-14 Oct 73-04	1	14.2	.043	256	154	23°S	8.9	± 3°
	3	10.9	.032		16.8	5°S	16.7	± 3°
	2	5.3	.063		48.2			
SAS 1-15 Oct 73-01	1	14.2	.043	343	215	17°S	6.0	± 3°
	3	8.1	.054		20.1	4°S	28.8	± 3°
	2	4.5	.096		82.0			
SAS 1-15 Oct 73-04	1	16.8	.096	442	246	26°S	0.2	± 1°
	2	5.0	.118		116	6°N	75.2	± 2°
SAS 1-16 Oct 73-01	1	14.2	.094	336	173	24°S	5.6	± 3°
	2	5.3	.065		111	3°N	70.9	± 4°
SAS 1-16 Oct 73-02	1	14.2	.064	329	234	21°S	0.5	± 2°
	2	5.3	.118		77.1	0°	76.8	± 3°
SAS 1-19 Oct 73-01	1	14.2	.054	882	334	24°S	0.1	± 2°
	3	9.8	.043		72.1	0°	15.2	± 4°
	2	5.0	.086		117			
SAS 1-19 Oct 73-03	1	16.8	.086	428	257	22°S	0.6	± 1°
	2	5.0	.107		98.1	2°N	43.0	± 2°
SAS 1-20 Oct 73-01	1	16.8	.054	492	170	28°S	0.8	± 3°
	3	9.8	.043		79.7	2°S	10.8	± 4°
	2	4.8	.086		151			

Appendix D. (Cont'd)

Run	Peak	Period (sec)	BW(Hz)	$E_T(cm^2)$	$E_p(cm^2)$	α_o	$P(\alpha_o)$%	$\Delta\alpha_o$
SAS 1-20 Oct 73-04	3	36.6	.032	741	82.1			
	1	16.8	.054		273	26°S	1.0	± 4°
	2	5.3	.107		208	1°S	11.4	± 3°
SAS 1-21 Oct 73-03	1	14.2	.107	496	358	26°S	16.7	± 4°
	2	4.1	.043		11.7	26°S	62.9	± 2°
SAS 1-21 Oct 73-04	2	16.8	.032	562	62.9	23°S	26.1	± 3°
	1	9.8	.075		412	16°S	30.5	± 3°
SAS 1-22 Oct 73-01	2	14.2	.043	791	179	22°S	13.7	± 3°
		9.8	.096		547	10°S	25.1	± 3°
SAS 1-22 Oct 73-03	2	14.2	.043	397	110	21°S	8.8	± 3°
	1	10.9	.129		270	2°S	21.8	± 3°
SAS 1-22 Oct 73-04	2	14.2	.064	363	154	20°S	9.4	± 2°
	1	8.1	.118		171	1°S	66.7	± 3°
SAS 1-23 Oct 73-01	1	12.3	.086	270	159	12°S	61.8	± 5°
	2	7.4	.104		86.2	19°S	72.7	± 4°
SAS 1-23 Oct 73-03	1	14.2	.075	167	102	22°S	8.5	± 2°
	2	7.4	.079		43.2	28°S	43.6	± 3°
SAS 1-23 Oct 73-04	1	12.3	.107	636	434	5°S	1.5	± 3°
	2	5.0			172	11°N	66.4	± 4°
SAS 1-24 Oct 73-01	1	14.2	.075	836	385	8°S	17.3	± 3°
	2	7.4	.107		322	10°N	71.2	± 4°
SAS 1-24 Oct 73-02	1	12.3	.075	991	516	5°S	9.4	± 3°
	2	7.4	.097		349	10°N	14.9	± 4°
SAS 1-25 Oct 73-01	1	10.9	.075	528	237	2°S	5.0	± 2°
	2	8.8	.075		155	2°N	9.8	± 3°
	3	5.3	.032		34.8			

Appendix D. (Cont'd)

Run	Peak	Period (sec)	BW(Hz)	$E_T(cm^2)$	$E_p(cm^2)$	α_o	$P(\alpha_o)$%	$\Delta\alpha_o$
SAS 1-25 Oct 73-02	2	16.8	.032	382	22.6	23°S	29.5	± 4°
	1	9.8	.182		335	0°	25.4	± 5°
SAS 1-25 Oct 73-03	2	16.8	.021	447	29.7	25°S	0.1	± 1°
	1	8.8	.177		394	3°S	22.2	± 3°
SAS 1-25 Oct 73-04	2	16.8	.032	426	27.3	28°S	22.3	± 4°
	1	8.8	.150		391	1°N	20.8	± 3°
SAS 1-26 Oct 73-01	2	14.2	.043	398	24.4	25°S	4.4	± 3°
	1	8.8	.161		347	3°N	3.1	± 2°
SAS 1-26 Oct 73-02	3	16.8	.021	421	42.3	25°S	0.3	± 1°
	1	9.8	.107		319	2°N	3.2	± 2°
	2	5.6	.054		51.2			
SAS 1-26 Oct 73-03	3	16.8	.043	232	37.6	26°S	0.6	± 3°
	2	9.8	.054		73.3	1°S	4.6	± 2°
	1	7.4	.091		86.0			
SAS 1-26 Oct 73-04	2	16.8	.032	307	31.1	28°S	1.6	± 3°
	1	8.8	.142		237	0°	6.2	± 3°
SAS 1-27 Oct 73-01	2	16.8	.043	193	26.9	23°S	0.6	± 2°
	1	8.8	.150		143	3°S	9.6	± 2°
SAS 1-27 Oct 73-04	1	14.2	.054	193	76.8	20°S	23.7	± 5°
	3	10.9	.032		29.2	2°S	9.1	± 3°
	2	6.9	.064		44.3			
SAS 1-28 Oct 73-03	1	14.2	.086	208	157	4°S	3.3	± 3°
SAS 1-28 Oct 73-04	1	14.2	.097	283	209	9°S	8.0	± 3°
SAS 1-29 Oct 73-01	1	12.3	.097	405	284	5°S	2.9	± 2°
	2	6.9	.121		97.4	4°N	4.0	± 1°

Appendix D. (Cont'd)

Run	Peak	Period (sec)	BW(Hz)	$E_T(cm^2)$	$E_p(cm^2)$	α_o	$P(\alpha_o)\%$	$\Delta\alpha_o$
SAS 1-29 Oct 73-02	1	16.8	.032	722	242	17°S	1.7	± 3°
	3	12.3	.032		190	2°S	1.7	± 2°
	2	8.1	.075		237			
SAS 1-29 Oct 73-04	1	14.2	.043	1470	919	4°S	0.4	± 3°
	2	9.8	.121		475	2°N	1.6	± 3°
SAS 1-30 Oct 73-01	2	60.2	.032	1380	55			
	1	14.2	.119		1291	5°S	1.4	± 3°
SAS 1-02 Nov 73-02	1	14.2	.078	411	228	17°S	25.6	± 4°
	2	8.1	.070		79.2	1°N	1.9	± 2°
SAS 1-03 Nov 73-01	1	8.8	.105	694	344	0°	0.7	± 2°
	2	7.4	.086		146	2°N	5.1	± 2°
SAS 1-03 Nov 73-02	1	12.3	.073	352	118	8°S	13.0	± 4°
	2	7.4	.035		49.8	1°N	6.9	± 2°
SAS 1-04 Nov 73-02	2	14.2	.054	452	62.3	17°S	4.3	± 3°
	1	6.0	.073		149	1°S	24.9	± 2°
SAS 1-04 Nov 73-04	2	16.8	.043	714	127	26°S	0.8	± 2°
	1	7.4	.105		356	1°N	1.2	± 2°
SAS 1-05 Nov 73-01	2	16.8	.059	688	141	18°S	4.7	± 3°
	1	7.4	.072		168	1°N	2.2	± 2°
SAS 1-05 Nov 73-02	1	16.8	.072	528	183	17°S	3.2	± 3°
	2	6.0	.086		156	4°N	43.1	± 4°
SAS 1-07 Nov 73-02	1	12.3	.107	534	345	5°S	4.8	± 3°
	2	6.0	.064		105			
SAS 1-08 Nov 73-01	2	14.2	.043	386	99.2	24°S	0.6	± 2°
	1	9.8	.059		104	2°N	1.5	± 2°
SAS 1-08 Nov 73-03	2	14.2	.024	406	39.2	25°S	0.7	± 3°
	1	9.8	.070		202	4°S	15.5	± 4°

Appendix D. (Cont'd)

Run	Peak	Period (sec)	BW(Hz)	$E_T(cm^2)$	$E_p(cm^2)$	α_o	$P(\alpha_o)$%	$\Delta\alpha_o$
SAS 1-09 Nov 73-01	1	14.2	.075	233	85.5	18°S	2.9	± 3°
	2	8.1	.054		60.4	8°S	53.2	± 3°
SAS 1-09 Nov 73-03	2	16.8	.032	244	42.5	24°S	0.6	± 2°
	1	10.9	.089		131	2°S	2.3	± 3°
SAS 1-10 Nov 73-01	2	14.2	.030	404	67.5	24°S	0.8	± 2°
	1	9.8	.107		284	4°S	14.0	± 2°
SAS 1-10 Nov 73-02	1	10.9	.134	364	310	8.S	7.5	± 2°
SAS 1-10 Nov 73-04	2	14.2	.024	391	53.9	24°S	1.3	± 3°
	1	9.8	.081		238	16°S	18.8	± 4°
SAS 1-11 Nov 73-03	2	14.2	.021	460	26.3	27°S	0.9	± 2°
	1	9.8	.102		370	11°S	28.2	± 3°
SAS 1-11 Nov 73-04	1	8.8	.152	255	225	26°S	59.7	± 4°
SAS 1-12 Nov 73-01	2	14.2	.027	330	22.3	25°S	0.7	± 3°
	1	9.8	.102		288	11°S	32.5	± 4°
SAS 1-12 Nov 73-02	1	12.3	.057	428	200	8°S	2.2	± 2°
	2	8.8	.093		189			
	3	5.0	.064		12.0			
SAS 1-12 Nov 73-03	1	12.3	.102	867	625	7°S	1.8	± 2°
	2	4.1	.097		218	30°S	61.6	± 3°
SAS 1-12 Nov 73-04	1	10.9	.123	795	579	2°S	1.4	± 2°
	2	4.8	.088		180	56°S	49.8	± 4°
SAS 1-13 Nov 73-01	1	10.9	.113	1080	872	1°S	0.8	± 2°
	2	5.3	.094		161	2°N	29.9	± 2°
SAS 1-13 Nov 73-03	1	9.8	.137	1040	820	2°S	12.6	± 2°
	2	5.6	.072		190			

Appendix D. (Cont'd)

Run	Peak	Period (sec)	BW(Hz)	$E_T(cm^2)$	$E_p(cm^2)$	α_o	$P(\alpha_o)$%	$\Delta\alpha_o$
SAS 1-20 Nov 73-04	1	12.3	.075	890	422	6°S	50.3	± 3°
	2	7.4	.086		290	5°N	51.2	± 3°
	3	4.5	.036		40.1			
SAS 1-21 Nov 73-01	1	10.9	.204	863	820	1°N	46.1	± 4°
SAS 1-01 Dec 73-02	1	14.2	.082	877	759	6°S	0.4	± 2°
	2	7.4	.091		49.6	22°S	30.8	± 3°
SAS 1-01 Dec 73-03	1	14.2	.064	638	564	12°S	2.1	± 3°
	2	7.4	.060		28.5	3°N	10.1	± 2°
SAS 1-01 Dec 73-04	1	14.2	.075	347	278	5°S	0.4	± 2°
	2	6.4	.043		11.8	2°S	8.1	± 2°
SAS 1-02 Dec 73-01	2	14.2	.032	545	199	8°S	0.4	± 1°
	1	10.9	.064		200	4°S	2.2	± 2°
	3	4.8	.107		67.6			
SAS 1-02 Dec 73-02	3	14.2	.043	780	214	10°S	4.0	± 2°
	1	9.8	.054		279	1°S	8.2	± 2°
	2	5.0	.107		222	25°S	17.1	± 3°
SAS 1-03 Dec 73-02	1	9.8	.215	771	730	3°S	2.3	± 2°
SAS 1-04 Dec 73-01	2	14.2	.030	459	28.6	19°S	2.2	± 3°
	1	8.8	.156		374	0°	1.6	± 3°
SAS 1-05 Dec 73-02	1	16.8	.059	258	102	6°S	0.3	± 2°
	2	8.8	.046		59.6	2°N	5.7	± 2°
	3	6.4	.072		51.0			
SAS 1-05 Dec 73-04	1	16.8	.107	594	334	7°S	0.1	± 1°
	2	4.8	.088		155	1°S	7.6	± 1°
SAS 1-06 Dec 73-01	1	14.2	.091	620	261	4°S	0.7	± 2°
	2	4.5	.110		167	0°	35.0	± 1°

Appendix D. (Cont'd)

Run	Peak	Period (sec)	BW(Hz)	$E_T(cm^2)$	$E_p(cm^2)$	α_o	$P(\alpha_o)\%$	$\Delta\alpha_o$
SAS 1-07 Dec 73-01	1	16.8	.107	798	754	7°S	0.2	± 1°
SAS 1-07 Dec 73-02	1	14.2	.128	437	396	7°S	0.4	± 1°
SAS 1-08 Dec 73-01	1	14.2	.113	679	546	5°S	0.8	± 1°
	2	6.4	.099		61.6	10°N	29.7	± 3°
SAS 1-08 Dec 73-02	1	14.2	.099	537	382	12°S	1.0	± 2°
	3	8.8	.043		50.2	15°S	6.5	± 2°
	2	6.4	.089		82.1			
SAS 1-08 Dec 73-03	1	14.2	.113	934	775	8°S	50.0	± 3°
	2	6.4	.097		93.6	2°S	50.0	± 3°
SAS 1-08 Dec 73-04	3	20.5	.025	516	38.7	9°S	0.1	± 1°
	1	14.2	.091		346	5°S	2.9	± 3°
	2	6.4	.059		76.9			
SAS 1-09 Dec 73-01	2	16.8	.029	593	87.3	12°S	1.0	± 2°
	1	12.3	.065		387	6°S	1.9	± 3°
	3	7.4	.097		62.5			
SAS 1-09 Dec 73-02	3	16.8	.030	529	60.2	12°S	0.5	± 2°
	1	12.3	.072		320	11°S	1.4	± 2°
	2	6.9	.113		119			
SAS 1-09 Dec 73-03	1	12.3	.097	397	279	9°S	8.1	± 3°
	2	6.9	.115		49.2	6°N	67.3	± 3°
SAS 1-09 Dec 73-04	1	14.2	.054	362	167	12°S	1.1	± 2°
	2	9.8	.038		83.2	0°	5.5	± 2°
	3	6.9	.032		36.4			
	4	5.6	.048		28.2			
SAS 1-10 Dec 73-01	1	14.2	.102	300	232	14°S	2.1	± 2°
	2	6.9	.123		37.0	18°S	55.0	± 3°

Appendix D. (Cont'd)

Run	Peak	Period (sec)	BW(Hz)	$E_T(cm^2)$	$E_p(cm^2)$	α_o	$P(\alpha_o)$%	$\Delta\alpha_o$
SAS 1-10 Dec 73-03	3	20.5	.032	299	54.6			
	1	14.2	.025		79.7	12°S	20.2	±3°
	2	10.9	.043		77.9	15°S	9.1	±2°
	4	6.9	.086		39.8			
SAS 1-12 Dec 73-01	1	14.2	.064	563	470	6°S	0.6	±2°
	3	8.1	.054		18.5	35°S	48.6	±4°
	2	4.3	.096		28.0			
SAS 1-12 Dec 73-02	1	14.2	.075	478	418	12°S	0.1	±2°
	3	6.9	.054		14.3	9°S	24.8	±3°
	2	4.3	.086		18.0			
SAS 1-12 Dec 73-03	1	14.2	.096	449	395	8°S	0.1	±2°
	2	4.1	.075		13.6	68°S	10.5	±3°
SAS 1-12 Dec 73-04	1	12.3	.076	704	610	8°S	0.6	±3°
	2	6.9	.068		50.4	10°S	11.2	±3°
	3	4.8	.057		20.6			
SAS 1-15 Dec 73-01	1	16.8	.043	1910	1070	2°S	7.2	±3°
	2	12.3	.095		612	1°N	13.8	±3°
	3	5.6	.086		140			
SAS 1-15 Dec 73-02	1	14.2	.089	1880	1610	5°S	21.6	±4°
	2	7.4	.098		201	67°N	20.4	±5°
SAS 1-15 Dec 73-03	1	16.8	.075	2010	1400	11°S	9.4	±3°
	2	8.1	.057		372	90°N	63.6	±8°
SAS 1-15 Dec 73-04	1	16.8	.100	1990	1730	7°S	6.9	±4°
	2	6.4	.065		185			
SAS 1-16 Dec 73-01	1	14.2	.075	1560	1300	9°S	28.7	±5°
	2	6.4	.096		185	47°N	28.4	±4°
SAS 1-16 Dec 73-02	1	14.2	.139	989	953	4°S	15.8	±4°

Appendix D. (Cont'd)

Run	Peak	Period (sec)	BW(Hz)	$E_T(cm^2)$	$E_p(cm^2)$	α_o	$P(\alpha_o)$%	$\Delta\alpha_o$
SAS 1-16 Dec 73-03	1	14.2	.150	720	680			
SAS 1-16 Dec 73-04	1	14.2	.149	629	604			
SAS 1-17 Dec 73-01	1	14.2	.054	508	249			
	2	9.8	.107		225			
	3	4.8	.053		7.5			
SAS 1-17 Dec 73-02	1	14.2	.064	405	304			
	2	8.1	.075		87.4			
SAS 1-17 Dec 73-03	1	12.3	.087	598	421			
	2	6.0	.098		161			
SAS 1-18 Dec 73-01	1	14.2	.064	725	460			
	2	6.9	.100		240			
SAS 1-18 Dec 73-02	2	14.2	.043	679	126			
	1	8.1	.108		457			
	3	4.5	.055		53.9			
SAS 1-18 Dec 73-03	2	14.2	.043	590	203	15°S	46.2	±5°
	1	7.4	.150		323	10°N	70.3	±3°
SAS 1-18 Dec 73-04	1	14.2	.064	906	565	11°S	51.7	±4°
	2	7.4	.128		312	43°S	56.1	±4°
SAS 1-19 Dec 73-01	1	14.2	.075	1120	897	8°S	51.9	±4°
	2	7.4	.054		129	13°N	55.8	±3°
	3	6.0	.065		47.6			
SAS 1-19 Dec 73-03	1	12.3	.064	411	319	10°S	51.2	±3°
	2	8.1	.043		64.7	20°N	56.5	±4°
	3	5.6	.086		37.7			
SAS 1-19 Dec 73-04	2	20.5	.021	449	19.9	17°S	45.8	±4°
	1	10.9	.108		387	89°N	67.5	±10°
	3	5.6	.065		18.4			

Appendix D. (Cont'd)

Run	Peak	Period (sec)	BW(Hz)	$E_T(cm^2)$	$E_p(cm^2)$	α_o	$P(\alpha_o)\%$	$\Delta\alpha_o$
SAS 1-20 Dec 73-04	1	14.2	.075	1230	1080	11°S	53.5	±4°
	2	7.4	.078		87.6	44°N	63.8	±4°
	3	5.0	.054		14.5			
SAS 1-21 Dec 73-01	3	60.2	.040	1370	39.0			
	1	14.2	.075		1240	12°S	53.5	±4°
	2	6.9	.108		75.0	9°S	64.6	±3°
SAS 1-21 Dec 73-02	3	36.6	.086	923	19.0			
	1	14.2	.097		865	13°S	51.1	±4°
	2	6.4	.032		22.0	33°N	61.0	±3°
SAS 1-21 Dec 73-04	2	60.2	.043	941	33.8			
	1	12.3	.085		829	13°S	20.3	±4°
	3	6.0	.090		25.1	13°S	65.5	±4°
SAS 1-22 Dec 73-01	1	12.3	.085	1100	878	12°S	16.9	±3°
	2	6.4	.096		211	9°N	83.1	±5°
SAS 1-22 Dec 73-02	1	12.3	.096	1100	895	10°S	18.6	±3°
	2	4.8	.098		153			
SAS 1-22 Dec 73-03	1	12.3	.075	1540	686	3°S	22.0	±4°
	2	6.9	.070		557	3°N	31.4	±3°
	3	4.8	.086		237			
SAS 1-22 Dec 73-04	1	12.3	.080	1780	1070	0°	24.1	±3°
	2	7.4	.075		444	9°N	39.0	±3°
	3	5.6	.043		141			
SAS 1-23 Dec 73-01	3	60.2	.032	3120	88.9			
	1	12.3	.069		2070	6°S	19.5	±4°
	2	8.1	.150		949	0°	31.8	±4°
SAS 1-24 Dec 73-04	1	16.8	.061	1590	869	12°S	16.0	±3°
	2	9.8	.043		430	4°S	27.8	±3°
	3	6.9	.096		208			

Appendix D. (Cont'd)

Run	Peak	Period (sec)	BW(Hz)	$E_T(cm^2)$	$E_p(cm^2)$	α_o	$P(\alpha_o)\%$	$\Delta\alpha_o$
SAS 1-28 Dec 73-05	1	12.3	.125	409	309	10°S	4.1	± 2°
	2	6.0	.082		84.4	0°	83.2	± 3°
SAS 1-29 Dec 73-01	1	12.3	.129	394	287	13°S	3.3	± 2°
	2	6.0	.079		81.6	0°	69.5	± 3°
SAS 1-29 Dec 73-02	2	12.3	.064	599	252	13°S	4.1	± 2°
	1	6.4	.089		277	1°N	39.9	± 3°
	3	5.0	.047		45.9			
SAS 1-20 Dec 73-04	1	16.8	.064	1250	734	9°S	4.8	± 2°
	2	7.4	.043		265	2°S	15.4	± 3°
	3	6.4	.043		146			
	4	5.0	.043		52.2			
SAS 1-30 Dec 73-01	1	14.2	.064	1550	926	6°S	7.4	± 3°
	2	8.1	.075		488	1°S	12.2	± 3°
	3	5.0	.068		69.6			
SAS 1-30 Dec 73-02	1	16.8	.082	1410	841	7°S	3.5	± 3°
	2	8.8	.146		548	1°S	12.4	± 3°
SAS 1-30 Dec 73-03	2	14.2	.054	1680	484	9°S	2.2	± 2°
	1	8.8	.168		1100	3°S	10.8	± 3°
SAS 1-30 Dec 73-04	1	14.2	.104	1880	1410	6°S	3.8	± 3°
	2	6.9	.089		361	3°N	34.6	± 3°
SAS 1-02 Jan 74-03	1	16.8	.064	470	335	17°S	18.4	± 4°
	2	8.1	.107		125	14°N	45.7	± 4°
SAS 1-02 Jan 74-04	2	16.8	.032	408	95.6	28°S	13.8	± 4°
	1	10.9	.068		219	6°S	22.2	± 3°
	3	6.4	.095		75.0			
SAS 1-03 Jan 74-01	2	14.2	.040	316	182	22°S	21.1	± 5°
	1	9.8	.110		117	2°N	27.1	± 4°

Appendix D. (Cont'd)

Run	Peak	Period (sec)	BW(Hz)	$E_T(cm^2)$	$E_p(cm^2)$	α_o	$P(\alpha_o)$%	$\Delta\alpha_o$
SAS 1-03 Jan 74-02	1	14.2	.056	429	303	25°S	13.7	±4°
	2	8.8	.135		103	4°S	7.8	±2°
SAS 1-03 Jan 74-04	1	14.2	.050	246	115	20°S	18.9	±4°
	2	9.8	.054		82.8	0°	54.3	±4°
	3	4.1	.090		31.3			
SAS 1-03 Jan 74-05	1	14.2	.040	173	78.4	27°S	15.5	±4°
	2	10.9	.193		76.6	5°S	2.0	±3°
SAS 1-04 Jan 74-01	2	14.2	.055	267	51.6	29°S	17.1	±4°
	1	6.0	.182		191	53°S	21.3	±3°
SAS 1-04 Jan 74-04	3	14.2	.032	1140	66.5	14°S	23.8	±4°
	1	7.4	.095		864	34°S	48.4	±4°
	2	5.3	.075		201			
SAS 1-04 Jan 74-05	2	14.2	.032	603	45.6	23°S	17.5	±4°
	1	8.1	.087		502	16°S	47.8	±4°
	3	4.3	.078		41.5			
SAS 1-05 Jan 74-01	2	16.8	.021	2180	82.1	12°S	14.6	±4°
	1	8.1	.193		2050	20°S	30.7	±3°
SAS 1-06 Jan 74-04	3	14.2	.032	816	94.4	15°S	19.0	±4°
	1	8.8	.043		397	17°S	37.6	±3°
	2	7.4	.128		297	19°S	40.9	±4°
SAS 1-06 Jan 74-05	2	12.3	.043	405	122	13°S	15.4	±3°
	3	7.4	.054		99.7	26°S	53.3	±3°
	1	5.3	.118		167			
SAS 1-07 Jan 74-01	1	10.9	.064	278	101	8°S	31.0	±4°
	3	8.1	.055		66.6	12°N	47.8	±3°
	2	5.0	.086		75.8			

Appendix D. (Cont'd)

Run	Peak	Period (sec)	BW(Hz)	E_T (cm^2)	E_p (cm^2)	α_o	$P(\alpha_o)$%	$\Delta\alpha_o$
SAS 1-02 Jan 74-02	1	12.3	.054	290	103	17°S	17.3	± 4°
	2	7.4	.075		83.8	0	56.7	± 4°
	3	5.3	.086		77.1			
SAS 1-07 Jan 74-03	2	12.3	.086	284	112	15°S	20.2	± 4°
	1	5.3	.134		134	51°S	71.6	± 3°
SAS 1-07 Jan 74-04	2	12.3	.055	348	79.1	21°S	19.7	± 5°
	1	6.9	.094		197	7°S	89.6	± 5°
	3	4.3	.050		64.9			
SAS 1-08 Jan 74-01	1	8.1	.110	705	534	41°S	38.7	± 4°
	2	5.3	.095		145	36°N	58.1	± 3°
SAS 1-08 Jan 74-02	1	8.8	.121	1160	879	43°S	39.1	± 4°
	2	5.6	.081		219	22°S	70.8	± 4°
SAS 1-08 Jan 74-03	1	8.8	.246	1590	1500	18°S	8.6	± 4°
SAS 1-09 Jan 74-01	1	8.1	.128	1660	1360	39°S	52.2	± 5°
	2	4.3	.076		281	14°S	49.7	± 4°
SAS 1-09 Jan 74-02	1	8.8	.240	974	938	30°S	52.6	± 5°
SAS 1-10 Jan 74-03	1	20.5	.043	440	238	17°S	8.2	± 3°
	2	9.8	.161		184	13°S	27.1	± 3°
SAS 1-11 Jan 74-01	1	16.8	.068	569	431	8°S	13.7	± 4°
	2	7.4	.113		98.0	34°S	48.6	± 4°
SAS 1-11 Jan 74-03	1	14.2	.075	224	175	15°S	14.1	± 3°
	2	7.4	.128		32.0	23°S	57.3	± 4°
SAS 1-11 Jan 74-04	1	14.2	.074	156	125	18°S	15.6	± 3°
	2	6.9	.118		21.0	5°N	81.7	± 3°
SAS 1-12 Jan 74-01	1	14.2	.061	239	206	15°S	16.1	± 3°
	2	7.4	.079		13.6	24°S	41.8	± 4°

Appendix D. (Cont'd)

Run	Peak	Period (sec)	BW(Hz)	$E_T(cm^2)$	$E_p(cm^2)$	α_o	$P(\alpha_o)$%	$\Delta\alpha_o$
SAS 1-12 Jan 74-02	2	60.2	.032	277	11.9			
	1	14.2	.086		258	13°S	10.7	±3°
	3	6.9	.045		7.0	19°S	56.9	±4°
SAS 1-12 Jan 74-03	1	14.2	.049	365	197	18°S	14.4	±4°
	2	9.8	.108		136	22°S	16.1	±4°
	3	4.1	.036		5.7			
SAS 1-12 Jan 74-04	1	14.2	.060	495	298	16°S	14.6	±3°
	2	8.1	.110		184	21°S	17.1	±3°
SAS 1-13 Jan 74-01	1	14.2	.182	768	740	14°S	11.2	±3°
SAS 1-13 Jan 74-02	1	14.2	.161	962	946	11°S	11.6	±3°
SAS 1-13 Jan 74-03	1	12.3	.089	1700	1520	14°S	11.2	±3°
	2	6.4	.112		160	12°S	38.1	±3°
SAS 1-13 Jan 74-04	1	14.2	.078	1310	1125	9°S	12.7	±3°
	2	7.4	.117		148	12°S	31.6	±3°
SAS 1-14 Jan 74-01	1	14.2	.092	1450	1250	12°S	12.7	±3°
	2	6.9	.054		74.5	5°S	37.1	±3°
	3	4.3	.065		13.9			
SAS 1-14 Jan 74-02	1	14.2	.203	931	888	9°S	10.1	±3°
SAS 1-15 Jan 74-01	1	12.3	.160	658	611	5°S	18.0	±3°
	2	4.3	.043		6.1	65°S	39.1	±2°
SAS 1-15 Jan 74-03	1	12.3	.128	512	490	8°S	7.8	±2°
SAS 1-15 Jan 74-04	2	16.8	.021	473	20.0			
	1	12.3	.119		332	5°S	16.5	±3°
	3	5.0	.053		12.0			
SAS 1-16 Jan 74-01	2	16.8	.036	385	56.6	6°S	16.1	±3°
	1	10.9	.096		285	11°S	22.6	±3°
	3	5.3	.064		10.6			

Appendix D. (Cont'd)

Run	Peak	Period (sec)	BW(Hz)	$E_T(cm^2)$	$E_p(cm^2)$	α_o	$P(\alpha_o)$%	$\Delta\alpha_o$
SAS 1-18 Jan 74-02	1	10.9	.182	651	618	10°S	55.1	± 3°
SAS 1-18 Jan 74-03	1	12.3	.150	721	692			
SAS 1-19 Jan 74-01	1	12.3	.155	611	592			
SAS 1-19 Jan 74-02	2	14.2	.030	387	49.9			
	1	9.8	.102		284			
SAS 1-19 Jan 74-03	1	10.9	.155	371	358			
SAS 1-19 Jan 74-04	1	10.9	.059	480	214			
	2	6.9	.075		190			
	3	4.5	.048		42.0			
SAS 1-20 Jan 74-01	1	10.9	.070	496	330			
	2	6.4	.065		72.3			
	3	4.5	.059		31.1			
SAS 1-20 Jan 74-02	1	14.2	.064	1920	1480	2°S	41.0	± 4°
	2	6.9	.139		349	3°S	45.4	± 3°
SAS 1-25 Jan 74-02	2	14.2	.036	220	146	14°S	27.9	± 4°
	1	9.8	.134		64.2	3°S	32.6	± 3°
SAS 1-26 Jan 74-01	2	14.2	.054	171	72.9	15°	14.3	± 4°
	1	7.4	.023		81.3	2°N	15.0	± 2°
SAS 1-26 Jan 74-02	2	14.2	.048	323	113	20°S	3.1	± 3°
	3	8.8	.059		33.4	1°S	2.1	± 2°
	1	4.5	.086		139			
SAS 1-26 Jan 74-03	2	12.3	.054	348	122	8°S	2.2	± 3°
	1	6.0	.161		207	4°N	54.2	± 3°
SAS 1-26 Jan 74-04	2	12.3	.051	856	161	4°S	3.8	± 3°
	1	8.1	.091		459	13°S	10.3	± 3°
	3	5.3	.048		151			

Appendix D. (Cont'd)

Run	Peak	Period (sec)	BW(Hz)	$E_T(cm^2)$	$E_p(cm^2)$	α_o	$P(\alpha_o)\%$	$\Delta\alpha_o$
SAS 1-27 Jan 74-01	2	14.2	.034	667	111	11°S	0.5	± 1°
	1	8.1	.171		444	0°	5.5	± 2°
SAS 1-27 Jan 74-02	2	10.9	.064	632	176	3°S	1.0	± 3°
	1	8.1	.134		401	0°	9.2	± 3°
SAS 1-27 Jan 74-03	2	12.3	.054	1030	288	4°S	1.8	± 3°
	1	8.1	.126		680	2°N	4.3	± 2°
	3	4.5	.042		37.7			
SAS 1-27 Jan 74-04	2	16.8	.040	1190	227	9°S	0.3	± 2°
	1	10.9	.039		790	4°S	1.7	± 3°
SAS 1-28 Jan 74-01	1	14.2	.061	697	377	6°S	4.7	± 3°
	2	6.9	.111		271	7°S	54.1	± 4°
SAS 1-28 Jan 74-03	1	14.2	.086	414	308	5°S	10.3	± 3°
	2	6.9	.085		90.3	0°	38.2	± 4°
SAS 1-28 Jan 74-04	2	14.2	.027	554	145	10°S	13.6	± 4°
	1	10.9	.075		321	4°N	47.9	± 3°
	3	6.4	.094		65.8			
SAS 1-29 Jan 74-01	1	12.3	.057	285	127	11°S	19.6	± 3°
	2	9.8	.036		70.7	5°S	22.9	± 3°
	3	7.4	.079		63.4			
SAS 1-29 Jan 74-02	1	12.3	.137	468	410	10°S	1.7	± 3°
	2	5.3	.075		36.4	4°N	43.9	± 3°
SAS 1-29 Jan 74-03	2	14.2	.062	437	210	14°S	0.1	± 1°
	1	9.8	.156		212	8°S	15.7	± 3°
SAS 1-29 Jan 74-04	2	14.2	.032	322	76.0	11°S	3.1	± 3°
	1	6.9	.129		223	4°N	0.8	± 2°
SAS 1-30 Jan 74-01	3	20.5	.021	416	17.3	12°S	0.1	± 1°
	2	12.3	.033		73.0	8°S	1.6	± 2°
	1	8.1	.121		281	5°S	9.8	± 3°

Appendix D. (Cont'd)

Run	Peak	Period (sec)	BW(Hz)	$E_T(cm^2)$	$E_p(cm^2)$	α_o	$P(\alpha_o)\%$	$\Delta\alpha_o$
SAS 1-30 Jan 74-03	2	14.2	.035	284	113	9°S	20.4	±3°
	1	6.9	.145		156	8°N	65.0	±3°
SAS 1-30 Jan 74-04	2	14.2	.040	267	76.9	7°S	18.7	±3°
	1	6.9	.145		173	6°N	32.6	±3°
SAS 1-31 Jan 74-01	1	14.2	.076	240	114	6°S	15.9	±3°
	2	6.9	.118		113	10°N	35.0	±3°
SAS 1-09 Feb 74-02	1	14.2	.086	130	106			
SAS 1-09 Feb 74-03	1	14.2	.075	115	86.0	20°S	19.5	±4°
	2	8.8	.075		12.2	2°N	34.6	±4°
SAS 1-10 Feb 74-01	1	14.2	.075	175	128	17°S	20.5	±4°
	2	8.1	.043		11.8	1°N	35.6	±4°
SAS 1-10 Feb 74-04	1	14.2	.051	274	239	11°S	1.6	±4°
	3	7.4	.054		7.1	8°N	52.5	±4°
	2	5.0	.070		11.0	41°S	50.2	±3°
SAS 1-11 Feb 74-01	1	14.2	.043	648	540	8°S	0.3	±2°
	2	6.9	.064		34.0	7°S	34.3	±3°
	3	4.8	.056		32.4	70°S	46.0	±4°
SAS 1-11 Feb 74-02	1	14.2	.054	527	446	6°S	1.5	±2°
	2	5.3	.145		67.8	74°S	30.5	±4°
SAS 1-11 Feb 74-03	1	14.2	.043	1180	1020	4°S	2.0	±2°
	2	6.9	.064		68.1	5°S	5.8	±3°
	3	5.0	.075		61.6	11°S	28.3	±3°
SAS 1-11 Feb 74-04	1	14.2	.054	698	607	11°S	1.0	±2°
	2	5.6	.137		68.0	1°S	36.1	±3°
SAS 1-12 Feb 74-01	1	14.2	.075	639	547	7°S	0.8	±2°
	2	5.6	.128		51.3	1°N	38.7	±3°

Appendix D. (Cont'd)

Run	Peak	Period (sec)	BW(Hz)	$E_T(cm^2)$	$E_p(cm^2)$	α_o	$P(\alpha_o)$	$\Delta\alpha_o$
SAS 1-12 Feb 74-02	2	16.8	.021	565	93.0	8°S	0.3	± 1°
	1	12.3	.067		368	5°S	0.8	± 1°
	3	5.3	.107		77.4			
SAS 1-26 Feb 74-02	1	14.2	.091	405	221	10°S	1.5	± 3°
	2	6.0	.129		162	4°N	13.6	± 2°
SAS 1-27 Feb 74-02	2	12.3	.078	655	277	5°S	1.0	± 2°
	1	6.9	.134		357	6°N	6.7	± 2°
SAS 1-27 Feb 74-04	1	14.2	.075	571	441	10°S	2.2	± 3°
	2	6.0	.124		103	0°	10.0	± 2°
SAS 1-28 Feb 74-01	1	12.3	.099	829	742	6°S	0.6	± 3°
SAS 1-28 Feb 74-07	1	12.3	.121	609	546	4°S	1.0	± 2°
SAS 1-01 Mar 74-01	1	10.9	.118	748	609	1°S	0.5	± 1°
SAS 1-07 Mar 74-03	3	9.8	.050	230	42.2	4°S	12.4	± 2°
	2	6.4	.059		73.1	78°N	2.3	± 4°
	1	4.8	.064		84.9			
SAS 1-07 Mar 74-04	2	14.2	.054	200	25.9	5°S	1.0	± 3°
	1	6.4	.150		139	46°S	0.4	± 2°
SAS 1-08 Mar 74-01	1	14.2	.078	625	444	6°S	0.2	± 2°
	2	6.9	.121		161	47°S	1.9	± 2°
SAS 1-08 Mar 74-04	2	14.2	.047	2100	90.1	6°S	3.2	± 3°
	1	8.8	.183		2000	2°S	2.2	± 2°
SAS 1-09 Mar 74-01	1	10.9	.164	1520	1400	1°N	3.1	± 2°
SAS 1-09 Mar 74-02	1	10.9	.070	1130	622	5°S	1.7	± 3°
	2	7.4	.118		482	24°S	63.1	± 4°
SAS 1-09 Mar 74-03	1	10.9	.215	411	388	6°S	4.2	± 2°

Appendix D. (Cont'd)

Run	Peak	Period (sec)	BW(Hz)	$E_T(cm^2)$	$E_p(cm^2)$	α_o	$P(\alpha_o)$%	$\Delta\alpha_o$
SAS 1-10 Mar 74-03	1	14.2	.064	124	50.2	13°S	3.2	± 2°
	2	8.8	.043		30.8	4°S	58.2	± 4°
	3	6.4	.085		30.0			
SAS 1-11 Mar 74-01	1	10.9	.075	153	66.0	6°S	2.9	± 2°
	2	6.9	.107		48.5	25°S	20.2	± 3°
SAS 1-15 Mar 74-03	1	16.8	.032	277	138	8°S	0.1	± 1°
	2	10.9	.149		122	6°S	1.2	± 2°
SAS 1-16 Mar 74-02	1	14.2	.054	170	136	12°S	0.7	± 1°
	2	8.8	.129		23.3	7°S	18.0	± 3°
SAS 1-16 Mar 74-03	1	16.8	.025	169	89.0	13°S	0.1	± 1°
	2	12.3	.039		54.9	11°S	0.9	± 2°
	3	8.1	.125		16.8			
SAS 1-17 Mar 74-01	1	14.2	.118	209	188	11°S	2.0	± 2°
SAS 1-17 Mar 74-02	1	16.8	.024	224	94.4	20°S	0.6	± 2°
	2	12.3	.030		86.7	6°S	7.3	± 3°
	3	8.8	.053		25.4	11°S	5.9	± 3°
	5	6.4	.042		6.5			
	4	4.1	.060		17.5			
SAS 1-17 Mar 74-03	1	14.2	.055	210	159	14°S	0.5	± 2°
	3	7.4	.070		11.7	10°S	6.6	± 2°
	2	4.3	.075		23.6			
SAS 1-22 Mar 74-01	1	14.2	.066	396	327	22°S	1.8	± 2°
	2	7.4	.078		32.3	11°S	10.1	± 2°
	3	4.3	.062		17.1	20°N	48.5	± 3°
SAS 1-22 Mar 74-02	1	14.2	.080	354	270	16°S	5.5	± 3°
	2	4.5	.137		53.0	67°S	41.0	± 3°
SAS 1-22 Mar 74-03	1	12.3	.095	188	131	11°S	7.3	± 2°
	2	5.0	.107		23.5	13°N	52.3	± 4°

Appendix D. (Cont'd)

Run	Peak	Period (sec)	BW(Hz)	$E_T(cm^2)$	$E_p(cm^2)$	α_o	$P(\alpha_o)$%	$\Delta\alpha_o$
SAS 1-22 Mar 74-04	3	26.2	.021	149	6.7			
	2	16.8	.028		54.0	22°S	0.4	± 2°
	1	12.3	.102		61.0	22°S	11.1	± 3°
SAS 1-26 Mar 74-01	1	20.5	.062	1440	1090	18°S	9.2	± 3°
	2	9.8	.048		136	12°S	27.7	± 3°
	3	6.0	.112		23.6			
SAS 1-26 Mar 74-02	1	16.8	.046	1660	1230	12°S	14.5	± 4°
	2	8.8	.054		295	9°S	25.8	± 3°
	3	6.0	.110		78.5			
SAS 1-26 Mar 74-03	3	60.2	.030	1430	22.9			
	1	16.8	.043		1200	13°S	14.9	± 4°
	2	8.8	.134		169	9°S	24.9	± 3°
SAS 1-27 Mar 74-01	1	16.8	.060	1910	1610	6°S	13.8	± 4°
	2	8.1	.065		189	6°S	29.7	± 3°
	3	5.3	.084		36.5			
SAS 1-27 Mar 74-02	1	16.8	.075	1300	1120	16°S	16.1	± 4°
	2	8.1	.115		183	4°N	74.7	± 5°
SAS 1-27 Mar 74-03	1	14.2	.151	2140	2090	11°S	20.7	± 4°
SAS 1-28 Mar 74-01	1	14.2	.161	1830	1780	8°S	18.7	± 4°
SAS 1-28 Mar 74-03	1	12.3	.155	1260	1200	9°S	20.7	± 3°
SAS 1-28 Mar 74-04	1	14.2	.144	1140	1110	9°S	19.3	± 3°
SAS 1-29 Mar 74-01	1	20.5	.214	1320	1270	19°S	7.9	± 3°
SAS 1-29 Mar 74-02	1	14.2	.155	1630	1490	8°S	19.2	± 3°
SAS 1-29 Mar 74-03	2	36.6	.022	2470	30.6			
	1	14.2	.142		2370	7°S	16.7	± 4°

Appendix D. (Cont'd)

Run	Peak	Period (sec)	BW(Hz)	$E_T(cm^2)$	$E_p(cm^2)$	α_o	$P(\alpha_o)\%$	$\Delta\alpha_o$
SAS 1-29 Mar 74-04	4	60.2	.040	2300	69.1			
	1	14.2	.064		1860	7°S	16.4	± 4°
	2	8.1	.053		225	13°S	32.5	± 4°
	3	4.5	.075		70.9			
SAS 1-30 Mar 74-01	3	60.2	.038	1390	59.2			
	1	14.2	.097		1150	7°S	17.7	± 4°
	2	4.5	.068		64.6	86°N	32.7	
SAS 1-30 Mar 74-02	1	14.2	.054	1580	1180	7°S	18.9	± 4°
	2	7.4	.044		221	15°S	41.3	± 3°
	3	5.0	.096		70.7			
SAS 1-30 Mar 74-03	1	14.2	.144	1110	1070	5°S	15.9	± 3°
SAS 1-30 Mar 74-04	2	60.2	.038	1180	44.4			
	1	14.2	.142		1080	12°S	17.7	± 4°
	3	4.5	.064		33.6	4°N	35.5	± 3°
SAS 1-31 Mar 74-01	1	12.3	.086	1440	1060	8°S	18.3	± 3°
	2	6.0	.110		333	16°S	80.3	± 3°
SAS 1=31 Mar 74-02	1	12.3	.064	2400	1190	8°S	19.7	± 4°
	2	8.1	.080		922	9°S	40.1	± 3°
	3	4.3	.065		192			
SAS 1-01 Apr 74-01	1	12.3	.059	2140	1610	7°S	20.1	± 3°
	3	8.1	.055		161	0°	36.9	± 4°
	2	6.0	.076		284			
SAS 1-01 Apr 74-02	3	60.2	.054	1680	35.3			
	1	12.3	.129		1480	8°S	20.1	± 3°
	2	5.6	.065		84.7	4°S	35.0	± 3°
SAS 1-01 Apr 74-03	1	12.3	.064	1590	918	4°S	2.0	± 3°
	2	8.1	.128		595	4°S	72.5	± 4°

Appendix D. (Cont'd)

Run	Peak	Period (sec)	BW(Hz)	$E_T(cm^2)$	$E_p(cm^2)$	α_o	$P(\alpha_o)$%	$\Delta\alpha_o$
SAS 1-01 Apr 74-04	1	14.2	.087	1660	1160	11°S	18.7	±3°
	2	6.0	.110		398	10°S	59.9	±4°
SAS 1-02 Apr 74-01	2	14.2	.070	1530	567	7°S	17.7	±4°
	1	5.6	.123		942	5°S	69.3	±4°
SAS 1-03 Apr 74-01	1	8.8	.172	1900	1790	3°S	3.3	±2°
SAS 1-03 Apr 74-03	1	9.8	.180	2500	2380	6°S	4.0	±2°
SAS 1-03 Apr 74-04	2	16.8	.043	1340	415	17°S	0.4	±1°
	1	8.8	.091		636	2°S	1.6	±3°
SAS 1-04 Apr 74-01	2	16.8	.064	1140	261	14°S	3.1	±3°
	1	9.8	.078		578	3°S	4.1	±2°
SAS 1-04 Apr 74-02	2	16.8	.043	963	235	21°S	0.7	±1°
	1	8.8	.142		665	7°S	1.6	±2°
SAS 1-05 Apr 74-01	1	12.3	.129	522	521	6°S	3.1	±3°
SAS 1-05 Apr 74-02	1	14.2	.140	487	440	14°S	3.1	±3°
SAS 1-05 Apr 74-04	1	14.2	.126	348	315	20°S	2.2	±4°
SAS 1-05 Apr 74-05	1	12.3	.145	424	291	9°S	0.9	±2°
SAS 1-07 Apr 74-02	2	14.2	.075	522	233	11°S	3.6	±3°
	1	8.1	.064		251	2°S	4.6	±2°
SAS 1-07 Apr 74-03	1	12.3	.054	1220	1030	6°S	0.8	±2°
SAS 1-09 Apr 74-04	1	12.3	.064	651	181	8°S	1.9	±3°
	2	8.8	.032		424	3°S	6.8	±2°
SAS 1-12 Apr 74-03	2	16.8	.032	442	22.2			
	1	12.3	.118		355			
SAS 1-13 Apr 74-01	1	12.3	.107	612	596	1°S	0.6	±2°

Appendix D. (Cont'd)

Run	Peak	Period (sec)	BW(Hz)	$E_T(cm^2)$	$E_p(cm^2)$	α_o	$P(\alpha_o)\%$	$\Delta\alpha_o$
SAS 1-13 Apr 74-02	2	16.8	.011	541	66.5	17°S	1.2	± 3°
	1	10.9	.096		451	1°S	0.8	± 3°
SAS 1-13 Apr 74-03	2	16.8	.032	443	80.4	11°S	1.0	± 2°
	1	10.9	.118		330	7°S	3.1	± 2°
SAS 1-13 Apr 74-04	2	16.8	.032	383	113	12°S	4.4	± 2°
	1	10.9	.140		236	2°S	1.7	± 2°
SAS 1-14 Apr 74-01	2	14.2	.048	338	139	8°S	5.6	± 3°
	1	10.9	.107		177	1°S	5.7	± 3°
SAS 1-14 Apr 74-03	2	14.2	.048	247	99.5	9°S	4.8	± 3°
	1	9.8	.161		126	7°S	32.0	± 4°
SAS 1-14 Apr 74-04	1	14.2	.139	229	212	16°S	5.2	± 3°
SAS 1-15 Apr 74-01	1	14.2	.115	266	168	17°S	3.5	± 3°
	2	4.5	.070		45.0	32°S	42.8	± 4°
SAS 1-15 Apr 74-03	1	14.2	.139	186	176	18°S	1.6	± 3°
SAS 1-15 Apr 74-04	1	14.2	.089	216	194	12°S	12.5	± 3°
SAS 1-16 Apr 74-01	1	14.2	.071	402	205	11°S	3.2	± 3°
	2	6.4	.105		162	5°N	12.0	± 3°
SAS 1-16 Apr 74-02	3	16.8	.019	744	45.6	30°S	0.3	± 1°
	2	12.3	.038		162	2°	1.6	± 3°
	1	7.4	.121		493			
SAS 1-16 Apr 74-03	1	12.3	.912	761	525	3°S	3.2	± 3°
	2	6.0	.617		167	5°N	35.5	± 4°
	3	4.3	.429		54			
SAS 1-16 Apr 74-04	1	9.8	.122	764	590	1°N	0.5	± 3°
	2	5.0	.075		123	0°	80.3	± 3°

Appendix D. (Cont'd)

Run	Peak	Period (sec)	BW(Hz)	$E_T(cm^2)$	$E_p(cm^2)$	α_o	$P(\alpha_o)\%$	$\Delta\alpha_o$
SAS 1-17 Apr 74-01	1	12.3	.067	366	184	10°S	1.5	± 3°
	2	8.8	.070		147	1°S	4.6	± 2°
SAS 1-17 Apr 74-02	1	10.9	.066	259	181	8°S	2.8	± 2°
	2	8.1	.048		34.1	4°S	16.4	± 3°
SAS 1-17 Apr 74-03	1	10.9	.140	237	185	7°S	2.1	± 2°
	2	4.3	.054		24.1	76°S	31.8	± 5°
SAS 1-18 Apr 74-01	2	16.8	.048	221	73.5	10°S	0.3	± 2°
	1	10.9	.099		104	8°S	2.9	± 3°
	3	4.1	.059		40.5			
SAS 1-18 Apr 74-02	1	16.8	.043	317	186	6°S	0.1	± 1°
	2	10.9	.097		65.3	8°S	3.6	± 2°
	3	4.3	.064		45.1			
SAS 1-18 Apr 74-03	1	14.2	.054	318	118	6°S	0.6	± 1°
	3	10.9	.054		37.7	10°S	2.4	± 3°
	2	5.3	.090		111			
SAS 1-18 Apr 74-04	2	14.2	.040	812	146	9°S	3.0	± 3°
	1	6.9	.129		576	3°S	4.0	± 2°
SAS 1-19 Apr 74-01	2	14.2	.054	1300	285	4°S	1.1	± 3°
	1	8.8	.097		890	3°S	5.3	± 2°
SAS 1-20 Apr 74-01	1	8.8	.097	625	593	11°S	11.8	± 4°
SAS 1-20	2	10.9	.032	498	92.0	9°S	3.5	± 2°
	1	7.4	.118		354	1°N	34.6	± 4°
SAS 1-20 Apr 74-03	1	10.9	.075	373	324	9°S	6.1	± 3°
SAS 1-20 Apr 74-04	2	16.8	.032	564	29.7	15°S	1.8	± 4°
	1	9.8	.150		490	9°S	5.0	± 3°

Appendix D.   (Cont'd)

Run	Peak	Period (sec)	BW(Hz)	$E_T(cm^2)$	$E_p(cm^2)$	α_o	$P(\alpha_o)\%$	$\Delta\alpha_o$
SAS 1-21 Apr 74-01	2	16.8	.043	406	73.3	11°S	0.9	± 4°
	1	8.1	.140		287	2°S	2.6	± 4°
SAS 1-21 Apr 74-02	2	16.8	.043	343	58.8	10°S	2.1	± 3°
	1	8.1	129		252	11°S	20.6	± 3°
SAS 1-21 Apr 74-03	2	16.8	.043	328	108	11°S	0.4	± 2°
	1	10.9	.107		147	4°S	1.0	± 2°
SAS 1-21 Apr 74-04	2	14.2	.054	434	112	11°S	2.1	± 3°
	1	8.8	.064		317	8°S	4.9	± 2°
SAS 1-22 Apr 74-01	2	14.2	.054	266	85.2	12°S	1.6	± 4°
	1	10.9	.064		138	1°S	0.9	± 3°
SAS 1-22 Apr 74-02	1	9.8	.107	245	141	3°S	7.0	± 2°
	2	6.0	.096		85.2	9°S	38.3	± 4°
SAS 1-22 Apr 74-03	3	20.5	.021	262	17.0	9°S	1.0	± 3°
	1	14.2	.043		118	9°S	2.0	± 3°
	2	4.8	.075		68.1			
SAS 1-22 Apr 74-04	3	20.5	.011	369	16.4			
	2	10.9	.064		93.1	3°S	0.7	± 3°
	1	5.0	.122		234	10°S	61.0	± 3°
SAS 1-23 Apr 74-01	3	16.8	.029	253	42.1	5°S	3.2	± 3°
	1	10.9	.093		122	0°	1.4	± 3°
	2	5.0	.093		71.8			
SAS 1-23 Apr 74-02	2	16.8	.032	302	120	2°S	0.3	± 1°
	1	10.9	.102		138	6°S	2.1	± 3°
	3	4.8	.051		23.7			
SAS 1-23 Apr 74-04	1	14.2	.118	356	327	10°S	1.4	± 3°
SAS 1-24 Apr 74-01	1	14.2	.078	262	246	8°S	1.6	± 3°

Appendix D. (Cont'd)

Run	Peak	Period (sec)	BW(Hz)	$E_T(cm^2)$	$E_p(cm^2)$	α_o	$P(\alpha_o)\%$	$\Delta\alpha_o$
SAS 1-24 Apr 74-02	1	14.2	.097	287	275	7°S	4.1	± 3°
SAS 1-25 Apr 74-03	1	10.9	.072	839	439	4°S	1.2	± 3°
	2	6.4	.097		313	2°N	23.3	± 4°
SAS 1-25 Apr 74-04	3	16.8	.032	806	90.5	24°S	0.3	± 2°
	2	12.3	.054		270	5°S	2.0	± 3°
	1	6.9	.107		275			
SAS 1-26 Apr 74-01	1	7.4	.097	839	810	12°S	23.2	± 3°
SAS 1-26 Apr 74-02	3	16.8	.024	753	52.2	26°S	0.3	± 2°
	2	10.9	.024		74.5	3°S	1.2	± 4°
	1	7.4	.136		584			
SAS 1-26 Apr 74-05	2	14.2	.043	467	100	23°S	1.0	± 1°
	1	6.9	.129		318	3°N	43.8	± 5°
SAS 1-27 Apr 74-01	2	14.2	.025	593	44.3	26°S	2.0	± 3°
	1	7.4	.129		531	1°N	34.6	± 4°
SAS 1-27 Apr 74-02	3	16.8	.064	244	59.8	24°S	0.9	± 1°
	2	8.1	.054		80.1	4°S	32.2	± 4°
	1	5.6	.107		93.5			
SAS 1-27 Apr 74-03	2	14.2	.032	222	34.3	23°S	8.8	± 3°
	1	8.8	.086		167	13°S	29.0	± 5°
SAS 1-27 Apr 74-04	2	14.2	.032	383	34.9	13°S	13.3	± 4°
	1	6.9	.129		293	14°S	25.6	± 4°
SAS 1-28 Apr 74-01	2	14.2	.032	526	62.4	23°S	3.0	± 4°
	1	8.8	.128		411	2°N	7.5	± 4°
SAS 1-28 Apr 74-02	2	14.2	.043	431	62.8	26°S	3.6	± 4°
	1	9.8	.107		298	1°S	12.3	± 4°
SAS 1-28 Apr 74-04	1	6.9	.183	480	428	6°N	22.1	± 4°

Appendix D. (Cont'd)

Run	Peak	Period (sec)	BW(Hz)	$E_T(cm^2)$	$E_p(cm^2)$	α_o	$P(\alpha_o)$%	$\Delta\alpha_o$
SAS 1-29 Apr 74-01	2	12.3	.054	533	137	0°	6.1	± 3°
	1	6.9	.105		384	5°N	7.0	± 2°
SAS 1-29 Apr 74-03	1	10.9	.104	323	188	1°S	1.1	± 3°
	2	6.9	.064		80.8	7°N	34.4	± 4°
SAS 1-29 Apr 74-04	1	10.9	.113	256	162	0°	1.2	± 3°
	2	6.0	.100		80.7	6°N	71.1	± 4°
SAS 1-30 Apr 74-01	2	10.9	.067	321	75.6	4°S	4.6	± 2°
	1	6.4	.126		216	19°S	58.2	± 4°
SAS 1-30 Apr 74-02	2	12.3	.067	189	44.9	10°S	9.2	± 2°
	1	6.0	.142		131	23°S	38.7	± 4°
SAS 1-30 Apr 74-03	2	12.3	.064	356	94.9	7°S	1.0	± 3°
	1	5.3	.136		250	3°N	74.6	± 5°
SAS 1-30 Apr 74-04	3	16.8	.027	352	36.8	24°S	0.3	± 3°
	2	12.3	.038		50.6	10°S	2.8	± 3°
	1	6.4	.104		182			
SAS 1-01 May 74-01	2	16.8	.032	563	77.6	28°S	0.3	± 2°
	3	12.3	.025		42.7	3°S	4.8	± 3°
	1	6.9	.136		411			
SAS 1-01 May 74-02	2	16.8	.043	268	84.1	26°S	0.1	± 1°
	3	12.3	.043		61.9	7°S	2.0	± 4°
	1	7.4	.114		100			
SAS 1-01 May 74-03	1	12.3	.144	274	241	5°S	1.6	± 3°
SAS 1-01 May 74-04	1	14.2	.086	206	195	23°S	0.8	± 2°
SAS 1-02 May 74-01	2	12.3	.075	478	170	6°S	2.4	± 3°
	1	6.0	.110		261	2°N	27.0	± 3°

Appendix D. (Cont'd)

Run	Peak	Period (sec)	BW(Hz)	$E_T(cm^2)$	$E_p(cm^2)$	α_o	$P(\alpha_o)$%	$\Delta\alpha_o$
SAS 1-02 May 74-02	2	14.2	.043	287	67.1	20°S	1.2	3°
	1	10.9	.054		191	9°S	2.4	3°
SAS 1-02 May 74-03	2	14.2	.043	241	66.6	25°S	0.9	2°
	1	10.9	.054		96.0	4°S	1.6	3°
SAS 1-02 May 74-04	1	14.2	.091	323	175	23°S	0.8	3°
	2	5.6	.091		100	5°N	57.8	4°
SAS 1-03 May 74-01	1	16.8	.048	311	116	22°S	0.4	1°
	2	10.9	.051		104	9°S	9.7	3°
	3	5.3	.070		51.5			
SAS 1-03 May 74-02	1	14.2	.097	617	422	17°S	4.0	3°
	2	6.4	.115		157	0°	10.0	3°
SAS 1-03 May 74-03	1	12.3	.094	567	400	4°S	1.0	3°
	2	5.3	.070		136	10°N	69.1	4°
SAS 1-04 May 74-01	1	16.8	.104	499	447	25°S	0.1	2°
	3	14.2	.032	482	99.1	27°S	0.2	1°
	1	10.9	.067		243	5°S	1.5	3°
	2	5.3	.094		108			
SAS 1-04 May 74-04	2	14.2	.043	323	65.1	28°S	0.6	1°
	1	10.9	.080		211	5°S	8.7	2°
SAS 1-05 May 74-01	2	14.2	.048	351	98.0	26°S	0.7	1°
	3	9.8	.048		69.8	2°S	5.2	2°
	1	4.8	.110		170			
SAS 1-05 May 74-02	1	14.2	.059	256	100	24°S	5.9	3°
	2	9.8	.070		69.1	1°S	5.6	2°
	3	5.0	.056		69.1			
SAS 1-05 May 74-03	3	14.2	.054	303	80.3	18°S	7.4	3°
	1	9.8	.064		104	3°S	1.3	2°
	2	5.3	.051		85.6			

Appendix D. (Cont'd)

Run	Peak	Period (sec)	BW(Hz)	$E_T (cm^2)$	$E_p (cm^2)$	α_o	$P(\alpha_o)\%$	$\Delta\alpha_o$
SAS 1-05 May 74-04	1	16.8	.102	235	146	21°S	0.1	± 2°
	2	6.0	.102		79.3	7°N	22.7	± 3°
SAS 1-06 May 74-01	2	14.2	.048	334	141	17°S	5.5	± 3°
	3	8.8	.022		20.3	3°S	6.0	± 2°
	1	6.0	.112		154			
SAS 1-06 May 74-02	1	16.8	.059	240	123	22°S	0.2	± 2°
	2	5.3	.128		92.3	6°N	86.8	± 3°
SAS 1-07 May 74-01	1	14.2	.054	282	167	20°S	3.3	± 3°
	2	7.4	.139		98.3	3°N	28.8	± 2°
SAS 1-07 May 74-04	1	14.2	.050	175	124	13°S	5.1	± 3°
	2	6.9	.135		34.0	3°S	23.5	± 2°
SAS 1-08 May 74-03	1	12.3	.075	165	114	6°S	34.1	± 3°
	2	6.4	.110		42.3	7°N	44.4	± 2°
SAS 1-08 May 74-04	1	12.3	.080	171	134	14°S	27.7	± 5°
	2	6.4	.112		21.8	29°S	32.0	± 3°
SAS 1-09 May 74-01	1	12.3	.118	213	199	10°S	12.0	± 4°
SAS 1-09 May 74-02	2	16.8	.027	249	84.6	9°S	2.0	± 4°
	1	12.3	.054		96.4	18°S	7.4	± 3°
	3	6.9	.108		54.5	-	-	-
SAS 1-09 May 74-03	1	16.8	.107	318	305	9°S	1.1	± 3°
SAS 1-09 May 74-04	1	14.2	.105	512	470	6°S	0.7	± 2°
	2	4.3	.064		24.0	27°N	70.2	± 2°
SAS 1-10 May 74-01	1	14.2	.095	457	376	10°S	6.6	± 2°
	2	4.3	.065		58.8	43°S	64.6	± 3°

Appendix D. (Cont'd)

Run	Peak	Period (sec)	BW(Hz)	$E_T(cm^2)$	$E_p(cm^2)$	α_o	$P(\alpha_o)\%$	$\Delta\alpha_o$
SAS 1-10 May 74-04	2	14.2	.032	471	107	13°S	4.3	± 3°
	1	10.9	.043		231	3°S	1.8	± 2°
	3	6.9	.085		133			
SAS 1-11 May 74-01	2	14.2	.043	731	267	22°S	3.6	± 3°
	1	8.8	.131		236	0°	2.0	± 2°
SAS 1-11 May 74-02	3	20.5	.013	678	15.1	15°S	0.2	± 3°
	2	12.3	.037		290	8°S	3.1	± 3°
	1	8.8	.139		345	1°S	2.5	± 3°
SAS 1-11 May 74-04	1	14.2	.054	525	195	16°S	13.7	± 4°
	2	10.9	.035		166	2°S	0.8	± 2°
	3	8.1	.065		138	0°	10.8	± 3°
SAS 1-12 May 74-01	1	14.2	.056	487	258	10°S	4.5	± 3°
	2	8.8	.086		216	3°S	5.3	± 2°
SAS 1-12 May 74-02	3	20.5	.021	594	23.5	17°S	0.2	± 3°
	2	14.2	.035		202	14°S	7.0	± 3°
	1	9.8	.117		316			
SAS 1-12 May 74-03	1	14.2	.077	414	304	8°S	1.7	± 3°
	2	6.4	.117		96.0	3°N	22.6	± 3°
SAS 1-12 May 74-04	2	16.8	.025	554	77.6	21°S	0.5	± 1°
	1	8.1	.171		421	1°S	4.1	± 2°
SAS 1-13 May 74-01	2	16.8	.025	567	60.1	20°S	0.5	± 1°
	1	12.3	.150		441	10°S	2.2	± 3°
SAS 1-13 May 74-02	2	16.8	.032	736	192	23°S	0.1	± 1°
	3	12.3	.032		72.0	20°S	5.9	± 2°
	1	8.1	.128		358			

Appendix D. (Cont'd)

Run	Peak	Period (sec)	BW(Hz)	$E_T(cm^2)$	$E_p(cm^2)$	α_o	$P(\alpha_o)\%$	$\Delta\alpha_o$
SAS 1-13 May 74-03	2	16.8	.032	805	151	25°S	0.2	± 1°
	3	12.3	.036		150	3°S	2.7	± 3°
	1	8.8	.110		387			
SAS 1-13 May 74-04	2	16.8	.038	1010	282	26°S	14.9	± 3°
	3	9.8	.032		216	1°N	4.3	± 2°
	1	8.1	.117		499			
SAS 1-14 May 74-02	1	16.8	.037	894	476	29°S	1.9	± 2°
	2	7.4	.112		380	3°N	3.0	± 2°
SAS 1-14 May 74-05	2	16.8	.048	736	245	21°S	4.3	± 3°
	1	9.8	.161		482	1°N	4.4	± 2°
SAS 1-14 May 74-06	1	16.8	.047	597	251	24°S	2.9	± 3°
	3	8.8	.043		145	3°N	5.1	± 2°
	2	6.9	.107		153			
SAS 1-15 May 74-02	1	16.8	.064	967	389	7°S	2.3	± 4°
	2	7.4	.128		355	2°N	17.9	± 2°
SAS 1-16 May 74-01	2	16.8	.048	778	204	23°S	0.5	± 2°
	1	9.8	.134		537	1°S	1.6	± 2°
SAS 1-16 May 74-02	1	14.2	.055	968	509	11°S	7.2	± 3°
	2	8.8	.053		303	2°N	7.5	± 2°
	3	6.0	.098		126			
SAS 1-16 May 74-04	2	14.2	.048	642	229	21°S	1.4	± 3°
	1	9.8	.123		380	2°S	2.7	± 2°
SAS 1-17 May 74-01	2	14.2	.043	574	164	20°S	3.8	± 3°
	1	8.1	.162		366	0°	3.0	± 2°
SAS 1-17 May 74-03	2	12.3	.063	1040	250	4°S	5.2	± 3°
	1	7.4	.134		762	3°S	7.2	± 2°

Appendix D. (Cont'd)

Run	Peak	Period (sec)	BW(Hz)	$E_T(cm^2)$	$E_p(cm^2)$	α_o	$P(\alpha_o)\%$	$\Delta\alpha_o$
SAS 1-17 May 74-04	2	12.3	.059	1250	255	10°S	6.3	± 3°
	1	6.4	.144		932	2°N	15.6	± 3°
SAS 1-18 May 74-01	2	12.3	.049	1720	195	5°S	2.5	± 3°
	1	6.9	.139		1440	4°S	51.7	± 4°
SAS 1-18 May 74-02	2	12.3	.043	2750	241	3°S	1.1	± 2°
	1	8.1	.131		2350	3°N	10.6	± 3°
SAS 1-18 May 74-03	2	12.3	.048	2620	203	4°S	1.7	± 3°
	1	8.1	.129		2380	7°N	9.4	± 3°
SAS 1-19 May 74-01	1	8.1	.171	2070	2000	8°S	17.5	± 3°
SAS 1-19 May 74-02	2	14.2	.032	1420	36.2	23°S	0.5	± 3°
	1	8.8	.150		1330	2°N	2.8	± 2°
SAS 1-19 May 74-03	1	8.8	.193	1100	1080	1°S	1.5	± 2°
SAS 1-19 May 74-04	3	14.2	.021	755	16.5	25°S	0.7	± 1°
	2	10.9	.032		50.1	3°S	2.0	± 2°
	1	7.4	.149		720	0°	5.2	± 2°
SAS 1-20 May 74-01	2	14.2	.032	840	25.2	23°S	0.4	± 2°
	1	8.1	.155		794	1°S	3.7	± 2°
SAS 1-20 May 74-04	2	14.2	.043	463	23.6	23°S	0.5	± 2°
	1	8.1	.182		333	1°S	2.3	± 2°
SAS 1-21 May 74-02	2	14.2	.054	462	42.3	23°S	0.8	± 2°
	1	8.1	.193		400	0°	1.6	± 2°
SAS 1-25 May 74-02	2	14.2	.043	283	107	23°S	0.7	± 2°
	1	8.8	.145		170	1°S	1.8	± 2°

Appendix D. (Cont'd)

Run	Peak	Period (sec)	BW(Hz)	$E_T(cm^2)$	$E_p(cm^2)$	α_o	$P(\alpha_o)$%	$\Delta\alpha_o$
SAS 1-25 May 74-03	1	16.8	.032	318	142	24°S	0.1	± 1°
	2	8.8	.044		97.9	2°S	5.7	± 2°
	3	7.4	.117		69.3	3°N	1.7	± 2°
SAS 1-25 May 74-04	2	16.8	.032	355	136	23°S	0.3	± 1°
	1	8.8	.118		207	1°N	1.0	± 1°
SAS 1-26 May 74-01	1	16.8	.030	609	296	26°S	0.1	± 1°
	2	8.1	.145		284	1°N	6.3	± 2°
SAS 1-28 May 74-04	2	14.2	.036	235	88.6	23°S	0.5	± 2°
	3	10.9	.030		46.7	2°S	0.9	± 2°
	1	7.4	.141		90.6	0°	5.7	± 2°
SAS 1-29 May 74-01	1	14.2	.035	264	124	22°S	0.6	± 2°
	2	10.9	.054		67.4	4°S	2.5	± 2°
	3	6.4	.095		63.7	12°S	68.4	± 4°

Definition of Terms:

Peak: In a multimodal energy spectrum the peaks are ordered with respect to their energies.

Period: The modal period for the defined peak of the data of all four sensors.

BW: The bandwidth, an average of the data of all four sensors.

E_T: The total energy of the spectrum, average of the data of all four sensors.

E_p: The energy contained in a spectral peak, average of the data of all four sensors.

α_o: The direction of the best fit to a single wave train for the four sensor array, measured from the vertical to the array. The fitting technique is based on the minimum value of $P(\alpha_o)$.

$P(\alpha_o)$: A measure of the effectiveness of the fit.

$\Delta\alpha_o$: The uncertainty assigned to α_o.

Appendix E. A tabular display of the variability of the energy levels of the various sensors for a given SAS run. The terms are defined at the end of the table and are derived in Appendix H.

Run	Sensor	E_T (cm^2)	Mean (cm^2)	Range (%)	E_{pl} (cm^2)	Mean (cm^2)	Range (%)
SAS 1-06 Feb 73-01	1	848	866	+3.3, -2.1	340	364	+11.5, -6.6
	2	895			354		
	3	873			357		
	4	851			406		
SAS 1-12 Feb 73-01	2	4130	3840	+7.5, -5.5	3290	3380	+4.7, -2.6
	3	3740			3300		
	4	3630			3540		
SAS 1-12 Feb 73-04	2	1600	1490	+7.4, -4.4	1200	1100	±9.1
	3	1450			1100		
	4	1420			1000		
SAS 1-13 Feb 73-01	2	1870	1650	+12.7, -8.6	1500	1200	+25, -10
	3	1570			1010		
	4	1510			1080		
SAS 1-13 Feb 73-02	2	1740	1720	+1.1, -2.9	1350	1220	+10.6, -3.3
	3	1750			1130		
	4	1670			1180		
SAS 1-13 Feb 73-04	2	1130	1060	+6.6, -8.9	996	965	+5.4, -8.3
	3	966			884		
	4	1090			1020		
SAS 1-14 Feb 73-01	2	1970	2050	+2.4, -3.9	1910	2000	+1.5, -4.5
	3	2100			2040		
	4	2090			2030		
SAS 1-14 Feb 73-02	2	1880	1860	+1.1, -1.6	1750	1640	+6.7, -3.6
	3	1830			1590		
	4	1860			1580		

Appendix E. (Cont'd)

Run	Sensor	E_T (cm^2)	Mean (cm^2)	Range (%)	E_{pl} (cm^2)	Mean (cm^2)	Range (%)
SAS 1-14 Feb 73-03	2	1460	1400	+4.1, -3.4	-	1060	± .9
	3	1410			1050		
	4	1350			1070		
SAS 1-14 Feb 73-04	2	749	748	+4.5, -6.1	723	770	+5.1, -6.1
	3	810			777		
	4	834			809		
SAS 1-15 Feb 73-03	2	1260	1120	+12.5, -9.8	735	670	+9.7,-17.9
	3	1010			550		
	4	1100			727		
SAS 1-16 Feb 73-02	2	1160	1110	+4.5, -3.6	1010	986	+3.4, -6.0
	3	1120			1020		
	4	1060			927		
SAS 1-17 Feb 73-01	2	860	746	+15.3, -8.0	819	623	+31.4,-13.0
	3	694			508		
	4	686			542		
SAS 1-17 Feb 73-04	2	861	849	+1.4, -1.3	716	631	+13.4, -7.4
	3	838			592		
	4	849			584		
SAS 1-18 Feb 73-01	2	1390	1430	+2.8, -2.4	1050	1070	+2.0, -2.5
	3	1420			1080		
	4	1470			1100		
SAS 1-18 Feb 73-02	2	1600	1690	+4.2, -5.2	1340	1420	+5.2, -4.9
	3	1710			1490		
	4	1760			1412		

Appendix E. (Cont'd)

Run	Sensor	E_T (cm^2)	Mean (cm^2)	Range (%)	E_{pl} (cm^2)	Mean (cm^2)	Range (%)
SAS 1-18 Feb 73-03	2	1710	1590	+7.6, -6.7	1310	1250	+4.9, -4.5
	3	1570			1250		
	4	1480			1190		
SAS 1-18 Feb 73-04	2	1650	1590	+3.8, -3.3	1510	1420	+4.4, -6.1
	3	1580			1400		
	4	1540			1360		
SAS 1-19 Feb 73-02	2	1170	1090	+7.8, -5.5	934	867	+6.7, -5.2
	3	1060			862		
	4	1030			831		
SAS 1-20 Feb 73-01	2	832	837	+1.5, -.60	467	473	+.84, -1.3
	3	830			474		
	4	850			477		
SAS 1-20 Feb 73-03	2	1360	1340	+1.5, -2.0	1110	1130	+1.9, -1.8
	3	1350			1150		
	4	1310			1130		
SAS 1-21 Feb 73-02	2	740	790	+3.5, -6.3	645	722	+4.8,-10.7
	3	812			765		
	4	818			757		
SAS 1-21 Feb 73-05	2	694	670	+3.6, -3.0	648	627	+3.3, -3.2
	3	667			627		
	4	650			607		
SAS 1-22 Feb 73-01	2	685	687	+2.2, -2.9	425	430	+4.4, -3.3
	3	674			416		
	4	702			449		
SAS 1-22 Feb 73-02	2	539	548	+1.3, -1.6	504	523	+2.7, -3.6
	3	555			537		
	4	551			527		

Appendix E. (Cont'd)

Run	Sensor	E_T (cm^2)	Mean (cm^2)	Range (%)	E_{pl} (cm^2)	Mean (cm^2)	Range (%)
SAS 1-23 Feb 73-01	1	244	217	±12.4	196	182	+7.7,-12.6
	2	223			187		
	3	211			185		
	4	190			159		
SAS 1-23 Feb 73-02	1	194	163	+19., -14.1	147	134	+9.7, -7.5
	2	173			139		
	3	147			124		
	4	139			127		
SAS 1-24 Feb 73-01	1	181	147	+23.1,-21.	152	129	+17.8,-20.2
	2	165			146		
	3	127			115		
	4	116			103		
SAS 1-24 Feb 73-02	1	182	150	+21.3,-18.7	144	127	+13.4,-28.3
	2	164			139		
	3	133			117		
	4	122			108		
SAS 1-24 Feb 73-03	1	715	745	+7.2, -4.0	643	697	+5.5, -7.0
	2	750			679		
	3	799			730		
	4	765			715		
SAS 1-24 Feb 73-04	1	1380	1390	+6.6, -6.9	1200	1250	+9.3,-11.1
	2	1290			1110		
	3	1440			1370		
	4	1480			1320		
SAS 1-25 Feb 73-01	1	2240	2190	+8.9,-13.6	1830	1870	+17.6,-16.0
	2	2260			1880		
	3	2390			2200		
	4	1900			1570		

Appendix E. (Cont'd)

Run	Sensor	E_T (cm^2)	Mean (cm^2)	Range (%)	E_{pl} (cm^2)	Mean (cm^2)	Range (%)
SAS 1-25 Feb 73-02	2	2970	3060	±3.1	2340	2420	±3.2
	3	3160			2490		
SAS 1-25 Feb 73-03	2	2770	2700	±2.1	2310	2320	± .3
	3	2660			2320		
SAS 1-25 Feb 73-04	2	2170	2140	±1.4	881	1000	±11.8
	3	2110			1120		
SAS 1-26 Feb 73-01	2	1680	1660	±1.3	1640	1590	±3.4
	3	1640			1530		
SAS 1-27 Feb 73-01	2	1820	1720	±5.9	1540	1490	±3.6
	3	1620			1490		
SAS 1-22 Mar 73-01	2	1080	1230	+6.5,-12.3	758	834	+17.1, -9.1
	3	1300			977		
	4	1310			767		
SAS 1-06 Apr 73-01	1	194	207	+6.3, -2.0	78	93	+16.1,-34.4
	2	219			66		
	3	206			125		
	4	211			105		
SAS 1-07 Apr 73-03	1	481	451	+11.5, -6.6	217	186	+16.7,-27.4
	2	471			135		
	3	399			212		
	4	456			180		
SAS 1-10 Apr 73-02	1	184	149	+23.5,-14.8	131	108	+22, -25.9
	2	127			80		
	3	132			88		
	4	154			132		

Appendix E. (Cont'd)

Run	Sensor	E_T (cm^2)	Mean (cm^2)	Range (%)	E_{pl} (cm^2)	Mean (cm^2)	Range (%)
SAS 1-10 Apr 73-03	1	182	160	+13.8, -15	111	107	+10.3, -13
	2	136			93		
	3	157			106		
	4	163			118		
SAS 1-11 Apr 73-01	1	166	147	+13, -13	99	90	+31, -23
	2	128			72		
	3	129			69		
	4	166			118		
SAS 1-11 Apr 73-03	1	209	172	+21.5, -18.7	93	88	+28.4, -19.5
	2	140			76		
	3	142			71		
	4	195			113		
SAS 1-12 Apr 73-02	1	219	198	+10.6, -10.6	101	117	+13.8, -13.8
	2	177			112		
	3	194			122		
	4	201			133		
SAS 1-12 Apr 73-03	1	1120	740	+50.8, -23.7	287	302	+16.5, -25.8
	2	613			346		
	3	656			352		
	4	574			224		
SAS 1-13 Apr 73-03	1	1570	1080	+44.7, -26.1	486	368	+32, -20.9
	2	799			291		
	3	975			314		
	4	985			381		

Appendix E. (Cont'd)

Run	Sensor	E_T (cm^2)	Mean (cm^2)	Range (%)	E_{pl} (cm^2)	Mean (cm^2)	Range (%)
SAS 1-14 Apr 73-01	1	934	760	+22.8,-13.8	321	284	+34.2,-31.4
	2	655			195		
	3	732			238		
	4	719			381		
SAS 1-14 Apr 73-03	1	1210	1070	+12.5,-13.2	571	659	+9.3,-19.1
	2	993			713		
	3	931			533		
	4	1160			820		
SAS 1-15 Apr 73-02	1	860	719	+19.7,-15.5	402	431	+13.2, -6.7
	2	617			426		
	3	683			426		
	4	716			488		
SAS 1-16 Apr 73-03	1	783	564	+13.8,-19.5	327	293	±20.5
	2	454			261		
	3	543			353		
	4	477			233		
SAS 1-17 Apr 73-01	1	806	463	+74.1,-32.2	157	145	+8.3, -5.5
	2	342			137		
	3	313			138		
	4	389			151		
SAS 1-17 Apr 73-03	1	794	679	+16.9,-13.8	204	208	+8.8, -5.3
	2	715			197		
	3	623			226		
	4	585			204		

Appendix E. (Cont'd)

Run	Sensor	E_T (cm^2)	Mean (cm^2)	Range (%)	E_{pl} (cm^2)	Mean (cm^2)	Range (%)
SAS 1-18 Apr 73-01	1	2440	2300	+11.3,-12.2	1750	1630	+7.4, -4.9
	2	2020			1670		
	3	2170			1550		
	4	2560			1560		
SAS 1-16 May 73-02	1	179	172	+5.8, -9.3	136	131	+4.6, -6.1
	2	182			137		
	3	173			128		
	4	156			123		
SAS 1-17 May 73-03	1	242	240	+3.3, -2.1	172	188	+4.3, -8.5
	2	235			187		
	3	236			194		
	4	248			196		
SAS 1-17 May 73-02	1	313	301	+3.8, -8.0	278	270	+3.0, -7.8
	2	309			275		
	3	305			276		
	4	277			249		
SAS 1-17 May 73-01	1	248	220	+12.7, -8.2	90	78	+15.4,-12.8
	2	224			85		
	3	208			70		
	4	202			68		
SAS 1-18 May 73-03	1	280	293	+9.2,-13.3	186	186	+5.9, -8.1
	2	312			197		
	3	320			188		
	4	254			173		
SAS 1-18 May 73-04	1	197	218	+19.7, -9.7	151	157	+12.1,-10.4
	2	229			176		
	3	261			155		
	4	183			144		

Appendix E. (Cont'd)

Run	Sensor	E_T (cm^2)	Mean (cm^2)	Range (%)	E_{pl} (cm^2)	Mean (cm^2)	Range (%)
SAS 1-19 May 73-01	1	262	270	+8.9, -8.8	222	227	+2.2, -3.1
	2	279			232		
	3	294			232		
	4	246			220		
SAS 1-19 May 73-02	1	230	261	+41.8,-23.8	139	111	+25.2,-17.1
	2	370			106		
	3	243			105		
	4	199			92		
SAS 1-19 May 73-04	1	199	204	+7.4, -9.3	157	154	+5.2, -5.2
	2	219			162		
	3	211			151		
	4	185			146		
SAS 1-20 May 73-01	1	235	234	+12.8,-14.1	143	149	+10.0, -5.4
	2	274			141		
	3	225			164		
	4	201			147		
SAS 1-20 May 73-02	1	226	241	+20.3,-14.1	108	115	+24.3,-14.3
	2	290			112		
	3	241			143		
	4	207			99.1		
SAS 1-20 May 73-03	1	245	244	+9.0,-14.3	86.7	86.0	+3.4, -5.3
	2	259			86.7		
	3	262			89.0		
	4	209			81.4		

Appendix E. (Cont'd)

Run	Sensor	E_T (cm^2)	Mean (cm^2)	Range (%)	E_{pl} (cm^2)	Mean (cm^2)	Range (%)
SAS 1-20 May 73-04	1	141	162	+29.0, -18.5	42.8	43.3	+3.2, -2.3
	2	165			43.3		
	3	209			44.7		
	4	132			42.3		
SAS 1-21 May 73-01	1	254	232	+9.5, -12.5	76.0	70.5	+7.8, -6.1
	2	244			72.8		
	3	227			67.2		
	4	203			66.2		
SAS 1-21 May 73-03	1	287	314	+13.1, -12.1	72.3	89.3	+24.3, -19.0
	2	338			79.9		
	3	355			111		
	4	276			94.2		
SAS 1-21 May 73-04	1	304	267	+13.8, -20.6	100	88.7	+12.7, -16.0
	2	286			91.5		
	3	-			-		
	4	212			74.6		
SAS 1-22 May 73-03	1	255	262	+1.9, -2.7	163	175	+10.8, -6.9
	2	267			167		
	3	-			-		
	4	265			194		
SAS 1-23 May 73-02	1	207	195	+8.2, -9.7	45.4	43.0	+5.6, -10.5
	2	211			45.0		
	3	-			-		
	4	166			38.5		

Appendix E. (Cont'd)

Run	Sensor	E_T (cm^2)	Mean (cm^2)	Range (%)	E_{pl} (cm^2)	Mean (cm^2)	Range (%)
SAS 1-23 May 73-03	1	181	175	+11.4,-15.5	94.6	101	+4.9, -6.3
	2	195			103		
	3	-			-		
	4	148			106		
SAS 1-24 May 73-01	1	273	271	+2.2, -2.9	97.3	110	+30.0,-19.6
	2	277			88.4		
	3	-			-		
	4	263			143		
SAS 1-24 May 73-02	1	311	284	+9.5,-19.4	238	229	+10.5,-14.0
	2	311			253		
	3	-			-		
	4	229			197		
SAS 1-24 May 73-03	1	172	159	+8.2,-11.3	121	107	+13.1,-12.1
	2	163			94.1		
	3	-			-		
	4	141			107		
SAS 1-24 May 73-04	1	238	212	+12.2,-17.9	96.6	85.8	+12.6,-18.3
	2	223			90.6		
	3	-			-		
	4	174			70.1		
SAS 1-25 May 73-01	1	695	853	+17.2,-18.5	262	323	+18.9,-21.3
	2	865			316		
	3	-			-		
	4	1000			392		

Appendix E. (Cont'd)

Run	Sensor	E_T (cm^2)	Mean (cm^2)	Range (%)	E_{pl} (cm^2)	Mean (cm^2)	Range (%)
SAS 1-25 May 73-03	1	396	373	+6.2,-11.8	185	168	+10.1,-17.3
	2	393			180		
	3	-			-		
	4	329			139		
SAS 1-25 May 73-04	1	393	358	+9.8,-14.2	116	113	+10.6,-14.1
	2	375			97.1		
	3	-			-		
	4	307			125		
SAS 1-26 May 73-01	1	664	600	+10.6,-14.0	271	248	+9.3, -9.3
	2	621			247		
	3	-			-		
	4	516			225		
SAS 1-26 May 73-02	1	786	733	+7.2, -4.2	581	502	+15.7,-15.1
	2	702			500		
	3	-			-		
	4	711			426		
SAS 1-26 May 73-03	1	550	548	+4.4, -4.9	310	270	+12.9,-14.4
	2	572			267		
	3	-			-		
	4	521			234		
SAS 1-26 May 73-04	1	763	670	+13.9,-12.5	414	328	+26.2,-26.5
	2	662			241		
	3	-			-		
	4	586			330		

Appendix E. (Cont'd)

Run	Sensor	E_T (cm^2)	Mean (cm^2)	Range (%)	E_{pl} (cm^2)	Mean (cm^2)	Range (%)
SAS 1-27 May 73-01	1	672	656	+5.2, -8.4	506	516	+1.2, -1.9
	2	690			521		
	3	-			-		
	4	605			522		
SAS 1-27 May 73-02	1	622	610	+11.0,-15.1	318	373	+12.1,-14.7
	2	677			418		
	3	-			-		
	4	530			384		
SAS 1-27 May 73-03	1	467	431	+8.4, -6.7	216	223	+8.5, -9.9
	2	430			230		
	3	426			242		
	4	402			203		
SAS 1-27 May 73-04	1	263	244	+7.8,-10.2	105	121	+28.1,-16.5
	2	260			155		
	3	235			121		
	4	219			101		
SAS 1-28 May 73-01	1	190	176	+8.0,-16.5	72.3	56	+28.6,-41.4
	2	187			32.6		
	3	178			59.0		
	4	147			59.9		
SAS 1-28 May 73-02	1	254	235	+8.1,-11.1	167	145	+15.2,-28.3
	2	245			148		
	3	231			160		
	4	209			104		

Appendix E. (Cont'd)

Run	Sensor	E_T (cm^2)	Mean (cm^2)	Range (%)	E_{pl} (cm^2)	Mean (cm^2)	Range (%)
SAS 1-28 May 73-04	1	121	124	+11.3, -4.8	32.8	44.1	+47.7,-25.0
	2	118			33.6		
	3	138			44.6		
	4	118			65.4		
SAS 1-29 May 73-02	1	181	176	+6.3, -8.5	89.4	99.1	+6.1,-10.1
	2	187			101		
	3	174			105		
	4	161			101		
SAS 1-29 May 73-03	1	104	105.9	+12.3, -6.6	34.9	33.2	+6.1, -3.0
	2	119			32.7		
	3	102			32.7		
	4	98.7			32.3		
SAS 1-29 May 73-04	1	120	121	+3.3, -5.0	40.7	45.3	+13.0,-10.9
	2	122			52.3		
	3	125			45.9		
	4	115			42.3		
SAS 1-30 May 73-01	1	132	176	+55.1,-25.0	43.9	51.2	+13.3,-14.3
	2	273			58.0		
	3	153			51.6		
	4	147			51.2		
SAS 1-30 May 73-02	1	137	133	±17.3	37.2	37.5	+9.3, -6.9
	2	156			41.0		
	3	128			37.8		
	4	110			34.9		

Appendix E. (Cont'd)

Run	Sensor	E_T (cm^2)	Mean (cm^2)	Range (%)	E_{pl} (cm^2)	Mean (cm^2)	Range (%)
SAS 1-30 May 73-03	1	111	106	+9.4,-16.0	39.8	46.1	+46.2,-19.3
	2	116			37.2		
	3	108			67.4		
	4	89.5			40.0		
SAS 1-30 May 73-04	1	128	142	+24.8,-14.8	35.1	35.2	+20.5,-33.0
	2	121			23.6		
	3	143			42.4		
	4	177			39.8		
SAS 1-31 May 73-01	1	1009	1080	+25.0,-21.3	640	525	+21.8,-38.8
	2	1354			601		
	3	1101			321		
	4	848			538		
SAS 1-31 May 73-02	1	222	209	+9.6,-12.4	124	102	+21.5,-12.6
	2	229			107		
	3	202			90.0		
	4	183			89.1		
SAS 1-31 May 73-03	1	271	254	+6.7,-13.4	123	116	+6.0,-11.2
	2	271			119		
	3	252			117		
	4	220			103		
SAS 1-31 May 73-04	1	289	333	+26.1,-20.4	75.7	74.2	+13.2,-12.9
	2	265			64.6		
	3	358			72.6		
	4	420			84.0		

Appendix E. (Cont'd)

Run	Sensor	E_T (cm^2)	Mean (cm^2)	Range (%)	E_{pl} (cm^2)	Mean (cm^2)	Range (%)
SAS 1-01 Jun 73-02	1	238	243	+12.3,-10.7	82.4	96.2	+47.6,-15.8
	2	273			81.0		
	3	245			142		
	4	217			79.3		
SAS 1-01 Jun 73-04	1	277	260	+6.5,-10.8	213	205	+3.9, -8.3
	2	258			210		
	3	271			209		
	4	232			188		
SAS 1-02 Jun 73-03	1	463	446	+13.9,-15.0	294	266	+10.5, -8.3
	2	508			267		
	3	380			244		
	4	433			258		
SAS 1-02 Jun 73-04	1	484	462	+5.2, -8.4	265	256	+7.4, -9.8
	2	467			252		
	3	476			275		
	4	423			231		
SAS 1-03 Jun 73-01	1	242	234	+5.5,-12.0	123	116	+8.6,-14.6
	2	247			126		
	3	241			115		
	4	206			99.1		
SAS 1-03 Jun 73-02	1	257	234	+9.8,-17.9	134	135	+7.4, -4.4
	2	248			132		
	3	238			145		
	4	192			129		

Appendix E. (Cont'd)

Run	Sensor	E_T (cm^2)	Mean (cm^2)	Range (%)	E_{p1} (cm^2)	Mean (cm^2)	Range (%)
SAS 1-03 Jun 73-03	1	200	198	+8.6, -7.6	154	157	+5.7, -5.7
	2	215			166		
	3	204			159		
	4	173			148		
SAS 1-03 Jun 73-04	1	400	357	+12.0,-12.0	322	280	+15.0,-16.1
	2	-			-		
	3	356			281		
	4	314			235		
SAS 1-04 Jun 73-01	1	282	274	+8.4,-12.0	115	120	+6.9, -4.2
	2	297			119		
	3	278			129		
	4	241			117		
SAS 1-04 Jun 73-02	1	198	193	+3.6, -6.7	89.5	90.1	+4.8, -5.3
	2	-			-		
	3	200			95.4		
	4	180			85.3		
SAS 1-04 Jun 73-03	1	194	182	+7.7,-11.0	141	130	+13.1,-16.9
	2	183			147		
	3	190			123		
	4	162			108		
SAS 1-04 Jun 73-04	1	166	170	+10.0,-10.6	95.5	87.2	+15.2, -7.9
	2	187			88.9		
	3	175			80.3		
	4	152			83.9		

Appendix E. (Cont'd)

Run	Sensor	E_T (cm^2)	Mean (cm^2)	Range (%)	E_{pl} (cm^2)	Mean (cm^2)	Range (%)
SAS 1-04 Jun 73-05	1	107	114	+36.0, -20.6	-	36.1	+2.5, -3.3
	2	155			37.0		
	3	104			36.3		
	4	90.5			34.9		
SAS 1-05 Jun 73-01	1	206	194	+6.2, -9.3	46.3	52.3	+9.9, -11.5
	2	-			-		
	3	199			57.5		
	4	176			53.1		
SAS 1-05 Jun 73-02	1	139	134	+16.4, -16.4	36.3	40.2	+12.4, -28.5
	2	156			32.8		
	3	129			45.9		
	4	112			45.9		
SAS 1-05 Jun 73-03	1	162	198	+33.3, -18.2	81.3	89.5	+17.3, -13.1
	2	169			77.8		
	3	196			94.1		
	4	264			105		
SAS 1-05 Jun 73-04	1	515	498	+46.1, -42.0	123	126	+64.3, -44.7
	2	289			69.7		
	3	728			207		
	4	460			104		
SAS 1-06 Jun 73-01	1	247	204	+21.1, -22.1	175	140	+25.0, -18.6
	2	207			126		
	3	202			145		
	4	161			114		

Appendix E. (Cont'd)

Run	Sensor	E_T (cm^2)	Mean (cm^2)	Range (%)	E_{pl} (cm^2)	Mean (cm^2)	Range (%)
SAS 1-06 Jul 73-05	1	637	625	+3.8, -9.1	451	488	+5.7, -7.6
	2	649			516		
	3	648			506		
	4	568			481		
SAS 1-06 Jul 73-06	1	889	811	+13.3,-16.0	501	632	+18.5,-20.7
	2	919			749		
	3	758			647		
	4	681			631		
SAS 1-06 Jul 73-07	1	678	692	+18.1,-11.5	579	584	+7.9, -8.0
	2	817			630		
	3	663			590		
	4	612			537		
SAS 1-07 Jul 73-01	1	393	346	+13.6,-11.0	205	196	+15.8,-13.3
	2	341			183		
	3	341			227		
	4	308			170		
SAS 1-07 Jul 73-02	1	306	305	+10.8, -8.8	211	210	+4.3, -3.8
	2	338			210		
	3	299			219		
	4	278			202		
SAS 1-07 Jul 73-03	1	394	372	+5.9, -8.6	264	191	+38.2,-27.7
	2	340			138		
	3	392			144		
	4	364			220		

Appendix E. (Cont'd)

Run	Sensor	E_T (cm^2)	Mean (cm^2)	Range (%)	E_{pl} (cm^2)	Mean (cm^2)	Range (%)
SAS 1-07 Jul 73-04	1	391	351	+11.4,-10.5	271	256	+5.9,-12.5
	2	337			269		
	3	361			260		
	4	314			224		
SAS 1-07 Jul 73-05	1	362	366	+4.9, -7.4	242	254	+10.2, -9.1
	2	381			262		
	3	384			231		
	4	339			280		
SAS 1-07 Jul 73-07	1	285	268	+11.6,-17.2	204	197	+7.6, -9.6
	2	299			212		
	3	250			196		
	4	240			178		
SAS 1-08 Jul 73-01	1	161	136	+18.4,-21.3	105	88	+19.3,-18.2
	2	147			98		
	3	129			76		
	4	107			72		
SAS 1-08 Jul 73-03	1	216	209	+9.6,-12.1	118	120	+5.0, -5.8
	2	229			126		
	3	206			123		
	4	184			113		
SAS 1-08 Jul 73-05	1	208	206	+4.8, -5.3	125	138	+2.9, -9.4
	2	216			142		
	3	203			141		
	4	195			142		

Appendix E. (Cont'd)

Run	Sensor	E_T (cm^2)	Mean (cm^2)	Range (%)	E_{pl} (cm^2)	Mean (cm^2)	Range (%)
SAS 1-08 Jul 73-07	1	185	188	+15.9, -8.5	106	109	+4.6, -3.7
	2	218			105		
	3	179			114		
	4	172			111		
SAS 1-09 Jul 73-01	1	156	152	+13.8, -8.5	60.7	76.3	+26.7,-20.4
	2	173			70.0		
	3	139			77.7		
	4	141			96.7		
SAS 1-09 Jul 73-03	1	190	187	+10.2, -5.3	136	137	+1.0, -1.0
	2	206			137		
	3	177			137		
	4	186			138		
SAS 1-10 Jul 73-01	1	213	226	+7.1, -5.8	123	123	+26.0,-30.0
	2	242			119		
	3	235			155		
	4	214			96		
SAS 1-10 Jul 73-02	1	260	268	+3.7, -3.0	177	174	+1.7, -2.3
	2	278			175		
	3	-			-		
	4	267			170		
SAS 1-11 Jul 73-01	1	341	327	+4.3, -8.9	221	194	+13.9,-27.6
	2	341			152		
	3	-			-		
	4	298			210		

Appendix E. (Cont'd)

Run	Sensor	E_T (cm^2)	Mean (cm^2)	Range (%)	E_{p1} (cm^2)	Mean (cm^2)	Range (%)
SAS 1-11 Jul 73-02	1	198	202	+8.9, -6.9	124	120	+4.2, -9.2
	2	220			109		
	3	204			125		
	4	188			120		
SAS 1-16 Jul 73-03	1	276	269	+8.6,-10.4	108	120	+20.0,-15.0
	2	292			125		
	3	266			144		
	4	241			102		
SAS 1-16 Jul 73-04	1	175	174	±0.6	49	39	+25.6,-28.2
	2	173			44		
	3	175			28		
	4	173			36		
SAS 1-17 Jul 73-01	1	263	260	+20.4,-14.6	152	145	+15.2,-35.9
	2	313			167		
	3	222			93		
	4	242			166		
SAS 1-18 Jul 73-04	1	215	208	+10.6,-11.5	63	61	+11.4,-13.1
	2	230			68		
	3	203			60		
	4	184			53		
SAS 1-19 Jul 73-01	1	294	304	+13.2,-11.5	116	124	+8.1, -6.5
	2	344			134		
	3	309			123		
	4	269			121		

Appendix E. (Cont'd)

Run	Sensor	E_T (cm^2)	Mean (cm^2)	Range (%)	E_{pl} (cm^2)	Mean (cm^2)	Range (%)
SAS 1-19 Jul 73-03	1	277	259	+12.4,-16.6	143	140	+5.7,-10.0
	2	291			148		
	3	255			142		
	4	216			126		
SAS 1-19 Jul 73-04	1	455	420	+8.3, -7.4	237	229	+3.5, -2.2
	2	424			224		
	3	413			229		
	4	389			224		
SAS 1-20 Jul 73-01	1	385	368	+4.6, -4.0	202	193	+5.2, -8.3
	2	356			190		
	3	353			177		
	4	376			203		
SAS 1-20 Jul 73-03	1	408	390	+4.6, -8.5	204	206	+8.7, -3.9
	2	414			198		
	3	380			224		
	4	357			198		
SAS 1-20 Jul 73-04	1	478	461	+8.9, -9.1	363	345	+5.5, -8.4
	2	502			364		
	3	447			339		
	4	419			316		
SAS 1-21 Jul 73-01	1	459	425	+8.2,-10.1	313	289	+17.6,-13.8
	2	400			249		
	3	460			340		
	4	686			255		

Appendix E. (Cont'd)

Run	Sensor	E_T (cm^2)	Mean (cm^2)	Range (%)	E_{pl} (cm^2)	Mean (cm^2)	Range (%)
SAS 1-21 Jul 73-02	1	701	740	+17.3, -7.3	439	453	+16.2,-12.1
	2	868			526		
	3	706			451		
	4	686			399		
SAS 1-21 Jul 73-03	1	404	395	+6.6, -5.0	141	143	±2.7
	2	421			147		
	3	381			146		
	4	375			139		
SAS 1-21 Jul 73-04	1	611	612	+4.4, -8.4	259	262	+8.0, -9.9
	2	638			281		
	3	639			271		
	4	561			236		
SAS 1-22 Jul 73-01	1	727	699	+4.0, -3.8	235	200	+17.5,-16.0
	2	696			211		
	3	698			185		
	4	674			168		
SAS 1-22 Jul 73-02	1	736	733	+3.1, -6.3	246	258	+2.7, -4.6
	2	756			258		
	3	754			265		
	4	687			264		
SAS 1-22 Jul 73-03	1	519	515	+8.0, -9.5	226	211	+9.0,-14.7
	2	556			230		
	3	518			206		
	4	466			180		

Appendix E. (Cont'd)

Run	Sensor	E_T (cm^2)	Mean (cm^2)	Range (%)	E_{pl} (cm^2)	Mean (cm^2)	Range (%)
SAS 1-22 Jul 73-04	1	420	442	+6.1, -5.0	153	166	+4.8, -7.8
	2	457			170		
	3	469			165		
	4	421			174		
SAS 1-23 Jul 73-01	1	527	495	+6.5, -8.5	378	260	+45.4,-21.5
	2	513			252		
	3	487			204		
	4	453			204		
SAS 1-23 Jul 73-03	1	505	466	+8.4, -9.9	230	241	+7.1, -8.3
	2	483			258		
	3	420			221		
	4	455			254		
SAS 1-24 Jul 73-02	1	848	882	+4.4, -3.9	564	625	+9.8, -9.8
	2	920			595		
	3	902			686		
	4	861			654		
SAS 1-27 Jul 73-04	1	242	220	+10.0, -5.4	123	118	+4.2, -6.8
	2	-			118		
	3	208			121		
	4	211			110		
SAS 1-28 Jul 73-02	1	155	141	+9.9, -8.5	70.3	64.2	+9.5,-10.3
	2	-			62.0		
	3	129			57.6		
	4	138			67.1		

Appendix E. (Cont'd)

Run	Sensor	E_T (cm^2)	Mean (cm^2)	Range (%)	E_{p1} (cm^2)	Mean (cm^2)	Range (%)
SAS 1-29 Jul 73-02	1	199	191	+4.7, -4.7	47.0	48.1	+6.2, -3.9
	2	-			-		
	3	192			51.1		
	4	182			46.2		
SAS 1-29 Jul 73-04	1	239	243	+4.1, -2.1	143	146	+4.8, -2.7
	2	-			-		
	3	253			153		
	4	238			142		
SAS 1-30 Jul 73-01	1	256	251	+2.7, -5.0	153	162	+6.9, -5.6
	2	-			-		
	3	258			174		
	4	238			160		
SAS 1-30 Jul 73-02	1	297	268	+11.2, -7.5	170	159	+6.5, -5.7
	2	-			-		
	3	258			157		
	4	248			150		
SAS 1-31 Jul 73-01	1	235	218	+7.8,-10.1	166	158	+5.1, -7.6
	2	-			-		
	3	194			161		
	4	226			146		
SAS -01 Aug 73-02	1	238	204	+16.7,-10.3	64.2	60.0	+7.0,-11.8
	2	189			54.7		
	3	183			60.1		
	4	204			52.9		

Appendix E. (Cont'd)

Run	Sensor	E_T (cm^2)	Mean (cm^2)	Range (%)	E_{pl} (cm^2)	Mean (cm^2)	Range (%)
SAS 1-01 Aug 73-03	1	161	149	+8.0, -4.7	67.9	70.8	+18.9,-15.0
	2	-			-		
	3	142			84.2		
	4	143			60.2		
SAS 1-02 Aug 73-01	1	252	245	+2.8, -2.8	95.9	103	+7.8, -6.9
	2	-			-		
	3	245			111		
	4	238			101		
SAS 1-02 Aug 73-03	1	260	233	+11.6, -5.6	148	149	+4.0, -4.0
	2	-			-		
	3	220			155		
	4	220			143		
SAS 1-02 Aug 73-04	1	272	220	+23.6,-12.3	125	127	+12.6,-11.8
	2	-			-		
	3	193			112		
	4	197			143		
SAS 1-03 Aug 73-01	1	211	181	+16.6,-11.0	91.9	83.6	+9.9,-12.8
	2	-			-		
	3	161			86.0		
	4	170			72.9		
SAS 1-10 Aug 73-01	1	918	917	+11.2, -6.2	326	328	+16.4,-14.3
	2	860			281		
	3	872			323		
	4	1020			382		

Appendix E. (Cont'd)

Run	Sensor	E_T (cm^2)	Mean (cm^2)	Range (%)	E_{pl} (cm^2)	Mean (cm^2)	Range (%)
SAS 1-10 Aug 73-03	1	220	207	+6.3,-11.6	87.6	83.4	+5.0, -6.7
	2	211			77.8		
	3	183			82.6		
	4	213			85.6		
SAS 1-11 Aug 73-01	1	200	178	+12.3, -7.3	85.0	81.4	+4.4, -8.9
	2	-			74.7		
	3	165			81.0		
	4	169			85.1		
SAS 1-11 Aug 73-02	1	181	175	+7.4,-10.9	63.9	56.3	+13.5,-13.8
	2	188			48.5		
	3	154			53.4		
	4	176			59.3		
SAS 1-11 Aug 73-03	1	356	322	+10.6, -7.8	115	95.1	+20.9,-16.1
	2	-			-		
	3	297			79.8		
	4	314			90.6		
SAS 1-11 Aug 73-04	1	365	314	+17.2,-26.1	73.6	63.1	+16.6,-17.1
	2	232			52.3		
	3	290			62.2		
	4	368			64.3		
SAS 1-12 Aug 73-01	1	404	391	+8.4,-11.5	145	134	+8.2, -4.5
	2	424			126		
	3	391			139		
	4	346			128		

Appendix E. (Cont'd)

Run	Sensor	E_T (cm^2)	Mean (cm^2)	Range (%)	E_{pl} (cm^2)	Mean (cm^2)	Range (%)
SAS 1-12 Aug 73-02	1	346	281	+23.1,-14.6	110	82.6	+33.2,-17.8
	2	282			77.9		
	3	240			74.7		
	4	255			67.9		
SAS 1-14 Aug 73-04	1	98.0	89.8	+14.7,-18.6	40.6	42.6	+6.8, -5.2
	2	85.2			40.4		
	3	73.1			45.5		
	4	103			44.1		
SAS 1-15 Aug 73-01	1	133	132	+6.8, -7.6	73.6	82.4	+14.4,-10.7
	2	122			73.9		
	3	132			88.0		
	4	141			94.3		
SAS 1-15 Aug 73-02	1	197	197	+12.7, -7.1	155	151	+13.2,-14.6
	2	183			129		
	3	187			148		
	4	222			171		
SAS 1-16 Aug 73-03	1	383	360	+6.4, -5.8	308	302	+3.6, -5.0
	2	339			287		
	3	351			313		
	4	367			300		
SAS 1-16 Aug 73-04	1	431	387	+11.4, -8.5	360	314	+14.6, -6.0
	2	386			302		
	3	354			295		
	4	377			298		

Appendix E. (Cont'd)

Run	Sensor	E_T (cm^2)	Mean (cm^2)	Range (%)	E_{pl} (cm^2)	Mean (cm^2)	Range (%)
SAS 1-20 Aug 73-03	1	253	246	+3.7, -4.9	109	125	+9.6,-12.8
	2	243			129		
	3	234			126		
	4	255			137		
SAS 1-20 Aug 73-04	1	176	169	+6.5, -6.5	44.2	41.2	+7.3,-11.9
	2	161			36.3		
	3	158			41.4		
	4	180			43.0		
SAS 1-21 Aug 73-01	1	319	291	+9.6, -4.8	90.9	84.2	+8.0, -5.1
	2	264			79.9		
	3	277			84.1		
	4	304			81.9		
SAS 1-21 Aug 73-02	1	304	264	+15.2, -4.5	107	107	+11.2,-13.3
	2	271			92.8		
	3	227			109		
	4	252			119		
SAS 1-21 Aug 73-03	1	361	369	+15.2, -9.2	192	183	+6.6, -7.1
	2	335			170		
	3	353			175		
	4	425			195		
SAS 1-22 Aug 73-02	1	613	572	+7.2,-15.2	400	349	+14.6,-16.6
	2	485			291		
	3	594			356		
	4	594			347		

Appendix E. (Cont'd)

Run	Sensor	E_T (cm^2)	Mean (cm^2)	Range (%)	E_{p1} (cm^2)	Mean (cm^2)	Range (%)
SAS 1-22 Aug 73-03	1	791	764	+3.5, -3.9	276	342	+15.5,-21.9
	2	778			395		
	3	755			367		
	4	734			329		
SAS 1-22 Aug 73-04	1	938	897	+9.6,-11.6	258	241	+7.0, -5.8
	2	782			248		
	3	886			227		
	4	983			230		
SAS 1-23 Aug 73-01	1	1330	1220	+9.0, -6.6	988	1010	+5.6, -5.6
	2	1140			953		
	3	1200			1040		
	4	1220			1070		
SAS 1-23 Aug 73-02	1	1230	1020	+20.0, -9.1	1052	851	+23.6,-14.2
	2	927			781		
	3	948			730		
	4	963			841		
SAS 1-23 Aug 73-03	1	991	937	+5.7, -7.0	579	556	+5.0, -5.6
	2	871			584		
	3	945			538		
	4	941			525		
SAS 1-24 Aug 73-02	1	707	674	+4.9, -7.0	594	552	+7.6, -3.6
	2	627			532		
	3	672			536		
	4	688			546		

Appendix E. (Cont'd)

Run	Sensor	E_T (cm^2)	Mean (cm^2)	Range (%)	E_{pl} (cm^2)	Mean (cm^2)	Range (%)
SAS 1-24 Aug 73-03	1	621	603	+3.0, -5.6	388	386	+8.5, -4.9
	2	601			370		
	3	569			367		
	4	621			419		
SAS 1-24 Aug 73-04	1	568	480	+18.3,-15.6	423	361	+17.2,-11.6
	2	405			319		
	3	423			319		
	4	525			384		
SAS 1-25 Aug 73-01	1	559	489	+14.3,-10.6	484	423	+14.4,-13.0
	2	478			420		
	3	483			422		
	4	437			368		
SAS 1-25 Aug 73-02	1	413	400	+4.0, -4.8	275	265	+9.1,-19.6
	2	371			213		
	3	400			289		
	4	416			284		
SAS 1-25 Aug 73-03	1	237	208	+12.0,-14.4	162	102	+58.8,-30.3
	2	231			98.6		
	3	186			71.1		
	4	178			75.8		
SAS 1-25 Aug 73-04	1	275	232	+18.5,-16.8	102	105	+15.2,-23.7
	2	223			80.1		
	3	193			118		
	4	238			121		

Appendix E. (Cont'd)

Run	Sensor	E_T (cm^2)	Mean (cm^2)	Range (%)	E_{pl} (cm^2)	Mean (cm^2)	Range (%)
SAS 1-26 Aug 73-01	1	241	247	+16.2,-16.2	139	142	+13.4,-12.7
	2	207			124		
	3	252			161		
	4	287			144		
SAS 1-26 Aug 73-02	1	148	129	+14.7,-22.5	84.9	72.0	+17.9,-13.9
	2	125			62.0		
	3	100			66.3		
	4	144			74.8		
SAS 1-26 Aug 73-03	1	136	121	+12.4,-10.7	83.2	73.9	+12.6, -7.0
	2	-			-		
	3	119			68.7		
	4	108			69.9		
SAS 1-26 Aug 73-04	1	136	127	+12.6,-18.1	49.2	46.3	+22.5,-39.7
	2	123			51.3		
	3	123			27.9		
	4	143			56.7		
SAS 1-27 Aug 73-01	1	231	219	+5.5,-10.5	108	95.6	+12.9,-25.2
	2	228			95.9		
	3	196			71.5		
	4	222			107		
SAS 1-27 Aug 73-02	1	234	208	+12.5, -8.2	76.1	77.7	+4.7, -2.1
	2	191			77.1		
	3	198			76.3		
	4	210			81.4		

Appendix E. (Cont'd)

Run	Sensor	E_T (cm^2)	Mean (cm^2)	Range (%)	E_{pl} (cm^2)	Mean (cm^2)	Range (%)
SAS 1-31 Aug 73-01	1	233	204	+14.2,-13.2	82.3	82.1	+4.1, -2.7
	2	207			80.8		
	3	177			85.5		
	4	200			79.9		
SAS 1-06 Sept 73-01	1	360	350	+8.9,-12.0	145	138	+23.9,-29.7
	2	-			-		
	3	381			171		
	4	308			97.3		
SAS 1-06 Sept 73-02	1	578	522	+10.7, -7.9	308	333	+4.5, -7.5
	2	-			-		
	3	481			348		
	4	507			342		
SAS 1-06 Sept 73-03	1	568	533	+6.6, -3.8	328	298	+10.1,-10.4
	2	-			-		
	3	513			298		
	4	518			267		
SAS 1-07 Sept 73-01	1	1000	934	+7.1, -8.6	671	646	+3.9, -7.6
	2	-			-		
	3	854			597		
	4	949			671		
SAS 1-07 Sept 73-02	1	-	678	+7.1, -6.6	-	317	+10.1,-10.1
	2	-			-		
	3	633			285		
	4	726			319		

Appendix E. (Cont'd)

Run	Sensor	E_T (cm^2)	Mean (cm^2)	Range (%)	E_{pl} (cm^2)	Mean (cm^2)	Range (%)
SAS 1-07 Sept 73-03	1	-	776	+5.7, -5.7	-	446	+3.1, -3.4
	2	-			-		
	3	732			431		
	4	820			460		
SAS 1-08 Sept 73-01	1	-	749	+0.9, -0.9	-	414	+1.4, -1.4
	2	-			-		
	3	742			408		
	4	756			420		
SAS 1-08 Sept 73-02	1	-	668	+6.7, -7.2	-	534	+10.3,-10.3
	2	-			-		
	3	620			589		
	4	716			479		
SAS 1-08 Sept 73-04	1	-	792	+8.5, -8.5	-	685	+7.0, -7.2
	2	-			-		
	3	725			636		
	4	859			733		
SAS 1-09 Sept 73-01	1	-	590	+1.7, -1.5	-	507	+4.5, -4.9
	2	-			-		
	3	581			483		
	4	600			531		
SAS 1-14 Sept 73-01	1	203	192	+5.7, -8.3	100	106	+17.9,-11.3
	2	-			-		
	3	197			93.5		
	4	176			125		

Appendix E. (Cont'd)

Run	Sensor	E_T (cm^2)	Mean (cm^2)	Range (%)	E_{pl} (cm^2)	Mean (cm^2)	Range (%)
SAS 1-14 Sept 73-02	1	-	199	- -	82.3	82.3	- -
	2	-					
	3	-					
	4	199					
SAS 1-14 Sept 73-03	1	224	197	+13.7, -7.1	102	88.8	+14.9, -7.9
	2	-			-		
	3	185			81.6		
	4	183			82.7		
SAS 1-15 Sept 73-01	1	212	184	+15.2,-11.4	110	87.8	+25. -14.8
	2	-			-		
	3	163			75.4		
	4	176			78.0		
SAS 1-17 Sept 73-02	1	343	323	+6.2, -9.3	114	111	+2.7, -5.4
	2	-			-		
	3	293			105		
	4	333			114		
SAS 1-17 Sept 73-03	1	276	263	+4.9, -3.0	107	112	+3.6, -4.5
	2	-			-		
	3	258			113		
	4	255			117		
SAS 1-17 Sept 73-04	1	211	203	+3.9, -3.0	96.4	87.3	+10.4, -7.2
	2	-			-		
	3	197			81.0		
	4	202			84.6		

Appendix E. (Cont'd)

Run	Sensor	E_T (cm^2)	Mean (cm^2)	Range (%)	E_{pl} (cm^2)	Mean (cm^2)	Range (%)
SAS 1-18 Sept 73-01	1	408	373	+9.4, -7.8	280	249	+12.4, -9.2
	2	-			-		
	3	366			242		
	4	346			226		
SAS 1-18 Sept 73-03	1	350	343	+2.0, -1.2	152	153	+1.3, -1.3
	2	-			-		
	3	339			155		
	4	339			151		
SAS 1-18 Sept 73-04	1	344	338	+1.2, -1.5	198	185	+7.0, -3.8
	2	-			-		
	3	338			178		
	4	333			180		
SAS 1-19 Sept 73-02	1	368	353	+4.2, -7.9	225	195	+15.4,-15.9
	2	-			-		
	3	325			164		
	4	366			196		
SAS 1-19 Sept 73-03	1	289	298	+15.8,-13.1	164	140	+17.1,-14.3
	2	-			-		
	3	345			136		
	4	259			120		
SAS 1-19 Sept 73-04	1	241	254	+6.3, -5.1	135	122	+9.6, -6.6
	2	-			-		
	3	270			114		
	4	251			116		

Appendix E. (Cont'd)

Run	Sensor	E_T (cm^2)	Mean (cm^2)	Range (%)	E_{pl} (cm^2)	Mean (cm^2)	Range (%)
SAS 1-20 Sept 73-01	1	251	243	+15.2,-18.5	89.6	79.8	+12.3,-10.2
	2	-			-		
	3	280			78.0		
	4	198			71.7		
SAS 1-20 Sept 73-03	1	392	346	+13.3, -8.7	203	213	+18.8,-14.6
	2	-			-		
	3	316			182		
	4	331			253		
SAS 1-20 Sept 73-04	1	418	461	+5.4, -9.3	195	220	+8.6,-11.4
	2	-			-		
	3	486			227		
	4	479			239		
SAS 1-21 Sept 73-01	1	473	431	+9.7, -5.3	245	211	+16.1,-11.8
	2	-			-		
	3	413			186		
	4	408			203		
SAS 1-21 Sept 73-02	1	955	876	+9.0, -5.1	683	625	+9.3, -5.0
	2	-			-		
	3	831			594		
	4	841			597		
SAS 1-21 Sept 73-03	1	718	663	+8.3, -8.3	313	317	+3.8, -2.8
	2	-			-		
	3	664			329		
	4	608			308		

Appendix E. (Cont'd)

Run	Sensor	E_T (cm^2)	Mean (cm^2)	Range (%)	E_{pl} (cm^2)	Mean (cm^2)	Range (%)
SAS 1-22 Sept 73-01	1	554	509	+8.8, -6.5	353	338	+4.4, -5.6
	2	-			-		
	3	496			343		
	4	476			319		
SAS 1-22 Sept 73-02	1	730	629	+16.1, -7.9	363	318	+14.2, -7.2
	2	-			-		
	3	579			296		
	4	579			295		
SAS 1-22 Sept 73-03	1	443	418	+6.0, -3.8	274	256	+15.2,-28.0
	2	-			-		
	3	409			295		
	4	402			200		
SAS 1-23 Sept 73-03	1	408	387	+5.4, -7.5	310	272	+14.0,-12.5
	2	-			-		
	3	394			268		
	4	358			238		
SAS 1-23 Sept 73-04	1	519	452	+14.8, -8.2	350	309	+13.3, -9.4
	2	-			-		
	3	421			298		
	4	415			280		
SAS 1-24 Sept 73-03	1	682	640	+15.0,-11.3	396	339	+16.8,-22.4
	2	736			373		
	3	568			263		
	4	572			322		

Appendix E. (Cont'd)

Run	Sensor	E_T (cm^2)	Mean (cm^2)	Range (%)	E_{pl} (cm^2)	Mean (cm^2)	Range (%)
SAS 1-24 Sept 73-04	1	771	693	+11.3, -7.4	292	261	+27.6, -21.1
	2	683			333		
	3	642			214		
	4	676			206		
SAS 1-25 Sept 73-01	1	658	632	+10.0, -13.6	373	336	+11.0, -14.3
	2	695			355		
	3	546			288		
	4	628			329		
SAS 1-27 Sept 73-01	1	503	475	+9.3, -9.9	316	246	+28.5, -19.1
	2	429			256		
	3	447			199		
	4	519			212		
SAS 1-02 Oct 73-01	1	100	104	+8.7, -7.7	43.9	58.6	+25.1, -25.1
	2	113			49.9		
	3	107			73.3		
	4	95.5			67.3		
SAS 1-02 Oct 73-02	1	130	131	+10.7, -8.4	67.9	54.8	+23.9, -15.7
	2	145			57.1		
	3	-			48.0		
	4	119			46.2		
SAS 1-02 Oct 73-03	1	112	119	+22.7, -16.0	49.6	44.3	+20.3, -27.5
	2	146			53.3		
	3	-			42.2		
	4	99.7			32.1		

Appendix E. (Cont'd)

Run	Sensor	E_T (cm^2)	Mean (cm^2)	Range (%)	E_{pl} (cm^2)	Mean (cm^2)	Range (%)
SAS 1-03 Oct 73-02	1	297	294	+4.4, -3.4	122	119	+2.5, -2.5
	2	284			117		
	3	307			116		
	4	287			122		
SAS 1-03 Oct 73-03	1	331	325	+4.0, -5.5	182	181	+5.5, -7.7
	2	338			191		
	3	-			183		
	4	307			167		
SAS 1-03 Oct 73-04	1	200	198	+9.1,-10.6	84.1	85.1	+12.3,-21.4
	2	216			66.9		
	3	-			95.6		
	4	177			93.8		
SAS 1-04 Oct 73-01	1	220	222	+10.8, -9.5	108	96.6	+11.3,-11.4
	2	246			85.6		
	3	-			93.6		
	4	201			99.8		
SAS 1-06 Oct 73-01	1	209	205	+3.4, -7.3	108	101	+6.9, -4.5
	2	208			101		
	3	212			95.5		
	4	190			99.7		
SAS 1-08 Oct 73-01	1	98.8	111	+41.4,-27.4	48.1	47.2	+11.0,-15.0
	2	108			52.4		
	3	157			48.0		
	4	80.6			40.1		

Appendix E. (Cont'd)

Run	Sensor	E_T (cm^2)	Mean (cm^2)	Range (%)	E_{pl} (cm^2)	Mean (cm^2)	Range (%)
SAS 1-08 Oct 73-02	1	313	310	+7.4, -8.4	144	131	+9.9, -9.2
	2	333			134		
	3	284			119		
	4	310			127		
SAS 1-09 Oct 73-02	1	1026	917	+11.9, -9.6	952	841	+13.2,-12.2
	2	915			848		
	3	829			738		
	4	897			827		
SAS 1-10 Oct 73-01	1	277	284	+19.4,-11.6	177	166	+13.3,-13.3
	2	339			188		
	3	270			144		
	4	251			154		
SAS 1-10 Oct 73-03	1	338	329	+2.7, -1.8	262	241	+8.7,-10.7
	2	323			232		
	3	-			215		
	4	326			255		
SAS 1-10 Oct 73-04	1	335	321	+4.4, -8.1	196	189	+9.5,-16.4
	2	334			207		
	3	-			158		
	4	295			193		
SAS 1-11 Oct 73-01	1	179	182	+18.1,-15.9	89.6	88.0	+21.5,-20.6
	2	215			107		
	3	-			85.6		
	4	153			69.9		

Appendix E. (Cont'd)

Run	Sensor	E_T (cm^2)	Mean (cm^2)	Range (%)	E_{pl} (cm^2)	Mean (cm^2)	Range (%)
SAS 1-11 Oct 73-02	1	227	213	+6.6, -7.5	134	118	+13.6,-11.9
	2	197			114		
	3	-			120		
	4	216			104		
SAS 1-11 Oct 73-03	1	217	213	+14.1,-16.0	45.7	44.8	+5.7, -3.9
	2	243			46.5		
	3	-			-		
	4	179			42.3		
SAS 1-12 Oct 73-04	1	144	146	+11.0,-10.3	45.6	44.8	+6.7,-11.4
	2	162			46.2		
	3	-			39.7		
	4	131			47.8		
SAS 1-13 Oct 73-02	1	169	187	+14.4, -9.6	63.8	66.4	+14.0, -8.1
	2	214			65.2		
	3	-			75.7		
	4	179			61.0		
SAS 1-13 Oct 73-03	1	144	151	+10.6, -5.3	80.6	83.2	+5.9, -3.1
	2	167			83.5		
	3	-			88.1		
	4	143			80.7		
SAS 1-14 Oct 73-01	1	200	190	+9.5,-14.7	95.8	91.2	+5.0, -3.9
	2	208			87.6		
	3	-			90.9		
	4	162			90.4		

Appendix E. (Cont'd)

Run	Sensor	E_T (cm^2)	Mean (cm^2)	Range (%)	E_{pl} (cm^2)	Mean (cm^2)	Range (%)
SAS 1-14 Oct 73-02	1	229	230	+13.5,-13.0	132	130	+8.5,-10.8
	2	261			132		
	3	-			141		
	4	200			116		
SAS 1-14 Oct 73-04	1	256	256	+0.3, -0.0	149	154	+13.6, -7.8
	2	257			143		
	3	-			147		
	4	256			175		
SAS 1-15 Oct 73-01	1	388	343	+13.1,-10.5	246	215	+14.4, -7.9
	2	333			200		
	3	-			-		
	4	307			198		
SAS 1-15 Oct 73-04	1	460	442	+4.1, -5.2	256	246	+4.1, -4.9
	2	446			249		
	3	-			-		
	4	419			234		
SAS 1-16 Oct 73-01	1	346	336	+5.7,-10.4	180	173	+8.8,-16.8
	2	355			188		
	3	341			144		
	4	301			178		
SAS 1-16 Oct 73-02	1	341	329	+5.8, -9.7	245	234	+6.8, -4.7
	2	348			239		
	3	-			-		
	4	297			218		

Appendix E. (Cont'd)

Run	Sensor	E_T (cm^2)	Mean (cm^2)	Range (%)	E_{p1} (cm^2)	Mean (cm^2)	Range (%)
SAS 1-19 Oct 73-01	1	945	882	+7.1, -7.6	357	334	+6.4, -3.3
	2	887			323		
	3	-			-		
	4	815			323		
SAS 1-19 Oct 73-03	1	437	428	+7.0, -8.9	243	257	+6.2, -5.4
	2	458			273		
	3	-			-		
	4	390			256		
SAS 1-20 Oct 73-01	1	501	492	+1.8, -2.6	189	170	+11.2, -6.5
	2	479			172		
	3	-			160		
	4	497			159		
SAS 1-20 Oct 73-04	1	775	741	+6.2,-11.3	273	273	+7.4,-12.5
	2	787			294		
	3	657			239		
	4	746			287		
SAS 1-21 Oct 73-03	1	518	496	+4.4, -4.4	361	358	+5.0, -5.6
	2	496			338		
	3	-			376		
	4	474			357		
SAS 1-21 Oct 73-04	1	590	562	+5.0, -6.6	445	412	+8.0, -7.4
	2	572			409		
	3	-			-		
	4	525			382		

Appendix E. (Cont'd)

Run	Sensor	E_T (cm^2)	Mean (cm^2)	Range (%)	E_{p1} (cm^2)	Mean (cm^2)	Range (%)
SAS 1-22 Oct 73-01	1	873	791	+10.4, -9.9	574	547	+4.9, -4.9
	2	787			520		
	3	-			-		
	4	713			546		
SAS 1-22 Oct 73-03	1	470	397	+18.4,-23.4	297	270	+10.0, -8.9
	2	397			246		
	3	304			283		
	4	418			253		
SAS 1-22 Oct 73-04	1	387	363	+6.6, -3.6	205	171	+19.9,-21.0
	2	352			173		
	3	-			-		
	4	350			135		
SAS 1-23 Oct 73-01	1	285	270	+14.1,-20.0	183	159	+15.1,-17.0
	2	308			162		
	3	-			-		
	4	216			132		
SAS 1-23 Oct 73-03	1	197	167	+18.0,-21.6	123	102	+20.6,-17.5
	2	174			101		
	3	-			-		
	4	131			84.1		
SAS 1-23 Oct 73-04	1	649	636	+5.8, -8.0	406	434	+13.1, -6.5
	2	673			432		
	3	-			491		
	4	585			406		

Appendix E. (Cont'd)

Run	Sensor	E_T (cm^2)	Mean (cm^2)	Range (%)	E_{pl} (cm^2)	Mean (cm^2)	Range (%)
SAS 1-24 Oct 73-01	1	880	836	+7.2,-12.3	472	385	+22.6,-22.1
	2	896			430		
	3	-			300		
	4	733			336		
SAS 1-24 Oct 73-02	1	1087	991	+8.8, -8.3	578	516	+12.0,-12.4
	2	978			518		
	3	-			-		
	4	909			452		
SAS 1-25 Oct 73-01	1	524	528	+3.0, -2.3	218	237	+5.9, -8.0
	2	544			240		
	3	-			-		
	4	516			254		
SAS 1-25 Oct 73-02	1	383	382	+8.4, -8.4	345	335	+3.0, -5.4
	2	414			342		
	3	-			-		
	4	350			317		
SAS 1-25 Oct 73-03	1	471	447	+5.4, -6.9	427	394	+8.4,-12.4
	2	466			422		
	3	433			345		
	4	416			381		
SAS 1-25 Oct 73-04	1	435	426	+9.4,-11.3	401	391	+4.4, -6.9
	2	466			409		
	3	-			-		
	4	378			364		

Appendix E. (Cont'd)

Run	Sensor	E_T (cm^2)	Mean (cm^2)	Range (%)	E_{pl} (cm^2)	Mean (cm^2)	Range (%)
SAS 1-26 Oct 73-01	1	407	398	+5.8, -8.0	358	347	+3.2, -4.6
	2	421			345		
	3	-			353		
	4	366			331		
SAS 1-26 Oct 73-02	1	452	421	+7.4,-13.3	302	319	+7.3, -8.5
	2	452			294		
	3	365			292		
	4	415			344		
SAS 1-26 Oct 73-03	1	243	232	+17.2,-15.5	94.2	86.0	+10.0,-12.1
	2	272			89.5		
	3	196			94.6		
	4	216			75.6		
SAS 1-26 Oct 73-04	1	307	307	+9.8, -7.8	225	237	+8.0, -5.1
	2	337			242		
	3	283			225		
	4	301			256		
SAS 1-27 Oct 73-01	1	195	193	+22.3,-14.0	153	143	+11.9, -9.1
	2	236			160		
	3	174			131		
	4	166			130		
SAS 1-27 Oct 73-04	1	219	193	+13.5,-17.6	90.0	76.8	+18.2,-18.0
	2	211			78.4		
	3	159			63.0		
	4	182			75.7		

Appendix E. (Cont'd)

Run	Sensor	E_T (cm^2)	Mean (cm^2)	Range (%)	$E_{pl.}$ (cm^2)	Mean (cm^2)	Range (%)
SAS 1-28 Oct 73-03	1	243	208	+20.7,-20.2	193	157	+22.9,-17.2
	2	251			163		
	3	172			130		
	4	166			140		
SAS 1-28 Oct 73-04	1	312	283	+18.2,-17.3	236	209	+12.9,-17.2
	2	336			228		
	3	234			173		
	4	250			197		
SAS 1-29 Oct 73-01	1	430	405	+9.9,-17.5	316	284	+11.3,-15.8
	2	445			283		
	3	344			239		
	4	400			299		
SAS 1-29 Oct 73-02	1	767	722	+6.2, -9.7	243	242	+5.8, -6.6
	2	732			256		
	3	652			226		
	4	735			244		
SAS 1-29 Oct 73-04	1	1610	1470	+2.7,-11.6	961	919	+6.1, -9.8
	2	1500			911		
	3	1300			829		
	4	1460			975		
SAS 1-30 Oct 73-01	1	1490	1380	+8.5,-12.3	1390	1290	+7.8,-12.4
	2	1460			1350		
	3	1210			1130		
	4	1370			1300		

Appendix E. (Cont'd)

Run	Sensor	E_T (cm^2)	Mean (cm^2)	Range (%)	E_{pl} (cm^2)	Mean (cm^2)	Range (%)
SAS 1-02 Nov 73-02	1	423	411	+8.5,-12.4	228	228	+6.1,-14.5
	2	360			195		
	3	416			230		
	4	446			242		
SAS 1-03 Nov 73-01	1	746	694	+7.5, -5.5	389	344	+13.1,-14.0
	2	679			364		
	3	696			326		
	4	656			296		
SAS 1-03 Nov 73-02	1	349	352	+15.9,-17.9	153	118	+29.7,-45.7
	2	408			125		
	3	363			131		
	4	289			63.5		
SAS 1-04 Nov 73-02	1	411	452	+18.4,-11.7	110	149	+29.5,-26.2
	2	461			152		
	3	535			193		
	4	399			139		
SAS 1-04 Nov 73-04	1	793	714	+11.1, -6.6	454	356	+27.5,-14.4
	2	705			348		
	3	667			318		
	4	691			304		
SAS 1-05 Nov 73-01	1	729	688	+5.6, -7.7	191	168	+25.0,-35.1
	2	716			160		
	3	666			210		
	4	639			109		

Appendix E. (Cont'd)

Run	Sensor	E_T (cm^2)	Mean (cm^2)	Range (%)	E_{pl} (cm^2)	Mean (cm^2)	Range (%)
SAS 1-05 Nov 73-02	1	514	528	+8.9, -7.6	181	183	+16.9,-14.8
	2	488			156		
	3	534			179		
	4	575			214		
SAS 1-07 Nov 73-02	1	555	534	+15.4,-10.9	360	345	+4.3, -6.7
	2	616			322		
	3	490			340		
	4	476			357		
SAS 1-08 Nov 73-01	1	373	386	+7.5, -3.6	169	129	+31.0,-24.8
	2	415			123		
	3	381			96.8		
	4	372			129		
SAS 1-08 Nov 73-03	1	421	406	+6.4, -7.1	188	202	+42.1,-22.3
	2	377			157		
	3	432			287		
	4	395			176		
SAS 1-09 Nov 73-01	1	246	233	+7.3,-12.9	95.6	85.5	+12.9,-15.9
	2	250			90.8		
	3	231			82.7		
	4	203			71.9		
SAS 1-09 Nov 73-03	1	269	244	+12.7,-14.3	137	131	+5.8,-14.9
	2	275			114		
	3	221			139		
	4	209			134		

Appendix E. (Cont'd)

Run	Sensor	E_T (cm^2)	Mean (cm^2)	Range (%)	E_{pl} (cm^2)	Mean (cm^2)	Range (%)
SAS 1-10 Nov 73-01	1	466	404	+15.3, -9.2	346	284	+21.8,-12.0
	2	376			264		
	3	406			276		
	4	367			250		
SAS 1-10 Nov 73-02	1	339	364	+10.4, -6.9	264	310	+17.7,-14.8
	2	363			291		
	3	402			365		
	4	352			320		
SAS 1-10 Nov 73-04	1	435	391	+11.3,-10.2	270	238	+13.4, -6.3
	2	402			230		
	3	401			229		
	4	351			223		
SAS 1-11 Nov 73-03	1	462	460	+2.4, -4.1	369	370	+4.6,-17.8
	2	464			344		
	3	471			387		
	4	441			379		
SAS 1-11 Nov 73-04	1	238	255	+5.9, -6.7	219	255	+8.9,-16.0
	2	250			189		
	3	270			245		
	4	261			244		
SAS 1-12 Nov 73-01	1	378	330	+18.2,-23.3	314	288	+9.0,-12.2
	2	390			285		
	3	298			298		
	4	253			253		

Appendix E. (Cont'd)

Run	Sensor	E_T (cm^2)	Mean (cm^2)	Range (%)	E_{pl} (cm^2)	Mean (cm^2)	Range (%)
SAS 1-12 Nov 73-02	1	437	428	+2.1, -3.0	202	200	+2.5, -4.0
	2	429			192		
	3	431			205		
	4	415			200		
SAS 1-12 Nov 73-03	1	1000	867	+15.3, -7.4	684	625	+9.4, -5.0
	2	850			637		
	3	815			594		
	4	803			586		
SAS 1-12 Nov 73-04	1	852	795	+7.2, -5.8	623	579	+7.1, -5.9
	2	749			545		
	3	829			590		
	4	750			557		
SAS 1-13 Nov 73-01	1	1040	1080	+10.2,-13.0	789	872	+19.3,-21.6
	2	940			683		
	3	1150			975		
	4	1190			1040		
SAS 1-13 Nov 73-03	1	1140	1040	+10.6,-17.8	820	820	+10.1,-22.2
	2	855			638		
	3	1150			918		
	4	1000			903		
SAS 1-20 Nov 73-04	2	789	890	+7.3,-11.3	482	422	+12.4, -7.3
	3	927			392		
	4	955			391		
SAS 1-21 Nov 73-01	2	788	863	±8.8	650	820	+14.5,-19.6
	3	939			939		
	4	863			862		

Appendix E. (Cont'd)

Run	Sensor	E_T (cm^2)	Mean (cm^2)	Range (%)	E_{pl} (cm^2)	Mean (cm^2)	Range (%)
SAS 1-01 Dec 73-02	1	881	877	+3.6, -4.3	816	759	+7.5, -7.8
	2	879			700		
	3	909			750		
	4	839			771		
SAS 1-01 Dec 73-03	1	657	638	+3.0, -2.8	590	564	+4.6,-11.3
	2	624			500		
	3	651			595		
	4	620			571		
SAS 1-01 Dec 73-04	1	345	347	+15.6,-14.7	312	278	+12.2,-10.4
	2	401			249		
	4	296			273		
SAS 1-02 Dec 73-01	1	516	545	+16.1, -9.6	218	200	+9.0, -9.5
	2	539			198		
	3	633			181		
	4	492			204		
SAS 1-02 Dec 73-02	1	854	780	+9.5,-13.2	326	279	+16.8,-37.6
	2	800			289		
	3	790			326		
	4	677			174		
SAS 1-03 Dec 73-02	2	739	771	+5.8, -4.1	650	730	+9.2,-11.0
	3	816			797		
	4	757			744		
SAS 1-03 Dec 73-04	1	414	450	+22.2,-15.1	338	321	+5.3, -3.4
	2	455			320		
	3	550			317		
	4	382			310		

Appendix E. (Cont'd)

Run	Sensor	E_T (cm^2)	Mean (cm^2)	Range (%)	E_{pl} (cm^2)	Mean (cm^2)	Range (%)
SAS 1-04 Dec 73-01	1	449	459	+12.2,-10.2	389	374	+4.0, -2.9
	2	515			363		
	4	412			369		
SAS 1-05 Dec 73-02	1	276	258	+7.0,-12.4	123	102	+20.5,-17.4
	2	274			103		
	3	255			98.2		
	4	226			84.2		
SAS 1-05 Dec 73-04	1	613	594	+6.6, -5.6	346	334	+3.6, -6.6
	2	633			312		
	3	561			330		
	4	570			346		
SAS 1-06 Dec 73-01	1	563	620	+21.3,-13.7	272	261	+13.7,-11.1
	2	752			297		
	3	630			243		
	4	535			232		
SAS 1-07 Dec 73-01	1	785	798	+4.3, -1.8	747	754	+6.1, -6.0
	2	789			709		
	3	832			800		
	4	784			758		
SAS 1-07 Dec 73-02	1	451	437	+12.8,-16.0	441	396	+11.4, -9.3
	2	493			376		
	3	438			408		
	4	367			359		

Appendix E. (Cont'd)

Run	Sensor	E_T (cm^2)	Mean (cm^2)	Range (%)	E_{pl} (cm^2)	Mean (cm^2)	Range (%)
SAS 1-08 Dec 73-01	1	691	679	+4.3, -7.1	555	546	+7.7,-10.8
	2	631			487		
	3	708			588		
	4	684			553		
SAS 1-08 Dec 73-02	1	545	537	+12.7,-14.1	376	382	+7.8,-10.5
	2	605			399		
	3	535			412		
	4	461			342		
SAS 1-08 Dec 73-03	1	916	934	+7.1, -6.0	790	775	+9.4,-11.1
	2	878			689		
	3	1000			848		
	4	943			772		
SAS 1-08 Dec 73-04	1	562	516	+8.9, -6.6	453	346	+30.9,-13.0
	2	523			319		
	3	496			301		
	4	482			309		
SAS 1-09 Dec 73-01	1	619	593	+4.4, -5.7	-	387	±4.9
	2	559			406		
	3	611			386		
	4	584			368		
SAS 1-09 Dec 73-02	1	503	529	+7.9, -4.9	341	320	+6.2, -4.7
	2	571			315		
	3	528			319		
	4	514			305		

Appendix E. (Cont'd)

Run	Sensor	E_T (cm^2)	Mean (cm^2)	Range (%)	E_{pl} (cm^2)	Mean (cm^2)	Range (%)
SAS 1-09 Dec 73-03	1	379	397	+5.0, -4.5	308	279	+10.4, -9.3
	2	400			281		
	3	417			253		
	4	393			275		
SAS 1-09 Dec 73-04	1	328	362	+11.3, -9.3	156	167	+8.3, -6.6
	2	403			155		
	3	384			181		
	4	334			175		
SAS 1-10 Dec 73-01	1	272	300	+12.3, -9.3	221	232	±4.7
	2	337			224		
	3	308			243		
	4	284			240		
SAS 1-10 Dec 73-03	1	291	299	±10.0	99.0	79.7	+24.2,-20.2
	2	305			72.6		
	3	329			63.6		
	4	269			83.6		
SAS 1-12 Dec 73-01	1	627	563	+11.2,-17.8	546	470	+16.2,-15.1
	2	626			479		
	3	535			454		
	4	463			399		
SAS 1-12 Dec 73-02	1	441	478	+5.6, -7.7	394	418	±5.7
	2	505			396		
	3	494			440		
	4	473			442		

Appendix E. (Cont'd)

Run	Sensor	E_T (cm^2)	Mean (cm^2)	Range (%)	E_{pl} (cm^2)	Mean (cm^2)	Range (%)
SAS 1-12 Dec 73-03	1	418	449	+3.8, -6.9	371	395	+7.8, -8.1
	2	466			363		
	3	459			420		
	4	451			426		
SAS 1-12 Dec 73-04	1	808	704	+14.8,-13.6	688	610	+12.8,-12.4
	2	714			612		
	3	686			606		
	4	608			534		
SAS 1-15 Dec 73-01	1	2000	1910	+4.7, -6.8	1050	1010	+6.9,-11.9
	2	1780			890		
	3	1950			1080		
SAS 1-15 Dec 73-02	1	1940	1880	+3.2, -5.9	1610	1560	+6.4, -9.6
	2	1770			1410		
	3	1920			1660		
SAS 1-15 Dec 73-03	1	2010	2010	+9.0, -9.4	1430	1400	±2.1
	2	1820			1410		
	3	2190			1370		
SAS 1-15 Dec 73-04	1	2010	1990	+7.0, -8.5	1790	1730	+4.6, -7.5
	2	1820			1600		
	3	2130			1810		
SAS 1-16 Dec 73-01	1	1620	1560	+3.8, -4.5	1340	1300	+3.1, -6.1
	2	1490			1220		
	3	1560			1330		
SAS 1-16 Dec 73-02	1	955	989	+5.2, -3.4	955	953	+7.0, -7.2
	2	972			884		
	3	1040			1020		

Appendix E. (Cont'd)

Run	Sensor	E_T (cm^2)	Mean (cm^2)	Range (%)	E_{pl} (cm^2)	Mean (cm^2)	Range (%)
SAS 1-16 Dec 73-03	1	752	720	±4.4	703	680	±3.4
	3	689			650		
SAS 1-16 Dec 73-04	1	572	629	±9.1	553	604	±8.3
	3	686			654		
SAS 1-17 Dec 73-01	1	496	508	±2.2	266	249	±6.8
	3	519			232		
SAS 1-17 Dec 73-02	1	410	405	±1.3	307	304	±1.2
	3	399			300		
SAS 1-17 Dec 73-03	1	601	598	±1.0	432	421	±2.6
	3	594			410		
SAS 1-18 Dec 73-01	1	721	725	±0.01	448	460	±2.6
	3	729			472		
SAS 1-18 Dec 73-02	1	662	679	±2.5	443	457	±3.0
	3	696			470		
SAS 1-18 Dec 73-03	1	573	590	±2.9	332	323	±2.9
	3	607			314		
SAS 1-18 Dec 73-04	1	947	906	+5.6, -5.3	563	565	±0.01
	3	858			561		
	4	902			571		
SAS 1-19 Dec 73-01	1	1200	1120	+7.1, -9.8	971	897	+8.3, -7.1
	3	1130			886		
	4	1020			833		
SAS 1-19 Dec 73-03	1	360	411	+10.9,-12.4	306	319	±4.1
	3	456			332		
	4	417			319		

Appendix E. (Cont'd)

Run	Sensor	E_T (cm^2)	Mean (cm^2)	Range (%)	E_{pl} (cm^2)	Mean (cm^2)	Range (%)
SAS 1-19 Dec 73-04	1	437	449	+3.3, -2.7	367	387	+5.7, -5.2
	3	445			386		
	4	464			409		
SAS 1-20 Dec 73-04	1	1260	1230	+2.4, -3.3	1090	1080	+2.8, -2.7
	3	1240			1110		
	4	1190			1050		
SAS 1-21 Dec 73-01	1	1400	1370	+5.8, -8.0	1260	1240	+7.3, -8.1
	3	1450			1330		
	4	1260			1140		
SAS 1-21 Dec 73-02	1	945	923	+2.4, -3.1	876	865	+1.3, -2.3
	3	930			873		
	4	894			845		
SAS 1-21 Dec 73-04	1	921	941	+17.9,-13.2	860	829	+4.2, -8.1
	2	1110			829		
	3	916			864		
	4	816			762		
SAS 1-22 Dec 73-02	1	1580	1540	+13.6,-11.7	731	686	+4.1,-13.1
	2	1450			596		
	3	1750			702		
	4	1360			714		
SAS 1-22 Dec 73-01	1	1200	1100	+9.1,-14.6	949	878	+8.1,-13.9
	2	1110			878		
	3	1170			929		
	4	939			756		

Appendix E. (Cont'd)

Run	Sensor	E_T (cm^2)	Mean (cm^2)	Range (%)	E_{pl} (cm^2)	Mean (cm^2)	Range (%)
SAS 1-22 Dec 73-02	1	1200	1100	+9.1,-14.6	949	895	+6.0,-15.5
	2	1110			946		
	3	1170			929		
	4	939			756		
SAS 1-22 Dec 73-03	1	1580	1540	+13.6,-11.7	731	686	+6.6,-13.1
	2	1450			596		
	3	1750			702		
	4	1360			714		
SAS 1-22 Dec 73-04	1	1760	1780	+11.2, -6.7	1000	1070	+11.2, -6.5
	2	1660			1060		
	3	1980			1190		
	4	1720			1040		
SAS 1-23 Dec 73-01	1	3250	3120	+4.2, -3.8	2020	2070	+11.1, -4.3
	2	3000			1980		
	3	3160			1990		
	4	3060			2300		
SAS 1-24 Dec 73-04	2	1590	1590	±1.9	776	869	+6.9,-10.7
	3	1620			929		
	4	1560			902		
SAS 1-28 Dec 73-05	1	-	409	+4.2, -5.1	-	309	+3.9, -5.5
	2	428			323		
	3	412			313		
	4	388			292		

Appendix E. (Cont'd)

Run	Sensor	E_T (cm^2)	Mean (cm^2)	Range (%)	E_{pl} (cm^2)	Mean (cm^2)	Range (%)
SAS 1-29 Dec 73-01	1	-	394	+8.1, -15.1	260	287	+11.1, -5.9
	2	336			319		
	3	426			282		
	4	419			-		
SAS 1-29 Dec 73-02	1	-	599	+2.5, -4.0	-	252	+3.2, -2.0
	2	584			244		
	3	623			257		
	4	589			256		
SAS 1-29 Dec 73-04	1	-	1250	+2.4, -4.8	-	734	+3.5, -4.5
	2	1220			701		
	3	1330			760		
	4	1190			742		
SAS 1-30 Dec 73-01	1	-	1550	+7.7, -8.4	-	926	+2.9, -2.2
	2	1420			906		
	3	1670			953		
	4	1560			918		
SAS 1-30 Dec 73-02	1	-	1410	+2.8, -3.5	-	841	+7.7, -8.6
	2	1410			906		
	3	1460			848		
	4	1370			769		
SAS 1-30 Dec 73-03	1	-	1680	+4.8, -3.6	-	1100	+13.6, -12.4
	2	1660			1100		
	3	1760			1250		
	4	1620			964		

Appendix E. (Cont'd)

Run	Sensor	E_T (cm^2)	Mean (cm^2)	Range (%)	E_{pl} (cm^2)	Mean (cm^2)	Range (%)
SAS 1-30 Dec 73-04	1	-	1830	+3.8, -6.0		1410	+7.1,-12.8
	2	1880			1510		
	3	1900			1480		
	4	1720			1230		
SAS 1-02 Jan 74-03	2	470	470	+6.0, -6.1	390	335	+16.4,-14.0
	3	498			327		
	4	441			288		
SAS 1-02 Jan 74-04	1	433	408	+6.1, -5.4	235	219	+7.3, -8.7
	2	421			223		
	3	386			200		
	4	391			218		
SAS 1-03 Jan 74-01	2	313	316	+4.4, -3.8	141	182	+9.9,-22.5
	3	330			204		
	4	304			200		
SAS 1-03 Jan 74-02	2	424	429	±0.01	329	309	+6.5, -4.2
	3	432			296		
	4	430			302		
SAS 1-03 Jan 74-04	2	256	246	+4.1, -2.4	125	115	+8.7,-11.3
	3	240			102		
	4	243			119		
SAS 1-03 Jan 74-05	1	183	173	+5.8, -4.6	89.5	78.4	+14.1, -9.6
	2	166			70.9		
	3	165			75.0		
	4	176			78.0		
SAS 1-04 Jan 74-01	2	281	267	+8.9,-13.8	206	191	+10.5,-18.3
	3	291			211		
	4	230			156		

Appendix E. (Cont'd)

Run	Sensor	E_T (cm^2)	Mean (cm^2)	Range (%)	E_{pl} (cm^2)	Mean (cm^2)	Range (%)
SAS 1-04 Jan 74-04	2	1240	1140	+8.8, -7.0	931	864	+7.8, -5.4
	3	1120			845		
	4	1060			817		
SAS 1-04 Jan 74-05	2	639	603	+6.0, -6.8	507	502	+2.8, -3.8
	3	607			516		
	4	562			483		
SAS 1-05 Jan 74-01	2	2170	2180	+8.7, -8.3	2050	2050	±9.8
	3	2370			2250		
	4	2000			1850		
SAS 1-06 Jan 74-04	2	836	816	±2.5	436	397	+9.8, -7.0
	3	816			385		
	4	797			369		
SAS 1-06 Jan 74-05	2	392	405	+3.0, -3.2	172	167	+7.2,-10.2
	3	417			150		
	4	406			179		
SAS 1-07 Jan 74-01	2	296	278	+6.5, -9.0	82.3	101	+11.9,-18.5
	3	284			112		
	4	253			110		
SAS 1-07 Jan 74-02	1	299	290	+4.1, -6.2	132	103	+28.1,-10.8
	2	288			91.9		
	3	302			95.2		
	4	272			93.6		
SAS 1-07 Jan 74-03	1	300	284	+5.6, -6.7	108	112	+1.8, -3.6
	2	265			113		
	3	288			114		
	4	284			112		

Appendix E. (Cont'd)

Run	Sensor	E_T (cm^2)	Mean (cm^2)	Range (%)	E_{pl} (cm^2)	Mean (cm^2)	Range (%)
SAS 1-07 Jan 74-04	1	350	348	+1.1, -3.2	189	197	+9.6, -8.6
	2	337			180		
	3	351			216		
	4	352			201		
SAS 1-08 Jan 74-01	1	732	705	+4.7,-16.5	574	534	+10.1,-21.2
	2	761			588		
	3	738			552		
	4	589			421		
SAS 1-08 Jan 74-02	1	1130	1160	+11.2, -5.2	830	879	+8.4, -5.6
	2	1120			840		
	3	1290			953		
	4	1100			894		
SAS 1-08 Jan 74-03	1	1890	1590	+18.9,-16.3	1640	1500	+9.3,-12.0
	2	1550			1450		
	3	1590			1570		
	4	1330			1320		
SAS 1-09 Jan 74-01	2	1500	1660	+8.4, -9.6	1270	1360	+5.1, -6.6
	3	1800			1380		
	4	1690			1430		
SAS 1-09 Jan 74-02	1	922	974	+14.0, -7.9	887	938	+15.1, -8.3
	2	897			860		
	3	1110			1080		
	4	966			926		

Appendix E. (Cont'd)

Run	Sensor	E_T (cm^2)	Mean (cm^2)	Range (%)	E_{pl} (cm^2)	Mean (cm^2)	Range (%)
SAS 1-10 Jan 74-03	1	435	440	+6.4, -7.0	214	238	+10.9,-10.1
	2	409			217		
	3	468			258		
	4	446			264		
SAS 1-11 Jan 74-01	2	570	569	±6.9	450	431	+4.4, -6.7
	3	608			442		
	4	529			402		
SAS 1-11 Jan 74-03	2	212	224	+3.1, -5.4	163	175	±6.9
	3	230			174		
	4	231			187		
SAS 1-11 Jan 74-04	1	152	156	+7.1, -5.1	124	125	±4.8
	2	148			119		
	3	167			126		
	4	158			131		
SAS 1-12 Jan 74-01	1	225	239	+8.8, -5.9	189	206	+6.3, -8.2
	2	225			200		
	3	260			219		
	4	247			217		
SAS 1-12 Jan 74-02	2	286	277	+4.3, -7.2	268	258	+3.9, -7.0
	3	289			266		
	4	257			240		
SAS 1-12 Jan 74-03	1	359	365	+7.5, -3.8	196	197	+14.2,-13.2
	2	363			171		
	3	385			197		
	4	351			225		

Appendix E. (Cont'd)

Run	Sensor	E_T (cm^2)	Mean (cm^2)	Range (%)	E_{pl} (cm^2)	Mean (cm^2)	Range (%)
SAS 1-12 Jan 74-04	1	517	495	+4.4, -7.5	313	298	+5.0 -7.4
	2	496			299		
	3	510			302		
	4	458			276		
SAS 1-13 Jan 74-01	1	802	768	+7.8,-10.3	775	740	+8.4,-10.0
	2	828			802		
	3	752			717		
	4	689			666		
SAS 1-13 Jan 74-02	1	926	962	+6.0, -3.7	919	946	+6.7, -4.2
	2	958			948		
	3	1020			1010		
	4	943			906		
SAS 1-13 Jan 74-03	1	1620	1700	+3.5, -4.7	1510	1520	+4.6, -3.9
	2	1690			1520		
	3	1760			1590		
	4	1740			1460		
SAS 1-13 Jan 74-04	1	1250	1310	+7.6, -4.6	1070	1125	+9.3, -5.8
	2	1230			1060		
	3	1410			1230		
	4	1360			1140		
SAS 1-14 Jan 74-01	1	1240	1450	+13.1,-14.5	1050	1250	+12.8,-16.0
	2	1410			1220		
	3	1640			1410		
	4	1490			1330		

Appendix E. (Cont'd)

Run	Sensor	E_T (cm^2)	Mean (cm^2)	Range (%)	E_{p1} (cm^2)	Mean (cm^2)	Range (%)
SAS 1-14 Jan 74-02	1	1070	931	+14.9,-14.3	1000	888	+12.6,-13.2
	2	971			940		
	3	883			840		
	4	798			770		
SAS 1-15 Jan 74-01	1	766	658	+16.4,-10.0	658	611	+7.7, -4.9
	2	628			594		
	3	644			609		
	4	592			581		
SAS 1-15 Jan 74-03	2	503	512	+7.6, -5.9	479	490	+8.4, -5.9
	3	551			531		
	4	482			461		
SAS 1-15 Jan 74-04	2	486	473	+2.7, -2.5	337	332	+1.5, -2.4
	3	461			336		
	4	471			324		
SAS 1-16 Jan 74-01	2	362	385	+11.2, -6.0	283	285	+3.2, -2.5
	3	428			294		
	4	364			278		
SAS 1-18 Jan 74-02	2	720	651	±10.6	697	618	±12.8
	3	582			538		
SAS 1-18 Jan 74-03	2	747	721	±3.6	734	692	±6.1
	3	695			650		
SAS 1-19 Jan 74-01	2	551	611	±9.8	550	592	±6.9
	3	671			633		
SAS 1-19 Jan 74-02	2	352	387	±9.0	271	284	±4.6
	3	422			297		

Appendix E. (Cont'd)

Run	Sensor	E_T (cm^2)	Mean (cm^2)	Range (%)	E_{pl} (cm^2)	Mean (cm^2)	Range (%)
SAS 1-19 Jan 74-03	2	402	371	±8.4	396	358	±10.6
	3	340			319		
SAS 1-19 Jan 74-04	2	477	480	±0.6	226	214	±5.6
	3	483			202		
SAS 1-20 Jan 74-01	2	451	496	±9.1	255	330	±22.7
	3	541			405		
SAS 1-25 Jan 74-02	1	240	220	+9.1, -9.5	127	146	+9.6,-13.0
	2	222			152		
	4	199			160		
SAS 1-26 Jan 74-01	1	180	171	+5.3, -3.5	73.9	72.9	+6.2, -7.5
	2	169			77.4		
	4	165			67.4		
SAS 1-26 Jan 74-02	1	343	323	+6.2,-11.8	120	113	+6.2, -8.8
	2	322			120		
	3	342			107		
	4	285			103		
SAS 1-26 Jan 74-03	1	342	348	+6.9, -4.9	215	207	+3.9, -3.4
	2	347			202		
	3	372			200		
	4	331			212		
SAS 1-26 Jan 74-04	1	821	856	+6.4, -6.8	436	459	±9.8
	2	911			482		
	3	888			504		
	4	798			414		

Appendix E. (Cont'd)

Run	Sensor	E_T (cm^2)	Mean (cm^2)	Range (%)	E_{pl} (cm^2)	Mean (cm^2)	Range (%)
SAS 1-27 Jan 74-01	1	707	667	+9.4, -9.9	464	444	+10.1,-10.6
	2	730			397		
	3	629			489		
	4	601			425		
SAS 1-27 Jan 74-02	1	718	632	+13.6,-11.1	499	401	+24.4,-21.4
	2	625			457		
	3	587			334		
	4	502			315		
SAS 1-27 Jan 74-03	1	1180	1030	+14.5, -8.4	805	680	+18.4, -8.9
	2	1030			660		
	3	959			619		
	4	943			634		
SAS 1-27 Jan 74-04	2	1270	1190	+6.7,-10.1	742	790	±6.1
	3	1240			790		
	4	1070			838		
SAS 1-28 Jan 74-01	1	685	697	+5.0, -3.4	386	377	+4.2, -6.6
	2	673			393		
	4	732			352		
SAS 1-28 Jan 74-03	1	385	414	+8.9, -7.0	286	308	+10.1, -7.1
	2	405			298		
	4	451			339		
SAS 1-28 Jan 74-04	1	520	554	+7.0, -6.1	284	321	+10.9,-11.5
	2	526			289		
	3	593			356		
	4	578			353		

Appendix E. (Cont'd)

Run	Sensor	E_T (cm^2)	Mean (cm^2)	Range (%)	E_{pl} (cm^2)	Mean (cm^2)	Range (%)
SAS 1-29 Jan 74-01	1	279	285	+1.0, -2.1	122	127	+4.7, -3.9
	2	288			126		
	4	287			133		
SAS 1-29 Jan 74-02	1	464	468	+4.1, -4.7	404	410	+2.9, -3.4
	2	487			416		
	3	475			422		
	4	446			396		
SAS 1-29 Jan 74-03	1	442	437	+1.1, -1.6	206	210	±5.2
	2	430			199		
	3	439			215		
	4	438			221		
SAS 1-29 Jan 74-04	1	333	322	+4.1, -5.0	231	223	+4.0, -5.8
	2	335			210		
	3	315			232		
	4	306			220		
SAS 1-30 Jan 74-01	1	418	416	±5.5	265	281	+17.4, -7.5
	2	414			260		
	3	439			330		
	4	393			270		
SAS 1-30 Jan 74-03	1	324	284	+14.1,-12.3	180	156	+15.4,-16.7
	2	298			177		
	3	264			130		
	4	249			136		
SAS 1-30 Jan 74-04	1	286	267	+7.5,-16.9	199	173	+15.0,-28.9
	2	271			182		
	3	287			188		
	4	222			123		

Appendix E. (Cont'd)

Run	Sensor	E_T (cm^2)	Mean (cm^2)	Range (%)	E_{p1} (cm^2)	Mean (cm^2)	Range (%)
SAS 1-31 Jan 74-01	1	246	240	+2.5, -2.9	121	114	+6.1, -3.5
	2	233			111		
	3	242			115		
	4	239			110		
SAS 1-09 Feb 74-02	1	138	130	+6.2, -4.6	112	106	+5.7, -4.7
	2	128			101		
	3	128			101		
	4	124			105		
SAS 1-09 Feb 74-03	1	115	115	+9.6, -5.2	91.5	86.0	+6.4, -6.2
	2	110			86.6		
	3	126			85.1		
	4	109			80.7		
SAS 1-10 Feb 74-01	1	187	175	+6.9, -5.7	132	128	+4.5, -3.1
	2	180			131		
	3	169			124		
	4	165			125		
SAS 1-10 Feb 74-04	1	247	274	+11.7, -9.9	217	239	+8.8, -9.2
	2	267			234		
	3	306			260		
	4	274			243		
SAS 1-11 Feb 74-01	1	631	648	+4.6, -2.6	515	540	+5.0, -4.6
	2	643			534		
	3	678			567		
	4	638			544		

Appendix E. (Cont'd)

Run	Sensor	E_T (cm^2)	Mean (cm^2)	Range (%)	E_{pl} (cm^2)	Mean (cm^2)	Range (%)
SAS 1-11 Feb 74-02	1	542	527	+2.8, -4.7	440	446	+3.8, -4.7
	2	502			425		
	3	534			463		
	4	530			457		
SAS 1-11 Feb 74-03	1	1210	1180	+2.5, -9.3	1030	1020	+3.9, -9.7
	2	1080			921		
	3	1210			1050		
	4	1210			1060		
SAS 1-11 Feb 74-04	1	663	698	+5.3, -5.0	570	607	+6.6, -6.1
	2	672			585		
	3	735			647		
	4	720			626		
SAS 1-12 Feb 74-01	1	681	639	+6.6, -5.5	583	547	+6.6, -4.9
	2	643			546		
	3	629			539		
	4	604			520		
SAS 1-12 Feb 74-02	1	570	565	+0.9, -2.7	360	368	+3.8, -2.7
	2	570			382		
	3	569			370		
	4	550			358		
SAS 1-26 Feb 74-02	1	379	405	+13.1,-13.3	187	221	+18.1,-15.4
	2	351			190		
	3	458			246		
	4	430			261		

Appendix E. (Cont'd)

Run	Sensor	E_T (cm^2)	Mean (cm^2)	Range (%)	E_{pl} (cm^2)	Mean (cm^2)	Range (%)
SAS 1-27 Feb 74-02	1	633	655	+3.8, -3.4	372	357	+5.3,-12.3
	2	654			368		
	3	651			313		
	4	680			376		
SAS 1-27 Feb 74-04	1	641	571	+12.3,-12.6	506	441	+14.7,-12.9
	2	589			471		
	3	555			384		
	4	499			401		
SAS 1-28 Feb 74-01	1	891	829	+7.5, -7.2	778	742	+4.9, -7.0
	2	821			740		
	3	836			761		
	4	769			690		
SAS 1-28 Feb 74-07	1	521	609	+28.1,-14.4	499	546	+6.4, -8.6
	2	780			581		
	3	577			561		
	4	559			542		
SAS 1-01 Mar 74-01	1	701	748	+31.1,-13.5	623	609	+11.7, -7.6
	2	981			680		
	3	663			571		
	4	647			563		
SAS 1-07 Mar 74-03	1	224	230	+9.1, -7.0	80.2	84.9	+9.0,-11.7
	2	251			91.8		
	3	232			92.5		
	4	214			75.0		

Appendix E. (Cont'd)

Run	Sensor	E_T (cm^2)	Mean (cm^2)	Range (%)	$E_{pl.}$ (cm^2)	Mean (cm^2)	Range (%)
SAS 1-07 Mar 74-04	1	194	200	+8.5, -3.0	129	139	+12.2, -7.2
	2	195			131		
	3	217			156		
	4	196			139		
SAS 1-08 Mar 74-01	1	637	625	+1.9, -4.0	478	444	+7.7,-14.2
	2	628			459		
	3	500			381		
	4	634			459		
SAS 1-08 Mar 74-04	1	2310	2100	+10.0,-10.5	2180	2000	+9.0, -9.5
	2	2230			2120		
	3	1990			1910		
	4	1880			1800		
SAS 1-09 Mar 74-01	1	1630	1520	+7.2, -5.3	1520	1400	+8.6, -6.4
	2	1530			1420		
	3	1440			1310		
	4	1460			1350		
SAS 1-09 Mar 74-02	1	1240	1130	+12.4,-17.6	544	622	+16.9,-12.5
	2	1270			655		
	3	931			563		
	4	1090			727		
SAS 1-09 Mar 74-03	1	415	411	+2.9, -5.4	395	388	+3.0, -4.9
	2	389			369		
	3	415			389		
	4	423			400		

Appendix E. (Cont'd)

Run	Sensor	E_T (cm^2)	Mean (cm^2)	Range (%)	E_{pl} (cm^2)	Mean (cm^2)	Range (%)
SAS 1-10 Mar 74-03	1	124	124	+9.7,-11.3	55.3	50.2	+10.8,-24.1
	2	127			55.6		
	3	136			38.8		
	4	110			50.9		
SAS 1-11 Mar 74-01	1	153	153	+4.6, -5.9	70.6	66.0	+7.0, -6.8
	2	160			66.7		
	3	142			61.7		
	4	155			65.2		
SAS 1-15 Mar 74-03	1	294	277	+6.1,-13.7	143	138	+5.1,-10.9
	2	294			145		
	3	279			140		
	4	239			123		
SAS 1-16 Mar 74-02	1	172	170	+3.5, -7.1	142	136	+4.4, -5.1
	2	173			140		
	3	176			132		
	4	158			129		
SAS 1-16 Mar 74-03	1	172	169	+4.1, -9.5	91.0	89.0	±2.2
	2	175			87.0		
	3	176			-		
	4	153			-		
SAS 1-17 Mar 74-01	1	225	209	+7.7,-13.9	201	188	+6.9, -8.5
	2	213			191		
	3	216			197		
	4	180			162		

Appendix E. (Cont'd)

Run	Sensor	E_T (cm^2)	Mean (cm^2)	Range (%)	E_{pl} (cm^2)	Mean (cm^2)	Range (%)
SAS 1-17 Mar 74-02	1	215	224	+12.1, -9.8	92.1	94.4	±2.4
	2	229			96.7		
	3	251			-		
	4	202			-		
SAS 1-17 Mar 74-03	1	213	210	+10.0,-11.0	164	159	+3.1, -2.5
	2	207			157		
	3	231			160		
	4	187			155		
SAS 1-22 Mar 74-01	1	401	396	+8.1,-11.6	336	327	+8.9,-15.3
	2	404			337		
	3	428			356		
	4	350			277		
SAS 1-22 Mar 74-02	1	389	354	+9.9,-13.3	284	270	+7.4,-11.9
	2	371			290		
	3	348			267		
	4	307			238		
SAS 1-22 Mar 74-03	1	193	188	+2.7, -6.4	138	131	±5.3
	2	191			137		
	3	193			124		
	4	176			125		
SAS 1-22 Mar 74-04	1	155	149	+5.4, -8.1	57.4	54.0	+7.6,-10.9
	2	145			52.3		
	3	157			58.1		
	4	131			78.1		

Appendix E. (Cont'd)

Run	Sensor	E_T (cm^2)	Mean (cm^2)	Range (%)	E_{pl} (cm^2)	Mean (cm^2)	Range (%)
SAS 1-26 Mar 74-01	1	1280	1440	+11.8, -11.1	1090	1250	+14.4, -12.8
	2	1410			1210		
	3	1610			1430		
	4	1450			1260		
SAS 1-26 Mar 74-02	1	1650	1660	±1.8	1180	1230	+3.1, -4.1
	2	1690			1220		
	3	1630			1270		
	4	1660			1250		
SAS 1-26 Mar 74-03	1	1510	1430	+7.0, -7.7	1240	1200	±5.0
	2	1530			1260		
	3	1350			1140		
	4	1320			1170		
SAS 1-27 Mar 74-01	1	1990	1910	±6.3	1710	1610	+6.2, -5.0
	2	2030			1650		
	3	1820			1560		
	4	1790			1530		
SAS 1-27 Mar 74-02	1	1430	1300	+10.0, -10.8	1250	1120	+11.6, -12.5
	2	1390			1190		
	3	1230			1040		
	4	1160			980		
SAS 1-27 Mar 74-03	1	2270	2140	+6.1, -11.4	2220	2090	+6.2, -11.0
	2	2310			2270		
	3	2070			2010		
	4	1900			1860		

Appendix E. (Cont'd)

Run	Sensor	E_T (cm^2)	Mean (cm^2)	Range (%)	E_{pl} (cm^2)	Mean (cm^2)	Range (%)
SAS 1-28 Mar 74-01	1	1860	1830	+2.7, -3.8	1810	1780	+2.8, -3.4
	2	1880			1830		
	3	1810			1760		
	4	1760			1720		
SAS 1-28 Mar 74-03	1	1160	1260	+9.5, -7.9	1080	1200	±10.0
	2	1190			1140		
	3	1380			1320		
	4	1320			1270		
SAS 1-28 Mar 74-04	1	1190	1140	+4.4, -8.8	1160	1110	+4.5, -9.0
	2	1180			1150		
	3	1150			1110		
	4	1040			1010		
SAS 1-29 Mar 74-01	1	1320	1320	+6.1, -3.8	1260	1270	+6.3, -2.4
	2	1400			1350		
	3	1270			1240		
	4	1290			1240		
SAS 1-29 Mar 74-02	1	1570	1630	+2.5, -3.7	1430	1490	+4.7, -4.0
	2	1610			1450		
	3	1660			1530		
	4	1670			1560		
SAS 1-29 Mar 74-03	1	2610	2470	+6.1, -6.9	2490	2370	+5.9, -7.2
	2	2620			2530		
	3	2300			2200		
	4	2350			2260		

Appendix E. (Cont'd)

Run	Sensor	E_T (cm^2)	Mean (cm^2)	Range (%)	E_{pl} (cm^2)	Mean (cm^2)	Range (%)
SAS 1-29 Mar 74-04	1	2230	2300	+4.3, -4.8	1770	1860	+4.3, -4.8
	2	2390			1930		
	3	2400			1940		
	4	2190			1780		
SAS 1-30 Mar 74-01	1	1390	1390	+3.6, -2.9	1130	1150	+8.7, -3.5
	2	1440			1250		
	3	1360			1110		
	4	1350			1110		
SAS 1-30 Mar 74-02	1	1760	1580	+11.4,-15.6	1300	1180	+10.2,-15.8
	2	1680			1260		
	3	1330			994		
	4	1530			1180		
SAS 1-30 Mar 74-03	1	1150	1110	+6.3, -2.7	1100	1070	+2.8, -1.9
	2	1100			1060		
	3	1100			1050		
	4	1080			1050		
SAS 1-30 Mar 74-04	1	1140	1180	±3.4	1060	1080	±1.4
	2	1150			1070		
	3	1220			1080		
	4	1190			1090		
SAS 1-31 Mar 74-01	1	1520	1440	±5.0	1080	1060	+2.8, -4.7
	2	1440			1020		
	3	1420			1030		
	4	1360			1090		

Appendix E. (Cont'd)

Run	Sensor	E_T (cm^2)	Mean (cm^2)	Range (%)	E_{pl} (cm^2)	Mean (cm^2)	Range (%)
SAS 1-31 Mar 74-02	1	2520	2400	+5.0, -2.5	1380	1190	+16.0,-11.8
	2	2330			1130		
	3	-			-		
	4	2340			1050		
SAS 1-01 Apr 74-01	1	2120	2140	+2.8, -2.3	1730	1610	+7.5,-13.0
	2	2090			1400		
	3	-			-		
	4	2200			1690		
SAS 1-01 Apr 74-02	1	1720	1680	+8.3,-10.1	1520	1480	+3.4, -6.8
	2	1820			1530		
	3	-			-		
	4	1510			1380		
SAS 1-01 Apr 74-03	1	1550	1590	+3.1, -2.5	899	918	+1.3, -2.1
	2	1640			930		
	3	-			-		
	4	1590			925		
SAS 1-01 Apr 74-04	1	1620	1660	+9.0, -8.4	1150	1160	+6.0, -7.8
	2	1680			1190		
	3	1810			1230		
	4	1520			1070		
SAS 1-02 Apr 74-01	1	1520	1530	+2.6, -1.3	934	942	+5.7, -3.4
	2	1510			910		
	3	1570			926		
	4	1520			996		

Appendix E. (Cont'd)

Run	Sensor	E_T (cm^2)	Mean (cm^2)	Range (%)	E_{pl} (cm^2)	Mean (cm^2)	Range (%)
SAS 1-03 Apr 74-01	1	1820	1900	+9.5, -5.8	1790	1790	+3.9, -2.2
	2	1910			1770		
	3	2080			1860		
	4	1790			1750		
SAS 1-03 Apr 74-03	1	2020	2500	+26.4,-19.2	1820	2380	+30.7,-23.5
	2	2460			2400		
	3	3160			3110		
	4	2350			2190		
SAS 1-03 Apr 74-04	1	1340	1340	+4.3, -6.7	624	636	+8.6, -9.6
	2	1400			575		
	3	1360			691		
	4	1250			654		
SAS 1-04 Apr 74-01	1	1240	1140	+8.8, -7.0	626	578	+8.3, -5.4
	2	1170			553		
	3	1060			547		
	4	1080			586		
SAS 1-04 Apr 74-02	1	1020	936	+7.0,-14.1	755	665	+13.5,-25.0
	2	1030			736		
	3	974			671		
	4	827			499		
SAS 1-05 Apr 74-01	1	517	522	+3.2, -4.8	509	521	+8.4, -6.5
	2	539			565		
	3	536			522		
	4	497			487		

Appendix E. (Cont'd)

Run	Sensor	E_T (cm^2)	Mean (cm^2)	Range (%)	E_{pl} (cm^2)	Mean (cm^2)	Range (%)
SAS 1-05 Apr 74-02	1	483	487	+7.4, -3.5	431	440	+9.3, -6.1
	2	470			413		
	3	471			438		
	4	523			481		
SAS 1-05 Apr 74-04	1	303	348	+10.6,-12.9	281	315	+7.3,-10.7
	2	335			302		
	3	385			340		
	4	367			338		
SAS 1-05 Apr 74-05	1	449	424	+5.9, -4.2	301	291	+4.1, -6.2
	2	422			286		
	3	420			303		
	4	406			273		
SAS 1-07 Apr 74-02	1	495	522	+3.7, -5.2	225	233	+5.2, -5.6
	2	542			214		
	3	542			245		
	4	507			220		
SAS 1-07 Apr 74-03	1	1270	1220	+4.1, -5.7	1100	1030	+6.8, -3.2
	2	1260			1010		
	3	1190			997		
	4	1150			1010		
SAS 1-12 Apr 74-03	1	419	442	+7.7, -5.2	344	355	+8.5, -8.5
	2	476			385		
	3	447			325		
	4	424			367		

Appendix E. (Cont'd)

Run	Sensor	E_T (cm^2)	Mean (cm^2)	Range (%)	E_{pl} (cm^2)	Mean (cm^2)	Range (%)
SAS 1-13 Apr 74-01	1	656	612	+6.7, -6.4	634	594	+6.3, -6.9
	2	645			623		
	3	573			555		
	4	575			555		
SAS 1-13 Apr 74-02	1	551	541	+4.4, -4.8	467	451	+6.4, -7.3
	2	565			480		
	3	531			440		
	4	515			418		
SAS 1-13 Apr 74-03	1	430	443	+2.9, -2.9	343	330	+3.9, -7.2
	2	435			341		
	3	456			306		
	4	451			330		
SAS 1-13 Apr 74-04	1	366	383	+4.2, -4.4	241	236	+7.6,-10.6
	2	392			254		
	3	399			239		
	4	374			211		
SAS 1-14 Apr 74-01	1	336	338	+6.2, -5.9	154	177	+7.3,-13.0
	2	359			184		
	3	318			180		
	4	338			190		
SAS 1-14 Apr 74-03	1	193	247	+8.5,-21.8	93.7	126	+20.6,-25.4
	2	268			152		
	3	267			149		
	4	259			109		

Appendix E. (Cont'd)

Run	Sensor	E_T (cm^2)	Mean (cm^2)	Range (%)	E_{pl} (cm^2)	Mean (cm^2)	Range (%)
SAS 1-14 Apr 74-04	1	-	229	+3.5, -5.2	-	212	±4.2
	2	232			212		
	3	237			221		
	4	217			204		
SAS 1-15 Apr 74-01	1	330	266	+24.1,-21.0	109	168	+20.2,-35.1
	2	270			202		
	3	253			184		
	4	210			176		
SAS 1-15 Apr 74-03	1	201	186	+13.4,-18.8	190	176	+13.6,-17.6
	2	211			200		
	3	182			167		
	4	151			145		
SAS 1-15 Apr 74-04	1	221	216	+6.0,-11.1	197	194	+7.2,-10.3
	2	229			208		
	3	220			195		
	4	192			174		
SAS 1-16 Apr 74-01	1	368	402	+15.9, -8.5	168	205	+16.1,-18.0
	2	394			200		
	3	466			238		
	4	381			213		
SAS 1-16 Apr 74-02	1	753	744	+3.2, -7.0	483	493	+11.4, -5.7
	2	768			549		
	3	692			475		
	4	764			465		

Appendix E. (Cont'd)

Run	Sensor	E_T (cm^2)	Mean (cm^2)	Range (%)	E_{pl} (cm^2)	Mean (cm^2)	Range (%)
SAS 1-16 Apr 74-03	1	772	761	+1.4, -1.2	509	525	+2.3, -3.0
	2	752			530		
	3	-			-		
	4	760			537		
SAS 1-16 Apr 74-04	1	806	764	+5.5, -8.8	620	590	+5.1, -6.6
	2	788			599		
	3	-			-		
	4	697			551		
SAS 1-17 Apr 74-01	1	307	366	+16.4,-16.1	149	184	+10.1,-19.0
	2	360			198		
	3	426			203		
	4	368			187		
SAS 1-17 Apr 74-02	1	253	259	+6.9, -8.9	186	181	+2.8, -6.1
	2	269			183		
	3	277			186		
	4	236			170		
SAS 1-17 Apr 74-03	1	261	237	+10.1,-14.3	197	185	+7.6,-11.9
	2	245			199		
	3	237			181		
	4	203			163		
SAS 1-18 Apr 74-01	1	209	221	+13.6, -8.1	97.0	104	+26.9,-11.6
	2	222			96.6		
	3	251			91.9		
	4	203			132		

Appendix E. (Cont'd)

Run	Sensor	E_T (cm^2)	Mean (cm^2)	Range (%)	E_{pl} (cm^2)	Mean (cm^2)	Range (%)
SAS 1-18 Apr 74-02	1	313	317	+3.8,-11.4	185	186	+11.8,-10.2
	2	320			185		
	3	355			208		
	4	281			167		
SAS 1-18 Apr 74-03	1	307	318	+6.3, -6.9	98.4	118	+17.8,-16.6
	2	296			105		
	3	338			139		
	4	331			128		
SAS 1-18 Apr 74-04	1	876	812	+8.0, -8.3	595	576	+16.1,-14.1
	2	877			669		
	3	751			495		
	4	745			546		
SAS 1-19 Apr 74-01	1	1310	1300	+5.4, -6.2	837	890	+16.8,-10.8
	2	1370			1040		
	3	-			-		
	4	1220			794		
SAS 1-19 Apr 74-01	1	711	651	+9.2,-10.4	495	424	+16.7, -9.0
	2	660			386		
	3	-			-		
	4	583			391		
SAS 1-20 Apr 74-01	1	643	625	+7.2,-10.4	630	593	+6.2, -9.4
	2	670			611		
	3	-			-		
	4	561			537		

Appendix E. (Cont'd)

Run	Sensor	E_T (cm^2)	Mean (cm^2)	Range (%)	E_{pl} (cm^2)	Mean (cm^2)	Range (%)
SAS 1-20 Apr 74-02	1	501	498	+2.2, -2.8	362	354	+2.3, -4.2
	2	484			339		
	3	-			-		
	4	509			362		
SAS 1-20 Apr 74-03	1	378	373	+6.4, -7.8	325	324	+10.4,-10.4
	2	397			358		
	3	-			-		
	4	344			290		
SAS 1-20 Apr 74-04	1	577	564	+3.7, -5.9	506	490	+3.3, -4.9
	2	585			499		
	3	-			-		
	4	531			466		
SAS 1-21 Apr 74-01	1	385	406	+7.1, -8.6	294	287	+7.0, -8.0
	2	371			264		
	3	431			283		
	4	435			307		
SAS 1-21 Apr 74-02	1	335	343	+2.3, -2.3	247	252	+10.7, -6.7
	2	351			235		
	3	-			-		
	4	342			275		
SAS 1-21 Apr 74-03	1	349	328	+6.1,-10.1	155	147	+5.4, -4.8
	2	334			140		
	3	332			144		
	4	295			150		

Appendix E. (Cont'd)

Run	Sensor	E_T (cm^2)	Mean (cm^2)	Range (%)	E_{pl} (cm^2)	Mean (cm^2)	Range (%)
SAS 1-21 Apr 74-04	1	413	434	+4.6, -4.8	319	317	+1.8, -2.5
	2	436			323		
	3	-			-		
	4	454			309		
SAS 1-22 Apr 74-01	1	259	266	+7.9, -2.3	135	138	+13.8,-15.3
	2	269			117		
	3	287			157		
	4	250			142		
SAS 1-22 Apr 74-02	1	243	245	+3.3, -4.1	139	141	+5.7, -8.5
	2	250			129		
	3	253			148		
	4	235			149		
SAS 1-22 Apr 74-03	1	268	262	+5.3,-10.7	122	118	+3.3, -2.5
	2	276			119		
	3	268			116		
	4	234			115		
SAS 1-22 Apr 74-04	1	402	369	+8.9,-13.0	254	234	+8.5, -7.3
	2	383			232		
	3	-			-		
	4	321			217		
SAS 1-23 Apr 74-01	1	262	253	+3.6, -4.7	127	122	+4.1, -4.9
	2	241			116		
	3	-			-		
	4	257			122		

Appendix E. (Cont'd)

Run	Sensor	E_T (cm^2)	Mean (cm^2)	Range (%)	E_{pl} (cm^2)	Mean (cm^2)	Range (%)
SAS 1-23 Apr 74-02	1	317	302	+5.0, -5.0	147	138	+6.5, -4.3
	2	303			140		
	3	300			133		
	4	287			132		
SAS 1-23 Apr 74-04	1	375	356	+8.7, -8.7	340	327	+3.9, -4.2
	2	368			327		
	3	-			-		
	4	325			313		
SAS 1-24 Apr 74-01	1	269	262	+2.8, -4.2	257	246	+4.5, -4.9
	2	265			248		
	3	-			-		
	4	251			234		
SAS 1-24 Apr 74-02	1	278	287	+4.5, -3.1	268	275	+6.5, -4.0
	2	282			268		
	3	-			-		
	4	300			293		
SAS 1-25 Apr 74-03	1	795	839	+4.4, -5.5	418	439	+3.0, -4.0
	2	876			452		
	3	-			-		
	4	845			448		
SAS 1-25 Apr 74-04	1	794	806	+8.3,-14.3	252	275	+16.0,-8.4
	2	867			266		
	3	873			319		
	4	691			266		

Appendix E. (Cont'd)

Run	Sensor	E_T (cm^2)	Mean (cm^2)	Range (%)	E_{pl} (cm^2)	Mean (cm^2)	Range (%)
SAS 1-26 Apr 74-01	1	842	839	+1.7, -2.0	755	810	+5.3, -7.0
	2	853			853		
	3	-			-		
	4	822			822		
SAS 1-26 Apr 74-02	1	803	753	+6.6,-11.6	644	584	+10.3, -6.8
	2	803			571		
	3	741			577		
	4	666			544		
SAS 1-26 Apr 74-05	1	479	467	+2.6, -2.6	328	318	+3.1, -3.5
	2	467			320		
	3	-			-		
	4	455			307		
SAS 1-27 Apr 74-01	1	622	593	+12.5,-17.4	578	531	+8.8,-19.6
	2	667			588		
	3	-			-		
	4	490			427		
SAS 1-27 Apr 74-02	1	252	244	+3.3, -6.1	98.0	93.5	+4.8, -7.4
	2	252			95.9		
	3	-			-		
	4	229			86.6		
SAS 1-27 Apr 74-03	1	234	222	+5.4, -8.1	186	167	+11.3, -8.9
	2	228			164		
	3	-			-		
	4	204			152		

Appendix E. (Cont'd)

Run	Sensor	E_T (cm^2)	Mean (cm^2)	Range (%)	E_{pl} (cm^2)	Mean (cm^2)	Range (%)
SAS 1-27 Apr 74-04	1	390	383	+1.8, -2.3	325	293	+9.6, -15.6
	2	374			307		
	3	-			-		
	4	386			247		
SAS 1-28 Apr 74-01	1	541	526	+2.9, -2.7	411	411	+6.1, -5.8
	2	525			387		
	3	-			-		
	4	512			436		
SAS 1-28 Apr 74-02	1	424	431	+1.2, -1.6	286	298	+7.4, -4.0
	2	436			320		
	3	-			-		
	4	434			288		
SAS 1-28 Apr 74-04	1	514	480	+7.1, -13.1	449	428	+10.0, -15.4
	2	508			471		
	3	-			-		
	4	417			362		
SAS 1-29 Apr 74-01	1	515	533	+9.8, -6.4	353	384	+8.3, -8.1
	2	534			383		
	3	583			416		
	4	499			386		
SAS 1-29 Apr 74-03	1	325	323	+4.0, -7.7	200	188	+6.4, -5.9
	2	336			189		
	3	333			187		
	4	298			177		

Appendix E. (Cont'd)

Run	Sensor	E_T (cm^2)	Mean (cm^2)	Range (%)	E_{p1} (cm^2)	Mean (cm^2)	Range (%)
SAS 1-29 Apr 74-04	1	250	256	+7.8, -5.9	142	162	+10.5,-12.3
	2	239			151		
	3	276			176		
	4	258			179		
SAS 1-30 Apr 74-01	1	290	321	+16.8, -9.7	203	216	+10.2,-10.6
	2	308			238		
	3	375			299		
	4	312			193		
SAS 1-30 Apr 74-02	1	204	189	+7.9, -7.4	150	131	+14.5, -6.1
	2	191			124		
	3	187			123		
	4	175			127		
SAS 1-30 Apr 74-03	1	384	356	+7.9, -6.2	258	250	+3.2, -8.4
	2	346			229		
	3	360			255		
	4	334			256		
SAS 1-30 Apr 74-04	1	323	352	+7.7, -8.2	192	182	+5.4, -8.8
	2	369			178		
	3	379			166		
	4	337			190		
SAS 1-01 May 74-01	1	535	563	+5.9, -5.0	411	411	+5.6, -4.6
	2	574			434		
	3	596			419		
	4	548			381		

Appendix E. (Cont'd)

Run	Sensor	E_T (cm^2)	Mean (cm^2)	Range (%)	E_{pl} (cm^2)	Mean (cm^2)	Range (%)
SAS 1-01 May 74-02	1	273	268	+5.2, -6.3	126	100	+26.0,-17.2
	2	282			95.4		
	3	265			96.9		
	4	251			82.8		
SAS 1-01 May 74-03	1	319	274	+16.4,-24.1	287	241	+19.0,-30.7
	2	298			272		
	3	272			238		
	4	208			167		
SAS 1-01 May 74-04	1	217	206	+8.3,-13.6	211	195	+8.2,-12.8
	2	223			210		
	3	207			187		
	4	178			170		
SAS 1-02 May 74-01	1	483	478	+8.4,-10.3	269	261	+17.6,-19.2
	2	482			258		
	3	518			307		
	4	429			211		
SAS 1-02 May 74-02	1	239	287	+18.1,-16.7	161	191	+22.5,-20.9
	2	319			234		
	3	251			151		
	4	339			219		
SAS 1-02 May 74-03	1	244	241	+5.8,-10.0	100	96.0	+4.2,-10.6
	2	247			98.3		
	3	255			100		
	4	216			85.8		

Appendix E. (Cont'd)

Run	Sensor	E_T (cm^2)	Mean (cm^2)	Range (%)	E_{pl} (cm^2)	Mean (cm^2)	Range (%)
SAS 1-02 May 74-04	1	349	323	+8.0, -4.3	189	175	+8.0, -7.4
	2	319			182		
	3	314			162		
	4	309			167		
SAS 1-03 May 74-01	1	307	311	+11.6, -8.7	138	116	+19.8,-27.6
	2	305			139		
	3	347			104		
	4	284			84.4		
SAS 1-03 May 74-02	1	665	617	+7.2, -9.4	419	422	+3.8, -2.8
	2	624			420		
	3	619			438		
	4	559			410		
SAS 1-03 May 74-03	1	576	567	+4.8, -9.7	388	400	+6.3, -6.8
	2	586			425		
	3	594			413		
	4	512			373		
SAS 1-04 May 74-01	1	503	499	+1.8, -3.6	481	447	+7.6,-13.1
	2	508			474		
	3	504			388		
	4	481			444		
SAS 1-04 May 74-03	1	476	482	+11.6,-12.4	251	243	+10.3,-11.1
	2	491			268		
	3	538			237		
	4	422			216		

Appendix E. (Cont'd)

Run	Sensor	E_T (cm^2)	Mean (cm^2)	Range (%)	E_{pl} (cm^2)	Mean (cm^2)	Range (%)
SAS 1-04 May 74-04	1	334	323	+3.4, -7.7	212	211	+5.7, -5.7
	2	326			209		
	3	333			223		
	4	298			199		
SAS 1-05 May 74-01	1	337	351	+8.5, -5.1	146	170	+19.4,-14.1
	2	353			157		
	3	381			203		
	4	333			175		
SAS 1-05 May 74-02	1	237	256	+5.1, -8.2	84.6	100	+16.0,-15.4
	2	260			86.3		
	3	269			113		
	4	258			116		
SAS 1-05 May 74-03	1	282	303	+10.2, -6.9	108	104	+14.4,-23.1
	2	298			110		
	3	334			119		
	4	298			80.0		
SAS 1-05 May 74-04	1	236	234	+6.4, -4.7	153	146	+15.8,-15.8
	2	250			169		
	3	231			123		
	4	224			137		
SAS 1-06 May 74-01	1	349	334	+5.4, -9.6	197	154	+27.9,-24.0
	2	352			159		
	3	334			142		
	4	302			117		

Appendix E. (Cont'd)

Run	Sensor	E_T (cm^2)	Mean (cm^2)	Range (%)	E_{p1} (cm^2)	Mean (cm^2)	Range (%)
SAS 1-06 May 74-02	1	217	240	+12.9, -9.6	102	123	+17.9,-17.1
	2	229			110		
	3	271			145		
	4	244			136		
SAS 1-07 May 74-01	1	254	282	+15.6, -9.9	155	167	+17.4,-10.2
	2	278			150		
	3	326			196		
	4	269			167		
SAS 1-07 May 74-04	1	198	175	+7.4, -6.3	136	124	+9.7,-15.3
	2	187			127		
	3	172			127		
	4	144			105		
SAS 1-08 May 74-03	1	171	165	+13.6, -5.5	117	114	±11.4
	2	156			101		
	3	162			112		
	4	169			127		
SAS 1-08 May 74-04	1	168	171	+4.7, -6.4	122	134	+5.2, -8.9
	2	179			138		
	3	175			141		
	4	160			136		
SAS 1-09 May 74-01	1	236	213	+10.8,-16.0	224	199	+12.6,-16.6
	2	233			210		
	3	203			194		
	4	179			166		

Appendix E. (Cont'd)

Run	Sensor	E_T (cm^2)	Mean (cm^2)	Range (%)	E_{pl} (cm^2)	Mean (cm^2)	Range (%)
SAS 1-09 May 74-02	1	242	249	+9.6, -9.2	88.6	96.4	+14.1, -8.1
	2	256			96.3		
	3	273			110		
	4	226			90.6		
SAS 1-09 May 74-03	1	329	318	+5.7, -8.1	316	305	+7.2, -8.2
	2	313			298		
	3	339			327		
	4	292			280		
SAS 1-09 May 74-04	1	537	512	+9.9,-17.8	492	470	+11.4,-19.9
	2	563			524		
	3	527			478		
	4	421			387		
SAS 1-10 May 74-01	1	399	457	+7.2,-12.7	320	376	+9.3,-14.9
	2	470			367		
	3	484			411		
	4	476			405		
SAS 1-10 May 74-04	1	480	471	+9.9,-13.8	213	231	+17.7,-11.7
	2	518			272		
	3	480			234		
	4	406			204		
SAS 1-11 May 74-01	1	748	731	+4.5, -9.7	411	436	+15.6,-14.0
	2	764			504		
	3	750			452		
	4	660			375		

Appendix E. (Cont'd)

Run	Sensor	E_T (cm^2)	Mean (cm^2)	Range (%)	E_{pl} (cm^2)	Mean (cm^2)	Range (%)
SAS 1-11 May 74-02	1	672	678	+8.6, -9.8	312	345	+14.8,-11.0
	2	691			307		
	3	736			396		
	4	611			364		
SAS 1-11 May 74-04	1	509	525	+5.5, -3.0	126	195	+16.9,-35.3
	2	515			193		
	3	554			231		
	4	521			288		
SAS 1-12 May 74-01	1	469	487	±3.7	270	258	+4.7,-12.4
	2	495			267		
	3	505			269		
	4	480			226		
SAS 1-12 May 74-02	1	588	594	+4.7, -5.5	323	316	+4.4, -5.4
	2	603			318		
	3	622			330		
	4	561			291		
SAS 1-12 May 74-03	1	416	414	+4.8, -6.5	316	304	+10.2,-16.8
	2	419			311		
	3	434			335		
	4	387			253		
SAS 1-12 May 74-04	1	547	554	+4.2, -6.9	437	421	+20.4,-17.8
	2	576			507		
	3	577			392		
	4	516			346		

Appendix E. (Cont'd)

Run	Sensor	E_T (cm^2)	Mean (cm^2)	Range (%)	E_{pl} (cm^2)	Mean (cm^2)	Range (%)
SAS 1-13 May 74-01	1	569	567	+9.9,-11.6	458	441	+9.5,-18.6
	2	623			465		
	3	574			482		
	4	501			359		
SAS 1-13 May 74-02	1	741	736	+5.0, -5.9	310	358	+9.5,-13.4
	2	773			357		
	3	736			373		
	4	692			392		
SAS 1-13 May 74-03	1	866	805	+7.6, -4.3	431	387	+12.7,-22.2
	2	778			436		
	3	802			378		
	4	770			301		
SAS 1-13 May 74-04	1	-	1010	+8.9, -6.9	-	499	+15.4,-11.6
	2	1100			576		
	3	983			441		
	4	940			480		
SAS 1-14 May 74-02	1	-	894	+8.7, -5.0	-	476	+3.4, -6.1
	2	861			490		
	3	972			492		
	4	849			447		
SAS 1-14 May 74-05	1	-	736	+4.2, -2.9	-	482	+8.1, -5.2
	2	767			521		
	3	715			457		
	4	725			468		

Appendix E. (Cont'd)

Run	Sensor	E_T (cm^2)	Mean (cm^2)	Range (%)	E_{pl} (cm^2)	Mean (cm^2)	Range (%)
SAS 1-14 May 74-06	1	-	597	+3.7, -3.2	-	251	+5.6, -3.2
	2	595			245		
	3	619			265		
	4	578			243		
SAS 1-15 May 74-02	1	-	967	±1.0	-	389	±7.1
	2	972			412		
	3	-			-		
	4	962			363		
SAS 1-16 May 74-01	1	746	778	+2.4, -4.1	442	537	+12.3,-17.7
	2	794			544		
	3	797			560		
	4	773			603		
SAS 1-16 May 73-02	1	1010	968	+4.3, -9.4	529	509	+8.1,-12.0
	2	1010			550		
	3	973			509		
	4	877			448		
SAS 1-16 May 74-04	1	656	642	+4.5, -5.8	410	380	±6.3
	2	671			407		
	3	637			360		
	4	605			344		
SAS 1-17 May 74-01	1	547	574	+8.5, -5.4	366	366	+13.4, -7.7
	2	581			343		
	3	623			415		
	4	543			338		

Appendix E. (Cont'd)

Run	Sensor	E_T (cm^2)	Mean (cm^2)	Range (%)	E_{pl} (cm^2)	Mean (cm^2)	Range (%)
SAS 1-17 May 73-03	1	943	1040	+10.6, -6.3	662	762	+13.4,-13.1
	2	1110			832		
	3	1150			864		
	4	974			689		
SAS 1-17 May 74-04	1	1210	1250	+6.4, -8.8	841	932	+11.5, -9.8
	2	1330			1040		
	3	1310			994		
	4	1140			854		
SAS 1-18 May 74-01	1	1720	1720	+11.6, -5.8	1450	1440	+9.0, -7.6
	2	1920			1570		
	3	1630			1330		
	4	1620			1440		
SAS 1-18 May 74-02	1	2780	2750	+7.3, -9.5	2390	2350	±7.2
	2	2950			2520		
	3	2760			2310		
	4	2490			2180		
SAS 1-18 May 74-03	1	2840	2620	+8.4,-11.5	2670	2380	+12.2,-13.4
	2	2750			2470		
	3	2590			2300		
	4	2320			2060		
SAS 1-19 May 74-01	1	2050	2070	+10.1,-11.1	1960	2000	+12.5, -9.5
	2	2100			1990		
	3	2280			2250		
	4	1840			1810		

Appendix E. (Cont'd)

Run	Sensor	E_T (cm^2)	Mean (cm^2)	Range (%)	E_{pl} (cm^2)	Mean (cm^2)	Range (%)
SAS 1-19 May 74-02	1	1350	1420	+9.2, -4.9	1300	1360	+5.9, -4.4
	2	1550			1440		
	3	1400			1360		
	4	1370			1330		
SAS 1-19 May 74-03	1	1120	1100	+4.5, -5.5	1070	1080	±4.6
	2	1150			1130		
	3	1100			1090		
	4	1040			1030		
SAS 1-19 May 74-04	1	898	755	+15.9,-17.9	869	720	+20.7,-21.4
	2	801			773		
	3	699			673		
	4	620			566		
SAS 1-20 May 74-01	1	841	840	+6.8,-10.7	800	794	+8.3,-12.3
	2	897			860		
	3	870			820		
	4	750			696		
SAS 1-20 May 74-04	1	475	463	+4.8, -7.1	341	333	+5.7, -9.3
	2	461			352		
	3	485			335		
	4	430			302		
SAS 1-21 May 74-02	1	474	462	+4.8, -6.9	411	400	+5.3, -7.3
	2	460			396		
	3	484			421		
	4	430			371		

Appendix E. (Cont'd)

Run	Sensor	E_T (cm^2)	Mean (cm^2)	Range (%)	E_{pl} (cm^2)	Mean (cm^2)	Range (%)
SAS 1-25 May 74-02	1	292	283	+6.4, -9.9	177	170	+9.4,-14.7
	2	282			172		
	3	301			186		
	4	255			145		
SAS 1-25 May 74-03	1	322	318	+4.4, -8.5	127	142	+8.5,-10.6
	2	325			145		
	3	332			154		
	4	291			140		
SAS 1-25 May 74-02	1	356	355	+6.5,-10.4	214	207	+5.3,-10.1
	2	378			218		
	3	367			210		
	4	318			186		
SAS 1-26 May 74-01	1	626	609	+7.2, -5.6	297	296	+8.1, -8.8
	2	653			320		
	3	580			270		
	4	575			296		
SAS 1-28 May 74-04	1	238	235	+5.5, -7.2	103	90.6	+13.7,-17.4
	2	237			100		
	3	248			84.7		
	4	218			74.8		
SAS 1-29 May 74-01	1	257	264	+6.4, -2.3	119	124	+8.1, -4.0
	2	261			122		
	3	281			134		
	4	258			120		

Appendix E. (Cont'd)

Definition of Terms:

E_T:	The total energy of the spectrum given for each sensor.
E_{p1}:	The energy of the major peak in the spectrum for each sensor.
Range:	The maximum deviations of the data from the mean.

APPENDIX F

TABULAR COMPARISONS OF SENSORS

Table F-1. Comparisons of the energy density values, total energy, and peak energy obtained from the frequency spectra of the four pressure sensors. The terms are defined at the end of the table.

Run	R_B(%)	R_T(%)	R_p(%)
SAS 1-17 May 73-02	34.8	11.8	10.8
SAS 1-18 May 73-01	64.3	20.9	4.4
SAS 1-18 May 73-03	63.4	22.5	8.7
SAS 1-18 May 73-04	75.5	29.4	13.2
SAS 1-19 May 73-01	57.6	17.7	9.1
SAS 1-19 May 73-02	119.0	65.6	16.4
SAS 1-19 May 73-04	54.0	16.7	10.3
SAS 1-20 May 73-01	94.0	26.9	10.9
SAS 1-20 May 73-02	81.7	34.4	11.8
SAS 1-20 May 73-03	66.5	23.3	7.3
SAS 1-20 May 73-04	65.3	47.5	7.3
SAS 1-21 May 73-01	69.4	22.0	14.1
SAS 1-21 May 73-03	61.6	25.2	14.8
Average	69.8	28.0	10.7
SAS 1-09 Feb 74-02	72.9	10.8	9.2
SAS 1-09 Feb 74-03	77.5	14.8	10.9
SAS 1-10 Feb 74-01	53.5	12.6	9.3
SAS 1-10 Feb 74-04	70.1	21.6	17.1
SAS 1-11 Feb 74-02	51.0	7.5	8.7
SAS 1-11 Feb 74-03	59.1	11.8	13.7
SAS 1-11 Feb 74-04	56.4	10.3	12.7
SAS 1-12 Feb 74-01	49.1	12.1	11.2
SAS 1-12 Feb 74-02	56.8	3.6	6.5
SAS 1-26 Feb 74-02	50.9	26.4	33.0
SAS 1-27 Feb 74-02	61.4	7.2	14.2
SAS 1-27 Feb 74-04	54.6	24.9	15.6
SAS 1-28 Feb 74-01	53.8	14.7	11.9
SAS 1-11 Feb 74-01	50.6	7.2	9.6
Average	58.4	13.3	13.1

Definition of Terms:

Define $S_i(n\Delta f)$ as the energy density in $cm^2/\Delta f$ of the i^{th} sensor at frequency equal to $n\Delta f$, where n is the band number and Δf the resolution of the grouped frequency band.

Definition of terms: (Cont'd)

R_B: The mean range of the energy density values of the spectra of the four sensors averaged over the first 25 frequency bands:

$$R_B(\%) = \sum_{n=1}^{24} \frac{S_m(n\Delta f) - S_\ell(n\Delta f)}{\bar{S}(n\Delta f)} \times \frac{100}{24} ,$$

where m = sensor with maximum energy density frequency band n, ℓ = sensor with minimum energy density in frequency band n, and $\bar{S}(n\Delta f)$ is the average of the values of the four sensors.

R_T: The range in the total energy of the frequency spectra of the four pressure sensors. The total energy is defined as the sum area under the first 25 frequency bands.

R_p: The range in the energy of the dominant spectral peak of the frequency spectra of the four pressure sensors. The method of obtaining peak energy and bandwidth is discussed in Appendix A.

Table F-2. A comparison of the characteristic parameters of the wave spectra measured with a pressure sensor array with visibly observed wave parameters.

SAS Run and Date	$E_T(cm^2)$	T(sec)	$E_p(cm^2)$	BW(Hz)	H_b (cm)	α_b Degrees	T_v(sec)	$(H_b)_v$ (cm)	α_v Degrees
SAS-1-13 Feb 73-02	1720	12.3	1220	.107	178	0°	8.0	240	0°
		6.4	452	.110	91				
SAS-1-14 Feb 73-02	1860	14.2	1640	.143	225	1°N	14.0	210	0°
		6.4	103		60	1°N			
SAS-1-20 Feb 73-03	1330	16.8	1130	.089	185	0°	15.0	190	0°
		8.8	135	.043	75	0°			
		5.9	38	.043	42				
		5.0	9.3	.021	22				
SAS-1-21 Feb 73-02	790	16.8	722	.111	191	0°	14.2	180	0°
		6.9	12	.021	27	0°			
		5.6	15	.038	28				
SAS-1-22 Feb 73-02	584	14.2	523	.136	137	1°S	13.0	120	0°
		5.0	7.5	.068	19	1°N			
SAS-1-23 Feb 73-02	163	12.3	134	.097	95	1°N	9.0	90	0°
		6.9	6.8	.043	24	3°S			
		4.5	4.7	.048	15				
SAS-1-10 Apr 73-03	160	12.3	107	.062	85		13.0	90	5°N
		9.8	35	.056	53				
		6.8	5	.048	21				
		4.3	3	.035	12				
SAS-1-12 Apr 73-03	740	14.2	302	.064	135		11.0	120	0°
		6.4	193	.070	69				

Table F-2. (Cont'd)

SAS Run and Date	E_T (cm^2)	T(sec)	E_p (cm^2)	BW(Hz)	H_b(cm)	α_b Degrees	T_v(sec)	$(H_b)_v$ (cm)	α_v Degrees
SAS-1-13 Apr 73-03	1081	14.2	283	.067	131		8.0	140	0°
		5.9	368	.075	82				
		4.1	135	.030	46				
SAS-1-16 Apr 73-03	564	16.8	101	.048	91		11.0	160	0°
		6.9	293	.086	84				
SAS-1-17 Apr 73-03	679	12.3	208	.056	90		12.0	150	5°N
		9.8	69	.026	57				
		6.4	154	.047	65				
		5.3	133	.054	54				
SAS-1-16 May 73-02	172	14.2	19	.029	49	1°S	10.5	100	0°
		9.8	131	.110	79	2°N			
		4.3	15	.059	22	0°			
SAS-1-17 May 73-02	301	10.9	270	.140	101	2°N	11.0	80	5°N
		4.5	21	.059	26	1°N			
SAS-1-18 May 73-03	292	12.3	186	.089	86	0°	8.5	120	0°
		4.5	60	.059	37	3°N			
SAS-1-21 May 73-03	314	14.2	89.3	.064	82	1°S	9.0	100	5°N
		5.6	120	.078	55				
SAS-1-22 May 73-03	262	10.9	175	.093	87	2°N	10.0	160	5°N
		6.0	62.7	.061	47				
SAS-1-23 May 73-03	175	10.9	101	.125	86	2°N	9.0	110	5°N
		6.0	50.6	.050	42	10°N			

Table F-2. (Cont'd)

SAS Run and Date	E_T (cm^2)	T(sec)	E_p (cm^2)	BW(Hz)	H_b (cm)	α_b Degrees	T_v (sec)	$(H_b)_v$ (cm)	α_v Degrees
SAS-1-24 May 73-03	159	14.2	25	.054	53	2°S	8.5	90	5°N
		6.9	107	.122	60	3°N			
SAS-1-25 May 73-03	373	12.3	168	.082	106	1°N	12.0	160	5°N
		6.4	79	.047	52	1°N			
SAS-1-29 May 73-03	106	14.2	33.1	.059	57	1°S	8.6	80	0°
		8.8	32.3	.067	51	2°N			
SAS-1-30 May 73-03	106	14.2	38.4	.075	61	1°S	9.3	80	0°
		7.4	46	.088	49				
SAS-1-31 May 73-03	254	16.8	116	.040	92	1°S	8.0	120	5°N
		10.9	58.5	.043	66	2°N			
		7.4	38.3	.051	41				
SAS-1-01 Jun 73-02	243	16.8	96.2	.036	89	1°S	12.0	100	0°
		12.3	90.3	.056	78	2°N			
		6.4	25.3	.083	36				
SAS-1-04 Jun 73-03	182	12.3	130	.027	93	0°	8.0	80	5°N
		8.8	32.8	.126	52	3°N			
		4.3	11.9	.043	20				
SAS-1-05 Jun 73-03	198	12.3	34.7	.051	54	1°N	9.5	70	5°N
		8.8	89.5	.081	66	2°N			
SAS-1-09 Jul 73-03	187	16.8	25	.043	48	1°S	7.7	60	5°N
		8.1	137	.115	76	3°N			

Table F-2. (Cont'd)

SAS Run and Date	E_T(cm^2)	T(sec)	E_p(cm^2)	BW(Hz)	H_b(cm)	α_b Degrees	T_v(sec)	$(H_b)_v$ (cm)	α_v Degrees
SAS-1-10 Jul 73-02	268	14.2	24.9	.039	52	1°S	9.0	60	0°
		8.8	174	.093	85	3°N			
		4.8	33.4	.036	31				
SAS-1-11 Jul 73-02	202	14.2	23.6	.043	51	1°S	8.0	90	0°
		9.8	120	.094	75	2°N			
		5.3	33.5	.064	74				
SAS-1-16 Jul 73-03	269	14.2	27.6	.035	55	1°S	6.7	80	5°N
		9.8	120	.070	75	2°N			
		5.9	86	.083	51				
SAS-1-19 Jul 73-03	259	16.8	140	.070	101	1°S	7.0	80	5°N
		5.9	98	.126	55	4°N			
SAS-1-20 Jul 73-03	390	16.8	151	.061	99	1°S	7.0	90	5°N
		6.9	195	.139	72	2°N			
SAS-1-23 Jul 73-03	466	14.2	58.7	.048	71	1°S	11.0	120	5°S
		9.8	241	.075	99	3°N			5°N
		5.6	123	.075	55				
SAS-1-24 Jul 73-02	680	16.8	64.3	.037	78	2°S	10.5	150	5°N
		8.1	625	.097	119	4°N			
SAS-1-30 Jul 73-02	268	14.2	162	.061	99	2°S	14.0	100	5°S
		8.8	30	.047	49	2°N	9.0		5°N
		5.3	64.1	.093	42				
SAS-1-01 Aug 73-03	149	14.2	42.7	.071	64	1°S	8.0	80	5°S
		6.9	93.9	.143	56	4°N			

Table F-2. (Cont'd)

SAS Run and Date	E_T (cm^2)	T(sec)	E_p (cm^2)	BW(Hz)	H_b(cm)	α_b Degrees	T_v(sec)	$(H_b)_v$ (cm)	α_v Degrees
SAS-1-02 Aug 73-03	233	14.2	44.9	.046	66	1°S	8.3	70	0°
		8.1	170	.161	74	4°N			
SAS-1-10 Aug 73-03	207	14.2	83.4	.064	80	1°S	8.0	140	5°N
		8.1	100	.153	65	4°N			
SAS-1-15 Aug 73-02	197	16.8	151	.099	105	1°S	11.5	60	5°S
		5.6	20	.113	32	3°N			
SAS-1-16 Aug 73-03	360	16.8	302	.048	128	1°S	15.0	140	5°S
		8.1	45.4	.140	47	3°N			
SAS-1-20 Aug 73-03	246	12.6	74.7	.069	71	1°S	8.0	90	5°N
		5.6	125	.083	56	4°N			
SAS-1-21 Aug 73-03	369	16.8	183	.056	109	2°S	14.0	80	5°S
		8.1	122	.068	72		8.0		5°N
SAS-1-22 Aug 73-03	764	16.8	167	.056	104	2°S	7.5	120	5°N
		7.4	342	.070	96				
		6.0	284	.099	76				
SAS-1-23 Aug 73-03	937	14.2	114	.043	86	1°S	8.0	150	0°
		8.1	556	.081	113	3°N			
		6.4	228	.075	75	1°N			
SAS-1-24 Aug 73-03	603	16.8	454	.046	65	1°S	8.3	110	0°
		8.1	386	.148	100	2°N			
SAS-1-27 Aug 73-02	208	16.8	67.7	.040	80	1°S	15.0	80	5°S
		9.8	77.7	.078	61	2°N			
		5.0	30.7	.078	36				

Table F-2. (Cont'd)

SAS Run and Date	$E_T(cm^2)$	T(sec)	$E_p(cm^2)$	BW(Hz)	$H_b(cm)$	α_b Degrees	$T_v(sec)$	$(H_b)_v$ (cm)	α_v Degrees
SAS-1-06 Sep 73-03	533	16.8	203	.043	102	1°S	7.0	90	5°N
		8.8	298	.132	97	2°N			
SAS-1-07 Sep 73-03	776	14.2	309	.059	137	2°S	9.6	110	5°N
		8.8	446	.097	112	3°N			
SAS-1-14 Sep 73-03	197	14.2	80.3	.054	70	1°S	11.4	60	0°
		10.9	88.8	.086	81	2°N			
SAS-1-17 Sep 73-03	263	16.8	112	.032	83	1°S	14.0	80	5°N
		12.3	70.3	.057	75	2°N			
		5.0	60.6	.097	40				
SAS-1-18 Sep 73-03	343	14.2	88.5	.036	73	1°S	10.0	90	0°
		9.8	75.7	.043	60	2°N			
		6.4	153	.129	65				
SAS-1-19 Sep 73-03	298	14.2	67.8	.075	64	1°S	8.6	100	0°
		6.0	140	.160	59	2°N			
SAS-1-20 Sep 73-03	346	14.2	152	.064	96	1°S	8.5	110	5°N
		9.8	34.4	.021	52	2°N			
		6.4	213	.125	72				
SAS-1-21 Sep 73-03	663	12.3	317	.072	54	1°N	8.0	150	5°N
		7.4	315	.140	92	2°N			
SAS-1-24 Sep 73-03	640	10.9	197	.067	93	2°N	8.0	150	0°
		7.4	339	.072	90	5°N			

Table F-2. (Cont'd)

SAS Run and Date	E_T (cm^2)	T(sec)	E_p (cm^2)	BW(Hz)	H_b (cm)	α_b Degrees	T_v (sec)	$(H_b)_v$ (cm)	α_v Degrees
SAS-1-02 Oct 73-03	119	16.8	23.2	.040	49	0°	8.5	60	5°S
		10.9	44.3	.067	57	1°S			
		6.4	23.8	.043	35				
SAS-1-03 Oct 73-02	294	16.8	49.8	.054	68	0°	7.5	110	5°N
		8.1	119	.072	71	2°N			
SAS-1-08 Oct 73-02	310	14.2	26.8	.043	58	1°S	8.0	50	5°N
		7.4	131	.081	67	3°N			
		5.0	123	.086	49				
SAS-1-09 Oct 73-02	917	16.8	47.9	.043	74	1°S	6.0	140	5°N
		7.4	841	.161	59	3°N			
SAS-1-10 Oct 73-03	329	14.2	69.8	.043	65	1°S	6.5	110	5°N
		6.9	241	.172	80	3°N			
SAS-1-11 Oct 73-03	213	14.2	44.8	.036	65	1°S	8.5	100	0°
		9.8	43.0	.043	59	2°N			
SAS-1-16 Oct 73-02	329	14.2	234	.064	119	1°S	8.0	90	
		5.3	77.1	.118	46	3°N			
SAS-1-19 Oct 73-03	428	16.8	257	.086	127	1°S	11.5	110	5°S
		5.0	98.1	.107	46	4°N			
SAS-1-22 Oct 73-03	397	14.2	110	.043	82	1°S	14.0	140	5°S
		10.9	270	.129	101	2°N			
SAS-1-23 Oct 73-03	167	14.2	102	.075	79	1°S	12.0	80	5°S
		7.4	43.2	.079	47	2°S			

Table F-2. (Cont'd)

SAS Run and Date	E_T(cm^2)	T(sec)	E_p(cm^2)	BW(Hz)	H_b(cm)	α_b Degrees	T_v(sec)	$(H_b)_v$ (cm)	α_v Degrees
SAS-1-24 Oct 73-02	991	12.3 7.4	516 349	.075 .097	132 92	1°N 5°N	13.0	160	5°N
SAS-1-25 Oct 73-03	447	16.8 8.8	29.7 394	.021 .177	55 105	1°S 2°N	8.0	150	5°N
SAS-1-26 Oct 73-01	232	16.8 9.8 7.4	37.6 73.3 86.0	.043 .054 .091	63 59 62	1°S 2°N	8.4	120	5°N
SAS-1-29 Oct 73-02	722	16.8 12.3 8.1	242 190 237	.032 .032 .075	111 87 88	1°S 2°N	11.5	120	5°N
SAS-1-02 Nov 73-02	411	14.2 8.1	228 79.2	.078 .070	118 58	1°S 2°N	7.5	90	5°N
SAS-1-05 Nov 73-02	528	16.8 6.0	183 156	.072 .086	107 62	0° 4°N	14.0	90	0°
SAS-1-07 Nov 73-02	534	12.3 6.0	345 105	.107 .164	117 54	1°N	10.3	110	5°N
SAS-1-08 Nov 73-03	406	14.2 9.8	39.2 202	.024 .070	61 91	1°S 2°N	9.0	90	0°
SAS-1-09 Nov 73-03	244	16.8 10.9	42.5 131	.032 .089	67 75	1°S 2°N	9.5	60	0°
SAS-1-12 Nov 73-03	867	12.3 4.1	625 218	.102 .097	142 150	1°N 9°S	10.0	120	5°N

Table F-2. (Cont's)

SAS Run and Date	$E_T(cm^2)$	T(sec)	$E_p(cm^2)$	BW(Hz)	H_b(cm)	α_b Degrees	T_v(sec)	$(H_b)_v$ (cm)	α_v Degrees
SAS-1-13 Nov 73-03	1040	9.8	820	.137	142	2°N	11.3	170	5°N
		5.6	190	.072	62				
SAS-1-03 Dec 73-02	771	9.8	730	.215	142	2°N	8.5	120	0°
SAS-1-05 Dec 73-02	258	16.8	102	.059	91	1°N	11.0	80	0°
		8.8	59.6	.046	54	2°N			
		6.4	59.1	.072	42				
SAS-1-10 Dec 73-03	299	20.5	54.6	.032	78		12.0	90	5°S
		14.2	79.7	.025	78	0°			
		10.9	77.9	.043	76	0°			
		6.9	39.8	.086	42				
SAS-1-12 Dec 73-03	449	14.2	395	.096	119	1°N	10.7	180	5°S
		4.1	13.6	.075	20	9°S			
SAS-1-18 Dec 73-03	590	14.2	203	.043	111	0°	12.0	120	5°S
		7.4	323	.150	93	5°N	8.0	120	5°N
SAS-1-19 Dec 73-03	411	12.3	319	.064	112	0°	11.6	120	5°S
		8.1	64.7	.043	56	5°N			
		5.6	37.7	.086	36				
SAS-1-21 Dec 73-02	923	36.6	19.0	.086	74		11.8	190	5°S
		14.2	865	.097	176	0°			
		6.4	22.0	.032	34	7°N			
SAS-1-02 Jan 74-03	470	16.8	335	.064	131	0°	8.0	150	5°N
		8.1	125	.107	73	5°N			

Table F-2. (Cont'd)

SAS Run and Date	$E_T(cm^2)$	T(sec)	$E_p(cm^2)$	BW(Hz)	H_b(cm)	α_b Degrees	T_v(sec)	$(H_b)_v$ (cm)	α_v Degrees
SAS-1-03 Jan 74-02	429	14.2	309	.056	137	2°S	11.8	110	5°S
		8.8	103	.135	65	1°N			
SAS-1-08 Jan 74-03	1590	8.8	1500	.246	158	1°S	9.2	180	8°S
SAS-1-09 Jan 74-02	974	8.8	938	.240	145	4°S	8.0	120	5°S
SAS-1-10 Jan 74-03	440	20.5	238	.043	120	0°	15.5	170	5°S
		9.8	184	.161	87	0°			
SAS-1-11 Jan 74-03	224	14.2	175	.075	103	0°	16.0	180	5°S
		7.4	32.0	.128	41	2°S			
SAS-1-14 Jan 74-02	931	14.2	888	.203	179	1°N	13.0	170	5°S
SAS-1-15 Jan 74-03	512	12.3	490	.128	129	1°N	12.7	150	5°S
SAS-1-28 Jan 74-03	414	14.2	308	.086	137	1°N	10.0	100	0°
		6.9	80.3	.085	52	1°N			
SAS-1-29 Jan 74-03	437	14.2	210	.062	113	0°	9.7	120	5°N
		9.8	212	.156	93	1°N			
SAS-1-30 Jan 74-03	284	14.2	113	.035	83	0°	14.5	110	5°N
		6.9	156	.145	68	4°N			
SAS-1-11 Feb 74-03	1180	14.2	1020	.043	178	2°N	13.2	160	5°N
		6.9	68.1	.064	55	2°N			
		5.0	61.6	.075	40	0°			

Table F-2. (Cont'd)

SAS Run and Date	$E_T(cm^2)$	T(sec)	$E_p(cm^2)$	BW(Hz)	H_b(cm)	α_b Degrees	T_v(sec)	$(H_b)_v$ (cm)	α_v Degrees
SAS-1-12 Feb 74-02	565	16.8	93	.021	87	2°N	15.0	170	5°N
		12.3	368	.067	121	1°N			
		5.3	77.4	.107	46				
SAS-1-26 Feb 74-02	405	14.2	221	.091	116	1°N	11.0	80	0°
		6.0	162	.129	63	4°N			
SAS-1-27 Feb 74-02	655	12.3	277	.078	104	1°N	8.5	90	0°
		6.9	357	.134	88	5°N			5°N
SAS-1-07 Mar 74-03	230	9.8	42.2	.050	58	1°N	8.0	60	0°
		6.4	73.1	.059	51				
		4.8	84.9	.064	42				
SAS-1-22 Mar 74-03	188	12.3	131	.095	93	0°	12.5	80	5°S
		5.0	23.5	.107	28	5°N			
SAS-1-26 Mar 74-02	1660	16.8	1230	.046	193	2°N	15.7	210	0°
		8.8	295	.054	97	0°	12.3	110	5°S
		6.0	78.5	.110	49				
SAS-1-27 Mar 74-03	2140	14.2	2090	.151	233	0°	15.5	210	0°
SAS-1-28 Mar 74-03	1260	12.3	1200	.155	177	1°N	15.0	210	0°
SAS-1-29 Mar 74-03	2470	36.6	30.6	.022	82				
		14.2	2370	.142	237	1°N	14.0	180	0°
SAS-1-01 Apr 74-03	1590	12.3	918	.064	177	2°N	12.1	190	0°
		8.1	595	.128	117	2°N			

Table F-2. (Cont'd)

SAS Run and Date	E_T (cm^2)	T(sec)	E_p (cm^2)	BW(Hz)	H_b(cm)	α_b Degrees	T_v(sec)	$(H_b)_v$ (cm)	α_v Degrees
SAS-1-03 Apr 74-03	2500	9.8	2380	.180	200	2°N	7.0	180	0°
SAS-1-04 Apr 74-02	963	16.8	235	.043	120	1°S	11.5	150	0°
		8.8	665	.142	130	1°N			
SAS-1-05 Apr 74-02	487	14.2	440	.140	130	0°	10.7	100	0°
SAS-1-15 Apr 74-03	186	14.2	176	.139	103	1°S	11.1	70	5°N
SAS-1-16 Apr 74-03	761	12.3	525	.912	134	2°N	8.4	120	5°N
		6.0	167	.617	64	4°N			
		4.3	54.0	.429	33				
SAS-1-17 Apr 74-03	237	10.9	185	.140	90	1°N	12.0	110	0°
		4.3	24.1	.054	26	11°S			
SAS-1-18 Apr 74-03	318	14.2	118	.054	85	1°N	14.1	110	0°
		10.9	37.7	.054	53	0°			
		5.3	111	.090	52				
SAS-1-22 Apr 74-03	262	20.5	17.0	.021	50	0°	14.5	70	5°N
		14.2	118	.043	85	0°			
		4.8	68.1	.075	40				
SAS-1-23 Apr 74-02	302	16.8	120	.032	99	1°N	15.0	60	5°N
		10.9	138	.102	77	1°N			
		4.8	23.7	.051	28				
SAS-1-24 Apr 74-02	287	14.2	275	.097	129	1°N	14.0	50	0°
SAS-1-25 Apr 74-03	839	10.9	439	.072	128	2°N	8.0	100	0°
		6.4	313	.097	76	4°N			

Table F-2. (Cont'd)

SAS Run and Date	$E_T(cm^2)$	T(sec)	$E_p(cm^2)$	BW(Hz)	$H_b(cm)$	α_b Degrees	$T_v(sec)$	$(H_b)_v$ (cm)	α_v Degrees
SAS-1-26 Apr 74-02	753	16.8	52.2	.024	74	1°S	8.5	130	5°N
		10.9	74.5	.024	74	1°N			
		7.4	584	.136	107				
SAS-1-29 Apr 74-03	323	10.9	188	.104	91	2°N	8.5	110	5°N
		6.9	80.8	.064	52	4°N			
SAS-1-30 Apr 74-03	356	12.3	94.9	.064	79	1°N	8.5	90	5°N
		5.3	250	.136	74	5°N			
SAS-1-01 May 74-03	274	12.3	241	.144	97	1°N	8.1	90	5°N
SAS-1-02 May 74-03	241	14.2	66.6	.043	71	1°S	8.7	110	5°N
		10.9	96.0	.054	84	1°N			
SAS-1-06 May 74-02	240	16.8	123	.059	100	1°S	12.0	100	5°N
		5.3	92.3	.128	48	4°N			
SAS-1-08 May 74-03	165	12.3	114	.075	87	1°N	12.0	70	5°N
		6.4	42.3	.110	44	4°N			
SAS-1-13 May 74-03	805	16.8	151	.032	88	1°S	11.5	110	5°N
		12.3	150	.036	100	1°N			
		8.8	387	.110	104				
SAS-1-16 May 74-02	968	14.2	509	.055	135	0°	11.0	140	5°N
		8.8	303	.053	98	3°N			
		6.0	126	.098	59				
SAS-1-17 May 74-03	1040	12.3	250	.063	99	1°N	8.2	170	5°N
		7.4	762	.134	117	3°N			
SAS-1-21 May 74-02	462	14.2	42.3	.054	26	1°S	8.5	90	5°N
		8.1	400	.193	101	3°N			

Definition of Terms:

E_T: The total energy in the wave spectrum obtained from an average of the records of the four pressure sensors at a 10-meter depth.

T: The period of a peak in the wave spectrum.

E_p: The averaged energy of the particular spectral peak at a 10-meter depth.

BW: The bandwidth of the spectral peak.

H_b: The height of breaking depth of a single frequency wave with the energy of the spectral peak.

α_b: The best single direction at breaking depth of the waves at the dominant period of the spectral peak. This direction is relative to the normal to the coastline at the Torrey Pines Station.

T_v: The observed period of the waves obtained by counting the period of 10 crests.

$(H_b)_v$: The observed average height of the breaking waves.

α_v: The observed breaker angle.

Table F-3. Comparisons of directional information for some November runs. The period and E_p were obtained from pressure sensor data. Also shown are the angles obtained from current meter data, accelerometer data, and visual observations.

			Directional Comparisons						Visual Observations			Shoaled Array Data	
			Array			Current-Meter		Accelerometer					
Run	Peak	Period	E_p (cm^2)	α_o	$P(\alpha_o)$	α_m	$\bar{\alpha}$	α_a	T_v (sec)	$(H_b)_v$ (cm)	α_v	H_b (cm)	α_b
SAS 1-03 Nov 73-01	1	8.8	344	0°	0.7	2°S	2°S	2°N					
	2	7.4	146	2°N	5.1	1°N	2°N	3°N					
SAS 1-03 Nov 73-02	1	12.3	118	8°S	13.0	13°S	11°S	11°S					
	2	7.4	49.8	1°N	6.8	2°N	4°N	7°S					
SAS 1-04 Nov 73-02	2	14.2	62.3	18°S	4.3	23°S	23°S	16°S					
	1	6.0	149	1°S	24.9	11°S	10°S	4°S					
SAS 1-04 Nov 73-04	2	16.8	127	26°S	0.8	33°S	32°S	14°S					
	1	7.4	356	1°N	0.8	5°S	3°S	6°N					
SAS 1-05 Nov 73-01	2	16.8	141	18°S	4.7	28°S	29°S	18°S					
	1	7.4	168	1°N	2.2	3°S	0°	7°S					
SAS 1-05 Nov 73-02	1	16.8	183	17°S	3.2	18°S	17°S	15°S	14.0	91.5	0°	101	1°S
	2	6.0	156	4°N	43.1	14°N	33°N	6°N					
SAS 1-07 Nov 73-02	1	12.3	345	5°S	4.8	15°S	16°S	19°S	10.3	107	5°S	119	3°N
	2	6.0	105	24°S	80.1	15°S	15°S	19°S					
SAS 1-08 Nov 73-01	2	14.2	99.2	24°S	0.6	26°S	25°S	23°S					
	1	9.8	104	2°N	1.5	4°S	4°S	4°S					
SAS 1-08 Nov 73-03	2	14.2	39.2	25°S	0.7	27°S	27°S	27°S					
	1	9.8	202	4°S	15.5	10°S	10°S	9°S	9.0	91.5	0°	91.5	3°N
SAS 1-09 Nov 73-01	1	14.2	85.5	18°S	2.9	20°S	20°S	21°S					
	2	8.1	60.4	8°S	53.2	6°S	7°S	9°S					
SAS 1-09 Nov 73-03	2	16.8	42.5	24°S	0.6	25°S	25°S	21°S					
	1	10.9	131	2°S	2.3	2°S	2°S	3°S	9.5	61.0	0°	82.4	4°N
SAS 1-10 Nov 73-01	2	14.2	67.5	24°S	0.8	25°S	25°S	16°S					
	1	9.8	284	4°S	14.0	4°S	4°S	5°S					
SAS 1-10 Nov 73-02	1	10.9	310	8°S	7.5	16°S	15°S	16°S					
SAS 1-10 Nov 73-04	2	14.2	53.9	24°S	1.3	27°S	26°S	21°S					
	1	9.8	238	16°S	18.8	17°S	16°S	15°S					
SAS 1-11 Nov 73-03	2	14.2	26.3	27°S	0.9	28°S	27°S	21°S					
	1	9.8	370	11°S	28.2	17°S	16°S	14°S					
SAS 1-11 Nov 73-04	1	8.8	225	26°S	59.7	17°S	16°S	16°S					
SAS 1-12 Nov 73-01	2	14.2	22.3	25°S	0.7	28°S	28°S	23°S					
	1	9.8	288	11°S	32.5	11°S	11°S	10°S	10	104	5°S	122	0°

Table F-3 (Cont'd)

				Directional Comparisons					Visual Observations			Shoaled Array Data	
				Array		Current-meter		Accelerometer					
Run	Peak	Period	$E_p(cm^2)$	α_o	$P(\alpha_o)$	α_m	$\bar{\alpha}$	α_a	T_v(sec)	$(H_b)_v$(cm)	α_v	H_b(cm)	α_b
SAS 1-12 Nov 73-03	1	12.3	625	7°S	1.8	13°S	13°S	10°S					
	2	4.1	218	29°S	61.7	2°N	1°S	6°S					
SAS 1-12 Nov 73-04	1	10.9	579	2°S	1.2	10°S	11°S	10°S					
	2	4.8	180	55°S	50.2	3°S	1°S	5°N					
SAS 1-13 Nov 73-01	1	10.9	872	1°S	0.8	10°S	8°S	6°S	11.3	171		155	9°S
	2	5.3	161	2°N	29.9	12°S	10°S	4°N					

Definition of Terms:

Peak: In a multimodal energy spectra the peaks are ordered with respect to their energies.

Period: The modal period for the defined peak of the data of all four sensors.

E_p: The energy contained in a spectral peak at a 10-meter depth, average of the data of all four sensors.

α_o: The direction of the best fit to a single wave train for the four sensor array measured from the vertical to the array. The fitting technique is based on the minimum value of $P(\alpha_o)$.

$P(\alpha_o)$: A measure of the effectiveness of the fit.

α_m: The angle where the directional spectrum obtained from orbital velocity records reached a maximum, measured from the normal to the beach, but corrected to the alignment of the array.

$\bar{\alpha}$: The mean angle obtained from the current meter data as defined in the text.

α_a: The angle obtained from accelerometer data.

T_v: The period of the waves as determined from visual observations from the cliff above the CERC station by counting the period of 10 crests.

$(H_b)_v$: The observed average height of the breaking waves.

α_v: The observed breaker angle.

H_b: The height of a single frequency wave at breaking depth which contained the energy of the spectral peak at the station.

α_b: The best single direction at breaking depth of the waves at the dominant period of the spectral peak arriving at the station from the direction α_o.

Appendix G. A tabular display of the comparisons of the directional results obtained using various sensor combinations of the array. All terms are defined below the table and are derived in Appendix H.

Run	Period (sec)	Array	α_o	P (α_o)%	$\Delta\alpha_o$
SAS 1-06 Feb 73-01	14.2	1,2,3,4	0°	11.1	± 3°
		1,2,3	5°N	5.3	± 4°
		2,3,4	10°S	13.2	± 5°
		1,2,4	5°S	23.0	± 3°
		1,3,4	4°N	15.5	± 3°
SAS 1-23 Feb 73-01	14.2	1,2,3,4	7°S	2.0	± 2°
		1,2,3	5°S	.6	± 2°
		2,3,4	8°S	.7	± 2°
		1,2,4	9°S	3.9	± 2°
		1,3,4	7°S	5.3	± 2°
SAS 1-23 Feb 73-02	12.3	1,2,3,4	3°S	6.9	± 2°
		1,2,3	1°S	5.7	± 2°
		2,3,4	3°S	2.8	± 3°
		1,2,4	5°S	10.8	± 2°
		1,3,4	2°S	9.4	± 2°
SAS 1-24 Feb 73-01	12.3	1,2,3,4	3°S	4.9	± 2°
		1,2,3	1°S	4.5	± 2°
		2,3,4	2°S	1.2	± 2°
		1,2,4	4°S	12.5	± 2°
		1,3,4	3°S	4.1	± 2°
SAS 1-24 Feb 73-01	6.4	1,2,3,4	38°S	44.1	±3°
		1,2,3	40°S	42.6	±3°
		2,3,4	45°S	53.6	±3°
		1,2,4	34°S	54.4	±3°
		1,3,4	37°S	43.5	±2°
SAS 1-24 Feb 73-02	12.3	1,2,3,4	4°S	10.6	±2°
		1,2,3	3°S	8.2	±3°
		2,3,4	4°S	3.0	±3°
		1,2,4	5°S	21.1	±3°
		1,3,4	4°S	9.8	±2°
SAS 1-24 Feb 73-03	9.7	1,2,3,4	3°S	29.4	±3°
		1,2,3	1°N	19.5	±3°
		2,3,4	0°	15.7	±2°
		1,2,4	8°S	41.4	±3°
		1,3,4	3°S	12.4	±2°

Appendix G. (Cont'd)

Run	Period (sec)	Array	α_o	P (α_o)%	$\Delta\alpha_o$
SAS 1-24 Feb 73-04	9.7	1,2,3,4	10°S	40.7	±3°
		1,2,3	4°S	26.1	±2°
		2,3,4	6°S	39.3	±3°
		1,2,4	11°S	32.1	±3°
		1,3,4	10°S	40.4	±3°
SAS 1-06 Apr 73-01	14.2	1,2,3,4	7°N	92.0	±3°
		1,2,3	20°S	184	-
		2,3,4	25°N	8.5	±3°
		1,2,4	90°S	328	-
		1,3,4	90°N	378	-
SAS 1-16 May 73-02	14.2	1,2,3,4	22°S	4.8	±3°
		1,2,3	22°S	1.5	±2°
		2,3,4	22°S	1.1	±2°
SAS 1-16 May 73-02	9.8	1,2,3,4	0°	4.4	±2°
		1,2,3	0°	1.7	±2°
		2,3,4	1°S	2.2	±2°
SAS 1-16 May 73-02	4.3	1,2,3,4	28°S	76.0	±5°
		1,2,3	31°S	78.8	-
		2,3,4	27°S	83.3	±4°
SAS 1-17 May 73-01	10.9	1,2,3,4	6°S	11.1	±2°
		1,2,3	5°S	2.5	±2°
		2,3,4	6°S	6.0	±2°
SAS 1-17 May 73-01	4.3	1,2,3,4	30°N	66.4	±5°
		1,2,3	15°N	56.2	-
		2,3,4	34°N	74.1	±5°
SAS 1-17 May 73-02	10.9	1,2,3,4	2°S	2.0	±2°
		1,2,3	3°S	1.1	±3°
		2,3,4	2°S	0.5	±2°
SAS 1-17 May 73-02	4.5	1,2,3,4	8°N	25.4	±3°
		1,2,3	9°N	20.9	±2°
		2,3,4	59°S	25.4	±2°
SAS 1-18 May 73-01	14.2	1,2,3,4	26°S	0.4	±1°
		1,2,3	25°S	0.1	±1°
		2,3,4	25°S	0.1	±1°

Appendix G. (Cont'd)

Run	Period (sec)	Array	α_o	P (α_o)%	$\Delta\alpha_o$
SAS 1-18 May 73-01	9.8	1,2,3,4	2°S	17.4	±3°
		1,2,3	3°S	16.1	±3°
		2,3,4	3°S	14.2	±3°
SAS 1-18 May 73-01	4.5	1,2,3,4	22°S	74.1	±3°
		1,2,3	43°S	67.2	-
		2,3,4	42°N	54.7	±5°
SAS 1-18 May 73-03	12.3	1,2,3,4	10°S	5.2	±2°
		1,2,3	10°S	1.5	±2°
		2,3,4	10°S	2.3	±2°
SAS 1-18 May 73-03	4.5	1,2,3,4	2°S	54.2	±5°
		1,2,3	43°S	82.2	-
		2,3,4	40°N	65.4	±5°
SAS 1-18 May 73-04	12.3	1,2,3,4	13°S	4.6	±2°
		1,2,3	12°S	1.2	±2°
		2,3,4	12°S	1.2	±2°
SAS 1-18 May 73-04	4.8	1,2,3,4	43°S	63.2	±4°
		1,2,3	20°N	71.3	-
		2,3,4	38°S	57.7	-
SAS 1-19 May 73-01	12.3	1,2,3,4	11°S	5.7	±2°
		1,2,3	11°S	1.5	±2°
		2,3,4	12°S	2.5	±2°
SAS 1-19 May 73-01	4.8	1,2,3,4	40°S	69.4	-
		1,2,3	0°	69.5	±5°
		2,3,4	31°N	45.7	-
SAS 1-19 May 73-02	14.2	1,2,3,4	28°S	0.7	±1°
		1,2,3	28°S	0.5	±1°
		2,3,4	28°S	0.4	±1°
SAS 1-19 May 73-02	10.9	1,2,3,4	4°S	3.7	±2°
		1,2,3	5°S	1.6	±2°
		2,3,4	5°S	1.4	±2°
SAS 1-19 May 73-02	4.8	1,2,3,4	28°S	73.3	±4°
		1,2,3	34°N	74.1	±3°
		2,3,4	30°S	59.8	±3°

Appendix G. (Cont'd)

Run	Period (sec)	Array	α_o	P (α_o)%	$\Delta\alpha_o$
SAS 1-19 May 73-04	16.9	1,2,3,4	21°S	1.8	±2°
		1,2,3	21°S	0.2	±2°
		2,3,4	20°S	0.3	±1°
SAS 1-19 May 73-04	5.0	1,2,3,4	40°N	63.2	±5°
		1,2,3	36°S	51.7	-
		2,3,4	No fit.		
SAS 1-20 May 73-01	16.8	1,2,3,4	26°S	.4	±1°
		1,2,3	26°S	.1	±1°
		2,3,4	26°S	.2	±1°
SAS 1-20 May 73-01	4.5	1,2,3,4	48°S	87.1	±3°
		1,2,3	3°S	77.7	±5°
		2,3,4	10°N	90.0	±5°
SAS 1-20 May 73-02	14.2	1,2,3,4	24°S	.5	±1°
		1,2,3	23°S	.1	±1°
		2,3,4	24°S	.3	±1°
SAS 1-20 May 73-02	9.8	1,2,3,4	5°S	15.0	±3°
		1,2,3	3°S	5.5	±2°
		2,3,4	7°S	5.7	±3°
SAS 1-20 May 73-03	14.2	1,2,3,4	25°S	1.5	±1°
		1,2,3	25°S	.2	±1°
		2,3,4	25°S	.9	±1°
SAS 1-20 May 73-03	9.8	1,2,3,4	2°S	10.8	±2°
		1,2,3	1°S	5.1	±2°
		2,3,4	3°S	8.5	±2°
SAS 1-20 May 73-04	12.3	1,2,3,4	21°S	10.8	±4°
		1,2,3	20°S	5.6	±2°
		2,3,4	22°S	5.3	±2°
SAS 1-20 May 73-04	9.8	1,2,3,4	2°S	28.2	±3°
		1,2,3	1°S	8.2	±2°
		2,3,4	6°S	21.7	±3°
SAS 1-21 May 73-01	12.3	1,2,3,4	28°S	25.0	±5°
		1,2,3	27°S	18.1	±5°
		2,3,4	25°S	10.4	±5°

Appendix G. (Cont'd)

Run	Period (sec)	Array	α_o	$P(\alpha_o)\%$	$\Delta\alpha_o$
SAS 1-21 May 73-01	8.8	1,2,3,4	1°N	11.8	±2°
		1,2,3	1°N	12.5	±2°
		2,3,4	1°N	14.8	±3°
SAS 1-21 May 73-04	12.3	1,2,3,4	20°S	27.5	±4°
		1,2,3	19°S	11.2	±4°
		2,3,4	20°S	14.9	±4°
SAS 1-22 May 73-03	9.8	1,2,3,4	0°	7.9	±2°
		1,2,3	0°	5.1	±2°
		2,3,4	1°S	4.6	±2°
SAS 1-23 May 73-03	10.9	1,2,3,4	4°S	19.9	±3°
		1,2,3	5°S	28.0	±3°
		2,3,4	6°S	14.6	±3°
SAS 1-23 May 73-03	4.5	1,2,3,4	30°N	78.6	±5°
		1,2,3	28°N	70.3	±5°
		2,3,4	24°N	85.8	±5°
SAS 1-24 May 73-01	10.9	1,2,3,4	6°S	6.3	±2°
		1,2,3	5°S	5.6	±2°
		2,3,4	6°S	5.6	±2°
SAS 1-24 May 73-01	6.9	1,2,3,4	3°S	9.6	±2°
		1,2,3	5°S	4.6	±2°
		2,3,4	3°S	15.5	±2°
SAS 1-24 May 73-02	12.3	1,2,3,4	8°S	43.0	±5°
		1,2,3	-	-	-
		2,3,4	15°S	44.2	±5°
SAS 1-24 May 73-02	6.9	1,2,3,4	2°N	37.3	±3°
		1,2,3	4°N	47.9	±3°
		2,3,4	8°N	70.6	±3°
SAS 1-24 May 73-03	14.2	1,2,3,4	36°S	56.3	±6°
		1,2,3	37°S	50.1	±5°
		2,3,4	-	-	-
SAS 1-24 May 73-03	6.9	1,2,3,4	4°N	33.7	±3°
		1,2,3	2°N	48.3	±4°
		2,3,4	6°N	51.4	±3°

Appendix G. (Cont'd)

Run	Period (sec)	Array	α_o	P (α_o)%	$\Delta\alpha_o$
SAS 1-24 May 73-04	14.2	1,2,3,4	21°S	4.7	±3°
		1,2,3	21°S	2.6	±3°
		2,3,4	21°S	.7	±1°
SAS 1-25 May 73-01	12.3	1,2,3,4	2°S	5.5	±3°
		1,2,3	1°N	12.2	±4°
		2,3,4	3°S	4.3	±4°
SAS 1-25 May 73-01	4.1	1,2,3,4	18°S	92.2	±3°
		1,2,3	11°S	73.1	±3°
		2,3,4	35°N	84.9	±4°
SAS 1-25 May 73-03	12.3	1,2,3,4	5°S	4.5	±2°
		1,2,3	7°S	9.2	±2°
		2,3,4	6°S	2.3	±2°
SAS 1-25 May 73-03	6.4	1,2,3,4	5°S	82.3	±5°
		1,2,3	12°S	75.3	±5°
		2,3,4	9°N	70.5	±5°
SAS 1-25 May 73-04	12.3	1,2,3,4	7°S	8.5	±2°
		1,2,3	8°S	4.6	±2°
		2,3,4	7°S	1.9	±2°
SAS 1-25 May 73-04	6.4	1,2,3,4	25°S	66.5	±6°
		1,2,3	10°N	64.9	±5°
		2,3,4	27°S	69.2	±5°
SAS 1-26 May 73-01	12.3	1,2,3,4	5°S	1.1	±2°
		1,2,3	6°S	.5	±2°
		2,3,4	5°S	.1	±1°
SAS 1-26 May 73-01	6.4	1,2,3,4	2°N	42.1	±3°
		1,2,3	0°	55.3	±3°
		2,3,4	2°N	32.6	±4°
SAS 1-26 May 73-02	12.3	1,2,3,4	8°S	4.7	±2°
		1,2,3	9°S	1.7	±2°
		2,3,4	10°S	4.8	±2°
SAS 1-26 May 73-02	7.4	1,2,3,4	0°	30.6	±3°
		1,2,3	1°S	22.1	±3°
		2,3,4	1°S	21.0	±3°

Appendix G. (Cont'd)

Run	Period (sec)	Array	α_o	$P(\alpha_o)$%	$\Delta\alpha_o$
SAS 1-26 May 73-03	10.9	1,2,3,4	3°S	2.8	±2°
		1,2,3	2°S	2.7	±2°
		2,3,4	4°S	4.5	±2°
SAS 1-26 May 73-03	7.4	1,2,3,4	1°S	31.3	±3°
		1,2,3	1°S	11.7	±3°
		2,3,4	1°S	33.5	±2°
SAS 1-26 May 73-04	10.9	1,2,3,4	4°S	2.7	±3°
		1,2,3	5°S	15.4	±3°
		2,3,4	5°S	1.4	±3°
SAS 1-26 May 73-04	7.4	1,2,3,4	1°N	55.2	±4°
		1,2,3	2°N	42.6	±3°
		2,3,4	4°S	45.8	±4°
SAS 1-27 May 73-01	14.2	1,2,3,4	27°S	1.4	±3°
		1,2,3	26°S	.9	±2°
		2,3,4	26°S	.9	±2°
SAS 1-27 May 73-01	8.0	1,2,3,4	2°N	10.7	±4°
		1,2,3	2°N	9.9	±4°
		2,3,4	1°N	8.1	±2°
SAS 1-27 May 73-02	14.2	1,2,3,4	31°S	4.2	±3°
		1,2,3	34°S	6.1	±3°
		2,3,4	32°S	3.8	±3°
SAS 1-27 May 73-02	8.0	1,2,3,4	2°N	22.1	±4°
		1,2,3	2°N	14.1	±3°
		2,3,4	1°N	15.5	±3°
SAS 1-27 May 73-03	14.2	1,2,3,4	29°S	.3	±1°
		1,2,3	30°S	.3	±1°
		2,3,4	28°S	.3	±1°
SAS 1-27 May 73-03	8.0	1,2,3,4	1°S	53.2	±5°
		1,2,3	2°N	37.0	±4°
		2,3,4	3°S	37.1	±5°
SAS 1-27 May 73-04	14.2	1,2,3,4	30°S	1.3	±4°
		1,2,3	29°S	1.4	±3°
		2,3,4	29°S	.2	±1°

Appendix G. (Cont'd)

Run	Period (sec)	Array	α_o	$P(\alpha_o)$%	$\Delta\alpha_o$
SAS 1-27 May 73-04	7.4	1,2,3,4	2°N	26.1	± 5°
		1,2,3	1°N	29.3	± 4°
		2,3,4	2°N	31.2	± 3°
SAS 1-28 May 73-01	12.3	1,2,3,4	30°S	3.7	± 2°
		1,2,3	30°S	4.3	± 2°
		2,3,4	29°S	.8	± 1°
SAS 1-28 May 73-01	8.8	1,2,3,4	3°N	20.9	± 3°
		1,2,3	4°N	11.1	± 3°
		2,3,4	2°N	24.4	± 3°
SAS 1-28 May 73-02	12.3	1,2,3,4	32°S	3.6	± 3°
		1,2,3	34°S	5.2	± 3°
		2,3,4	31°S	1.3	± 3°
SAS 1-28 May 73-02	7.4	1,2,3,4	0°	38.2	± 3°
		1,2,3	2°N	33.0	± 3°
		2,3,4	1°S	42.0	± 3°
SAS 1-28 May 73-04	12.3	1,2,3,4	30°S	7.1	± 3°
		1,2,3	29°S	8.2	± 4°
		2,3,4	31°S	1.1	± 3°
SAS 1-28 May 73-04	8.8	1,2,3,4	3°S	8.7	± 2°
		1,2,3	1°S	2.2	± 2°
		2,3,4	4°S	12.3	± 3°
SAS 1-29 May 73-02	14.2	1,2,3,4	23°S	2.0	± 2°
		1,2,3	23°S	.3	± 1°
		2,3,4	22°S	.7	± 1°
SAS 1-29 May 73-02	8.0	1,2,3,4	1°N	13.0	± 2°
		1,2,3	0°	13.7	± 2°
		2,3,4	0°	10.9	± 3°
SAS 1-29 May 73-03	14.2	1,2,3,4	23°S	.5	± 1°
		1,2,3	24°S	.1	± 1°
		2,3,4	23°S	.5	± 1°
SAS 1-30 May 73-01	16.8	1,2,3,4	20°S	.8	± 1°
		1,2,3	22°S	.1	± 1°
		2,3,4	20°S	.6	± 1°

Appendix G. (Cont'd)

Run	Period (sec)	Array	α_o	P (α_o)%	$\Delta\alpha_o$
SAS 1-30 May 73-01	7.4	1,2,3,4	1°S	39.1	±3°
		1,2,3	3°S	29.8	±3°
		2,3,4	0°	40.1	±3°
SAS 1-30 May 73-02	14.2	1,2,3,4	23°S	.7	±1°
		1,2,3	23°S	.1	±1°
		2,3,4	24°S	.1	±1°
SAS 1-30 May 73-02	7.4	1,2,3,4	3°N	50.9	±3°
		1,2,3	8°N	37.9	±4°
		2,3,4	1°S	54.1	±4°
SAS 1-30 May 73-03	14.2	1,2,3,4	21°S	8.8	±3°
		1,2,3	21°S	3.5	±2°
		2,3,4	20°S	3.0	±2°
SAS 1-30 May 73-03	6.9	1,2,3,4	1°N	25.5	±4°
		1,2,3	2°N	24.1	±3°
		2,3,4	1°N	46.1	±3°
SAS 1-30 May 73-04	14.2	1,2,3,4	22°S	2.0	±2°
		1,2,3	23°S	1.1	±2°
		2,3,4	24°S	3.5	±2°
SAS 1-31 May 73-01	14.2	1,2,3,4	22°S	21.9	±4°
		1,2,3	23°S	5.1	±3°
		2,3,4	16°S	11.1	±5°
SAS 1-31 May 73-01	7.4	1,2,3,4	1°S	77.8	±4°
		1,2,3	-	-	-
		2,3,4	3°N	42.9	±5°
SAS 1-31 May 73-02	14.2	1,2,3,4	23°S	1.0	±1°
		1,2,3	23°S	.2	±1°
		2,3,4	22°S	.1	±1°
SAS 1-31 May 73-02	10.9	1,2,3,4	1°N	8.6	±2°
		1,2,3	2°N	6.8	±2°
		2,3,4	1°N	5.0	±2°
SAS 1-31 May 73-03	16.8	1,2,3,4	25°S	.3	±1°
		1,2,3	26°S	.1	±1°
		2,3,4	24°S	.1	±1°

Appendix G. (Cont'd)

Run	Period (sec)	Array	α_o	$P(\alpha_o)$%	$\Delta\alpha_o$
SAS 1-31 May 73-03	10.9	1,2,3,4	2°S	7.5	±2°
		1,2,3	3°S	6.8	±2°
		2,3,4	2°S	5.8	±2°
SAS 1-31 May 73-04	14.2	1,2,3,4	22°S	2.0	±2°
		1,2,3	22°S	.4	±1°
		2,3,4	22°S	1.0	±1°
SAS 1-01 Jun 73-02	16.8	1,2,3,4	23°S	.1	±1°
		1,2,3	24°S	.1	±1°
		2,3,4	24°S	.2	±1°
SAS 1-01 Jun 73-02	12.3	1,2,3,4	1°S	7.3	±2°
		1,2,3	2°S	7.2	±2°
		2,3,4	1°S	6.9	±2°
SAS 1-01 Jun 73-04	14.2	1,2,3,4	25°S	2.8	±2°
		1,2,3	24°S	.8	±1°
		2,3,4	24°S	1.1	±2°
SAS 1-02 Jun 73-03	7.4	1,2,3,4	2°N	11.5	±2°
		1,2,3	3°N	8.1	±2°
		2,3,4	1°N	11.0	±3°
SAS 1-02 Jun 73-04	12.3	1,2,3,4	12°S	18.4	±4°
		1,2,3	13°S	8.0	±3°
		2,3,4	13°S	7.6	±3°
SAS 1-03 Jun 73-01	10.9	1,2,3,4	1°S	8.1	±2°
		1,2,3	0°	5.1	±2°
		2,3,4	1°S	4.2	±3°
SAS 1-03 Jun 73-02	14.2	1,2,3,4	25°S	1.3	±2°
		1,2,3	24°S	.5	±1°
		2,3,4	25°S	.3	±1°
SAS 1-03 Jun 73-03	6.0	1,2,3,4	10°N	80.9	±6°
		1,2,3	-	-	-
		2,3,4	13°N	86.1	±6°
SAS 1-03 Jun 73-04	14.2	1,2,3,4	25°S	3.8	±3°
		1,2,3	26°S	1.9	±2°
		2,3,4	25°S	3.6	±3°

Appendix G. (Cont'd)

Run	Period (sec)	Array	α_o	P (α_o)%	$\Delta\alpha_o$
SAS 1-04 Jun 73-01	14.2	1,2,3,4	25°S	3.9	±3°
		1,2,3	25°S	1.7	±2°
		2,3,4	24°S	1.4	±3°
SAS 1-04 Jun 73-02	8.8	1,2,3,4	5°N	9.2	±3°
		1,2,3	4°N	3.8	±3°
		2,3,4	4°N	2.3	±2°
SAS 1-04 Jun 73-04	12.3	1,2,3,4	15°S	15.3	±3°
		1,2,3	14°S	5.3	±2°
		2,3,4	16°S	6.7	±2°
SAS 1-04 Jun 73-05	4.5	1,2,3,4	51°S	77.3	±4°
		1,2,3	43°S	72.9	±5°
		2,3,4	47°S	76.3	±5°
SAS 1-05 Jun 73-01	9.8	1,2,3,4	3°N	8.2	±2°
		1,2,3	2°N	5.0	±3°
		2,3,4	2°N	11.6	±3°
SAS 1-05 Jun 73-02	12.3	1,2,3,4	10°S	23.9	±4°
		1,2,3	14°S	12.9	±4°
		2,3,4	11°S	14.1	±4°
SAS 1-05 Jun 73-03	14.2	1,2,3,4	30°S	9.8	±3°
		1,2,3	28°S	5.5	±4°
		2,3,4	27°S	4.2	±3°
SAS 1-05 Jun 73-04	8.8	1,2,3,4	1°S	8.8	±2°
		1,2,3	2°S	11.2	±2°
		2,3,4	2°S	6.7	±2°
SAS 1-06 Jun 73-01	5.6	1,2,3,4	0°	63.9	±3°
		1,2,3	2°N	41.5	±3°
		2,3,4	1°N	49.9	±3°
SAS 1-06 Jul 73-05	14.2	1,2,3,4	23°S	2.3	±2°
		1,2,3	23°S	.9	±2°
		2,3,4	22°S	.4	±1°
SAS 1-06 Jul 73-06	9.8	1,2,3,4	0°	6.4	±2°
		1,2,3	0°	3.4	±2°
		2,3,4	1°S	2.3	±2°

Appendix G. (Cont'd)

Run	Period (sec)	Array	α_o	$P(\alpha_o)\%$	$\Delta\alpha_o$
SAS 1-06 Jul 73-07	5.0	1,2,3,4	20°S	83.7	±5°
		1,2,3	-	-	-
		2,3,4	-	-	-
SAS 1-07 Jul 73-01	14.2	1,2,3,4	27°S	.8	±1°
		1,2,3	26°S	.2	±2°
		2,3,4	27°S	.4	±1°
SAS 1-07 Jul 73-02	12.3	1,2,3,4	26°S	.8	±1°
		1,2,3	25°S	.4	±1°
		2,3,4	25°S	.4	±1°
SAS 1-07 Jul 73-03	6.0	1,2,3,4	10°N	51.5	±4°
		1,2,3	-	-	-
		2,3,4	9°N	69.3	±5°
SAS 1-07 Jul 73-04	8.8	1,2,3,4	5°N	45.2	±4°
		1,2,3	5°N	38.0	±4°
		2,3,4	4°N	41.1	±5°
SAS 1-07 Jul 73-05	8.8	1,2,3,4	5°S	4.3	±2°
		1,2,3	5°S	3.9	±2°
		2,3,4	5°S	.9	±1°
SAS 1-07 Jul 73-07	6.4	1,2,3,4	12°N	58.6	±4°
		1,2,3	10°N	43.3	±4°
		2,3,4	10°N	49.6	±4°
SAS 1-08 Jul 73-01	10.9	1,2,3,4	28°S	29.9	±3°
		1,2,3	26°S	12.0	±3°
		2,3,4	26°S	22.3	±3°
SAS 1-08 Jul 73-03	7.4	1,2,3,4	2°S	28.5	±4°
		1,2,3	4°S	33.3	±5°
		2,3,4	2°S	16.0	±4°
SAS 1-08 Jul 73-05	12.3	1,2,3,4	30°S	2.9	±3°
		1,2,3	29°S	3.0	±3°
		2,3,4	30°S	1.3	±2°
SAS 1-08 Jul 73-07	14.2	1,2,3,4	24°S	.5	±1°
		1,2,3	24°S	.2	±1°
		2,3,4	24°S	.2	±1°

Appendix G. (Cont'd)

Run	Period (sec)	Array	α_o	$P(\alpha_o)$%	$\Delta\alpha_o$
SAS 1-09 Jul 73-01	8.8	1,2,3,4	1°N	34.2	±3°
		1,2,3	2°N	9.7	±4°
		2,3,4	1°S	17.1	±4°
SAS 1-09 Jul 73-03	14.2	1,2,3,4	26°S	2.2	±3°
		1,2,3	25°S	.7	±1°
		2,3,4	25°S	1.0	±3°
SAS 1-10 Jul 73-01	8.8	1,2,3,4	2°S	26.3	±5°
		1,2,3	6°S	18.6	±4°
		2,3,4	3°S	39.3	±4°
SAS 1-10 Jul 73-02	14.2	1,2,3,4	24°S	.8	±1°
		1,2,3	24°S	.3	±1°
		2,3,4	24°S	.1	±1°
SAS 1-11 Jul 73-01	9.8	1,2,3,4	1°N	44.1	±3°
		1,2,3	3°N	40.2	±4°
		2,3,4	3°N	44.1	±4°
SAS 1-11 Jul 73-02	14.2	1,2,3,4	26°S	1.4	±3°
		1,2,3	25°S	.6	±2°
		2,3,4	26°S	.3	±2°
SAS 1-16 Jul 73-03	9.8	1,2,3,4	1°N	36.9	±4°
		1,2,3	2°N	32.8	±4°
		2,3,4	2°N	31.7	±4°
SAS 1-16 Jul 73-04	14.2	1,2,3,4	24°S	.3	±1°
		1,2,3	24°S	.1	±1°
		2,3,4	24°S	.1	±1°
SAS 1-17 Jul 73-01	14.2	1,2,3,4	22°S	.5	±1°
		1,2,3	22°S	.2	±1°
		2,3,4	21°S	.3	±1°
SAS 1-18 Jul 73-04	5.3	1,2,3,4	-	-	-
		1,2,3	62°S	48.6	±4°
		2,3,4	-	-	-
SAS 1-19 Jul 73-01	16.8	1,2,3,4	24°S	.9	±1°
		1,2,3	23°S	.1	±1°
		2,3,4	24°S	.3	±1°

Appendix G. (Cont'd)

Run	Period (sec)	Array	α_o	P (α_o)%	$\Delta\alpha_o$
SAS 1-19 Jul 73-03	5.6	1,2,3,4	9°N	76.8	±5°
		1,2,3	-	-	-
		2,3,4	-	-	-
SAS 1-19 Jul 73-04	16.8	1,2,3,4	24°S	.5	±1°
		1,2,3	25°S	.1	±1°
		2,3,4	24°S	.5	±1°
SAS 1-20 Jul 73-03	6.9	1,2,3,4	5°N	40.0	±2°
		1,2,3	5°N	26.6	±2°
		2,3,4	3°N	32.0	±2°
SAS 1-20 Jul 73-04	14.2	1,2,3,4	23°S	0.6	±1°
		1,2,3	22°S	0.2	±1°
		2,3,4	22°S	0.1	±1°
SAS 1-20 Jul 73-04	6.4	1,2,3,4	27°S	75.7	-
		1,2,3	4°S	65.7	-
		2,3,4	7°S	72.1	-
SAS 1-21 Jul 73-01	14.2	1,2,3,4	25°S	0.7	±1°
		1,2,3	25°S	0.1	±1°
		2,3,4	25°S	0.2	±1°
SAS 1-21 Jul 73-01	6.4	1,2,3,4	2°N	46.1	±5°
		1,2,3	1°N	37.8	±4°
		2,3,4	3°N	45.1	±4°
SAS 1-21 Jul 73-02	14.2	1,2,3,4	22°S	1.2	±2°
		1,2,3	22°S	0.1	±2°
		2,3,4	22°S	0.6	±2°
SAS 1-21 Jul 73-02	6.9	1,2,3,4	6°N	26.4	±3°
		1,2,3	7°N	25.3	±4°
		2,3,4	8°N	18.4	±3°
SAS 1-21 Jul 73-03	14.2	1,2,3,4	24°S	1.0	±2°
		1,2,3	24°S	0.4	±1°
		2,3,4	24°S	0.1	±1°
SAS 1-21 Jul 73-03	7.4	1,2,3,4	1°N	31.3	±3°
		1,2,3	1°N	10.0	±4°
		2,3,4	1°N	34.5	±4°

Appendix G. (Cont'd)

Run	Period (sec)	Array	α_o	$P(\alpha_o)\%$	$\Delta\alpha_o$
SAS 1-21 Jul 73-04	16.9	1,2,3,4	25°S	0.2	±1°
		1,2,3	25°S	0.1	±1°
		2,3,4	25°S	0.1	±1°
SAS 1-21 Jul 73-04	7.4	1,2,3,4	8°N	54.3	±3°
		1,2,3	7°N	50.0	±3°
		2,3,4	5°N	54.0	±3°
SAS 1-22 Jul 73-01	16.9	1,2,3,4	27°S	0.4	±1°
		1,2,3	27°S	0.1	±1°
		2,3,4	27°S	0.1	±1°
SAS 1-22 Jul 73-01	8.1	1,2,3,4	4°N	8.9	±2°
		1,2,3	4°N	9.6	±2°
		2,3,4	5°N	10.7	±2°
SAS 1-22 Jul 73-02	14.2	1,2,3,4	25°S	0.4	±1°
		1,2,3	24°S	0.1	±1°
		2,3,4	25°S	0.1	±1°
SAS 1-22 Jul 73-03	8.0	1,2,3,4	9°N	20.9	±4°
		1,2,3	10°N	19.7	±4°
		2,3,4	6°N	19.6	±4°
SAS 1-22 Jul 73-04	14.2	1,2,3,4	27°S	0.8	±1°
		1,2,3	26°S	0.2	±1°
		2,3,4	27°S	0.9	±1°
SAS 1-23 Jul 73-01	8.8	1,2,3,4	67°N	51.6	±5°
		1,2,3	-	-	-
		2,3,4	6°N	74.3	±5°
SAS 1-23 Jul 73-02	7.4	1,2,3,4	3°N	17.0	±2°
		1,2,3	2°N	13.7	±2°
		2,3,4	3°N	7.8	±2°
SAS 1-24 Jul 73-02	16.8	1,2,3,4	29°S	0.1	±1°
		1,2,3	29°S	0.7	±1°
		2,3,4	28°S	0.3	±1°
SAS 1-27 Jul 73-04	8.8	1,2,3,4	42°S	39.8	±5°
		1,2,3	42°S	31.4	±5°
		2,3,4	26°S	38.1	±5°

Appendix G. (Cont'd)

Run	Period (sec)	Array	α_o	P (α_o)%	$\Delta\alpha_o$
SAS 1-28 Jul 73-02	12.3	1,2,3,4	24°S	7.5	±2°
		1,2,3	23°S	5.2	±3°
		2,3,4	23°S	3.9	±3°
SAS 1-29 Jul 73-02	5.6	1,2,3,4	8°S	83.4	±5°
		1,2,3	-	-	-
		2,3,4	-	-	-
SAS 1-30 Jul 73-01	14.2	1,2,3,4	29°S	.2	±1°
		1,2,3	28°S	.3	±1°
		2,3,4	29°S	.5	±1°
SAS 1-31 Jul 73-01	8.0	1,2,3,4	2°N	20.1	±3°
		1,2,3	3°N	38.3	±3°
		2,3,4	2°N	12.6	±3°
SAS 1-01 Aug 73-03	14.2	1,2,3,4	24°S	.9	±1°
		1,2,3	24°S	.3	±1°
		2,3,4	24°S	.3	±1°
SAS 1-02 Aug 73-01	8.0	1,2,3,4	5°N	10.8	±3°
		1,2,3	4°N	8.0	±3°
		2,3,4	4°N	11.9	±3°
SAS 1-10 Aug 73-03	14.2	1,2,3,4	24°S	2.4	±2°
		1,2,3	24°S	.4	±1°
		2,3,4	23°S	1.5	±2°
SAS 1-23 Aug 73-02	14.2	1,2,3,4	24°S	.6	±1°
		1,2,3	24°S	.2	±1°
		2,3,4	25°S	.2	±1°
SAS 1-23 Aug 73-02	8.1	1,2,3,4	1°S	10.6	±2°
		1,2,3	2°S	18.5	±2°
		2,3,4	1°S	5.8	±2°
SAS 1-23 Aug 73-03	14.2	1,2,3,4	25°S	.1	±1°
		1,2,3	25°S	.1	±1°
		2,3,4	26°S	.1	±1°
SAS 1-23 Aug 73-03	6.4	1,2,3,4	7°S	41.3	±3°
		1,2,3	7°S	24.2	±2°
		2,3,4	6°S	34.5	±2°

Appendix G. (Cont'd)

Run	Period (sec)	Array	α_o	P (α_o)%	$\Delta\alpha_o$
SAS 1-24 Aug 73-02	14.2	1,2,3,4	25°S	1.6	±2°
		1,2,3	24°S	.3	±1°
		2,3,4	24°S	.9	±1°
SAS 1-24 Aug 73-02	8.1	1,2,3,4	6°S	37.2	±2°
		1,2,3	7°S	28.3	±3°
		2,3,4	6°S	23.7	±2°
SAS 1-24 Aug 73-03	16.8	1,2,3,4	24°S	1.7	±2°
		1,2,3	24°S	.6	±2°
		2,3,4	23°S	1.3	±2°
SAS 1-24 Aug 73-03	8.1	1,2,3,4	4°S	2.3	±2°
		1,2,3	4°S	1.9	±2°
		2,3,4	4°S	1.8	±2°
SAS 1-24 Aug 73-04	16.8	1,2,3,4	30°S	.4	±1°
		1,2,3	31°S	.1	±1°
		2,3,4	31°S	.2	±2°
SAS 1-24 Aug 73-04	8.1	1,2,3,4	2°S	23.9	±2°
		1,2,3	1°S	10.1	±2°
		2,3,4	5°S	18.7	±3°
SAS 1-25 Aug 73-01	14.2	1,2,3,4	26°S	10.1	±3°
		1,2,3	23°S	4.7	±3°
		2,3,4	24°S	3.7	±3°
SAS 1-25 Aug 73-01	8.8	1,2,3,4	1°S	.6	±1°
		1,2,3	1°S	.5	±1°
		2,3,4	1°S	.4	±1°
SAS 1-25 Aug 73-02	14.2	1,2,3,4	24°S	1.8	±2°
		1,2,3	24°S	.8	±1°
		2,3,4	24°S	.7	±1°
SAS 1-25 Aug 73-02	5.6	1,2,3,4	7°N	39.4	±2°
		1,2,3	8°N	36.2	±2°
		2,3,4	8°N	52.1	±2°
SAS 1-25 Aug 73-03	14.2	1,2,3,4	25°S	.9	±2°
		1,2,3	26°S	.3	±2°
		2,3,4	24°S	.4	±1°

Appendix G. (Cont'd)

Run	Period (sec)	Array	α_o	P (α_o)%	$\Delta\alpha_o$
SAS 1-25 Aug 73-03	8.1	1,2,3,4	0°	4.7	±2°
		1,2,3	0°	11.2	±3°
		2,3,4	0°	1.6	±2°
SAS 1-25 Aug 73-04	12.3	1,2,3,4	26°S	30.0	±3°
		1,2,3	31°S	36.3	±3°
		2,3,4	32°S	24.5	±3°
SAS 1-25 Aug 73-04	8.1	1,2,3,4	3°N	10.3	±2°
		1,2,3	4°N	10.9	±3°
		2,3,4	3°N	13.9	±2°
SAS 1-26 Aug 73-01	12.3	1,2,3,4	33°S	10.3	±2°
		1,2,3	24°S	11.8	±2°
		2,3,4	30°S	7.9	±2°
SAS 1-26 Aug 73-01	6.9	1,2,3,4	5°N	34.0	±2°
		1,2,3	6°N	22.6	±3°
		2,3,4	1°N	36.3	±3°
SAS 1-26 Aug 73-02	16.8	1,2,3,4	24°S	.1	±1°
		1,2,3	25°S	.1	±2°
		2,3,4	24°S	.1	±1°
SAS 1-26 Aug 73-02	6.9	1,2,3,4	9°N	60.9	±3°
		1,2,3	6°N	59.4	±4°
		2,3,4	6°N	50.8	±4°
SAS 1-26 Aug 73-03	16.8	1,2,3,4	23°S	.1	±1°
		1,2,3	24°S	.3	±2°
		2,3,4	23°S	.1	±2°
SAS 1-26 Aug 73-03	6.9	1,2,3,4	1°N	25.2	±2°
		1,2,3	2°N	48.6	±3°
		2,3,4	0°	11.3	±2°
SAS 1-26 Aug 73-04	16.8	1,2,3,4	26°S	.2	±1°
		1,2,3	26°S	.1	±1°
		2,3,4	26°S	.1	±1°
SAS 1-27 Aug 73-01	16.8	1,2,3,4	27°S	.1	±1°
		1,2,3	27°S	.3	±1°
		2,3,4	27°S	.1	±1°

Appendix G. (Cont'd)

Run	Period (sec)	Array	α_o	P (α_o)%	$\Delta\alpha_o$
SAS 1-27 Aug 73-02	10.9	1,2,3,4	1°S	5.2	±2°
		1,2,3	0°	2.9	±3°
		2,3,4	2°S	12.4	±2°
SAS 1-31 Aug 73-01	10.9	1,2,3,4	3°S	27.9	±3°
		1,2,3	6°S	34.2	±3°
		2,3,4	7°S	24.1	±2°
SAS 1-13 Apr 74-01	12.3	1,2,3,4	1°S	0.6	±2°
		1,2,3	2°S	0.6	±2°
		2,3,4	1°S	0.3	±2°
SAS 1-13 Apr 74-01	9.8	1,2,3,4	0°	1.2	±2°
		1,2,3	1°S	2.4	±2°
		2,3,4	0°	0.4	±2°
SAS 1-13 Apr 74-02	16.8	1,2,3,4	17°S	1.1	±3°
		1,2,3	18°S	0.2	±2°
		2,3,4	17°S	0.2	±2°
SAS 1-13 Apr 74-02	10.9	1,2,3,4	1°S	0.8	±3°
		1,2,3	1°S	0.5	±2°
		2,3,4	1°S	0.1	±1°
SAS 1-13 Apr 74-03	16.8	1,2,3,4	11°S	1.0	±2°
		1,2,3	11°S	0.1	±2°
		2,3,4	11°S	0.3	±2°
SAS 1-13 Apr 74-03	10.9	1,2,3,4	7°S	3.1	±2°
		1,2,3	8°S	1.0	±2°
		2,3,4	7°S	0.6	±2°
SAS 1-13 Apr 74-04	16.8	1,2,3,4	12°S	4.4	±2°
		1,2,3	14°S	0.2	±2°
		2,3,4	12°S	0.2	±2°
SAS 1-13 Apr 74-04	10.9	1,2,3,4	2°S	1.7	±2°
		1,2,3	2°S	0.4	±2°
		2,3,4	3°S	1.5	±3°
SAS 1-14 Apr 74-01	14.2	1,2,3,4	8°S	5.6	±3°
		1,2,3	12°S	3.2	±3°
		2,3,4	8°S	0.3	±2°

Appendix G. (Cont'd)

Run	Period (sec)	Array	α_o	P (α_o)%	$\Delta\alpha_o$
SAS 1-14 Apr 74-01	10.9	1,2,3,4	1°S	5.7	± 3°
		1,2,3	1°S	5.2	± 3°
		2,3,4	1°S	1.6	± 3°
SAS 1-14 Apr 74-03	14.2	1,2,3,4	9°S	4.8	± 3°
		1,2,3	9°S	0.6	± 2°
		2,3,4	11°S	0.8	± 2°
SAS 1-14 Apr 74-03	9.8	1,2,3,4	7°S	32.0	± 4°
		1,2,3	7°S	12.3	± 4°
		2,3,4	9°S	5.8	± 2°
SAS 1-14 Apr 74-04	14.2	1,2,3,4	16°S	5.2	± 3°
		1,2,3	16°S	0.9	± 3°
		2,3,4	15°S	0.3	± 2°
SAS 1-14 Apr 74-04	9.8	1,2,3,4	6°S	25.1	± 3°
		1,2,3	7°S	9.0	± 3°
		2,3,4	8°S	3.0	± 3°
SAS 1-15 Apr 74-01	14.2	1,2,3,4	17°S	3.5	± 3°
		1,2,3	15°S	0.6	± 3°
		2,3,4	17°S	0.2	± 2°
SAS 1-15 Apr 74-01	4.5	1,2,3,4	32°S	42.8	±4°
		1,2,3	31°S	36.3	±3°
		2,3,4	35°S	24.9	±3°
SAS 1-15 Apr 74-03	14.2	1,2,3,4	18°S	1.6	±3°
		1,2,3	18°S	0.6	±3°
		2,3,4	17°S	0.1	±1°
SAS 1-15 Apr 74-03	4.5	1,2,3,4	75°S	48.2	±4°
		1,2,3	88°S	34.9	±6°
		2,3,4	63°S	17.0	±5°
SAS 1-15 Apr 74-04	14.2	1,2,3,4	12°S	12.5	±3°
		1,2,3	14°S	3.3	±3°
		2,3,4	13°S	3.3	±3°
SAS 1-15 Apr 74-04	4.5	1,2,3,4	-	-	-
		1,2,3	44°N	75.3	±5°
		2,3,4	60°S	29.9	±4°

Appendix G. (Cont'd)

Run	Period (sec)	Array	α_o	P (α_o)%	$\Delta\alpha_o$
SAS 1-16 Apr 74-01	14.2	1,2,3,4	11°S	3.2	±3°
		1,2,3	11°S	0.4	±2°
		2,3,4	11°S	0.7	±2°
SAS 1-16 Apr 74-01	6.4	1,2,3,4	5°N	12.0	±3°
		1,2,3	5°N	19.8	±3°
		2,3,4	6°N	15.3	±3°
SAS 1-16 Apr 74-02	16.8	1,2,3,4	30°S	0.3	±1°
		1,2,3	32°S	0.1	±2°
		2,3,4	29°S	0.3	±2°
SAS 1-16 Apr 74-02	12.3	1,2,3,4	2°S	1.6	±3°
		1,2,3	2°S	0.8	±3°
		2,3,4	3°S	1.3	±3°
SAS 1-16 Apr 74-03	12.3	1,2,3,4	3°S	3.2	±3°
		1,2,3	3°S	0.2	±2°
		2,3,4	4°S	1.9	±3°
SAS 1-16 Apr 74-03	6.0	1,2,3,4	5°N	35.5	±4°
		1,2,3	7°N	15.5	±3°
		2,3,4	5°N	22.0	±3°
SAS 1-16 Apr 74-04	9.8	1,2,3,4	1°N	0.5	±3°
		1,2,3	1°N	1.5	±2°
		2,3,4	1°N	0.5	±2°
SAS 1-16 Apr 74-04	5.0	1,2,3,4	0°	80.3	±3°
		1,2,3	4°N	55.6	±2°
		2,3,4	33°N	46.4	±3°
SAS 1-17 Apr 74-01	12.3	1,2,3,4	10°S	1.5	±3°
		1,2,3	10°S	0.4	±2°
		2,3,4	10°S	0.5	±2°
SAS 1-17 Apr 74-01	8.8	1,2,3,4	1°S	4.6	±2°
		1,2,3	1°S	1.4	±2°
		2,3,4	2°S	4.7	±2°

Appendix G. (Cont'd)

Definition of Terms:

Period:	The period at which the directional information was obtained.
α_o:	The direction of the best fit to a single wave train for the four sensor array. The fitting technique is based on the minimum value of $P(\alpha_o)$.
$P(\alpha_o)$:	A measure of the effectiveness of the fit.
$\Delta\alpha_o$:	The uncertainty assigned to α_o.

APPENDIX H

COMPARISON OF SPECTRA OF WAVE STAFF AND PRESSURE SENSOR

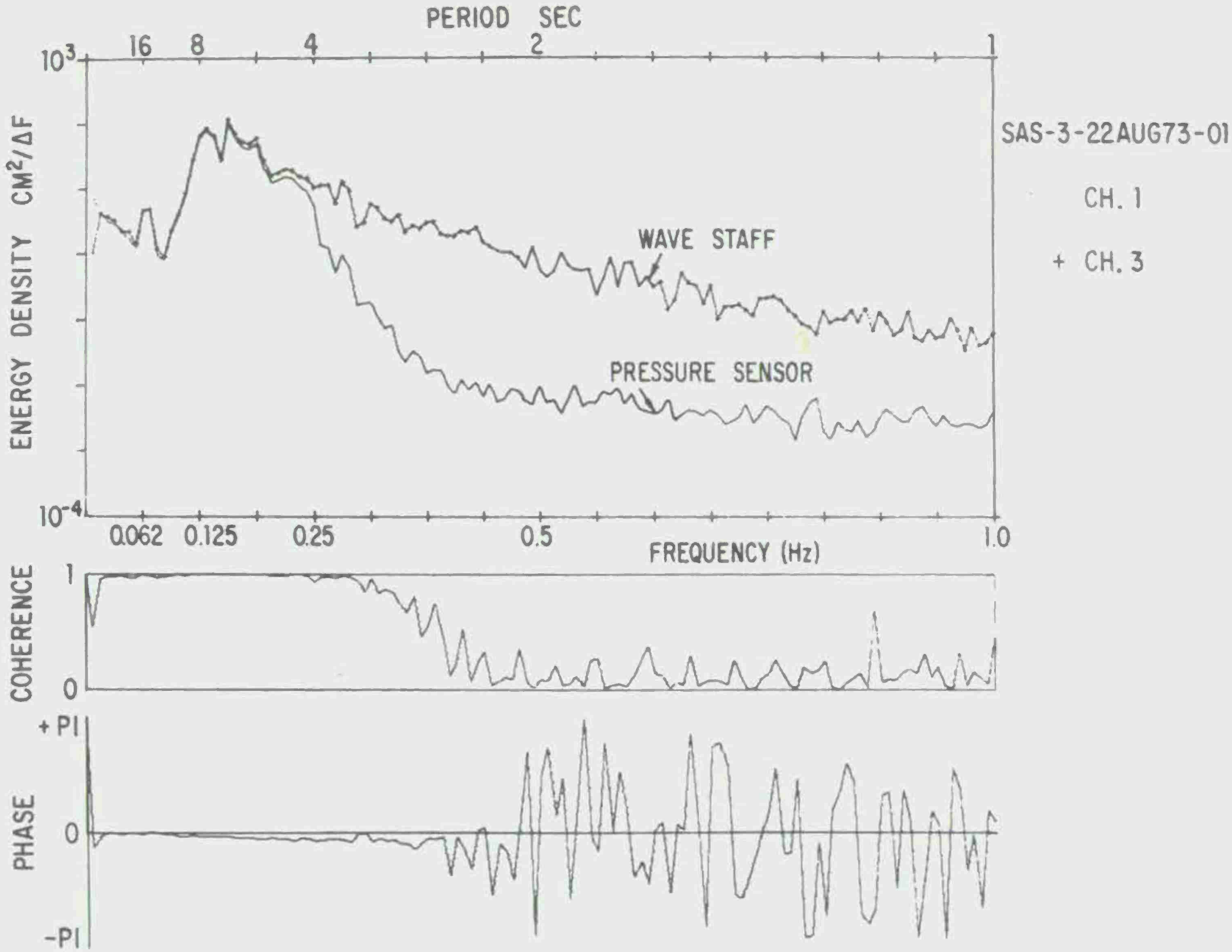

Figure H-1. Frequency and cross-spectra of a bottom-mounted pressure sensor and the surface-piercing resistive wire gage for simultaneous runs off Scripps Pier. The pressure-sensor spectrum is depth corrected for a 5.3-meter depth from 0.0 to 0.25 hertz. The sensors show good spectral agreement below 0.3 hertz.

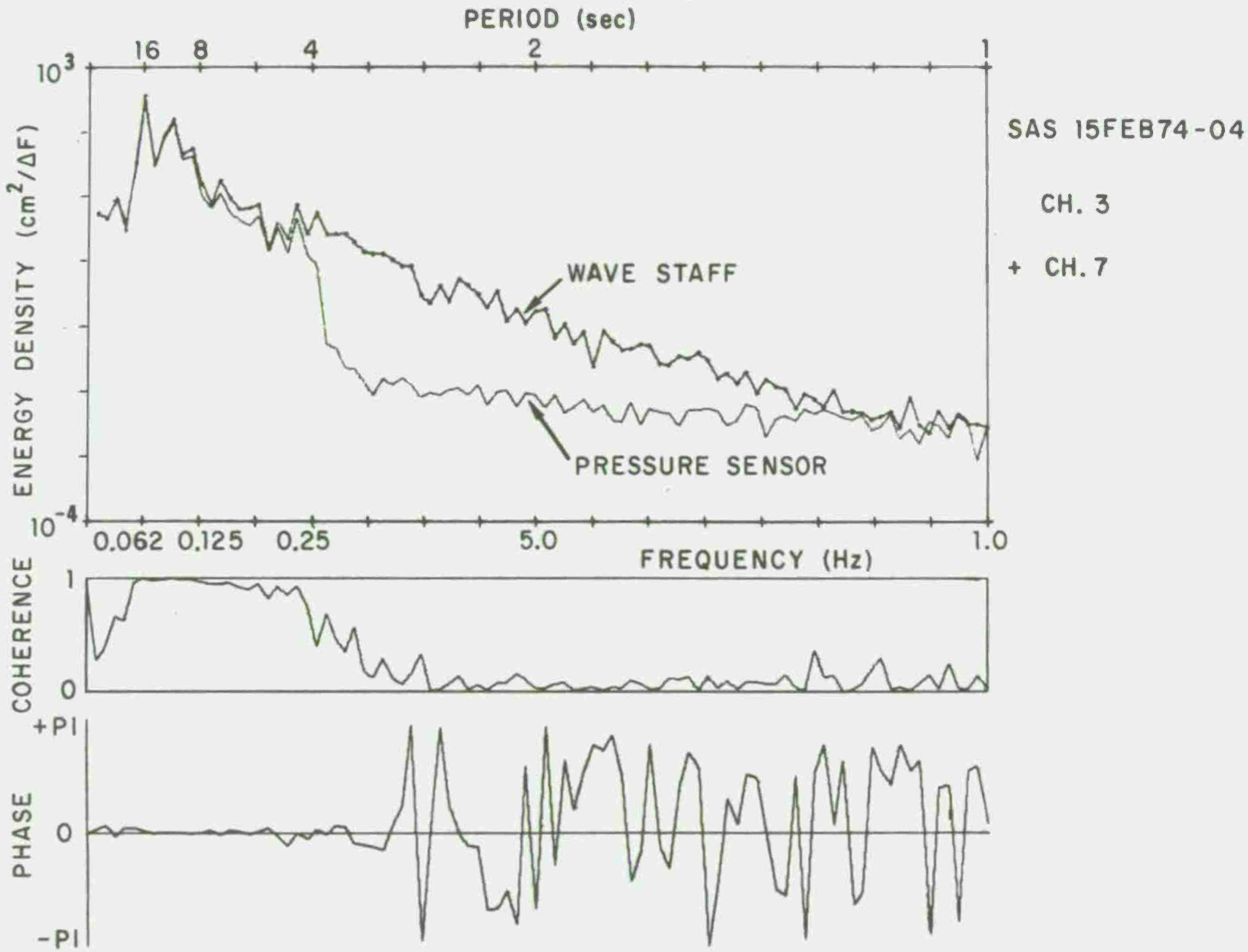

Figure H-2. Frequency and cross-spectra of pressure sensor 3 and the surface-piercing resistive wire gage mounted on the station. The station was temporarily tethered. The spectral values for the pressure sensor are depth corrected from 0.0 to 0.25 hertz.

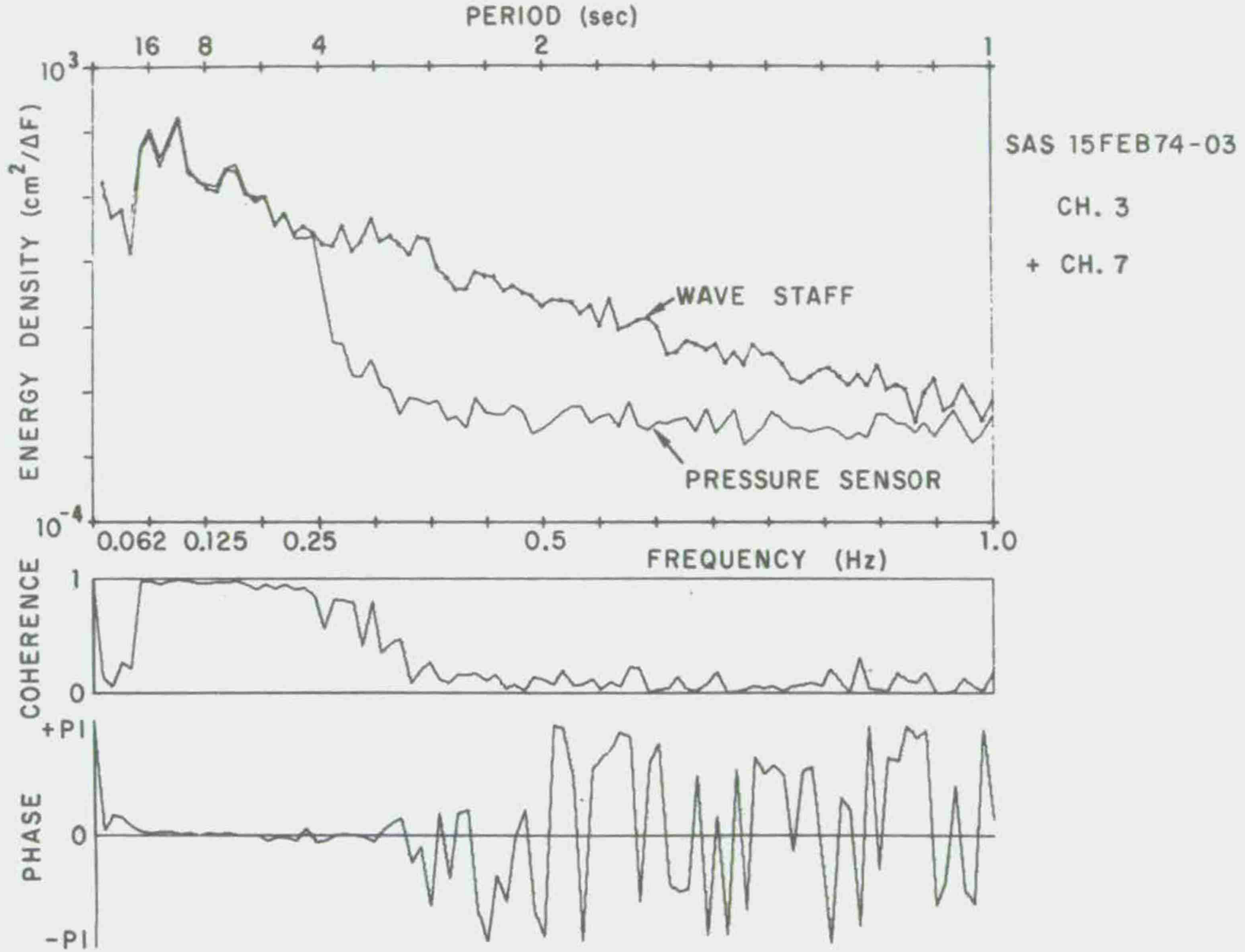

Figure H-3. Frequency and cross-spectra of pressure sensor 3 and the surface-piercin resistive wire gage mounted on the station. The station was temporarily tethered. The spectral values for the pressure sensor are depth correct from 0.0 to 0.25 hertz.

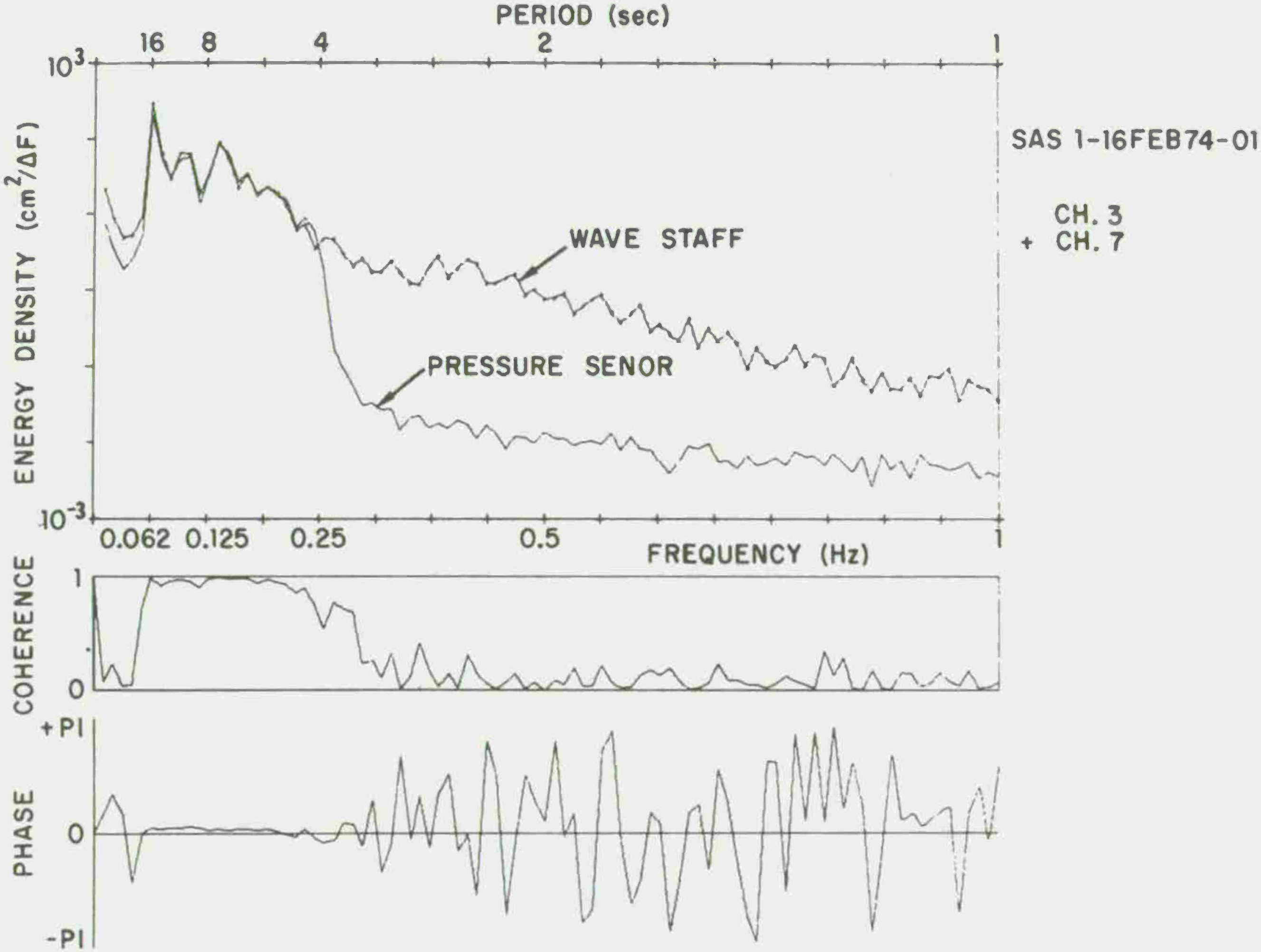

Figure H-4. Frequency and cross-spectra of pressure sensor 3 and the surface-piercing resistive wire gage mounted on the tethered spar. The pressure-sensor spectrum is depth corrected from 0.0 to 0.25 hertz for a 10-meter depth.

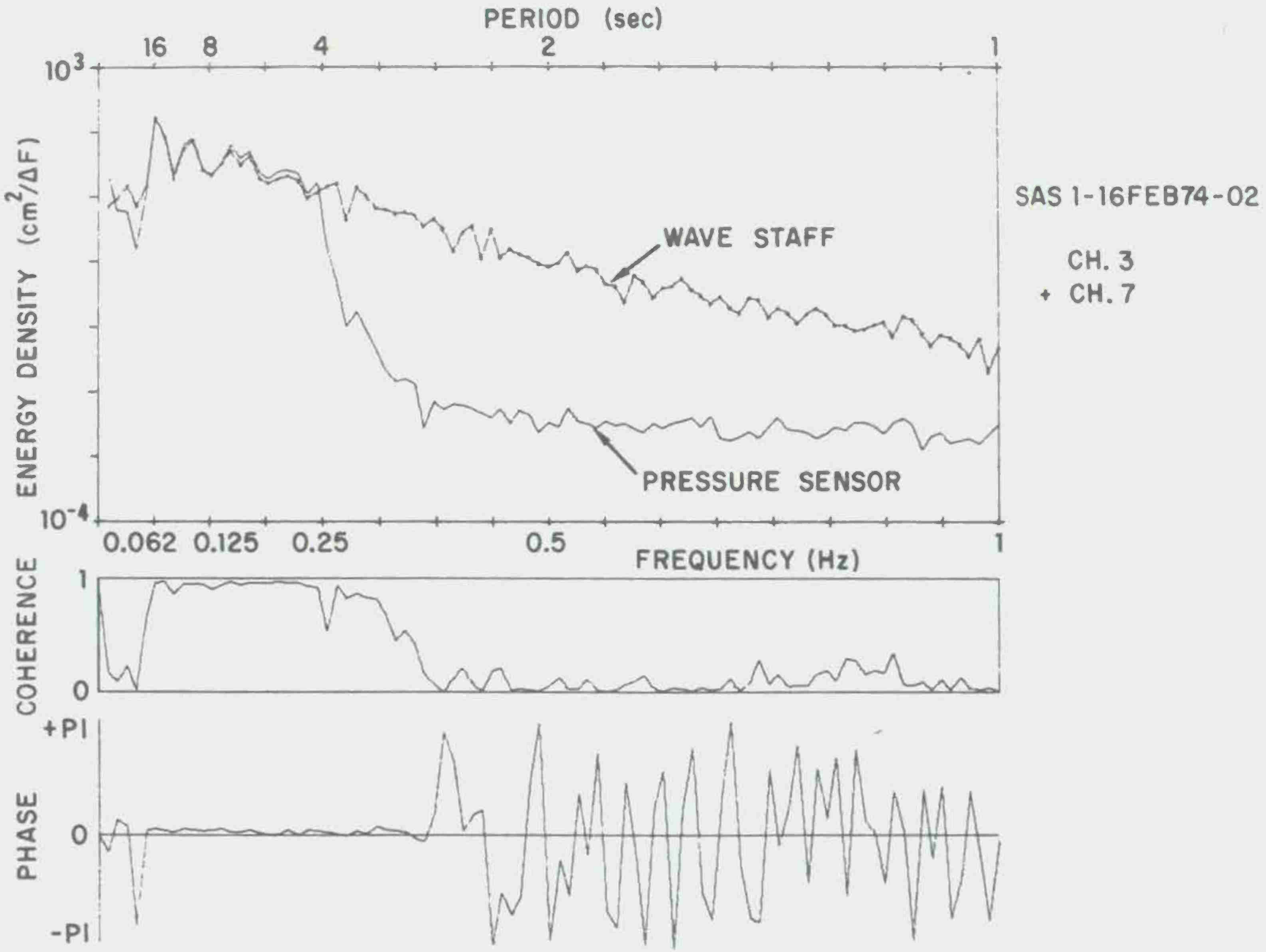

Figure H-5. Frequency and cross-spectra of pressure sensor 3 and the surface-piercing resistive wire gage mounted on the tethered spar. The pressure-sensor spectrum is depth corrected up to 0.25 hertz for a 10-meter depth.

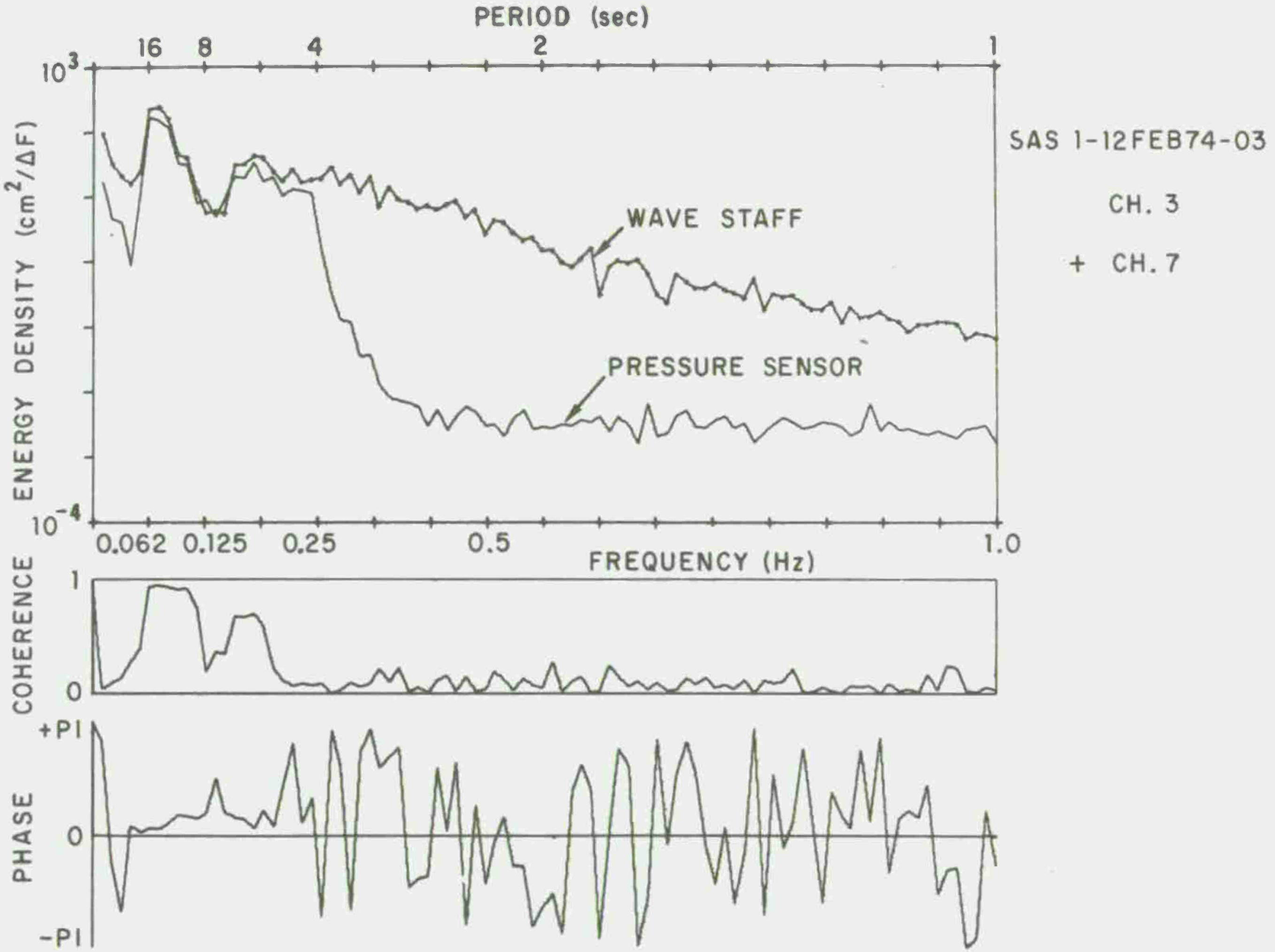

Figure H-6. Frequency and cross-spectra of pressure sensor 3 and the surface-piercing resistive wire gage mounted on the untethered station. The frequency spectra of the pressure sensor is depth corrected from 0.0 to 0.25 hertz.

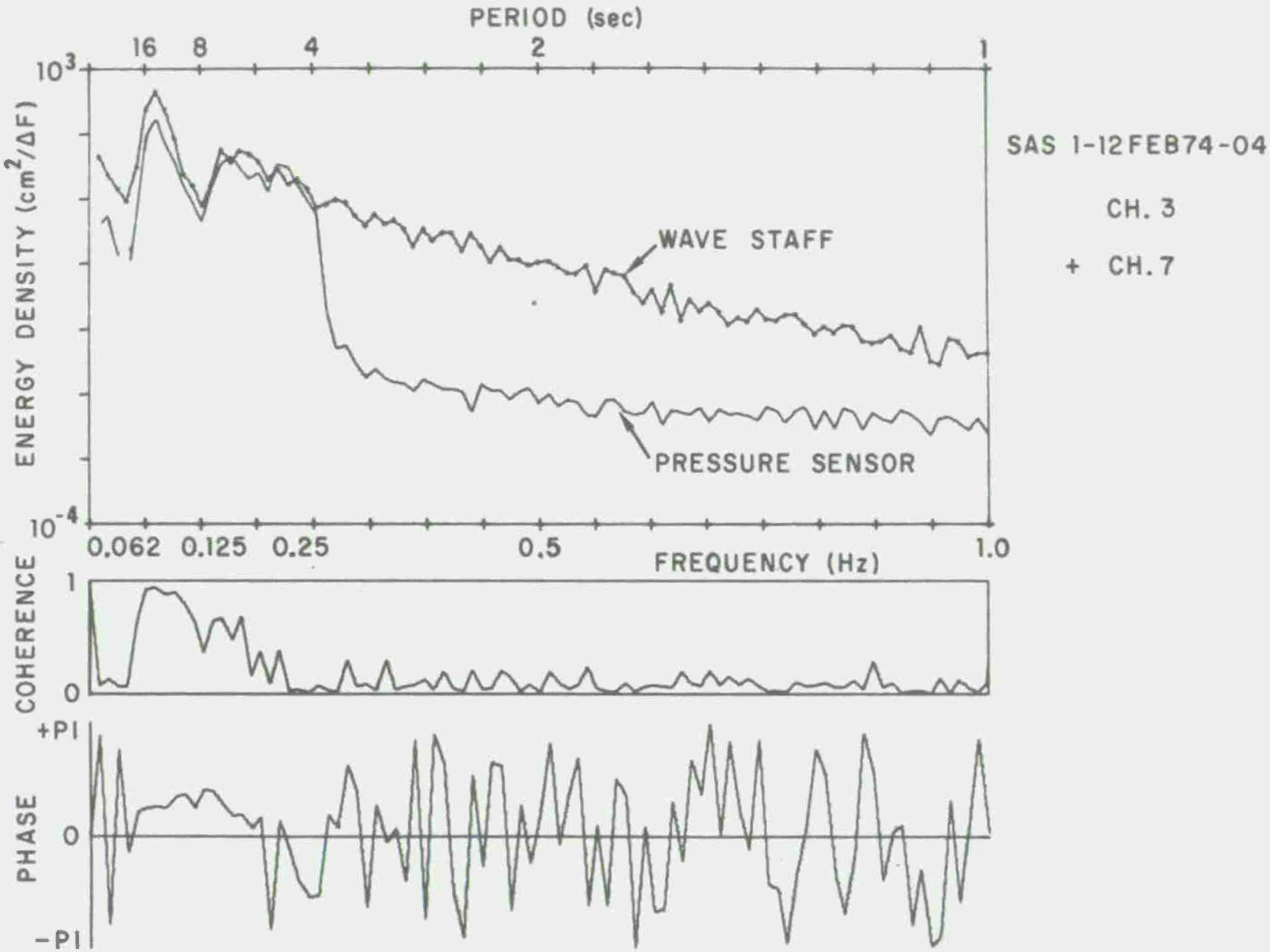

Figure H-7. Frequency and cross-spectra of pressure sensor 3 and the surface-piercing resistive wire gage mounted on the untethered station. The spectral values of the pressure sensor are depth corrected from 0.0 to 0.25 hertz. Although the low-frequency peak is coherent, the wave staff recorded more energy and the signals of the two different sensors are not in phase.

APPENDIX I

FREQUENCY OF OCCURRENCE OF SPECTRAL PEAKS

Tabular representation of the frequency distribution of spectral peaks as a function of direction, period, and height class.

Table I-1. Frequency distribution of peak energy versus direction of propagation and wave period. The directions are for a depth of 10 meters and are relative to the normal to the coast at Torrey Pines Beach, California. The frequencies of occurrence are given in percent for 109 runs in the summer months.

Direction	20° - 16° South				15° - 11° South					10° - 6° South						5° - 1° South			
Period (sec)	18.4-15.4	15.3-13.2	13.1-11.6	11.5-10.3	18.4-15.4	15.3-13.2	13.1-11.6	11.5-10.3	10.2-9.3	15.3-13.2	13.1-11.6	11.5-10.3	10.2-9.3	9.2-8.4	8.3-7.1	15.3-13.2	13.1-11.6	11.5-10.3	10.2-9.3
Energy (CM^2)																			
0 - 50	0.9		5.5		9.2	14.7	1.8			0.9									
50 - 100	1.8	0.9			5.5	14.7	0.9			1.8									
100 - 150		0.9			2.8	10.1				0.9							1.8		
150 - 200					6.4	2.8		0.9							0.9				
200 - 250					2.8	0.9				0.9							0.9		
250 - 300					0.9	0.9													
300 - 350					0.9	0.9													
350 - 400																			
400 - 450																			
450 - 500																			
500 - 550																			
550 - 600						0.9													
600 -650																			

Table I-1. (Cont'd)

Direction	0° - 5° North							6° - 10° North							11° - 15° North						
Period (sec)	13.1-11.6	11.5-10.3	10.2-9.3-	9.2-8.4	8.3-7.1	7.0-6.2	6.1-5.1	13.1-11.6	11.5-10.3	10.2-9.3	9.2-8.4	8.3-7.1	7.0-6.2	6.1-5.1	13.1-11.6	11.5-10.3	10.2-9.3	9.2-8.4	8.3-7.1	7.0-6.2	6.1-5.1
Energy (CM^2)																					
0 - 50								0.9									1.8	2.8	2.8	0.9	1.8
50 - 100						0.9	0.9					0.9	0.9	0.9	0.9		1.8	1.8	0.9	0.9	0.9
100 - 150																0.9	1.8	2.8	3.7		0.9
150 - 200	0.9					0.9				0.9			0.9				1.8	0.9	0.9		
200 - 250													0.9			0.9	0.9	1.8	0.9		
250 - 300	0.9										1.8							0.9	0.9	0.9	
300 - 350																			0.9		
350 - 400												0.9						0.9	0.9		
400 - 450																	0.9		0.9		
450 - 500																					
500 - 550																					
550 - 600												0.9							0.9		
600 - 650																	0.9	0.9			
650 - 700																			0.9		

Table I-1. (Cont'd)

Direction	16° - 20° North					21° - 25° North			No Direction Obtained						
Period (sec)	10.2-9.3	9.2-8.4	8.3-7.1	7.0-6.2	6.1-5.1	8.3-7.1	7.0-6.2	6.1-5.1	11.5-10.3	10.2-9.3	9.2-8.4	8.3-7.1	7.0-6.2	6.1-5.1	5.0-4.0
Energy (CM^2)															
0 - 50			0.9		0.9			0.9			0.9	0.9	5.5	4.6	5.5
50 - 100	0.9	0.9	0.9	2.8	1.8		0.9				0.9	0.9	1.8	7.3	4.6
100 - 150	0.9	0.9	2.8		0.9		0.9			0.9		0.9	1.8	0.9	2.8
150 - 200			0.9		0.9										0.9
200 - 250			1.8												
250 - 300											0.9				
300 - 350			0.9									0.9	0.9		
350 - 400															
400 - 450															
450 - 500				0.9											
500 - 550															
550 - 650															

Table I-2. Frequency distribution of peak energy versus direction of propagation and wave period. The directions are for a depth of 10 meters and are relative to the normal to the coast at Torrey Pines Beach, California. The frequencies of occurrence are given in percent for 120 runs in the fall months.

Direction	15° - 11° South							10° - 6° South							5° - 1° South				
Period (sec)	18.4-15.4	15.3-13.2	13.1-11.6	11.5-10.3	10.2-9.3	9.2-8.4	8.3-7.1	18.4-15.4	15.3-13.2	13.1-11.6	11.5-10.3	10.2-9.3	9.2-8.4	8.3-7.1	18.4-15.4	15.3-13.2	13.1-11.6	11.5-10.3	10.2-9.3
Energy (CM^2)																			
10 - 50	6.7	4.2					0.8	2.5	4.2						1.7			0.8	
50 - 100	2.5	5.8	0.8					4.2	5.8					0.8		1.7			
100 - 150	0.8	1.7						0.8	4.2										
150 - 200		0.8						0.8	4.2						0.8				
200 - 250	1.7	1.7				0.8			1.7						0.8	1.7			
250 - 300	0.8	0.8						0.8											0.8
300 - 350		1.7																	
350 - 400		1.7																	
400 - 450		0.8																	0.8
450 - 500																			
500 - 550																			
550 - 600																			
600 - 650																			
650 - 700																			
700 - 800																			
800 - 900																			
900 - 1000																			
1000 - 1200																			
1200 - 1400																			
1400 - 1600																			
1600 - 1800																			
1800 - 2000																			

Table I-2. (Cont'd)

Direction	0° - 4° North				5° - 9° North								10° - 14° North						
Period (sec)	15.3-13.2	13.1-11.6	11.5-10.3	10.2-9.3	15.3-13.2	13.1-11.6	11.5-10.3	10.2-9.3	9.2-8.4	8.3-7.1	7.0-6.2	6.1-5.1	13.1-11.6	11.5-10.3	10.2-9.3	9.2-8.4	8.3-7.1	7.0-6.2	6.1-5.1
Energy (cm^2)																			
10 - 50						0.8	1.7		0.8	0.8				0.8	3.3	1.7	0.8	0.8	
50 - 100						2.5	1.7		0.8	1.7			0.8	3.3	5.0		1.7		0.8
100 - 140						0.8		0.8				0.8	0.8	0.8		0.8			1.7
150 - 200		0.8				0.8							0.8	1.7			1.7		
200 - 250					0.8		0.8	0.8						0.8		0.8		0.8	0.8
250 - 300	0.8			0.8		0.8		0.8						1.7	0.8	1.7	1.7		
300 - 350		0.8				1.7	0.8						0.8		0.8	1.7	1.7		
350 - 400				0.8												1.7	0.8		
400 - 450					0.8	1.7										1.7			
450 - 500																			
500 - 550				0.8		0.8		0.8											
550 - 600														0.8					
600 - 650						0.8											0.8		
650 - 700																			
700 - 800														0.8					
800 - 900														0.8	0.8				
900 - 1000																			
1000 - 1200																			
1200 - 1400					0.8														
1400 - 1600																			
1600 - 1800																			
1800 - 2000																			

Table I-2. (Cont'd)

Direction	15° - 19° North								20° - 24° North				No Direction Obtained								
Period (sec)	13.1-11.6	11.5-10.3	10.2-9.3	9.2-8.4	8.3-7.1	7.0-6.2	6.1-5.1	5.0-4.0	8.3-7.1	7.0-6.2	6.1-5.1	5.0-4.0	18.4-15.4	15.3-13.2	13.1-11.6	11.5-10.3	9.2-8.4	8.3-7.1	7.0-6.2	6.1-5.1	5.0-4.0
Energy (cm^2)																					
10 - 50			0.8		1.7														3.3	4.0	5.0
50 - 100	0.8		0.8					0.8	0.8				0.8	0.8				1.7		3.3	1.7
100 - 150			0.8		3.3	0.8	0.8	0.8		0.8					0.8		0.8	0.8	0.8	0.8	1.7
150 - 200				0.8	0.8		2.5				0.8	0.8	0.8				0.8		2.5	0.8	1.7
200 - 250																		0.8			0.8
250 - 300					0.8						0.8										
300 - 350			0.8	0.8		0.8			2.5	0.8											
350 - 400																					
400 - 450																					
450 - 500			0.8																		
500 - 550															0.8						
550 - 600																					
600 - 650																					
650 - 700																0.8					
700 - 800																					
800 - 900					0.8																
900 - 1000																					
1000 - 1200																					
1200 - 1400																					
1400 - 1600																					
1600 - 1800																					
1800 - 2000																					

Table I-3. Frequency distribution of peak energy versus direction of propagation and wave period. The directions are for a depth of 10 meters and are relative to the normal to the coast at Torrey Pines Beach, California. The frequencies of occurrence are given in percent for 181 runs in winter months.

Direction	30° - 21° South				20° - 16° South									15° - 11° South						
Period (sec)	9.2-8.4	8.3-7.1	7.0-6.2	6.1-5.1	15.3-13.2	13.1-11.6	11.5-10.3	10.2-9.3	9.2-8.4	8.3-7.1	7.4-6.2	6.1-5.1	5.0-4.0	18.4-15.4	15.3-13.2	13.1-11.6	11.5-10.3	10.2-9.3	9.2-8.4	8.3-7.1
Energy (cm^2)																				
10 - 50										0.6		1.1	0.6							0.6
50 - 100		0.6			0.6									0.6	0.6					0.6
100 - 150				0.6																
150 - 200				0.6																
200 - 250									0.6											
250 - 300																				
300 - 350		0.6								0.6					0.6					
350 - 400													0.6							
400 - 450																				
450 - 500																				
500 - 550		0.6																		
550 - 600																				
600 - 650																				
650 - 700																				
700 - 800																				
800 - 900	0.6	0.6								0.6										
900 - 1000																				
1000 - 1200																				
1200 - 1400		0.6																		
1400 - 1600																				
1600 - 1800																				
1800 - 2000																				

Table I-3. (Cont'd)

Direction	10° - 6° South									5° - 1° South							
Period (sec)	15.3-13.2	13.1-11.6	11.5-10.3	10.2-9.3	9.2-8.4	8.3-7.1	7.0-6.1	6.1-5.1	5.0-4.0	18.4-15.4	15.3-13.2	13.1-11.6	11.5-10.3	10.2-9.3	9.2-8.4	8.3-7.1	7.0-6.2
Energy (cm^2)																	
10 - 50	1.1					1.1	0.6										
50 - 100	0.6	0.6									1.7		0.6		0.6		
100 - 150	2.2			0.6							1.1	1.1			0.6		
150 - 200	1.1					0.6					0.6						
200 - 250								0.6	0.6		2.2						
250 - 300						0.6					0.6	0.6					
300 - 350										0.6							
350 - 400											0.6				0.6		
400 - 450																	
450 - 500																	
500 - 550											0.6					0.6	
550 - 600																	
600 - 650																	
650 - 700																	
700 - 800											0.6						
800 - 900											0.6						
900 - 1000				0.6							0.6						
1000 - 1200												1.1		0.6			
1200 - 1400																	
1400 - 1600					0.6							0.6					
1600 - 1800																	
1800 - 2000						0.6											
2000 - 2500																	
2500 - 3000																	
3000 - 3500											0.6						

Table I-3. (Cont'd)

Direction	0° - 4° North										5° - 9° North								
Period (sec)	18.4-15.4	15.3-13.2	13.1-11.6	11.5-10.3	10.2-8.3	9.2-8.4	8.3-7.1	7.0-6.2	6.1-5.1	5.0-4.0	18.4-15.4	15.3-13.2	13.1-11.6	11.5-10.3	10.2-9.3	9.2-8.4	8.3-7.1	7.0-6.2	6.1-5.1
Energy (cm^2)																			
10 - 50								1.1	0.6									0.6	
50 - 100	1.7	1.1						1.1		0.6	1.1	0.6		1.1	0.6			1.1	2.2
100 - 150		1.7	1.1				1.1	1.1			0.6	0.6	0.6			0.6	0.6	1.1	0.6
150 - 200		0.6			0.6			0.6				1.1	0.6	0.6				0.6	
200 - 250	0.6	1.7	0.6	0.6									0.6	0.6	0.6		0.6	0.6	
250 - 300		0.6	1.1	0.6						0.6		1.1					1.1	0.6	
300 - 350			1.7								0.6	1.1	1.1						
350 - 400		0.6		0.6								1.7							
400 - 450		1.1	0.6								0.6	0.6	1.7		0.6				
450 - 500		0.6					0.6					0.6							
500 - 550		0.6	0.6									1.1							
550 - 600		0.6											0.6						
600 - 650		1.1	1.1	0.6															
650 - 700													1.1						
700 - 800	1.1	0.6									0.6	1.1		0.6					
800 - 900	0.6	1.1	1.7								0.6	1.1	0.6						
900 - 1000		0.6										1.1							
1000 - 1200		1.1										1.7							
1200 - 1400	0.6	2.2	0.6																
1400 - 1600	0.6	0.6										1.1							
1600 - 1800		0.6									0.6	0.6							
1800 - 2000		0.6																	
2000 - 2500																			
2500 - 3000																			
3000 - 3500			0.6																

Table I-3. (Cont'd)

Direction	10° - 14° North									15° - 19° North						20° - 24° North		
Period (sec)	15.3-13.2	13.1-11.6	11.5-10.3	10.2-9.3	9.2-8.4	8.3-7.1	7.0-6.2	6.1-5.1	5.0-4.0	11.5-10.3	10.2-9.3	9.2-8.4	8.3-7.1	7.0-6.2	6.1-5.1	8.3-7.1	7.0-6.2	6.1-5.1
Energy (cm^2)																		
10 - 50					0.6	0.6	1.1					0.6	0.6	1.1			0.6	
50 - 100				1.7		0.6	1.1					0.6	0.6		0.6	1.1	0.6	
100 - 150		1.7								0.6						1.1	0.6	
150 - 200			0.6						1.1					0.6	0.6		0.6	0.6
200 - 250														0.6	0.6			
250 - 300				0.6		1.1	0.6											
300 - 350							0.6			0.6						0.6		
350 - 400	0.6				0.6	0.6								1.1				
400 - 450																0.6		
450 - 500						0.6												
500 - 550																		
550 - 600					0.6		0.6							0.6				
500 - 650		0.6																
650 - 700		0.6		0.6									0.6					
700 - 800				0.6														
800 - 900																		
900 - 1000						0.6												
1000 - 1200	0.6	0.6			0.6													
1200 - 1400		0.6																
1400 - 1600	0.6																	
1600 - 1800																		
1800 - 2000																		

Table I-3. (Cont'd)

Direction	No Direction Obtained									
Period (sec)	18.4-15.4	15.3-13.2	13.1-11.6	11.5-10.3	10.2-9.3	9.2-8.4	8.3-7.1	7.0-6.2	6.1-5.1	5.0-4.0
Energy (cm^2)										
10 - 50	0.6							1.1	2.8	6.6
50 - 100							2.2	3.9	1.7	4.4
100 - 150		0.6						1.7	2.8	1.1
150 - 200							0.6	2.8	1.7	0.6
200 - 250		0.6		0.6	0.6			1.1	0.6	0.6
250 - 300					0.6					
300 - 350		0.6		0.6						
350 - 400				1.1			0.6			
400 - 450		0.6	0.6							
450 - 500		0.6					0.6	0.6		0.6
500 - 550										
550 - 600										
600 - 650			0.6							
650 - 700		1.1	0.6							
700 - 800										
800 - 900										
900 - 1000		0.6		0.6						
1000 - 1200										
1200 - 1400										
1400 - 1600		0.6	0.6							
1600 - 1800										
1800 - 2000		0.6								
2000 - 2500										
2500 - 3000			0.6							

Table I-4. Frequency distribution of peak energy versus direction of propagation and wave period. The directions are for a depth of 10 meters and are relative to the normal to the coast at Torrey Pines Beach, California. The frequencies of occurrence are given in percent for 247 runs in the spring months.

Direction	30°-21° South		20° - 16° South			15° - 11° South										10° - 6° South			
Period (sec)	6.1-5.1	5.0-4.0	18.4-15.4	15.3-13.2	13.1-11.6	18.4-15.4	15.3-13.2	13.1-11.6	11.5-10.3	10.2-9.3	9.2-8.4	8.3-7.1	7.0-6.2	6.1-5.1	5.0-4.0	18.4-15.4	15.3-13.2	13.1-11.6	11.5-10.3
Energy (cm^2)																			
10 - 50		1.2	0.4	2.0	1.2	0.4	2.0						0.4				4.9	0.4	
50 - 100		0.4		3.2		2.4	3.2									2.0	4.4	1.2	
100 - 150						1.2								0.4		1.6	0.8		
150 - 200						0.4										0.8	2.0		
200 - 250															0.4	1.2	0.4		
250 - 300						1.2											0.4		
300 - 350																	0.8		
350 - 400																			
400 - 450																			
450 - 500												0.4							
500 - 550																			
550 - 600																			
600 - 650																			
650 - 700																			
700 - 800																			
800 - 900																			
900 - 1000																			
1000 - 1200																			
1200 - 1400																			
1400 - 1600																			
1600 - 1800																			
1800 - 2000																			

Table I-4. (Cont'd)

Direction	5° - 1° South									0° - 4° North									
Period (sec)	18.4-15.4	15.3-13.2	13.1-11.6	11.5-10.3	10.2-9.3	9.2-8.4	8.3-7.1	7.0-6.2	6.1-5.1	18.4-15.4	15.3-13.2	13.1-11.6	11.5-10.3	10.2-9.3	9.2-8.4	8.3-7.1	7.0-6.2	6.1-5.1	5.0-4.0
Energy (cm^2)																			
10 - 50	0.4										0.4	0.4	0.4		0.4	0.8			
50 - 100	0.4									2.4	1.2	0.8	0.4				0.4	0.4	
100 - 150		0.4	0.4							0.8	2.4	0.4	0.4	0.4					
150 - 200		1.2									0.8	1.6	0.4		0.8				
200 - 250		0.8					0.4				0.8	0.4			0.4	0.4			0.4
250 - 300	0.4	0.4						0.4			0.4	0.8			0.4	0.4			
300 - 350									0.4	0.4	0.4	0.4	0.4						
350 - 400											0.4							0.4	
400 - 450	0.4	0.8										0.4		0.4					
450 - 500																			
500 - 550												0.4			0.4				
550 - 600																0.4			
600 - 650																			
650 - 700																			
700 - 800																			
800 - 900																0.4			
900 - 1000																			
1000 - 1200	0.4									0.4	1.2	0.4							
1200 - 1400										0.4									
1400 - 1600																			
1600 - 1800																			
1800 - 2000																			
2000 - 2500											0.4								

Table I-4. (Cont'd)

Direction	5° - 9° North								10° - 14° North									
Period (sec)	18.4-15.4	15.3-13.2	13.1-11.6	11.5-10.3	10.2-9.3	9.2-8.4	8.3-7.1	7.0-6.2	18.4-15.4	15.3-13.2	13.2-11.6	11.5-10.3	10.2-9.3	9.2-8.4	8.3-7.1	7.0-6.2	6.1-5.1	5.0-4.0
Energy (cm^2)																		
10 - 50	0.4	0.4	0.4		0.8	1.2	0.4				0.4	0.4	0.4	1.2	1.2	0.4		
50 - 100		0.4	1.2	2.4			0.4	0.4			0.4	2.4	1.6	0.8	0.8		0.4	0.4
100 - 150	0.4	0.8	1.6	2.0	0.4				0.4		1.2	1.2	0.8	0.4	0.8	0.4		0.4
150 - 200	0.4	0.8	1.2	2.4			0.4				0.8	2.4		0.4	0.4	0.4		0.8
200 - 250		0.4	1.6	0.4							0.4	1.2	0.4	1.2	0.8			
250 - 300		0.8	0.8									0.4	0.4		1.2			
300 - 350		0.4		0.4										0.4	0.8			
350 - 400	0.4		0.8	0.4		0.4									1.2			
400 - 450				0.4										0.4	0.4			
450 - 500		0.4										0.4	0.4		0.4			
500 - 550		0.4	0.4				0.4				0.4		0.4		0.4			
550 - 600		0.4		0.4									0.8	0.4		0.4		
600 - 650											0.4	0.4		0.4				
650 - 700															1.2			
700 - 800						0.4												
800 - 900							0.4							0.4			0.4	
900 - 1000		1.2																
1000 - 1200			0.4											0.4				
1200 - 1400		0.4.	1.2									0.4						
1400 - 1600		0.4						0.4										
1600 - 1800	0.4	0.4	0.4											0.4				
1800 - 2000		0.4	0.4				0.4							0.4				
2000 - 2500			0.4			0.4												

Table I-4. (Cont'd)

Direction	15° - 19° North					20° - 24° North				No Direction Obtained									
Period (sec)	9.2-8.4	8.3-7.1	7.0-6.2	6.1-5.1	5.0-4.0	8.3-7.1	7.0-6.2	6.1-5.1	5.0-4.0	18.4-15.4	15.3-13.2	13.1-11.6	11.5-10.2	10.2-9.3	9.2-8.4	8.3-7.1	7.0-6.2	6.1-5.1	5.0-4.0
Energy (cm^2)																			
10 - 50		0.4			0.4		0.4		0.4		0.4		0.4	0.8		1.6	2.0	1.2	6.1
50 - 100	0.4	0.8	0.4	1.2			0.4	0.4		0.8		1.2		0.4		0.8	2.0	2.0	5.3
100 - 150	0.4	0.4	0.4					0.4		0.4	0.8	1.2					0.8	2.0	1.2
150 - 200		0.4	0.4	0.4													2.4	0.4	0.8
200 - 250			0.8	0.4								0.4					0.8		0.4
250 - 300				0.4							0.4						1.2		
300 - 350	0.4		0.8						0.4		0.4			0.4			0.4	0.4	
350 - 400		1.2					0.4					0.4			0.4	0.4		0.4	
400 - 450	0.4		0.4														0.8		
450 - 500																0.8			
500 - 550		0.4																	
550 - 600																			
600 - 650																			
650 - 700																	0.4		
700 - 800																			
800 - 900																			
900 - 1000			0.4																
1000 - 1200																			
1200 - 1400	0.4										0.4								
1400 - 1600																			
1600 - 1800																			
1800 - 2000																			
2000 - 2500		0.4				0.4													

APPENDIX J

SEASONAL ENERGY-DIRECTIONAL PLOTS FOR GIVEN FREQUENCY BANDS

Included are plots of the total energy versus direction of propagation for specific seasons and wave periods. Each plot indicates the summed energies for spectral peaks of a specific wave period centered in the given frequency band. The winter data consists of 181 runs taken during the months of December, January, and February; spring data consists of 247 runs taken during March, April, and May; summer data consists of 109 runs taken during June, July, and August; fall data consists of 120 runs taken during September, October, and November.

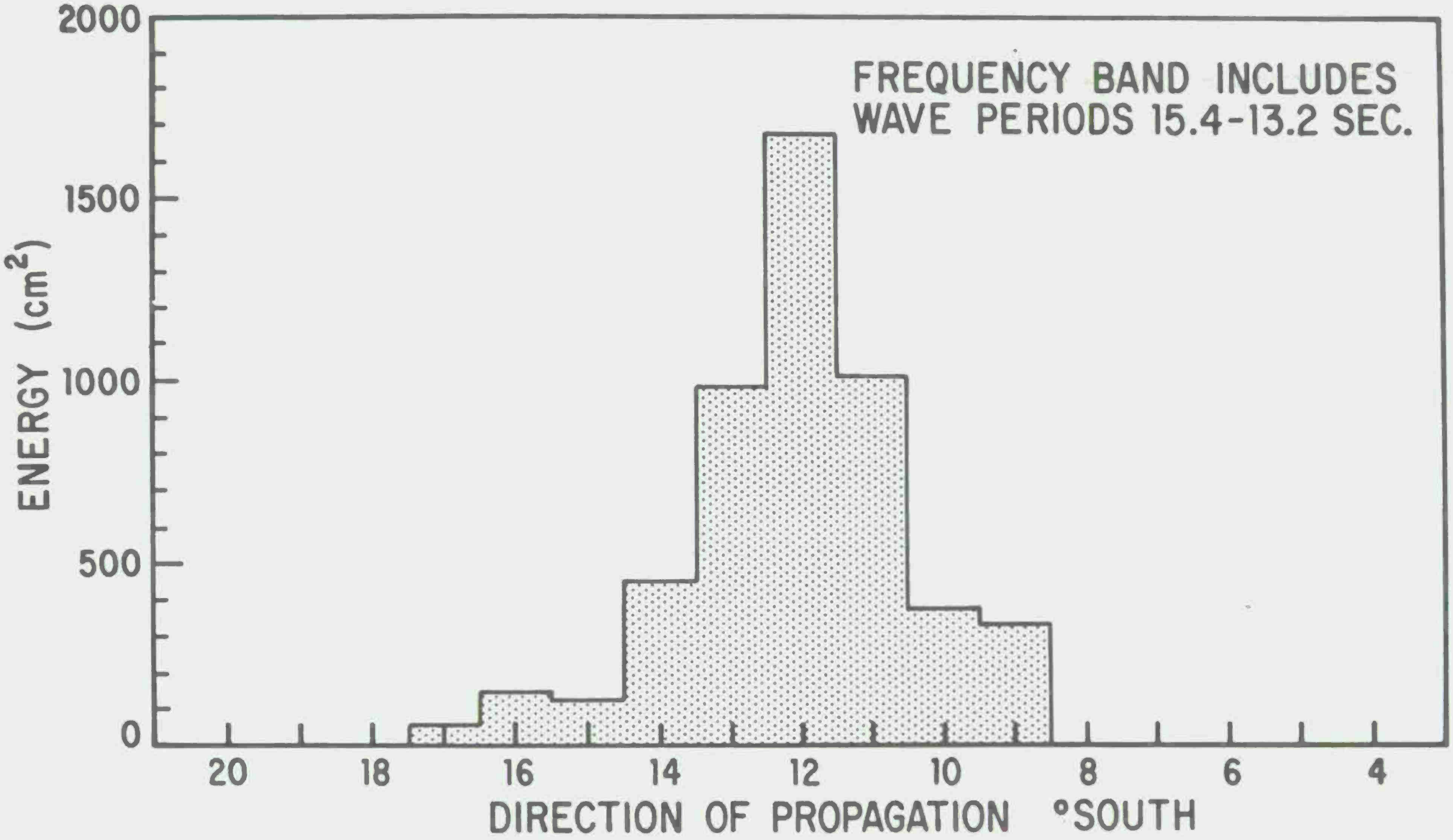

Figure J-1. A plot of the total energy versus direction of propagation during the summer months. The directions are in degrees from normal to the coast at Torrey Pines Station.

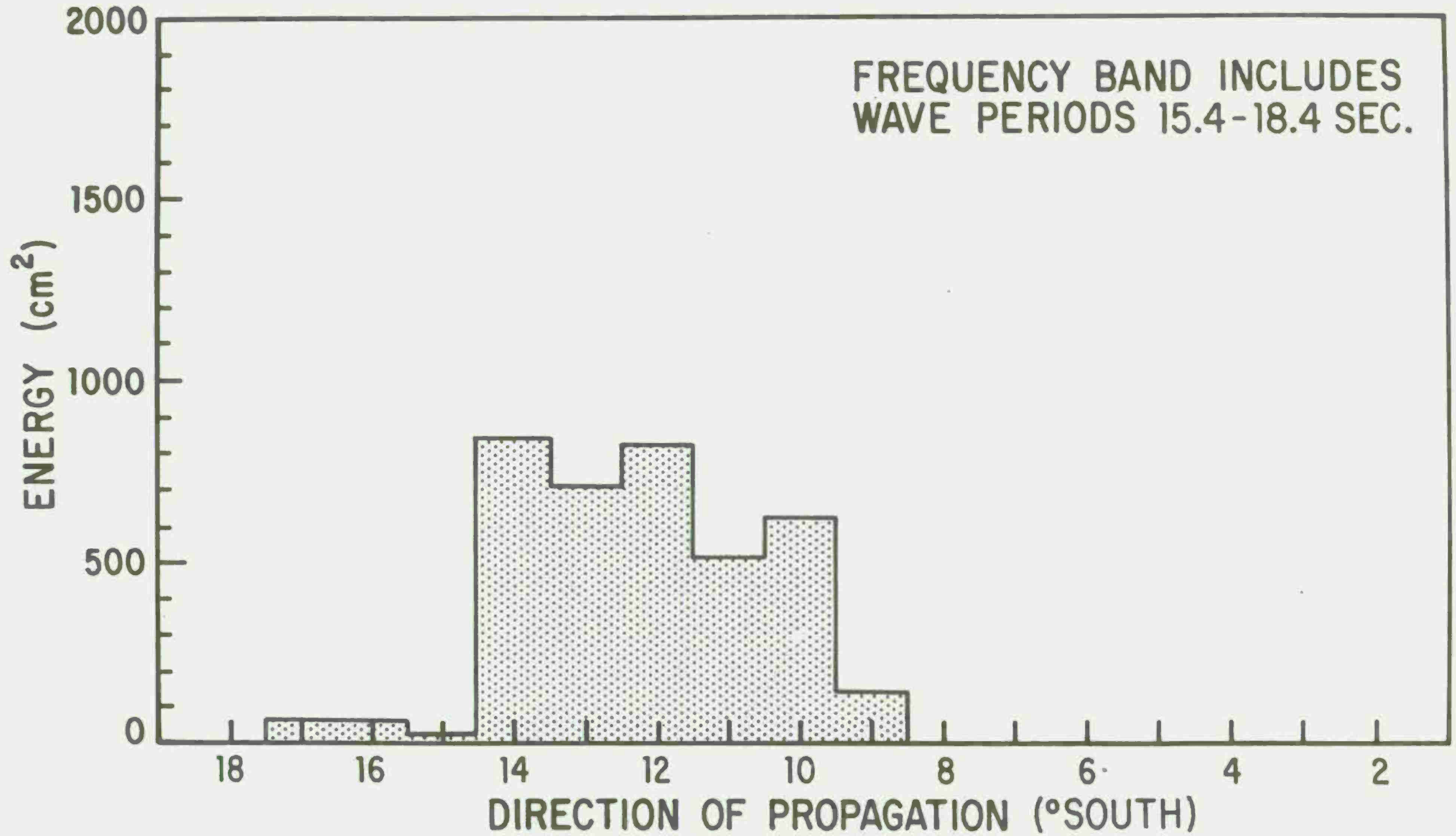

Figure J-2. A plot of the total energy versus direction of propagation during the summer months. The directions are in degrees from normal to the coast at Torrey Pines Station.

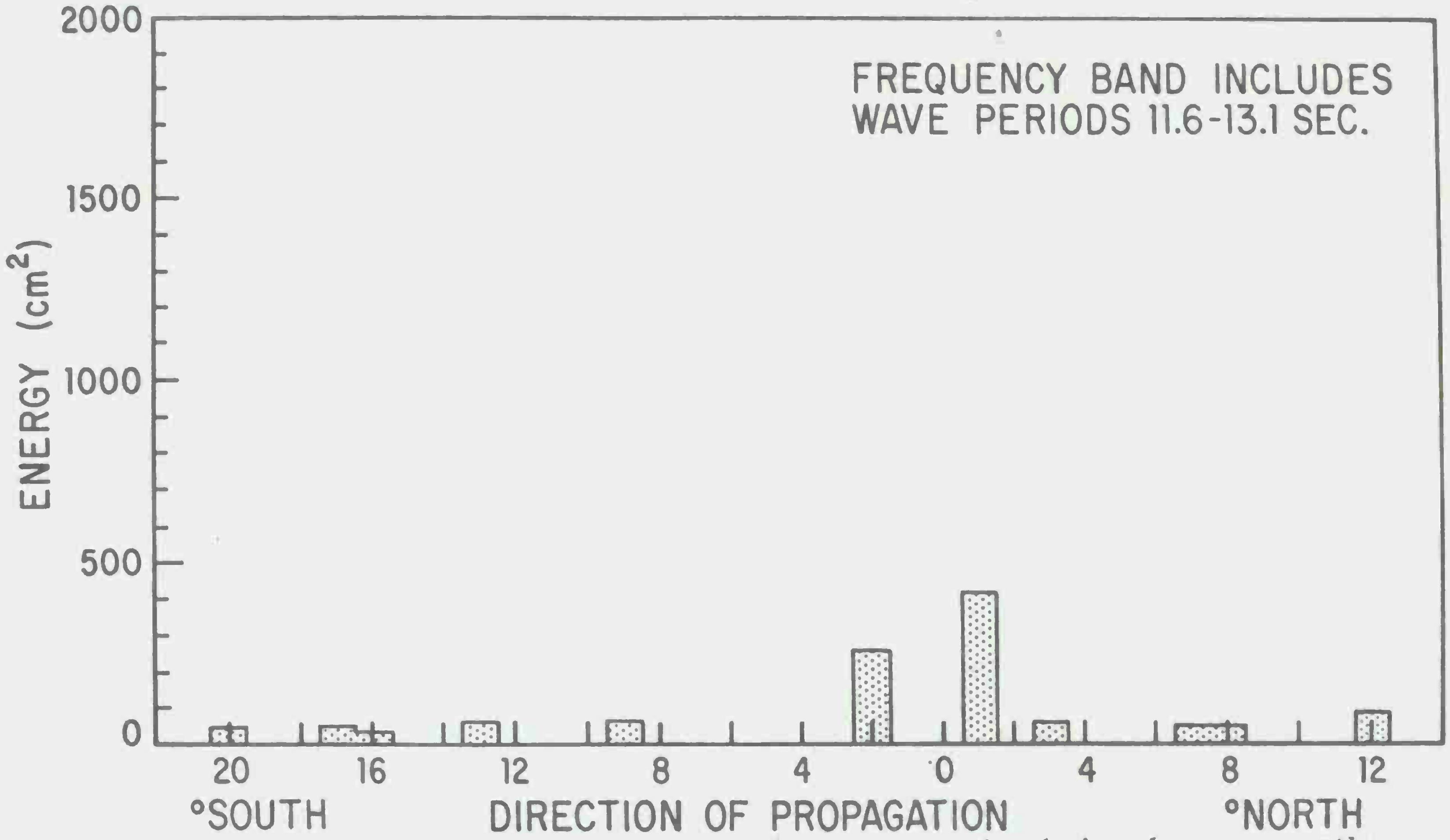

Figure J-3. A plot of the total energy versus direction of propagation during the summer months. The directions are in degrees from normal to the coast at Torrey Pines Station.

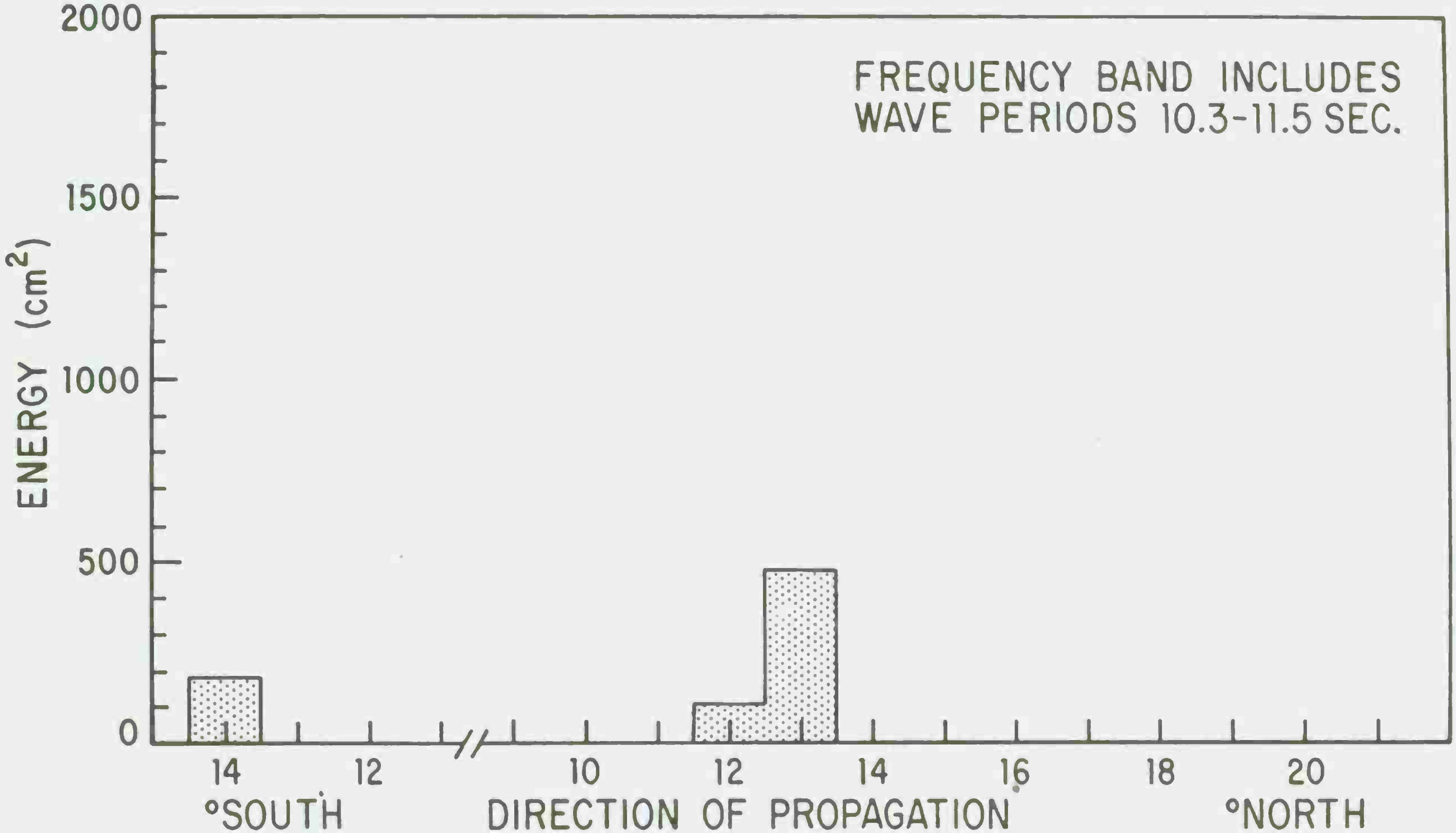

Figure J-4. A plot of the total energy versus direction of propagation during the summer months. The directions are in degrees from normal to the coast at Torrey Pines Station.

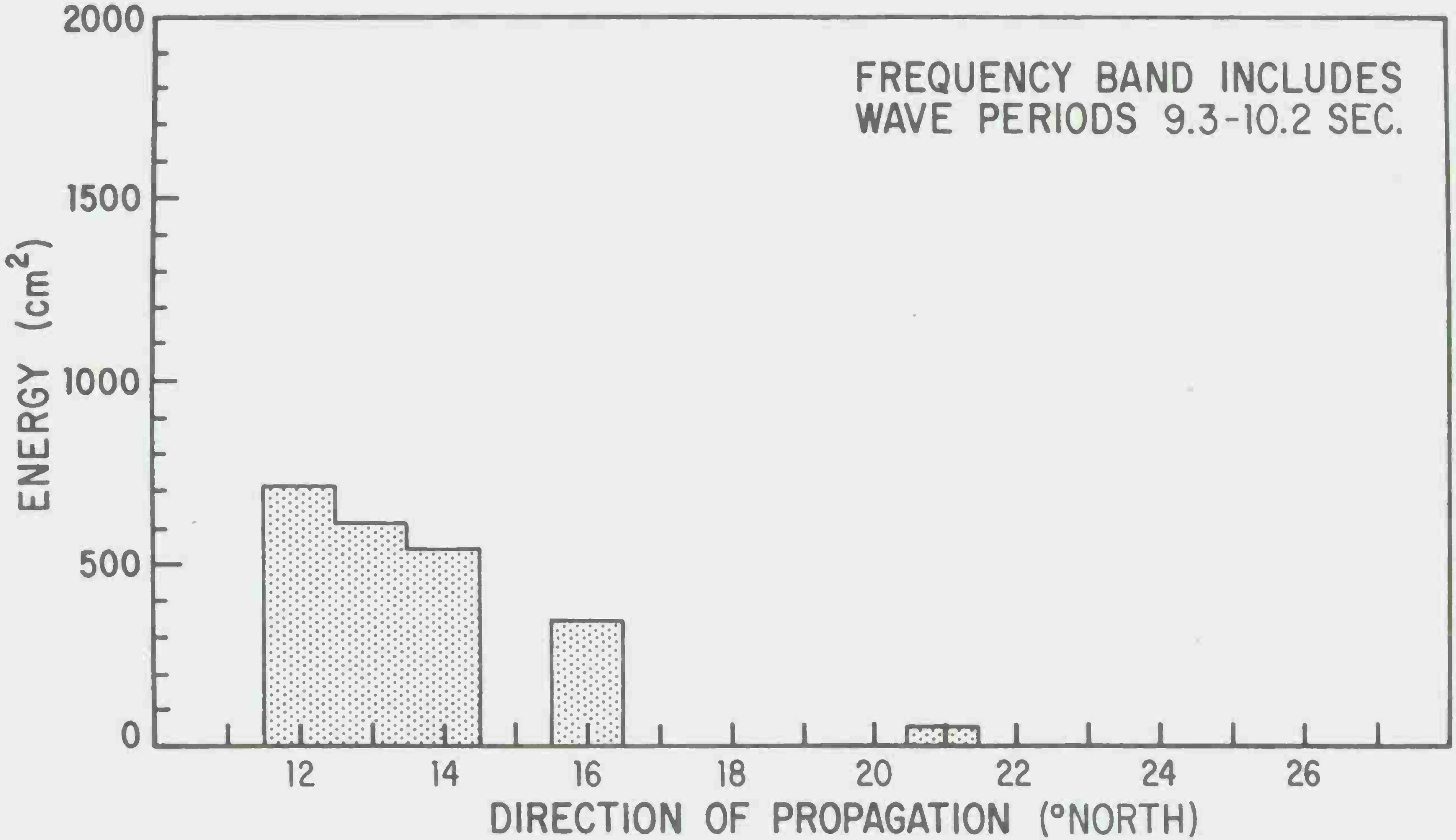

Figure J-5. A plot of the total energy versus direction of propagation during the summer months. The directions are in degrees from normal to the coast at Torrey Pines Station.

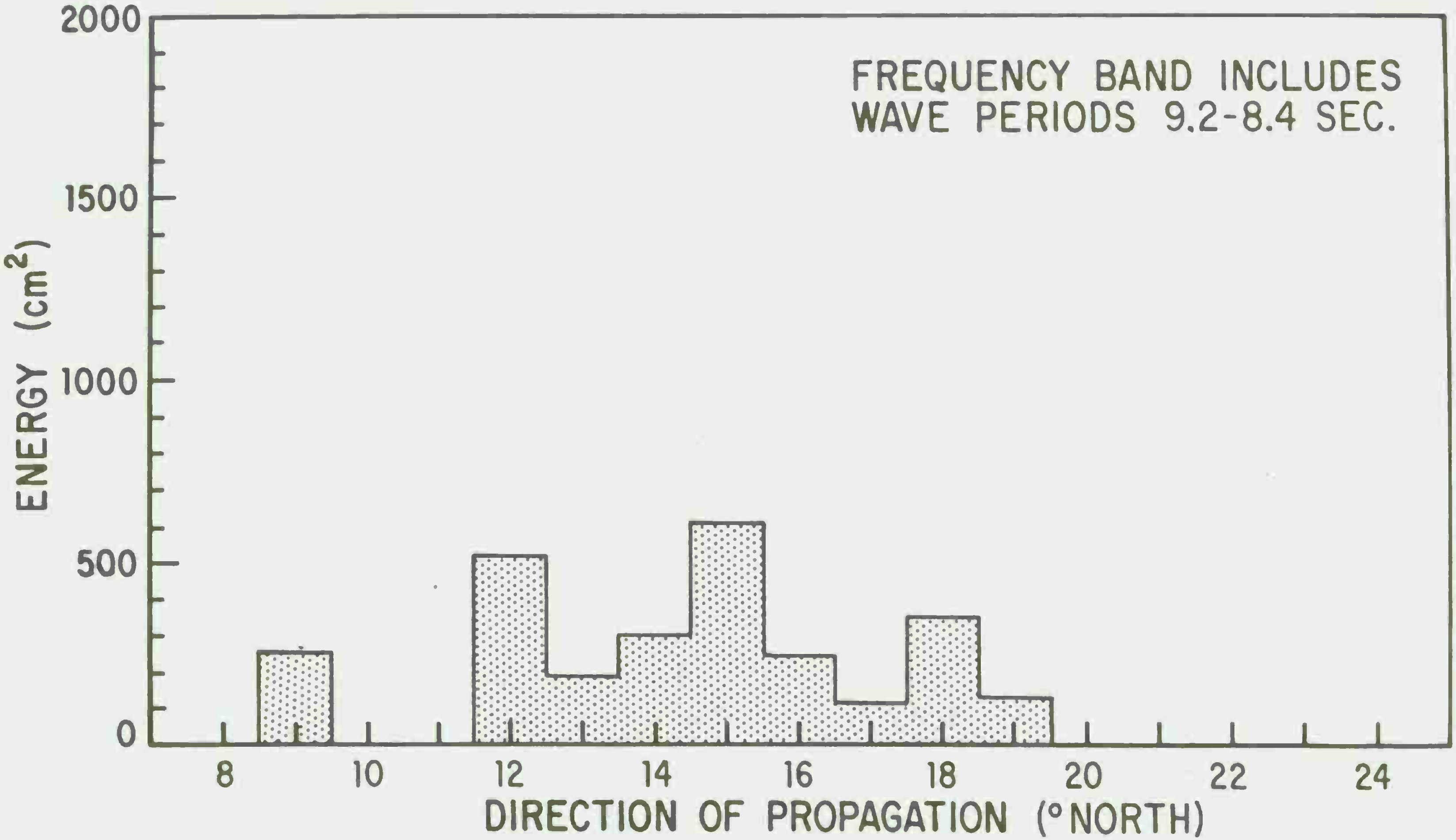

Figure J-6. A plot of the total energy versus direction of propagation during the summer months. The directions are in degrees from normal to the coast at Torrey Pines Station.

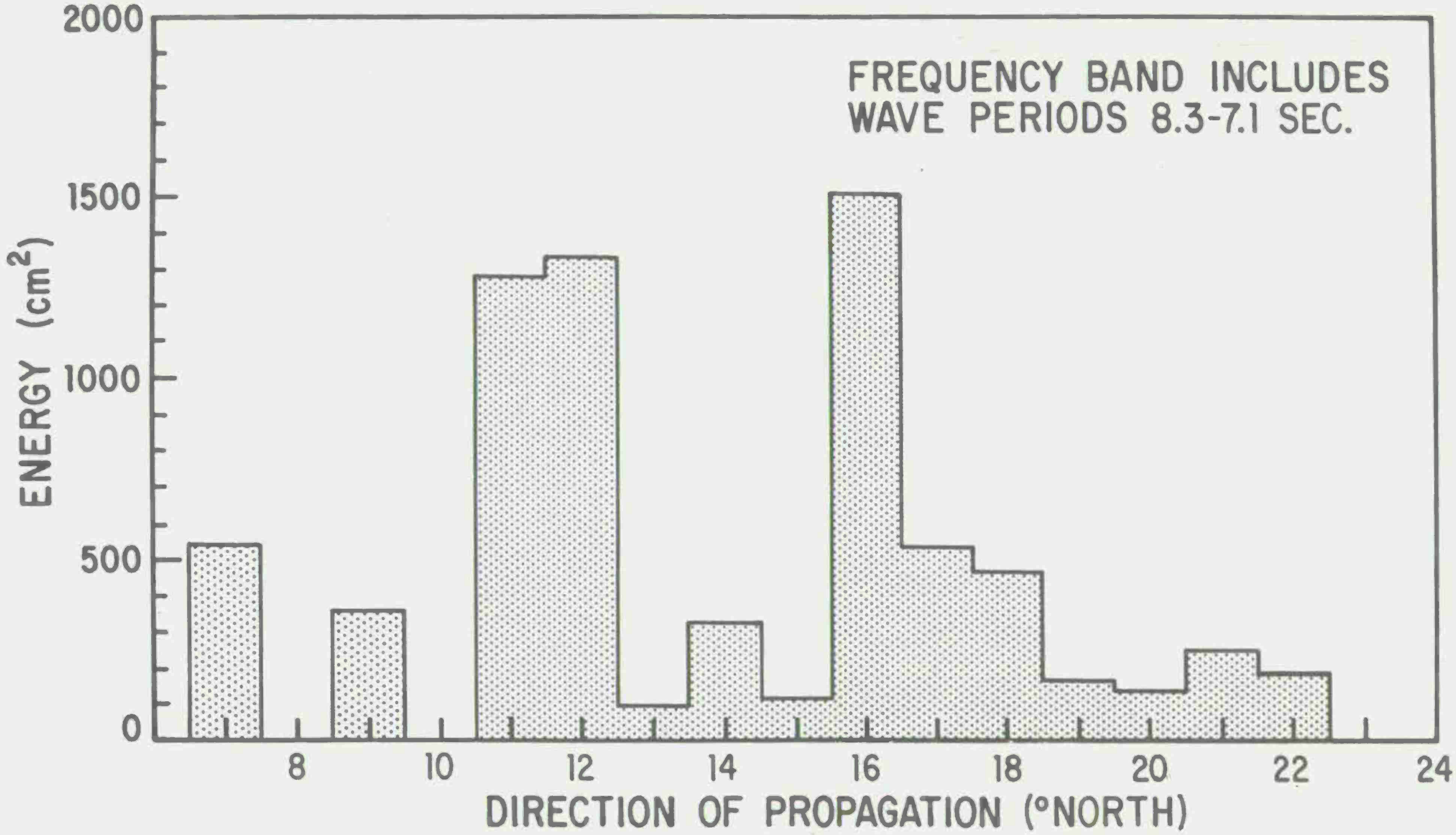

Figure J-7. A plot of the total energy versus direction of propagation during the summer months. The directions are in degrees from normal to the coast at Torrey Pines Station.

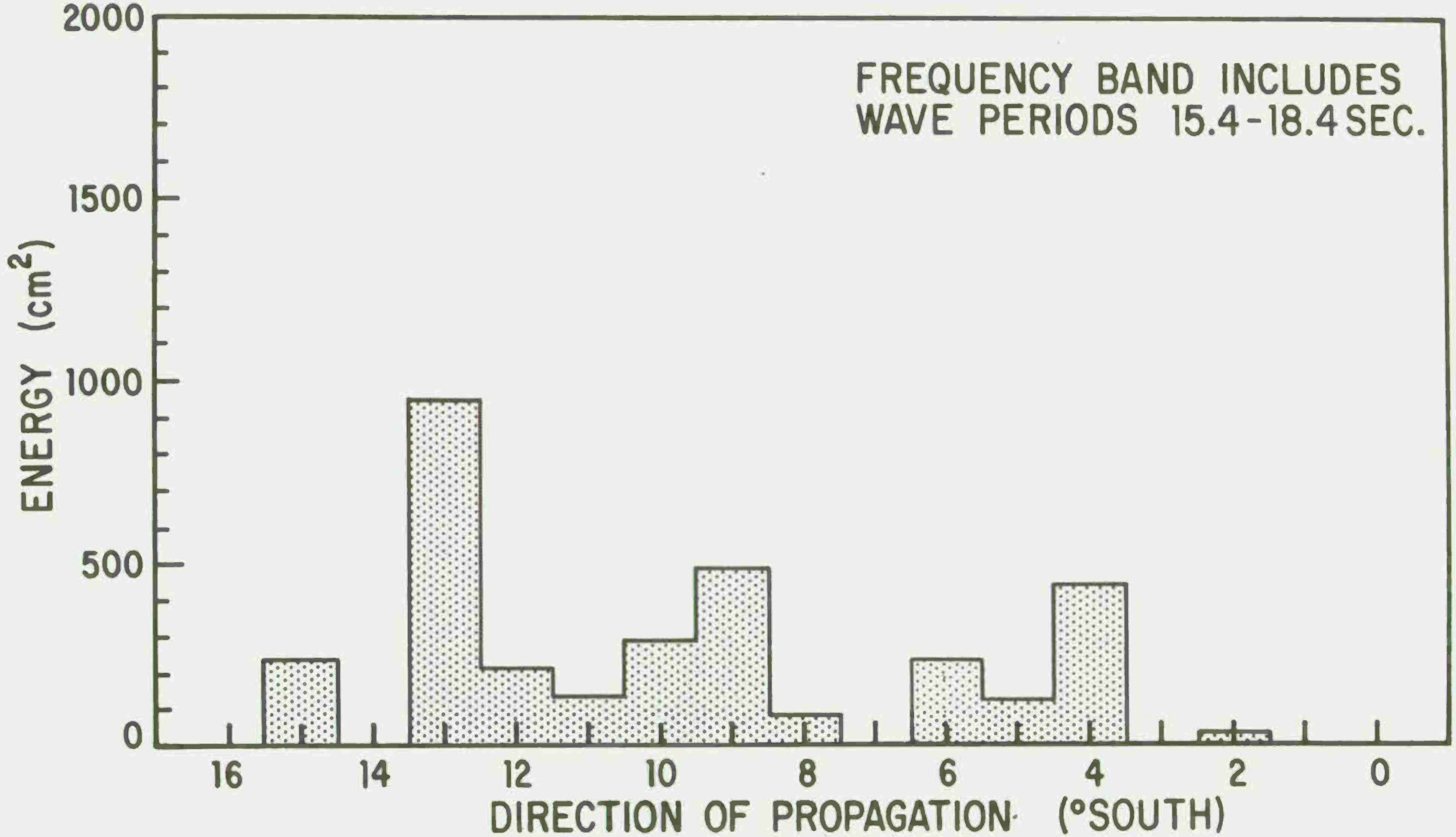

Figure J-8. A plot of the total energy versus direction of propagation during the fall months. The directions are in degrees from normal to the coast at Torrey Pines Station.

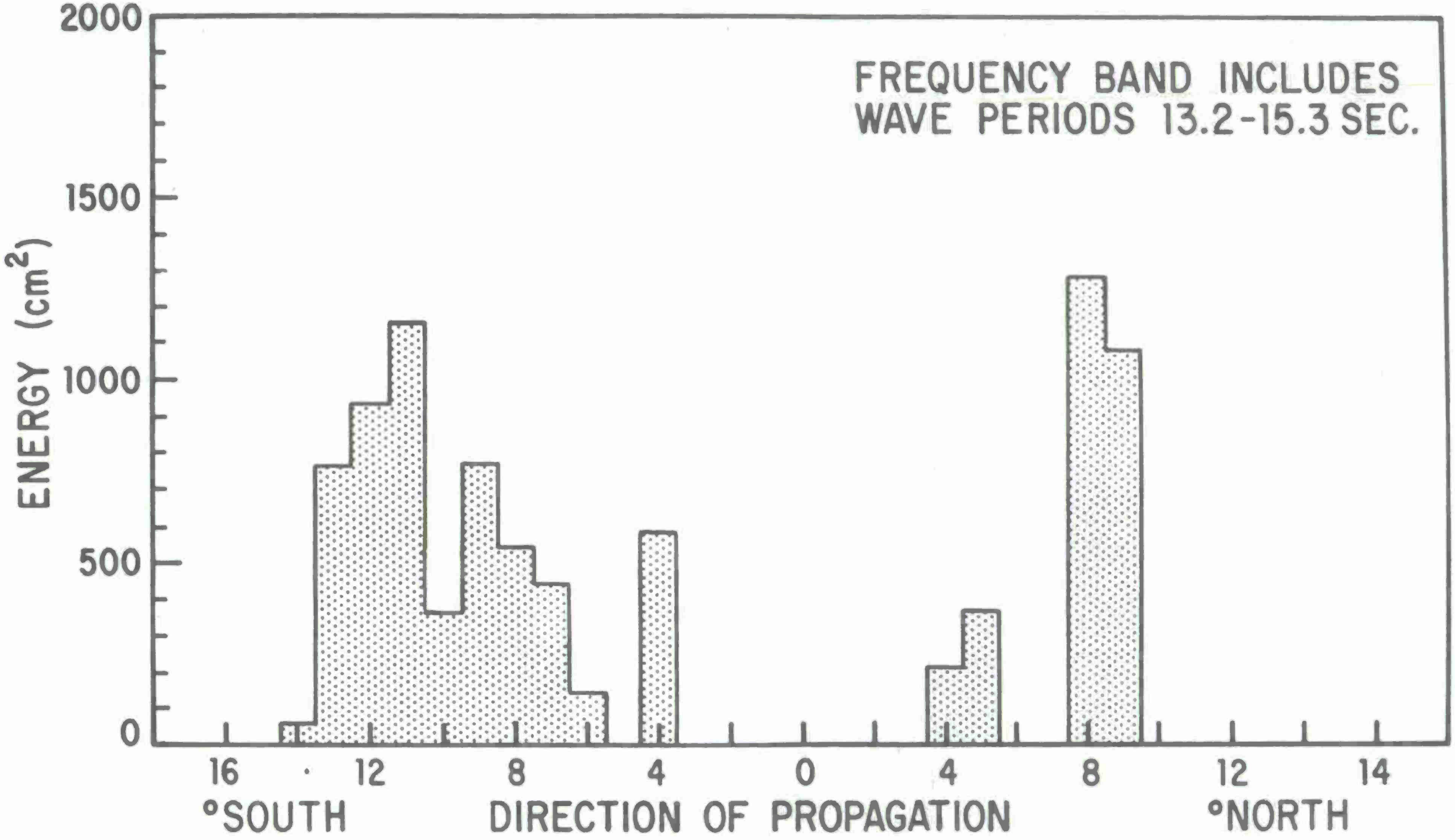

Figure J-9. A plot of the total energy versus direction of propagation during the fall months. The directions are in degrees from normal to the coast at Torrey Pines Station.

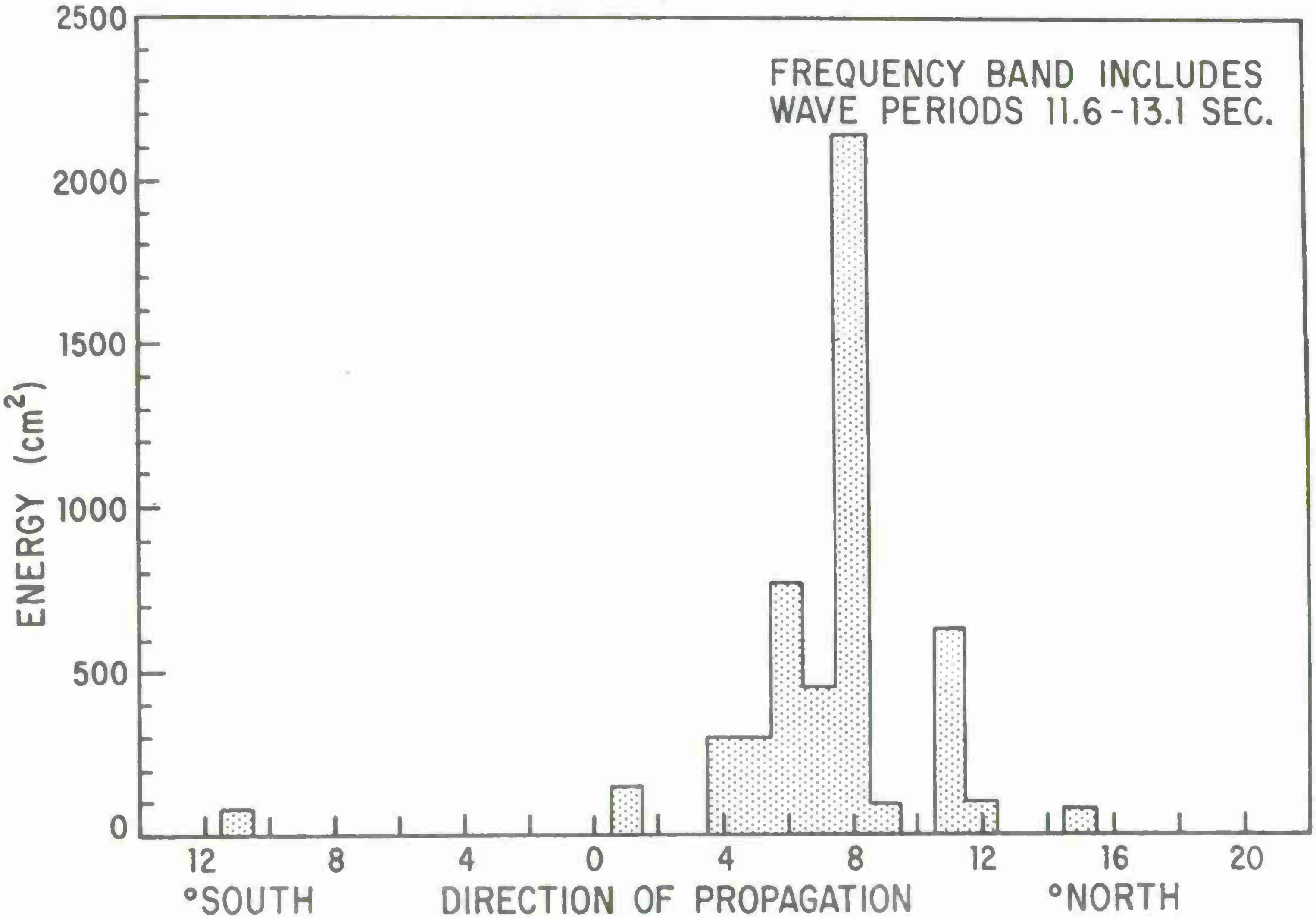

Figure J-10. A plot of the total energy versus direction of propagation during the fall months. The directions are in degrees from normal to the coast at Torrey Pines Station.

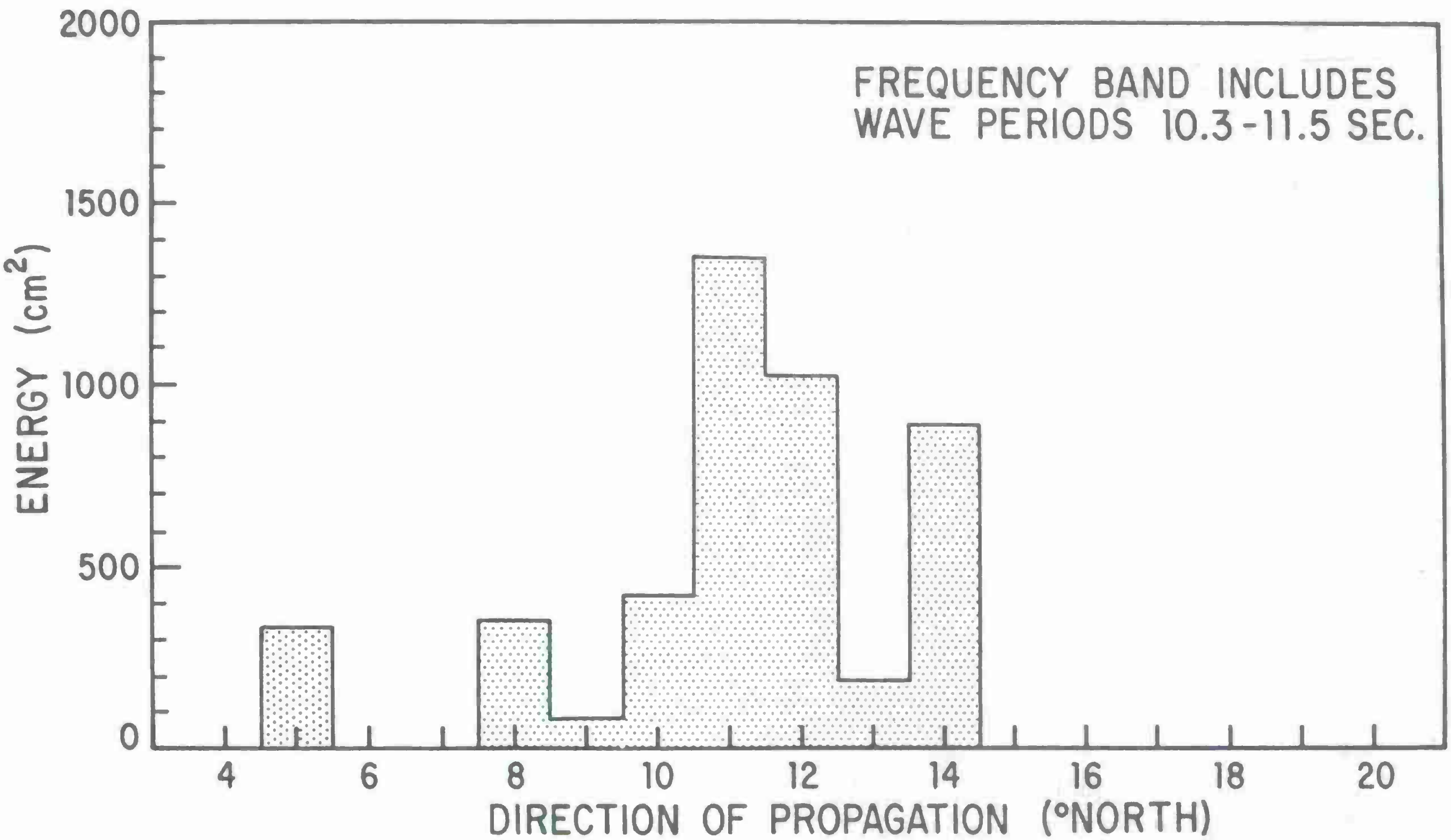

Figure J-11. A plot of the total energy versus direction of propagation during the fall months. The directions are in degrees from normal to the coast at Torrey Pines Station.

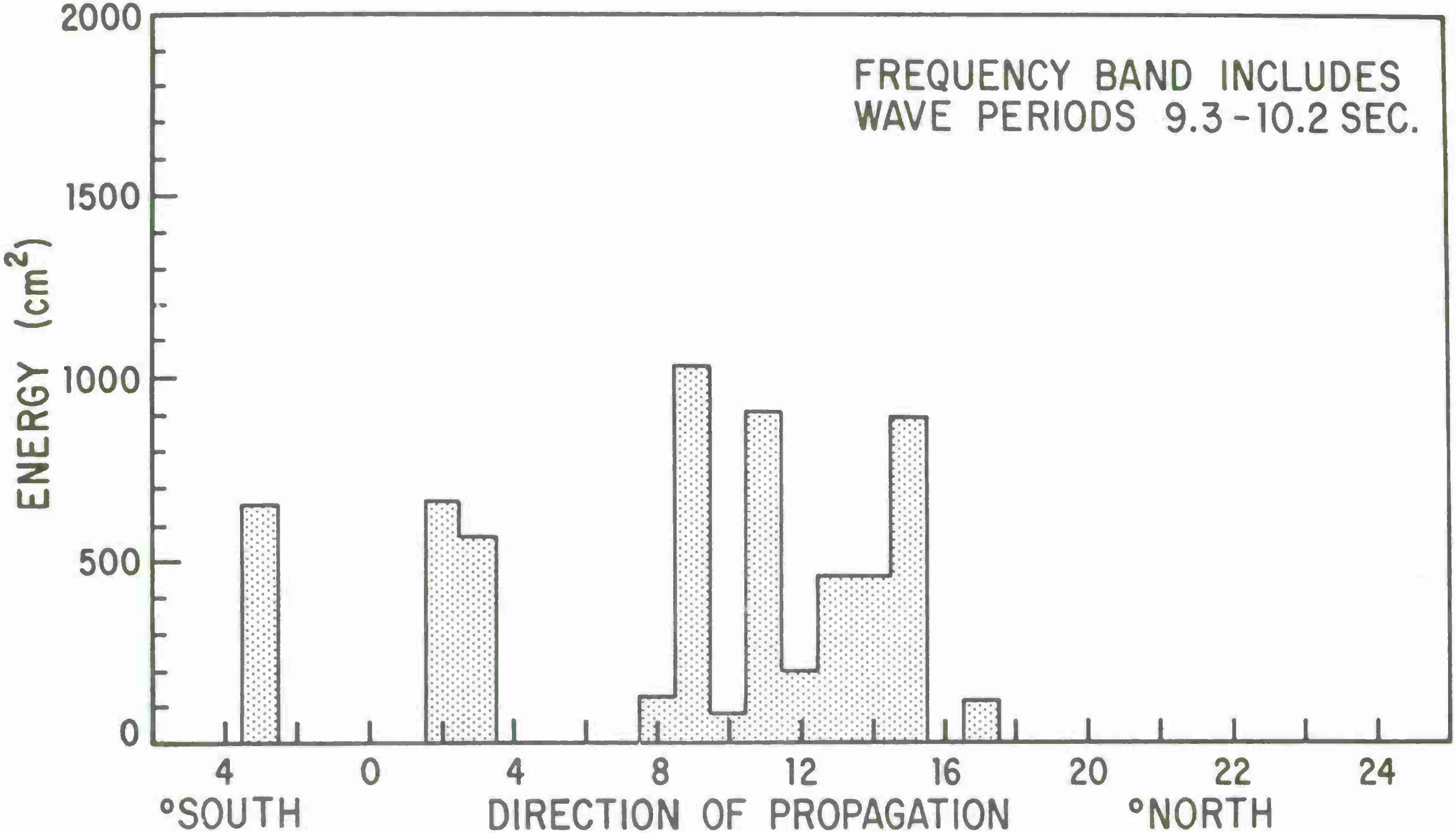

Figure J-12. A plot of the total energy versus direction of propagation during the fall months. The directions are in degrees from normal to the coast at Torrey Pines Station.

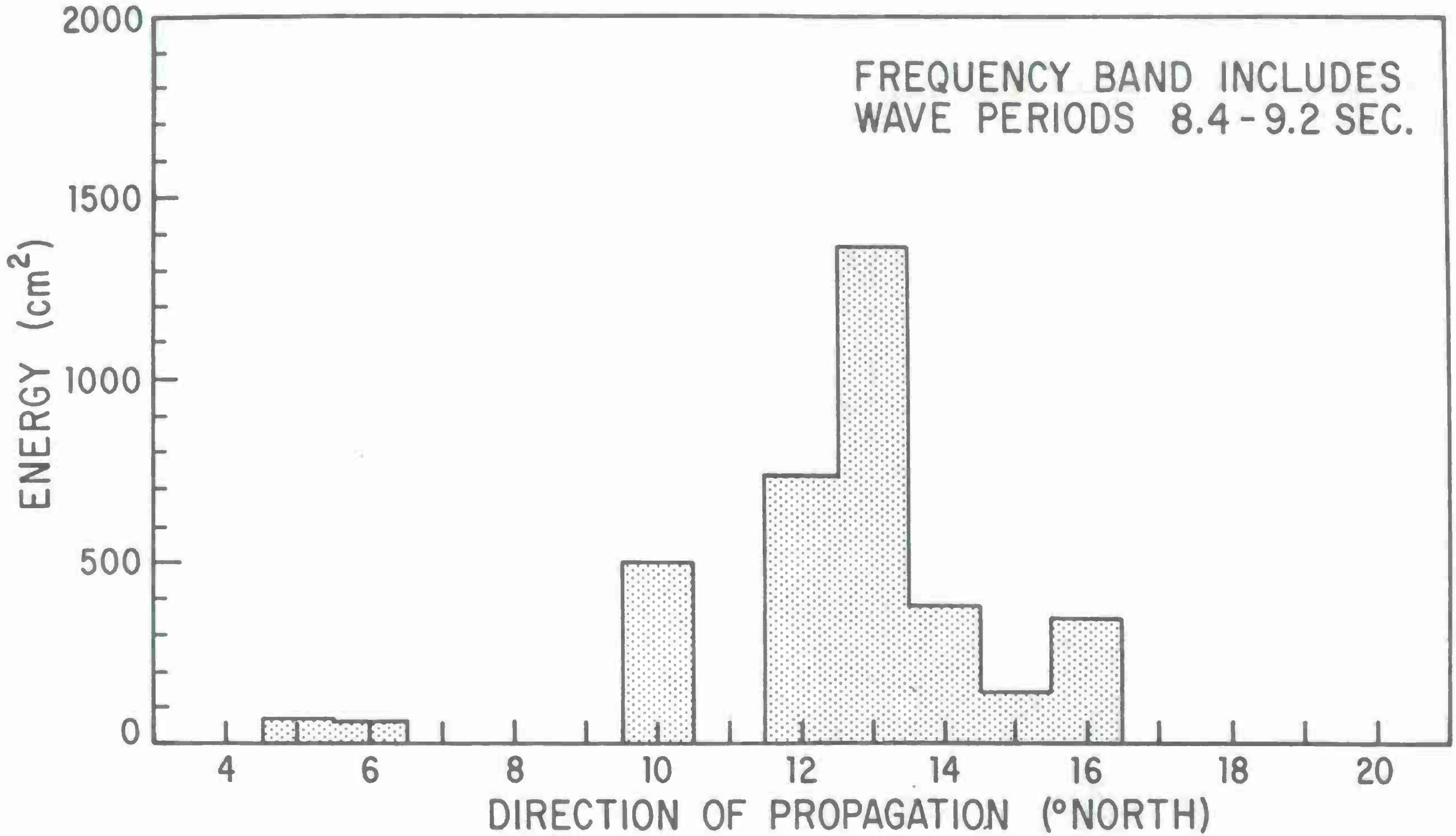

Figure J-13. A plot of the total energy versus direction of propagation during the fall months. The directions are in degrees from normal to the coast at Torrey Pines Station.

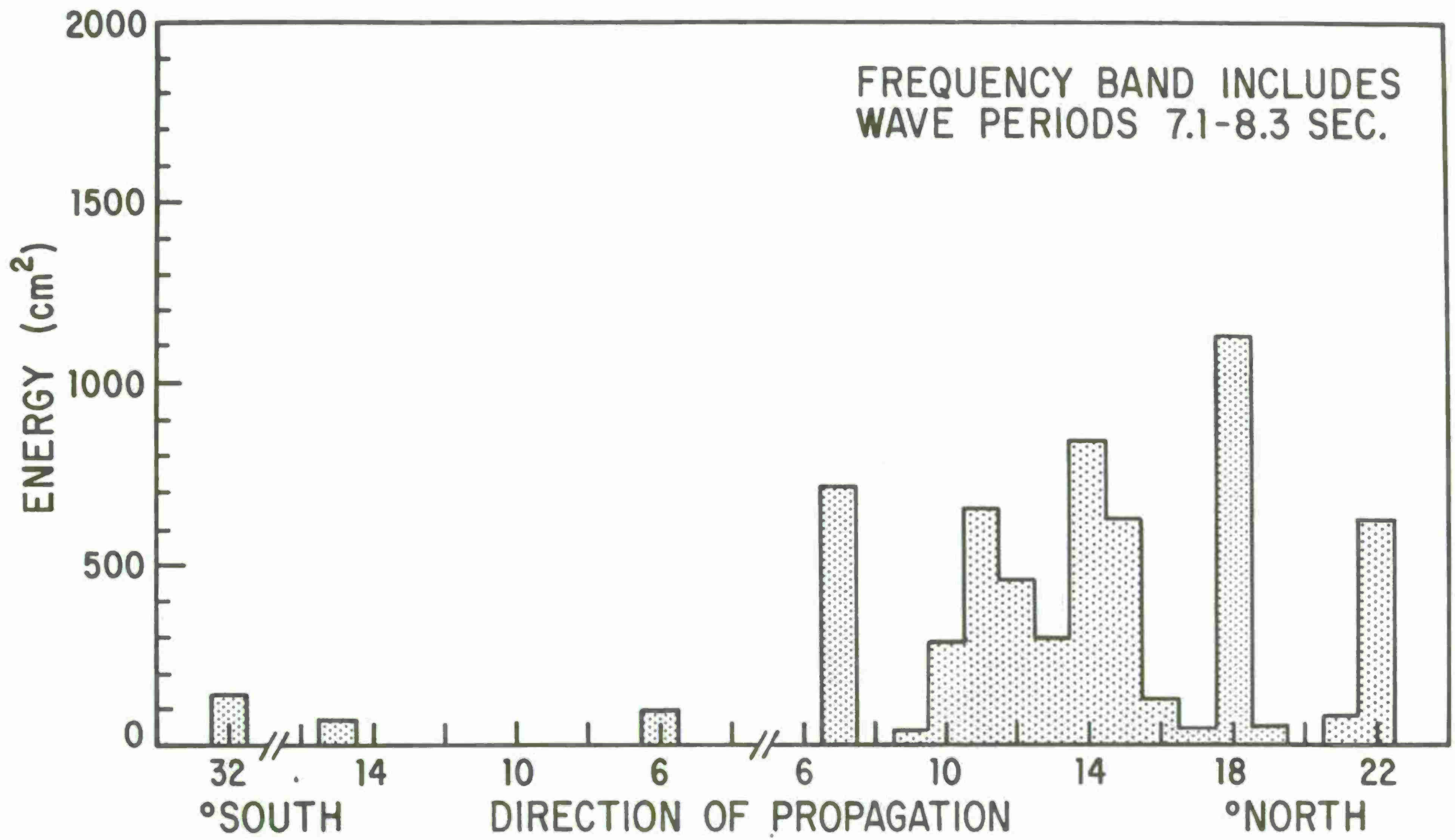

Figure J-14. A plot of the total energy versus direction of propagation during the fall months. The directions are in degrees from normal to the coast at Torrey Pines Station.

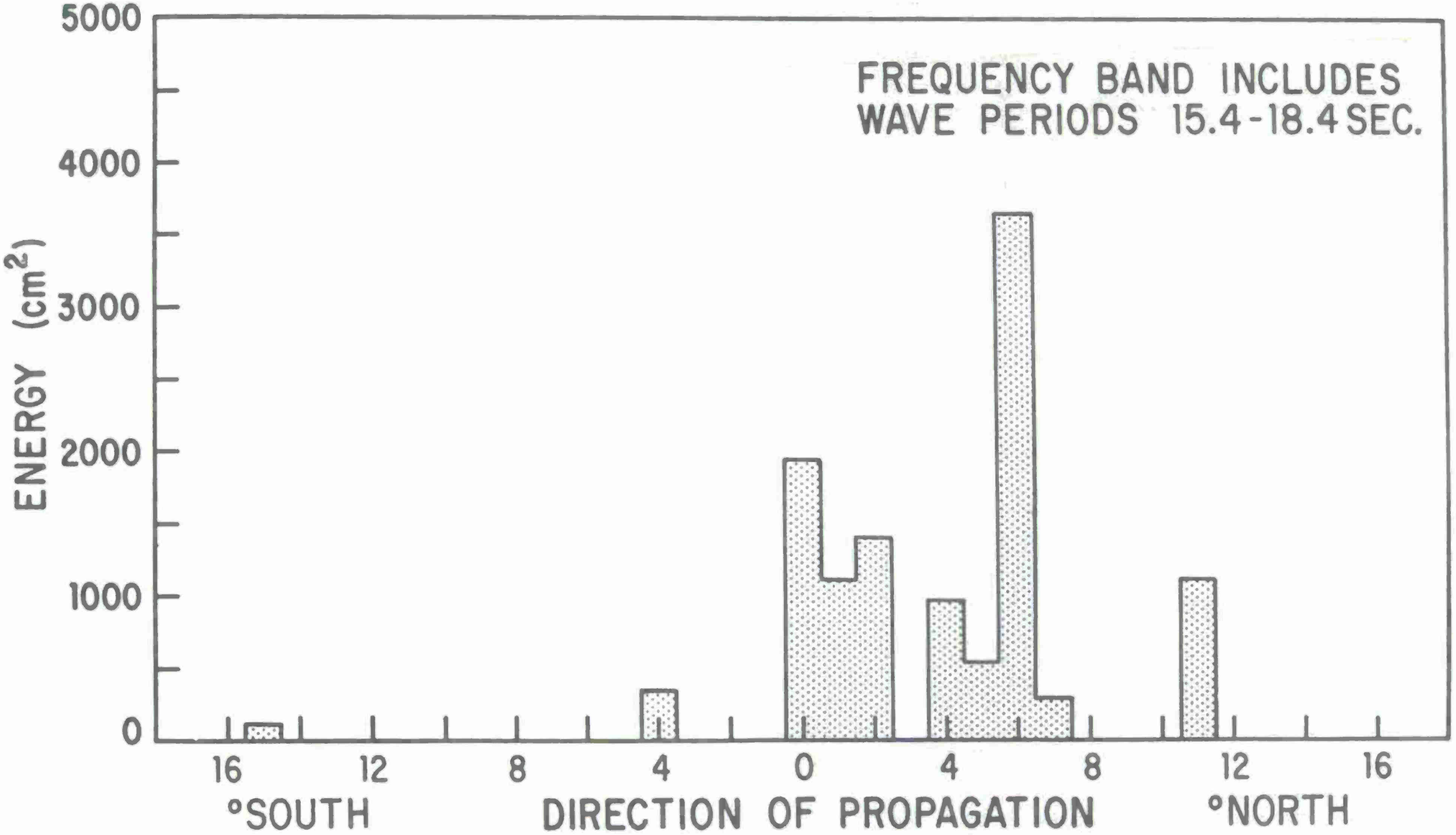

Figure J-15. A plot of the total energy versus direction of propagation during the winter months. The directions are in degrees from normal to the coast at Torrey Pines Station.

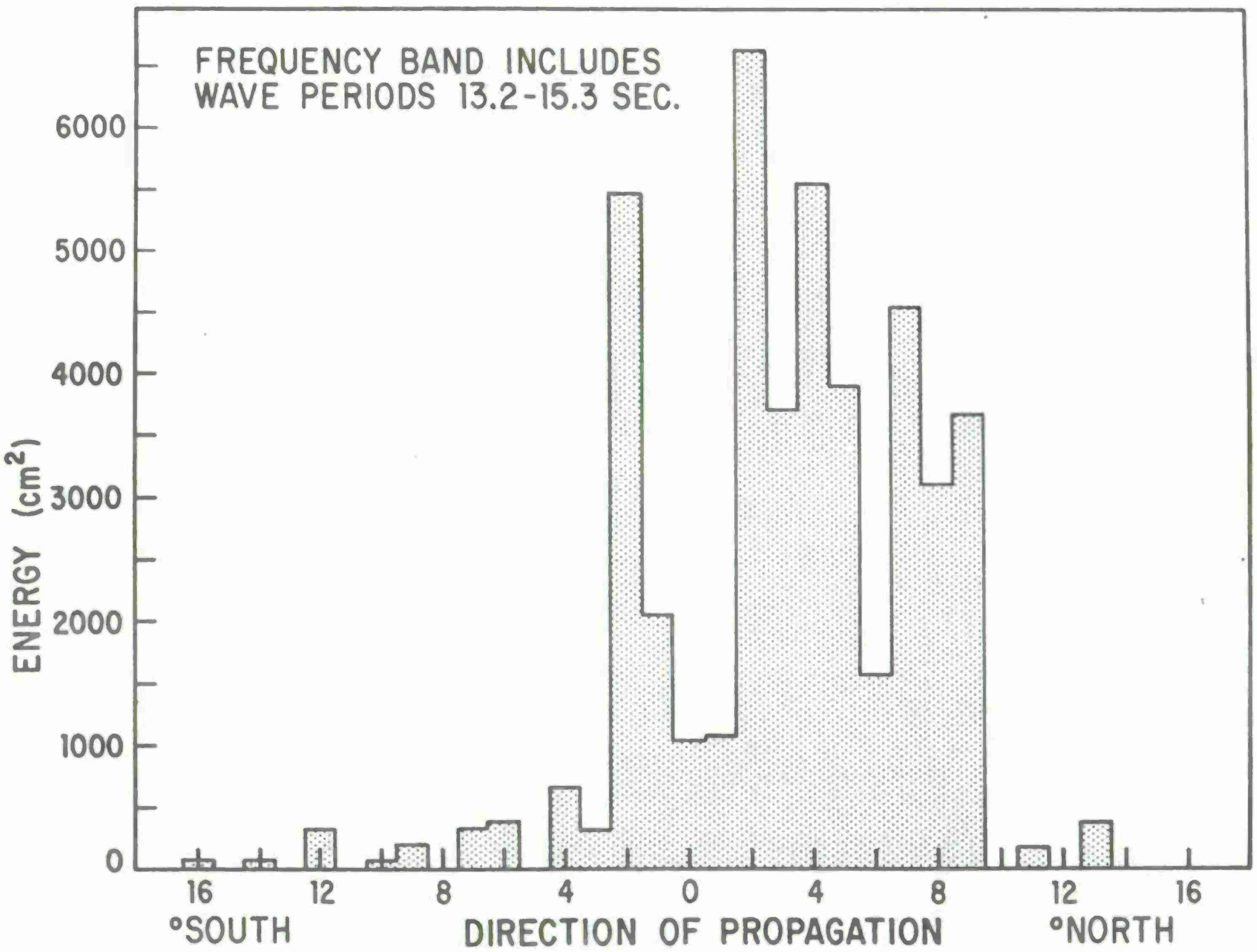

Figure J-16. A plot of the total energy versus direction of propagation during the winter months. The directions are in degrees from normal to the coast at Torrey Pines Station.

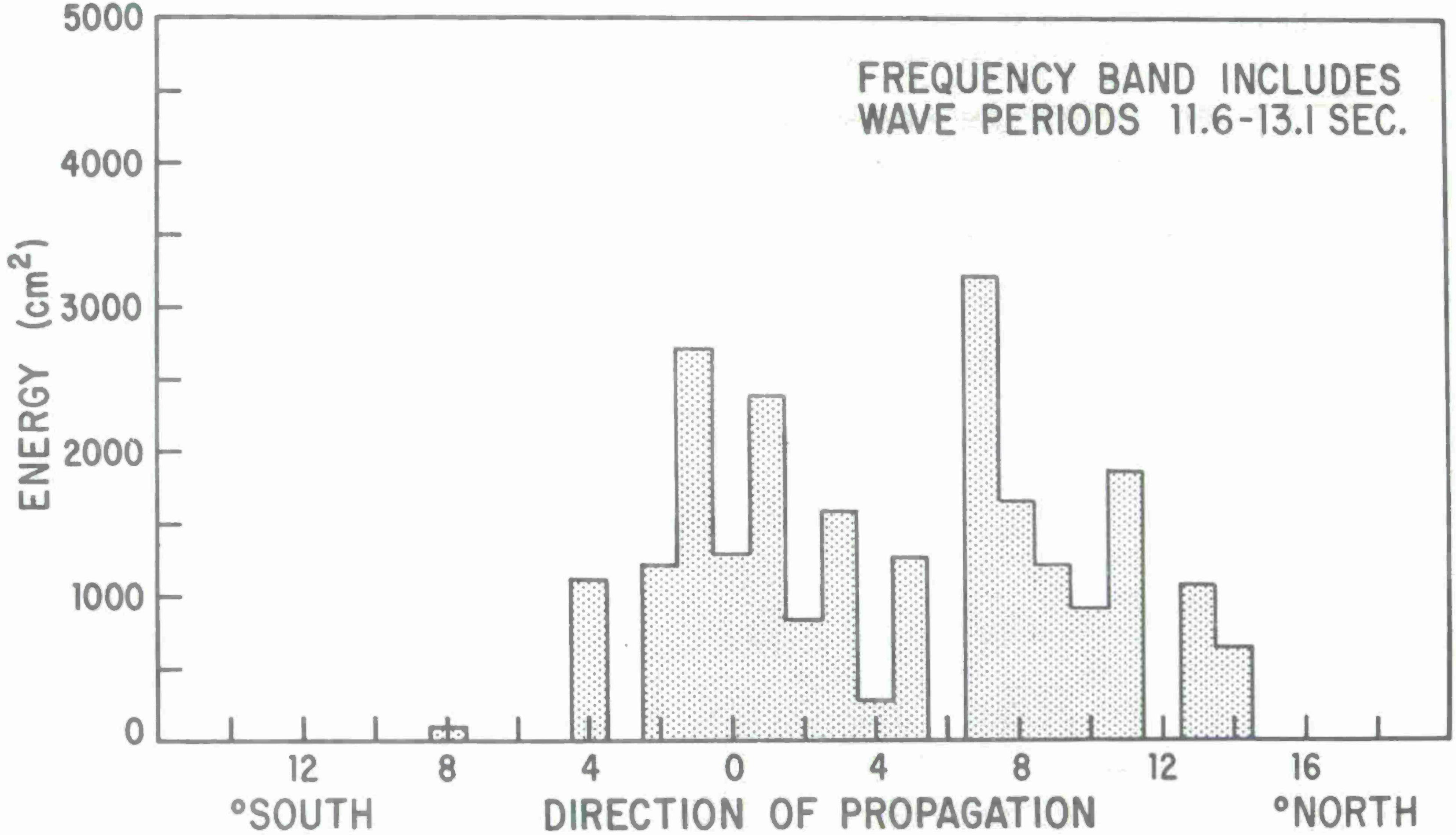

Figure J-17. A plot of the total energy versus direction of propagation during the winter months. The directions are in degrees from normal to the coast at Torrey Pines Station.

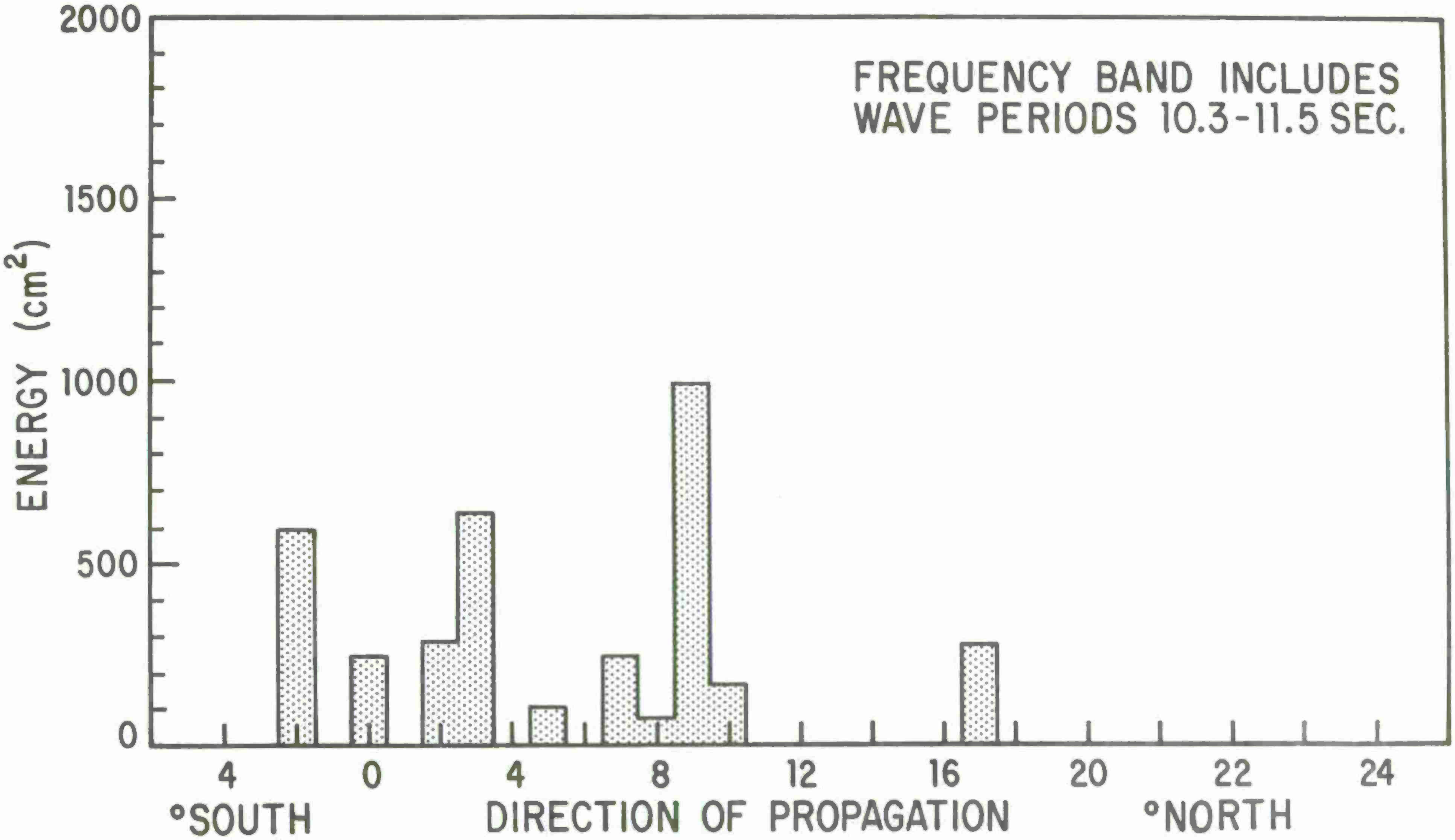

Figure J-18. A plot of the total energy versus direction of propagation during the winter months. The directions are in degrees from normal to the coast at Torrey Pines Station.

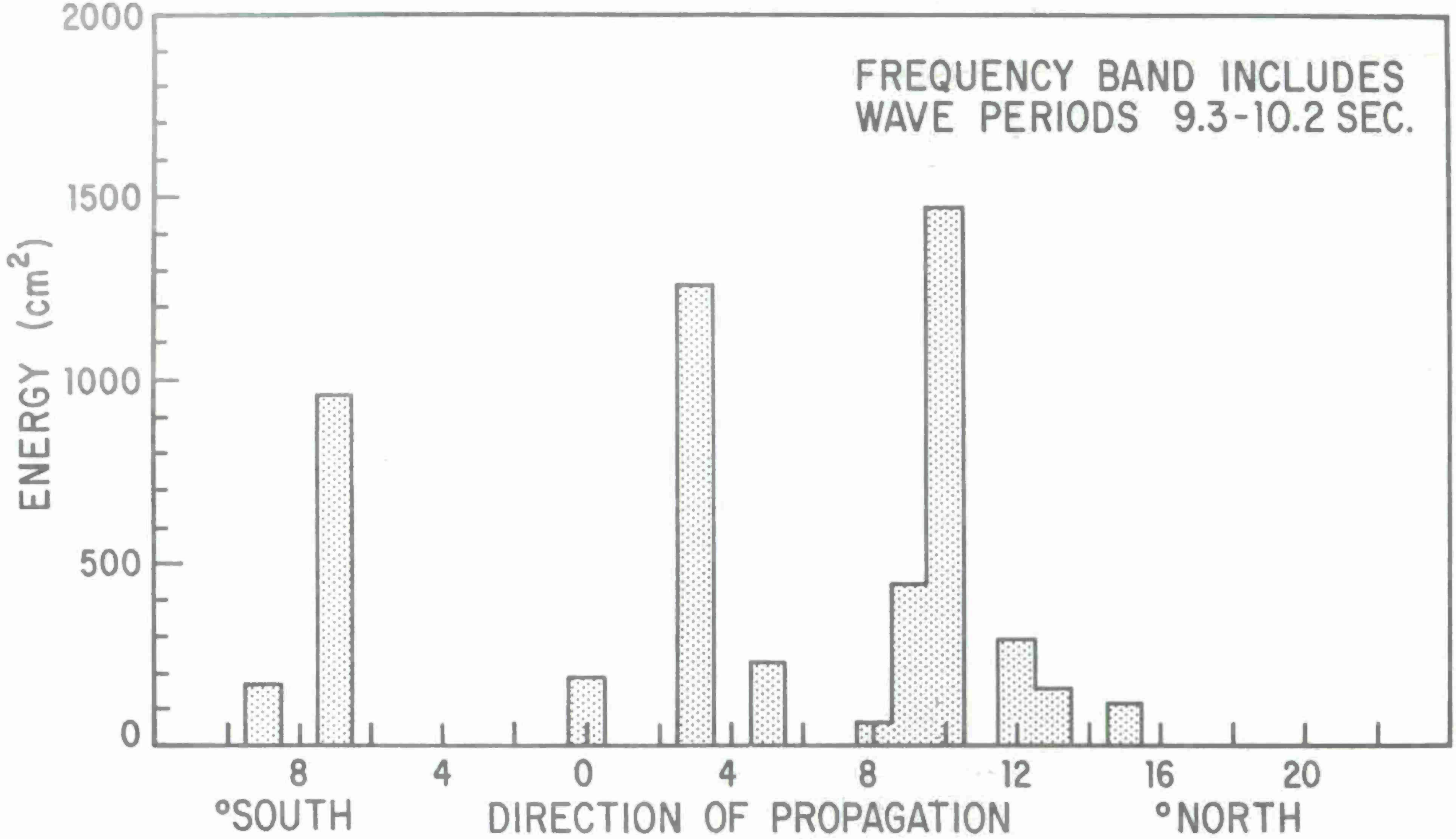

Figure J-19. A plot of the total energy versus direction of propagation during the winter months. The directions are in degrees from normal to the coast at Torrey Pines Station.

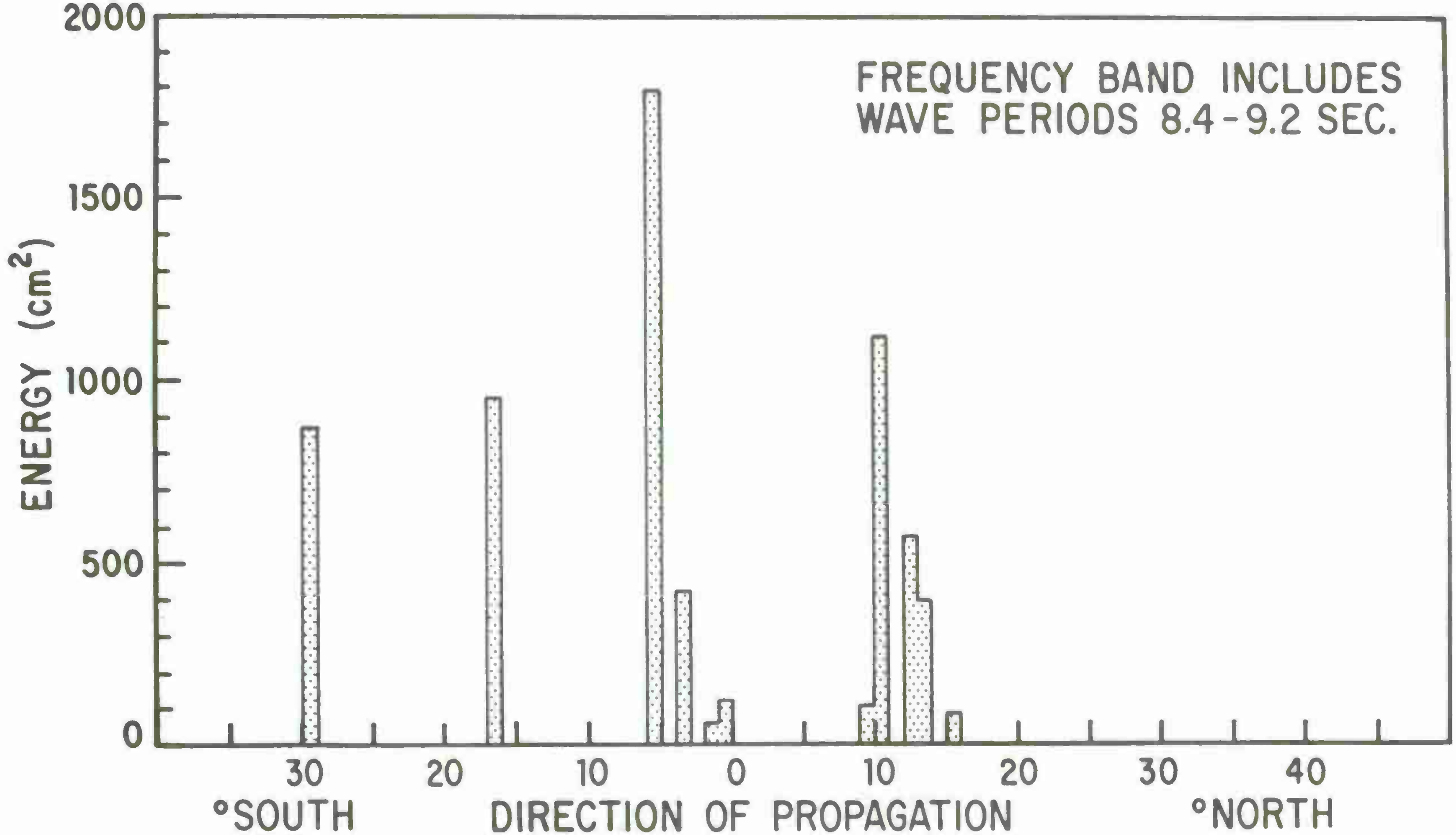

Figure J-20. A plot of the total energy versus direction of propagation during the winter months. The directions are in degrees from normal to the coast at Torrey Pines Station.

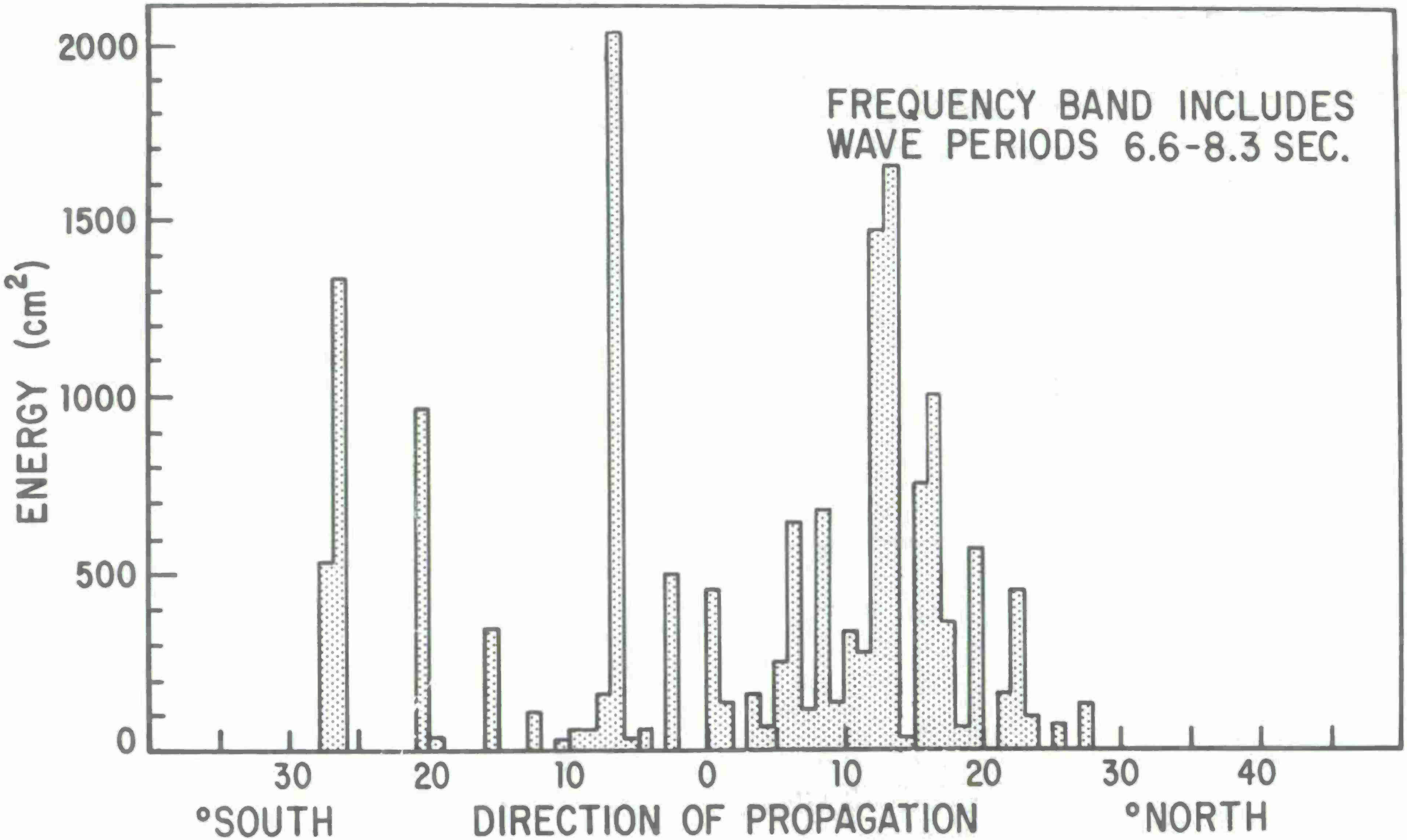

Figure J-21. A plot of the total energy versus direction of propagation during the winter months. The directions are in degrees from normal to the coast at Torrey Pines Station.

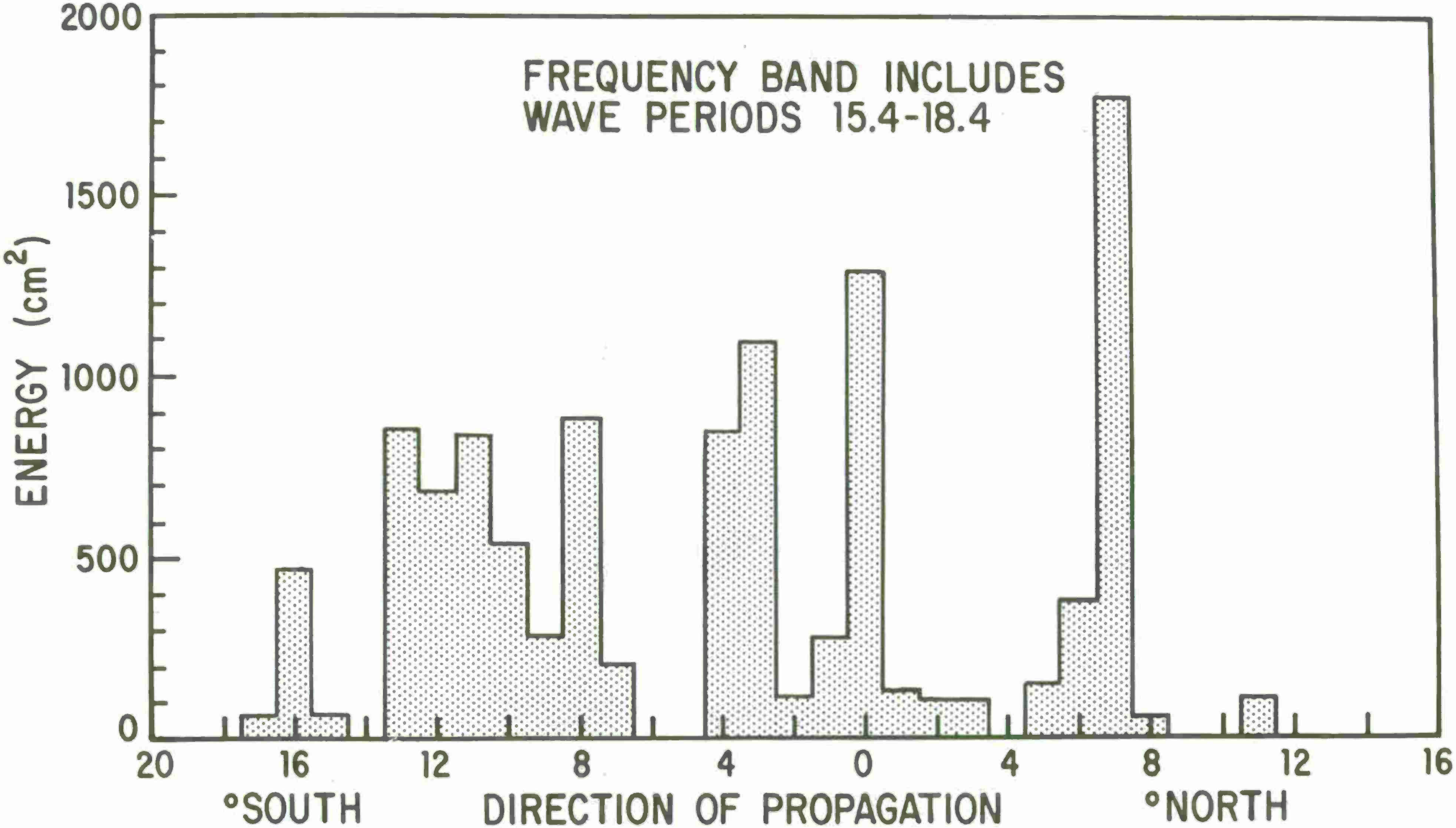

Figure J-22. A plot of the total energy versus direction of propagation during the spring months. The directions are in degrees from normal to the coast at Torrey Pines Station.

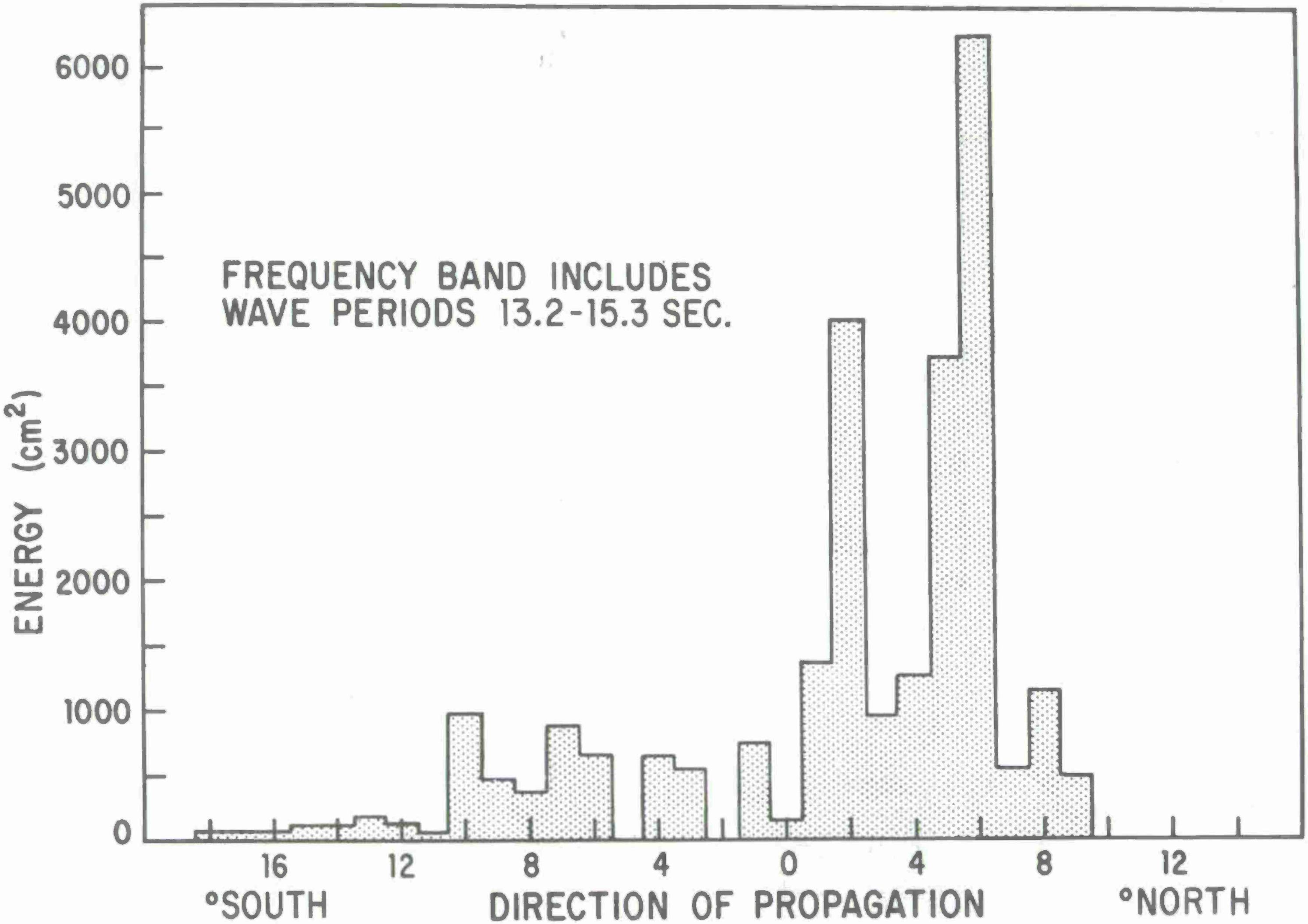

Figure J-23. A plot of the total energy versus direction of propagation during the spring months. The directions are in degrees from normal to the coast at Torrey Pines Station.

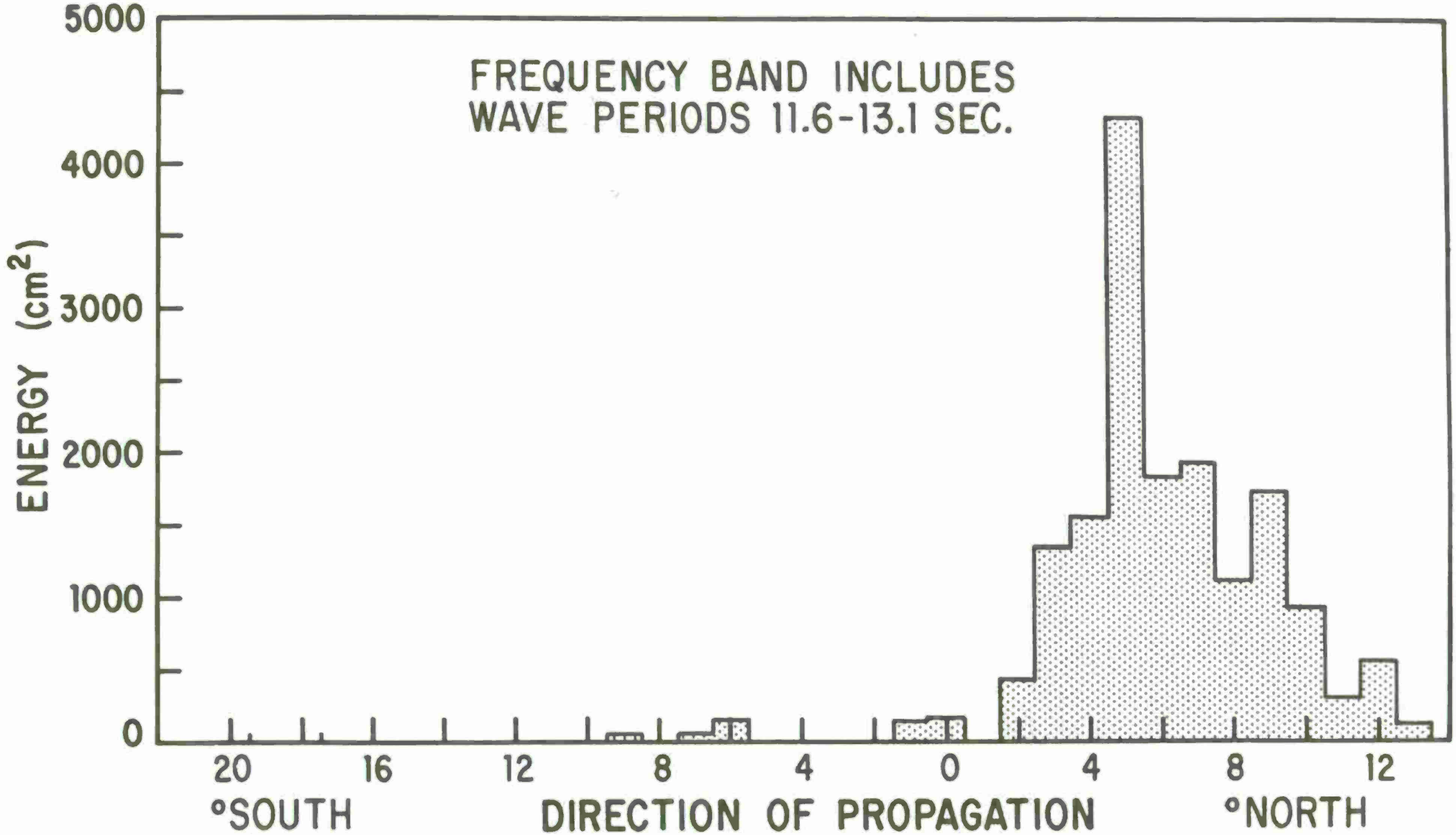

Figure J-24. A plot of the total energy versus direction of propagation during the spring months. The directions are in degrees from normal to the coast at Torrey Pines Station.

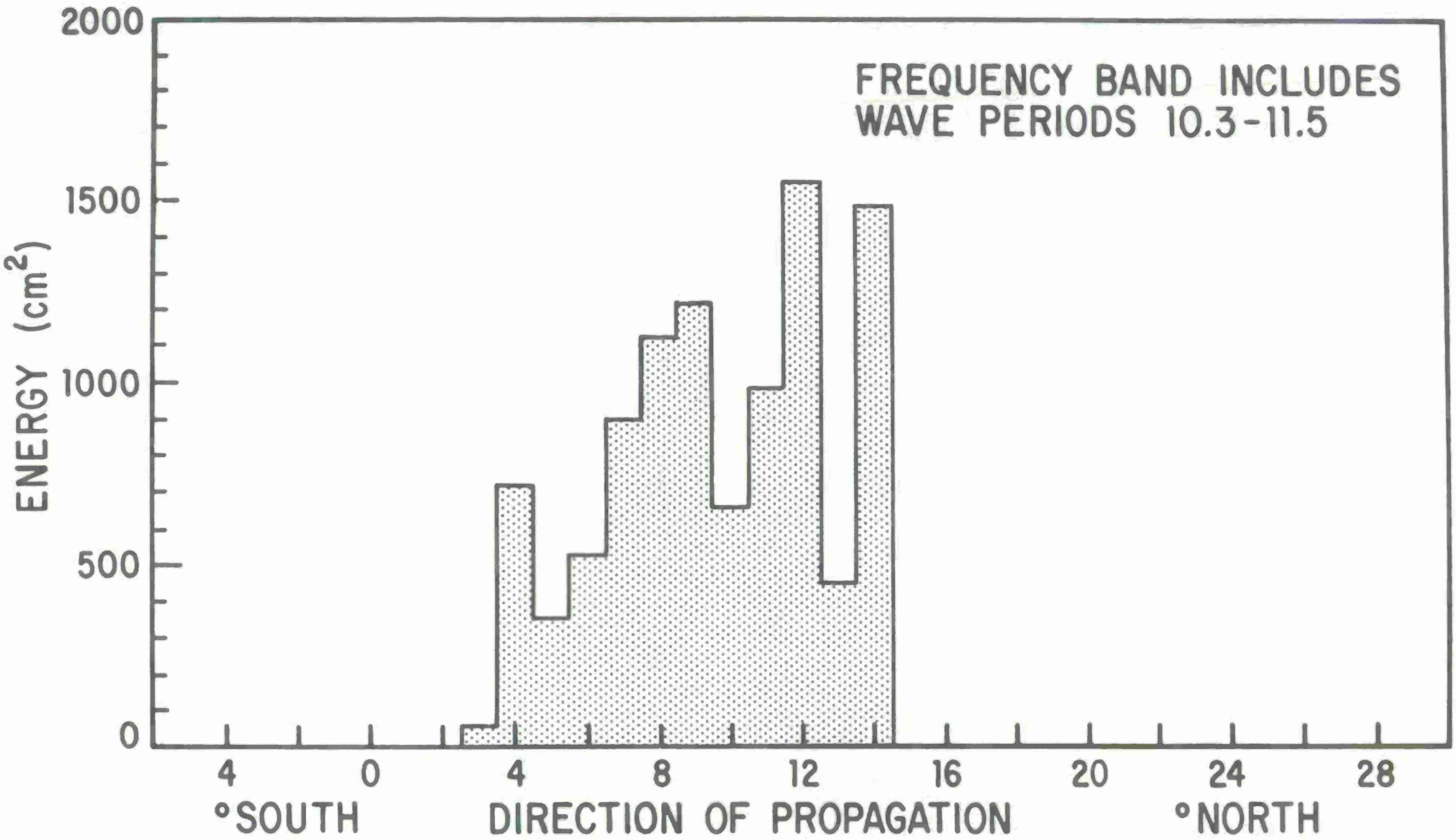

Figure J-25. A plot of the total energy versus direction of propagation during the spring months. The directions are in degrees from normal to the coast at Torrey Pines Station.

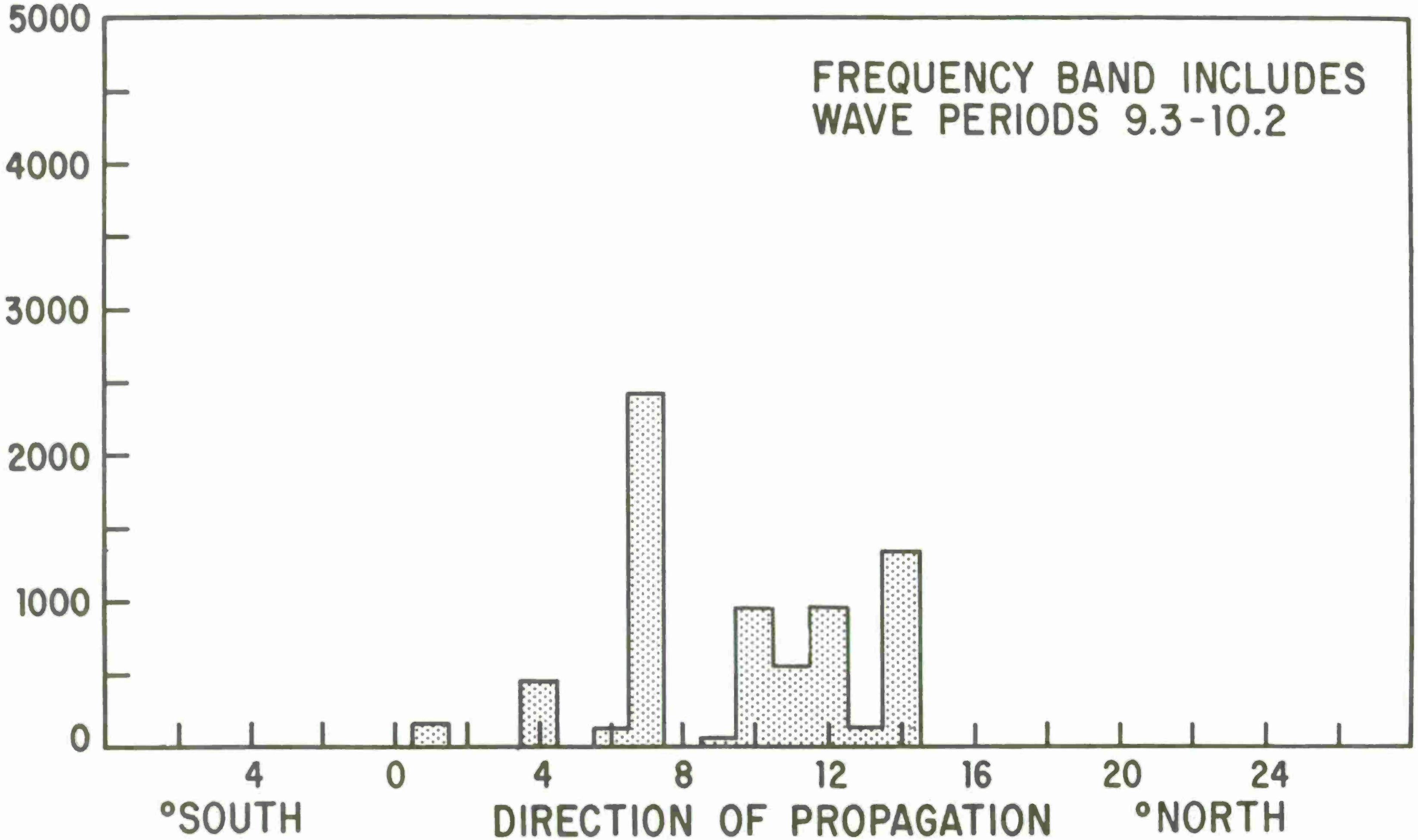

Figure J-26. A plot of the total energy versus direction of propagation during the spring months. The directions are in degrees from normal to the coast at Torrey Pines Station.

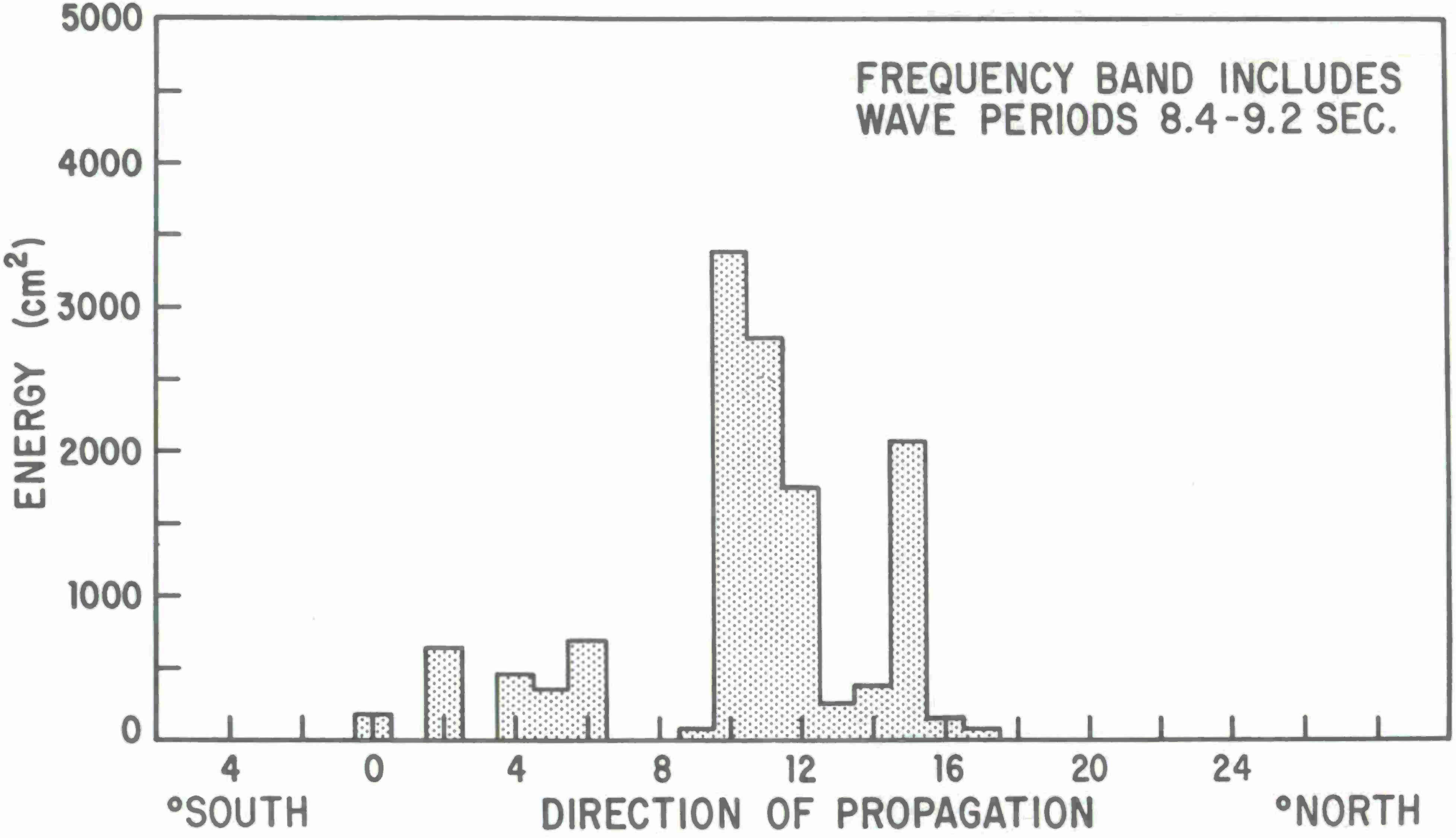

Figure J-27. A plot of the total energy versus direction of propagation during the spring months. The directions are in degrees from normal to the coast at Torrey Pines Station.

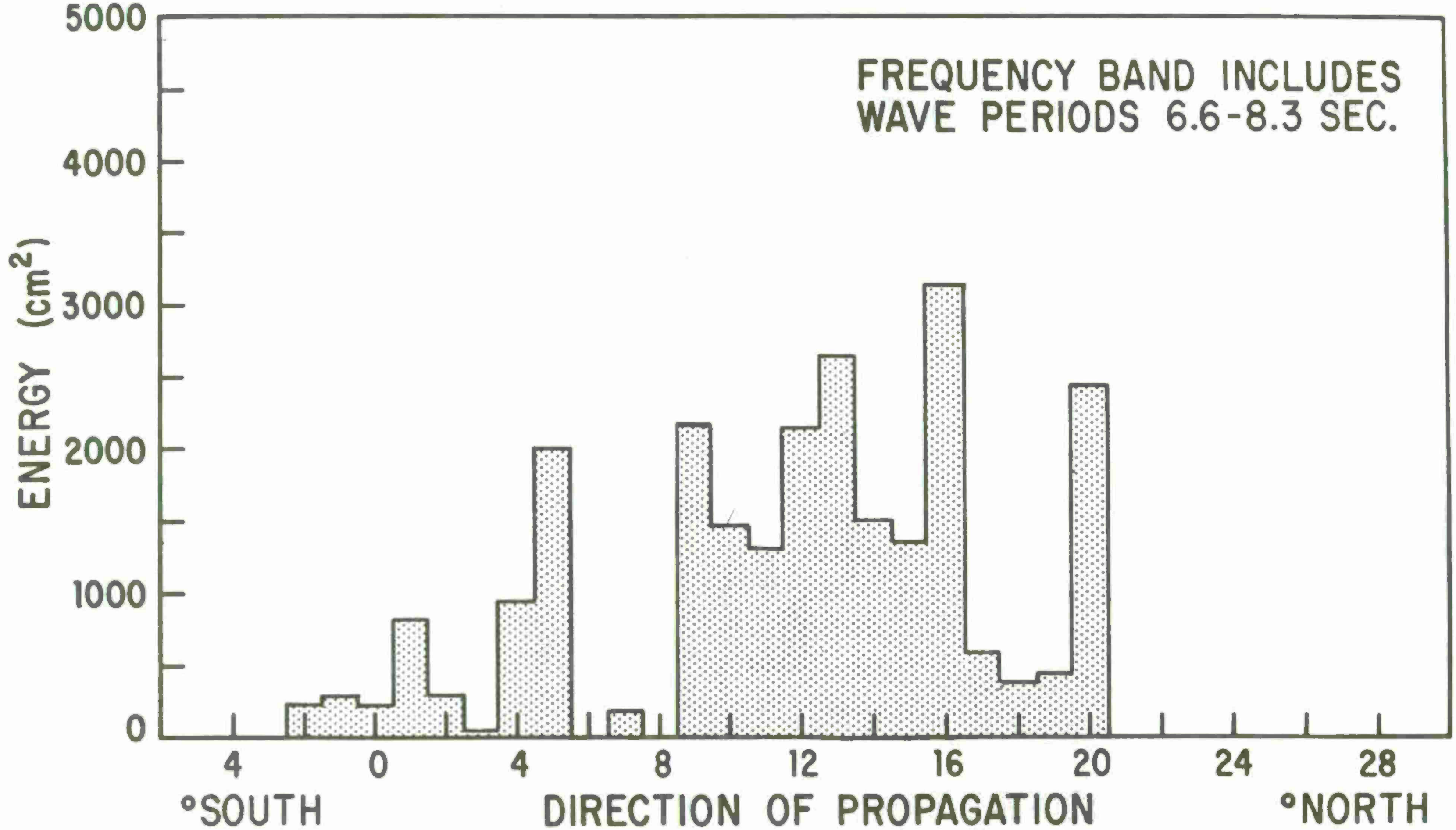

Figure J-28. A plot of the total energy versus direction of propagation during the spring months. The directions are in degrees from normal to the coast at Torrey Pines Station.

Pawka, Steven S.
Wave climate at Torrey Pines Beach, California / by Steven S. Pawka, Douglas L. Inman. . . [et al.]. - Fort Belvoir, Va. : U.S. Coastal Engineering Research Center, 1976.
372 p. : ill. (Technical paper - Coastal Engineering Research Center ; no. 76-5) (Contract - Coastal Engineering Research Center; DACW72-72-C-0021)
Bibliography : pp. 86-87.

Report presents a study of the wave climate at Torrey Pines Beach, California, using a line array of four pressure sensors which paralleled the coastline at a depth of 10 meters. Data from the array were used to calculate estimates of the frequency-directional spectra of the wave field.
1. Wave spectra. 2. Pressure sensors. 3. Ocean waves. I. Title. II. Inman, Douglas L. III. Series : U.S. Coastal Engineering Research Center. Contract DACW72-72-C-0021.

TC203 .U581tp no. 76-5 627 .U581tp

Pawka, Steven S.
Wave climate at Torrey Pines Beach, California / by Steven S. Pawka, Douglas L. Inman. . . [et al.]. - Fort Belvoir, Va. : U.S. Coastal Engineering Research Center, 1976.
372 p. : ill. (Technical paper - Coastal Engineering Research Center ; no. 76-5) (Contract - Coastal Engineering Research Center; DACW72-72-C-0021)
Bibliography : pp. 86-87.

Report presents a study of the wave climate at Torrey Pines Beach, California, using a line array of four pressure sensors which paralleled the coastline at a depth of 10 meters. Data from the array were used to calculate estimates of the frequency-directional spectra of the wave field.
1. Wave spectra. 2. Pressure sensors. 3. Ocean waves. I. Title. II. Inman, Douglas L. III. Series : U.S. Coastal Engineering Research Center. Contract DACW72-72-C-0021.

TC203 .U581tp no. 76-5 627 .U581tp

Pawka, Steven S.
Wave climate at Torrey Pines Beach, California / by Steven S. Pawka, Douglas L. Inman. . . [et al.]. - Fort Belvoir, Va. : U.S. Coastal Engineering Research Center, 1976.
372 p. : ill. (Technical paper - Coastal Engineering Research Center ; no. 76-5) (Contract - Coastal Engineering Research Center; DACW72-72-C-0021)
Bibliography : pp. 86-87.

Report presents a study of the wave climate at Torrey Pines Beach, California, using a line array of four pressure sensors which paralleled the coastline at a depth of 10 meters. Data from the array were used to calculate estimates of the frequency-directional spectra of the wave field.
1. Wave spectra. 2. Pressure sensors. 3. Ocean waves. I. Title. II. Inman, Douglas L. III. Series : U.S. Coastal Engineering Research Center. Contract DACW72-72-C-0021.

TC203 .U581tp no. 76-5 627 .U581tp

Pawka, Steven S.
Wave climate at Torrey Pines Beach, California / by Steven S. Pawka, Douglas L. Inman. . . [et al.]. - Fort Belvoir, Va. : U.S. Coastal Engineering Research Center, 1976.
372 p. : ill. (Technical paper - Coastal Engineering Research Center ; no. 76-5) (Contract - Coastal Engineering Research Center; DACW72-72-C-0021)
Bibliography : pp. 86-87.

Report presents a study of the wave climate at Torrey Pines Beach, California, using a line array of four pressure sensors which paralleled the coastline at a depth of 10 meters. Data from the array were used to calculate estimates of the frequency-directional spectra of the wave field.
1. Wave spectra. 2. Pressure sensors. 3. Ocean waves. I. Title. II. Inman, Douglas L. III. Series : U.S. Coastal Engineering Research Center. Contract DACW72-72-C-0021.

TC203 .U581tp no. 76-5 627 .U581tp